Western Research INSTITUTE

# Asphalt Research Consortium

## Quarterly Technical Progress Report
## January 1-March 31, 2011

April 2011

Prepared for
Federal Highway Administration
Contract No. DTFH61-07-H-00009

By
Western Research Institute
Texas A&M University
University of Wisconsin-Madison
University of Nevada-Reno
Advanced Asphalt Technologies

www.westernresearch.org
www.ARC.unr.edu

# TABLE OF CONTENTS


INTRODUCTION ..... 1

GENERAL CONSORTIUM ACTIVITIES ..... 3

PROGRAM AREA: MOISTURE DAMAGE ..... 5
- Category M1: Adhesion ..... 5
- Category M2: Cohesion ..... 9
- Category M3: Aggregate Surface ..... 16
- Category M4: Modeling ..... 17
- Category M5: Moisture Damage Prediction System ..... 18
- Table of Decision Points and Deliverables for Moisture Damage ..... 19
- Gantt Charts for Moisture Damage ..... 22

PROGRAM AREA: FATIGUE ..... 25
- Category F1: Material and Mixture Properties ..... 25
- Category F2: Test Method Development ..... 38
- Category F3: Modeling ..... 54
- Table of Decision Points and Deliverables for Fatigue ..... 73
- Gantt Charts for Fatigue ..... 77

PROGRAM AREA: ENGINEERED MATERIALS ..... 79
- Category E1: Modeling ..... 79
- Category E2: Design Guidance ..... 103
- Table of Decision Points and Deliverables for Engineered Materials ..... 130
- Gantt Charts for Engineered Materials ..... 135

PROGRAM AREA: VEHICLE-PAVEMENT INTERACTION ..... 137
- Category VP1: Workshop ..... 137
- Category VP2: Design Guidance ..... 137
- Category VP3: Modeling ..... 139
- Table of Decision Points and Deliverables for Vehicle-Pavement Interaction ..... 146
- Gantt Charts for Vehicle-Pavement Interaction ..... 147

PROGRAM AREA: VALIDATION ..... 149
- Category V1: Field Validation ..... 149
- Category V2: Accelerated Pavement Testing ..... 150
- Category V3: R&D Validation ..... 150
- Table of Decision Points and Deliverables for Validation ..... 158
- Gantt Charts for Validation ..... 160

PROGRAM AREA: TECHNOLOGY DEVELOPMENT ..... 163

PROGRAM AREA: TECHNOLOGY TRANSFER ..... 171
Category TT1: Outreach and Databases ..... 171
Table of Decision Points and Deliverables for Technology Transfer ..... 183
Gantt Charts for Technology Transfer ..... 184

# INTRODUCTION

This document is the Quarterly Report for the period of January 1 to March 31, 2011 for the Federal Highway Administration (FHWA) Contract DTFH61-07-H-00009, the Asphalt Research Consortium (ARC). The Consortium is coordinated by Western Research Institute with partners Texas A&M University, the University of Wisconsin-Madison, the University of Nevada Reno, and Advanced Asphalt Technologies.

The Quarterly Report is grouped into seven areas, Moisture Damage, Fatigue, Engineered Paving Materials, Vehicle-Pavement Interaction, Validation, Technology Development, and Technology Transfer. The format of the report is based upon the Research Work Plan that is grouped by Work Element and Subtask.

This Quarterly Report summarizes the work accomplishments, data, and analysis for the various Work Elements and Subtasks. This report is being presented in a summary form. The Quarter of January 1 to March 31, 2011 is fourth quarter of the Year 4 contract year. Reviewers may want to reference the previous Annual Work Plans and many other documents that are posted on the ARC website, www.ARC.unr.edu. The more detailed information about the research such as approaches to test method development, data collection, and analyses will be reported in research publications as part of the deliverables. This quarterly report contains updates to the Table of Deliverables and the Table of Journal Papers that were presented in the Year 5 Work Plan.

## SUPPORT OF FHWA AND DOT STRATEGIC GOALS

The Asphalt Research Consortium research is responsive to the needs of asphalt engineers and technologists, state DOT's, and supports the FHWA Strategic Goals and the Asphalt Pavement Road Map. More specifically, the research reported here supports the Strategic Goals of safety, mobility, and environmental stewardship. By addressing the causes of pavement failure and thus determining methods to improve asphalt pavement durability and longevity, this research will provide the motoring public with increased safety and mobility. The research directed at improved use of recycled asphalt pavement (RAP), warm mix asphalt, and cold mix asphalt supports the Strategic Goal of environmental stewardship.

# GENERAL CONSORTIUM ACTIVITIES

## PROGRESS THIS QUARTER

Many ARC members attended the TRB Annual Meeting in Washington DC during the week of January 23, 2011. Several presentations were made by ARC members on results of the research in both podium and poster sessions. Also just prior TRB week, presentations were made at the International Society of Asphalt Pavements (ISAP) Technical Committee meetings. ARC members also participate on TRB committees.

A brief ARC advisory board meeting was conducted during TRB week to keep all members up to date. The ARC Asphalt Microstructural Modeling team members met during TRB week to discuss project progress, coordination, and work plans.

ARC members attended and made presentations at the Association of Modified Asphalt Producers (AMAP) meeting on February 15 – 17, 2011 in Kansas City, Missouri and the Rocky Mountain Asphalt Conference in Denver, Colorado on February 24 & 25, 2011.

Several ARC members attended and made presentations at the Binder, Mix & Construction, and Fundamental Properties & Advanced Models ETG meetings in Phoenix, Arizona during the week of March 14, 2011. A considerable portion of the Fundamental Properties and Advanced Models ETG meeting was devoted to review of the ARC Year 5 Work Plan.

ARC members attended and presentations were made at the Association of Asphalt Paving Technologists meeting in Tampa, Florida during the week of March 27, 2011.

## WORK PLANNED FOR NEXT QUARTER

ARC members are planning on attending the RAP Expert Task Group meeting and the WMA TWG on May 10 - 13, 2011 that is being held at the Beckman Center in Irvine, California. An update on the RAP and WMA research being conducted by the ARC will be presented.

# PROGRAM AREA: MOISTURE DAMAGE

## CATEGORY M1: ADHESION

### Work Element M1a: Affinity of Asphalt to Aggregate (UWM)

Work Done This Quarter

The research group continued using the Sessile Drop method to measure contact angles of different asphalt binders with three liquids: distilled water, ethylene glycol, and formamide. Preliminary comparison between contact angle measurements, which can be used as a quantitative estimation of wettability, and Bitumen Bond Strength (BBS) results was conducted. The experimental results showed that the BBS and contact angle measurements are in agreement. Binders with higher pull-off tensile strength correspond to binders with higher wettability capacity (i.e., lower contact angles). Note that the comparison was performed based on Sessile Drop results with distilled water as probe liquid. The binders and aggregates used for BBS-Sessile Drop comparison are listed in table M1a.1.

Table M1a.1. Materials used for Contact Angle and BBS testing.

| | |
|---|---|
| **Solution** | Distilled Water, Ethylene Glycol, Formamide |
| **Aggregate** | Limestone and Granite |
| **Asphalt Binders** | FH 64-22 & CRM 58-28 |
| **Modified Asphalt Binders** | FH 64-22 +1% Polyphosphoric Acid (PPA),<br>FH 64-22+0.7% Elvaloy 4170+0.17% PPA<br>FH 64-22+0.7% Elvaloy AM+0.17% PPA<br>FH 64-22+0.5% Anti-Stripping<br>FH 64-22+2% Plastomer (CBE)<br>CRM 58-28 +1% PPA |

Significant Results

Table M1a.2 shows the values of the contact angel and the coefficient of variations (CV %) of the asphalt binders. It also shows the ranking based on contact angle measurements with distilled water. Table M1a.3 shows the ranking based on the pull-off strength results at dry and wet conditions (i.e., 96 hours) in granite substrate. It can be seen from tables M1a.2-M1a.3 that both tests rank the asphalt binders similarly. Lower contact angle with distilled water indicates higher wetting tendency. When wettability increases, the surface of aggregates to be wetted by the asphalt binder increases, thereby improving the adhesion between the asphalt and aggregate as observed in the BBS results.

Table M1a.2. Sessile Drop results for asphalt binders.

| Contact Angle in Water | | | | |
|---|---|---|---|---|
| **Sample** | **Average ( ° )** | **Std( ° )** | **CV (%)** | **Rank** |
| FH 64-22 + 2% CBE | 108.1 | 0.57 | 0.53 | 1 |
| FH 64-22 + 1% PPA | 108.7 | 0.74 | 0.68 | 2 |
| FH 64-22+0.7% Elv 4+0.17% PPA | 109.9 | 1.50 | 1.36 | 3 |
| FH 64-22+0.7% ElvM+0.17% PPA | 110.3 | 0.67 | 0.61 | 4 |
| FH 64-22 + 0.5% Anti-Stripping | 111.1 | 0.48 | 0.43 | 5 |
| FH 64-22 Neat | 111.1 | 0.61 | 0.55 | 5 |

Table M1a.3. BBS results at dry condition for asphalt binders.

| BBS test – Dry condition | | | | |
|---|---|---|---|---|
| | **Pull-off Strength (MPa)** | **Std (MPa)** | **CV (%)** | **Rank** |
| FH 64-22 + 2% CBE | 2.206 | 0.02 | 1 | 1 |
| FH 64-22 + 1% PPA | 2.138 | 0.03 | 1.5 | 2 |
| FH 64-22+0.7% Elv4+0.17% PPA | 2.019 | 0.08 | 3.8 | 3 |
| FH 64-22 + 0.5% Anti-Stripping | 2.010 | 0.07 | 3.3 | 4 |
| FH 64-22+0.7% ElvM+0.17% PPA | 1.869 | 0.11 | 5.8 | 5 |
| FH 64-22 Neat | 1.856 | 0.2 | 10.8 | 6 |
| **BBS test – Wet condition (96 hours)** | | | | |
| | **Pull-off Strength (MPa)** | **Std (MPa)** | **CV (%)** | **Rank** |
| FH 64-22 + 1% PPA | 1.924 | 0.09 | 4.8 | 1 |
| FH 64-22 + 0.5% Anti-Strip | 1.651 | 0.01 | 0.6 | 2 |
| FH 64-22 + 2% CBE | 1.240 | 0.02 | 1.9 | 3 |
| FH 64-22+0.7% Elv 4+0.17% PPA | 1.237 | 0.02 | 1.3 | 4 |
| FH 64-22+0.7% ElvM+0.17% PPA | 1.125 | 0.02 | 2 | 5 |
| FH 64-22 Neat | 1.004 | 0.03 | 2.9 | 6 |

It was also observed that contact angle decreases with asphalt binder modification. The increase in wettability is also evident from the increased hydrophilic characteristics of the asphalt binder with the addition of PPA. The different ranking observed for FH 64-22+0.5% Anti-stripping binder using contact angle and pull-off strength results can be explained by the fact that in the BBS test there is an interaction between the asphalt binder and the granite aggregate. A better adhesion can be achieved between an acidic binder and an acidic aggregate such as granite by using amines as anti-strip additives. Amines, which are basic organics, alter the surface of an acidic aggregate to provide better adhesion (Tunnicliff and Root 1984). The cohesive failure type observed for FH 64-22+0.5% Anti-Stripping binders (as shown in figure M1a.1) supports this explanation.

Figure M1a.1. Photograph. Cohesive failure for asphalt binder FH 64-22+0.5% anti-stripping with granite.

Figure M1a.2 shows contact angle results of asphalt binders measured with three probe liquids (i.e., distilled water, formamide, and ethylene glycol). These probe materials are pure and homogeneous liquids that do not react chemically or dissolve with asphalt binders.

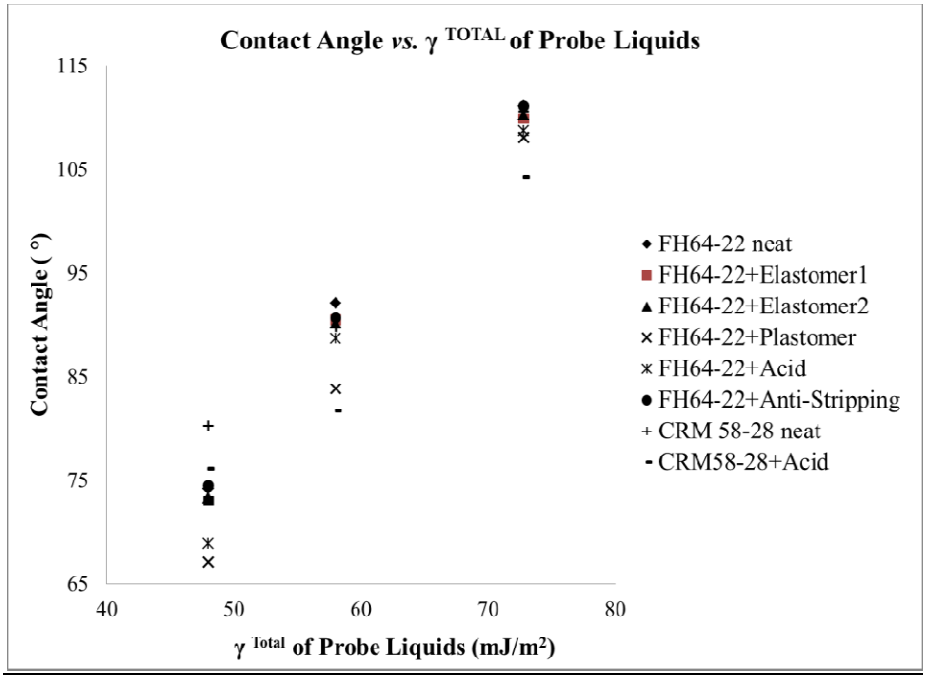


Figure M1a.2. Graph. Contact angles with water, formamide, and ethylene glycol.

The Young-Dupre equation, which relates the contact angle, the surface energy components of the probe liquid, and the surface energy components of the substrate, can be used to estimate the surface energy of the asphalt binders and aggregates. Then, by using the estimated surface free energy of both binder and aggregates, the adhesive bond in dry and wet conditions can be calculated using Gibbs free energy.

Significant Problems, Issues and Potential Impact on Progress

Aggregates for asphalt mixture preparation for Tensile Strength Ratio (TSR) testing were not available for the research team for the past quarter due to winter frozen conditions at quarries. The research team is expecting to obtained materials from a local pit once they are open after the winter season. The research team will double efforts in completing the TSR testing and will not expect delay in the progress of this work element.

Work Planned Next Quarter

Efforts will focus on the estimation of surface energy for both binders and aggregates indirectly with the contact angle measurements. Also, the adhesive bond between asphalt and aggregate in the presence of water will be calculated using Gibbs free energy for all materials and a comparison to the BBS results will be performed. The research team will use TSR testing results available from other work elements to continue the validation effort of the BBS test procedure.

Cited References

Tunnicliff, D. G., and R. E. Root, 1984, "Use of Anti-Stripping Additives in Asphalt Concrete Mixtures," National Cooperative Highway Research Program (NCHRP) Report 274.

## Work Element M1b: Work of Adhesion Based on Surface Energy

### *Subtask M1b-1: Surface Free Energy and Micro-Calorimeter Based Measurements for Work of Adhesion (TAMU)*

Work Done This Quarter

The main goal of this subtask is to provide material property inputs required in other work elements as required. Any data obtained from this subtask will be included in the material properties database. In the last quarter surface free energy of some aggregates and asphalt binders that are being used to develop test methods were measured.

Significant Results

None.

Significant Problems, Issues and Potential Impact on Progress

None.

Work Planned Next Quarter

Work on this subtask will be conducted in conjunction with and as required by other work elements.

***Subtask M1b-2: Work of Adhesion at Nano-Scale using AFM (WRI)***

Work Done This Quarter

No activity this quarter.

***Subtask M1b-3: Identify Mechanisms of Competition Between Water and Organic Molecules for Aggregate Surface (TAMU)***

Work Done This Quarter

This work element was completed and findings were reported in previous quarterly reports. There was no activity this quarter.

Work Planned Next Quarter

None.

**Work Element M1c: Quantifying Moisture Damage Using DMA (TAMU)**

Work Done This Quarter

This work element was completed and findings were reported in previous quarterly reports. There was no activity this quarter.

Work Planned Next Quarter

None.

**CATEGORY M2: COHESION**

**Work Element M2a: Work of Cohesion Based on Surface Energy**

***Subtask M2a-1: Methods to Determine Surface Free Energy of Saturated Asphalt Binders (TAMU)***

Note about Subtask M2a-1: Per the Year 5 work plan, the objectives of this work element will be accomplished in other tasks.

***Subtask M2a-2: Work of Cohesion Measured at Nano-Scale using AFM (WRI)***

Work Done This Quarter

Pursuant to the needs of this subtask and subtask M1b-2 the AFM metrology system that is used for nano-mechanical measurements was modified this past quarter. The modified system provides temperature and environmental control as well as improved sample positioning capabilities.

A miniature Peltier thermal stage was custom designed to mount directly to the 3-axis nano-positioning stage that is at the heart of our nano-mechanics system. The Peltier thermal stage uses a single miniature thermoelectric device with a 6.2-mm square gold-coated heat transfer surface. The miniature thermoelectric device is mounted to a copper heat sink/source. Gravity fed water-flow through a passage in the copper block maintains constant temperature for the heat sink/source without introducing any vibrations or pulsations to the sample. As currently configured the miniature thermal stage provides temperature control for the sample over the range of -10 through 100°C. This range can be expanded by increasing or decreasing the temperature of the water flow through the Peltier device heat sink/source. The miniature thermal stage has a 25-mm (1-inch) square footprint and is only 6.5-mm (~0.25-inch) in height.

The miniature Peltier stage can be used to either heat or cool the sample depending upon the direction of current flow through the device. This feature combined with the overall low thermal mass of the system allows for nearly instantaneous cooling of a heated sample. The extremely rapid cooling afforded by this new thermal stage may allow the morphology associated with elevated temperature to be frozen in place and imaged by AFM. The stage control is set up so that preset high and low temperatures can be toggled back and forth with the flip of a switch.

An acrylic housing was assembled to enclose the new thermal stage, the nano-positioning stage and the sample. The housing provides an enclosed controllable environment surrounding the sample and the AFM probe tip. The environmental housing allows the sample to be maintained under an inert and/or dry atmosphere during thermal cycling and pull-off force measurements. The environmental housing includes the necessary ports to provide access for the AFM scanning head as well as the various cables and tubes that are associated with the nano-positioning and thermal stages. The housing is set up so that it can be continuously purged with a gas stream, dry nitrogen for the current experiments, with only a very small flow needed to maintain a slight positive pressure in the sample chamber. With gas flow set to replace the entire enclosed volume of the chamber approximately once per minute the gas velocity in the chamber is low enough to have no perceptible affect on images or measurements made with the system while being sufficient to eliminate condensation on the sample surface and AFM cantilever.

Finally, the nano-stage, thermal-stage, and environmental chamber were all mounted on a low-profile X - Y translation stage. The manual translation stage allows for lateral positioning of the sample under the scan head without disrupting the inert environment within the sample chamber. Figure M2a-2.1 shows a photograph of the environmental system assembled on the granite base of the lithography AFM.

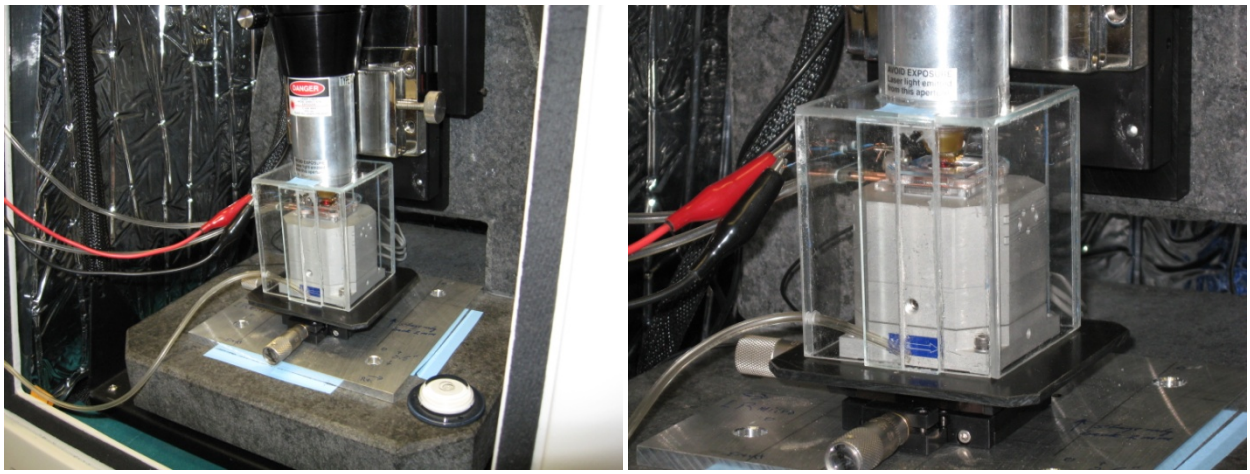

Figure M2a-2.1. Environmental system assembled on the granite base of the lithography AFM.

A calibration chart relating the voltage applied to the Peltier device with the measured temperature at the heat-transfer surface and the temperature of an asphalt film on a glass slide in contact with the surface was prepared. Preliminary experiments using the newly modified system began near the end of this past quarter. A few experiments have been completed at the time of this writing. A series of images that show the effect of mild heating on asphalt internal structuring is presented in the following results section. A method to analyze an AFM-based scratch test to measure rates of entropy production, as it relates to binder damage healing, was significantly refined during this quarter. Experiments designed to test this method are currently underway. Results of this testing will be reported next quarter.

Significant Results

Figure M2a-2.2 a, b, c, d, e shows phase (left image) and topography (right image) images of a thin film of SHRP core asphalt AAK-1 as the film is gently heated under an inert atmosphere. The sample was prepared by placing a small spot of asphalt on the center of a pre-cleaned glass microscope slide, covering the asphalt with a second slide topped with a 100-gram weight, and placing the whole stack in an oven at ~120° C for 30-minutes. After heating, the sample was removed from the oven and allowed to cool. It was then frozen by the drop-wise application of liquid nitrogen to the back of the top slide and popped apart. One of the slides was immediately mounted on the new thermal stage and blanketed under dry nitrogen. An area where the asphalt film appeared (in the optical microscope view) to have split such that a significant thickness of asphalt remained on both the top and bottom slide (i.e. a new plane representing the internal structuring of the film) was selected for imaging.

Figure M2a-2.2a shows this surface at ambient temperature. The phase contrast image (left image) assigns false coloring to the image in response to the phase angle between the incident and response signals from an oscillating tip as it is scanned across the sample surface, and, as such, gives a measure of changing viscoelastic properties at the sample surface. The wavemode® image (right image) assigns coloring based essentially upon the topography of the sample

surface. The phase contrast image clearly shows a two-phase system, and strongly indicates three dimensional structuring within the bulk of the film for this waxy asphalt. Similar three-dimensional structuring has been predicted based upon the results of small angle neutrons scattering (SANS) measurements (Schmets et al. 2010). We believe that these are some of the first AFM images to show internal structuring in an asphalt film. Note that no "bee-structures" are evident in the interior of the film. Instead, we see a relatively uniform distribution of two intermingled phases in a nondescript pattern.

Figure M2a-2.2b shows the same surface imaged at ambient temperature after the sample was heated to ~31° C for five minutes before being cooled. It appears that the relative amount of the darker colored phase increased somewhat with this heating. The topography image has changed very little showing a relatively flat surface with few notable features. The small amount of heating had little apparent effect on the internal structure of the sample with the overall appearance remaining quite similar to that shown in the previous image at ambient temperature.

Figure M2a-2.2c shows the sample surface imaged at ambient temperature after heating to ~41° C for five minutes followed by rapid cooling. This thermal cycle resulted in a dramatic change in the appearance of the sample surface. The maximum height of features in the topography image has nearly doubled with the appearance of distinct arrangements of several high spots. The phase image shows an apparent increase in the amount of the light-colored material phase as well as a complete rearrangement of the apparent structuring to form large islands of the light colored phase that seem to exhibit the beginnings of familiar football-like shapes. The "bee-structures" commonly seen at the surface of films of this asphalt are beginning to evolve in this image. If we accept the premise that "bee structures" are composed of paraffin waxes and wax-oils (Pauli et al. 2011) these images strongly indicate that these materials are distributed throughout the thickness of an asphalt film in a three-dimensional matrix. Heating apparently concentrates these materials in thin sheets at an asphalt air interface resulting in the familiar patterns seen in many AFM images of asphalt.

Figure M2a-2.2d shows further evolution of the "bee-structure" resulting when the sample was heated to ~48° C for five minutes and then cooled. A larger percentage of the sample surface is occupied by the lighter-colored phase, the football shape associated with this phase is becoming more pronounced, and the rippled appearance of the "bee-structures" is plainly evident. The maximum feature height in the topography image is about the same as in the previous image but the rippled "bee-structure" has become more distinct. Figure M2a-2.2e shows the phase boundaries appearing to begin to "melt" and become less distinct when the sample was heated to ~48° C for an additional 5 minutes. The maximum height of topographic features has begun to decrease compared to the previous image and the sharp color contrast between phases has become less distinct.

A corresponding series of experiments was conducted with similarly prepared samples using SHRP core asphalt AAA-1. This asphalt contains a minimal amount of paraffin waxes, and, as such, was expected to present a significantly different appearance when compared to the AAK-1 samples. Figures M2a-2.3a and M2a-2.3b show internal structuring for asphalt AAA-1. The images show the as prepared sample and the sample after several heating cycles respectively. Some structuring is evident in the phase image of the sample before thermal cycling, but the

contrast between phases and the phase boundaries are much less distinct for this low-wax asphalt when compared to the images of asphalt AAK. Unlike the more-waxy AAK sample, the structure seems to become finer and more dispersed after the sample has been heated.

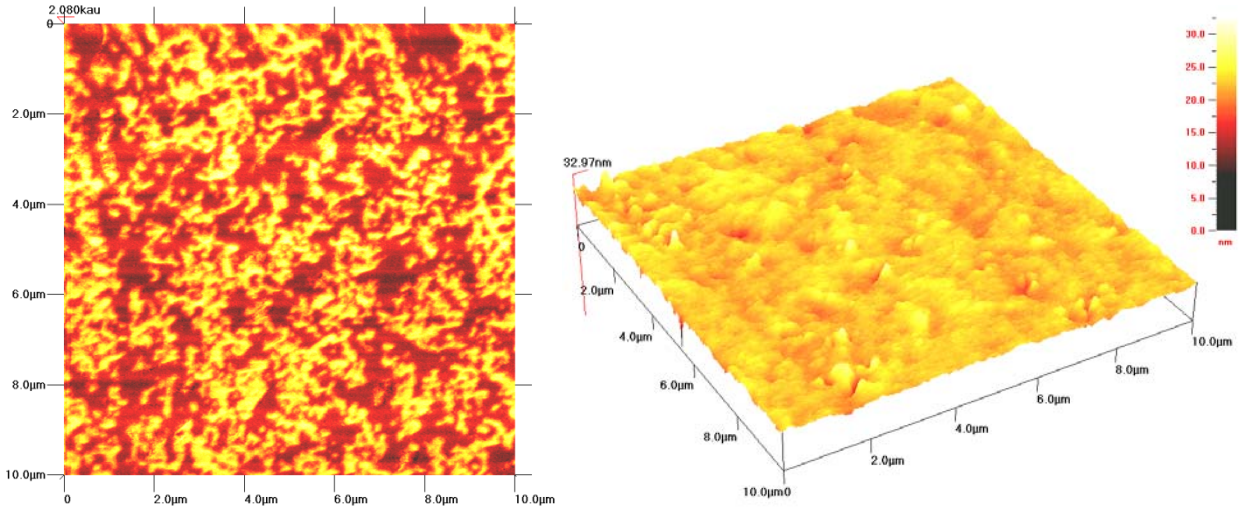


Figure M1b-2.2a. Internal structuring in SHRP core asphalt AAK-1 at ambient temperature.

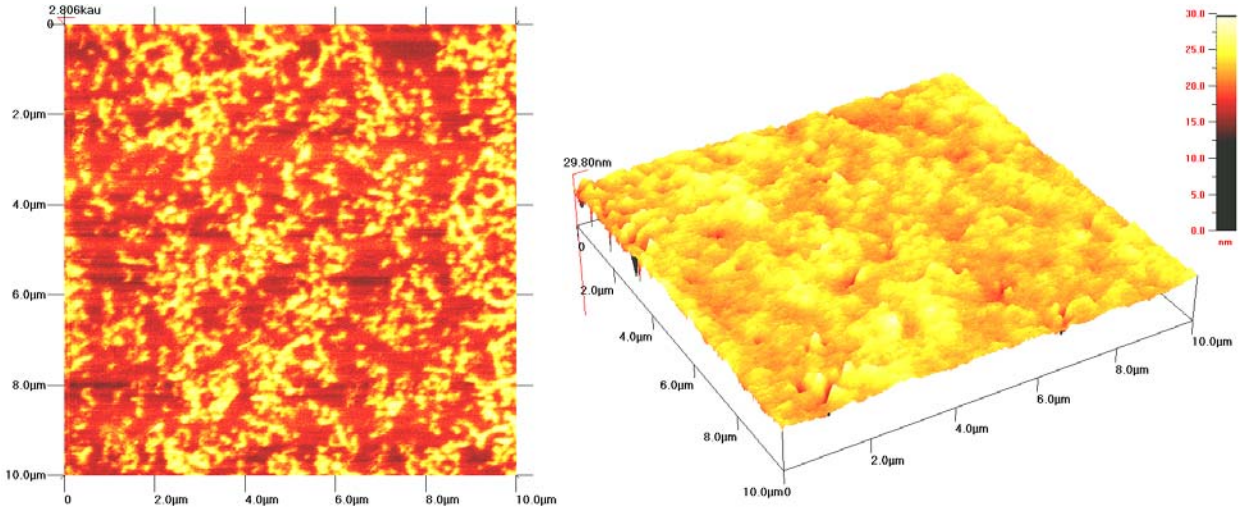


Figure M1b-2.2b. Internal structuring in SHRP core asphalt AAK-1 after heating to 31° C for five minutes. Imaged at ambient temperature.

The results of work conducted this quarter strongly indicate the existence of a three-dimensional microstructure within the bulk of an asphalt film involving waxy asphalt constituents. At an air/asphalt interface these same waxy constituents tend to spread out into thin sheets on the surface. We believe that instabilities within this thin surface film cause the surface to ripple forming the familiar “bee-structures” that are commonly observed in AFM images of the surface of asphalt films.

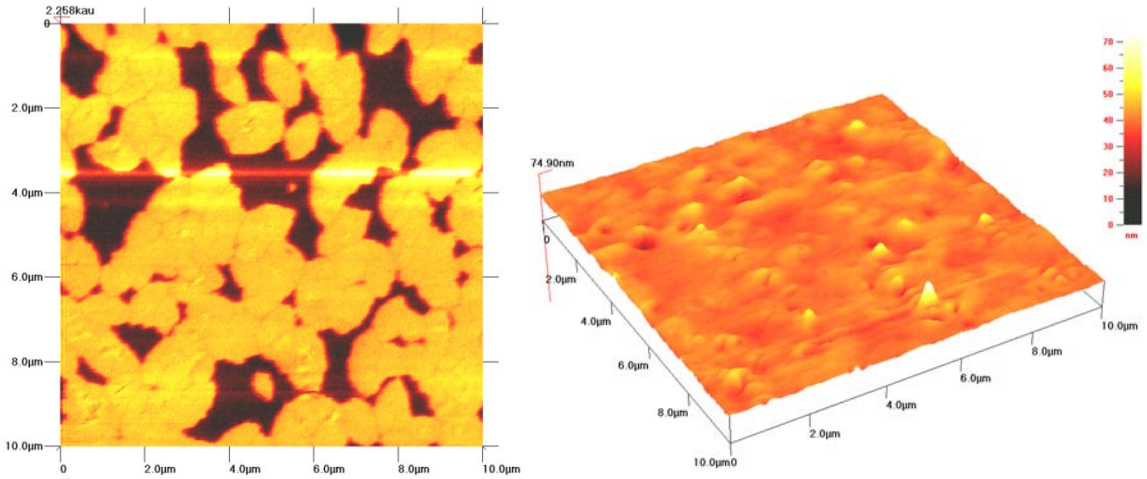


Figure M1b-2.2c. Internal structuring in SHRP core asphalt AAK-1 after heating to 41° C for five minutes. Imaged at ambient temperature.

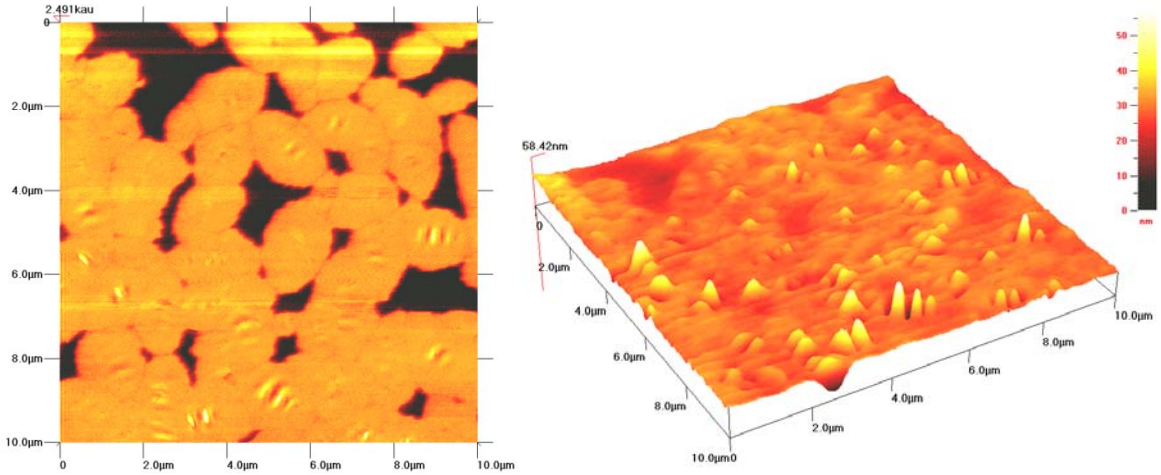


Figure M1b-2.2d. Internal structuring in SHRP core asphalt AAK-1 after heating to 48° C for five minutes. Imaged at ambient temperature.

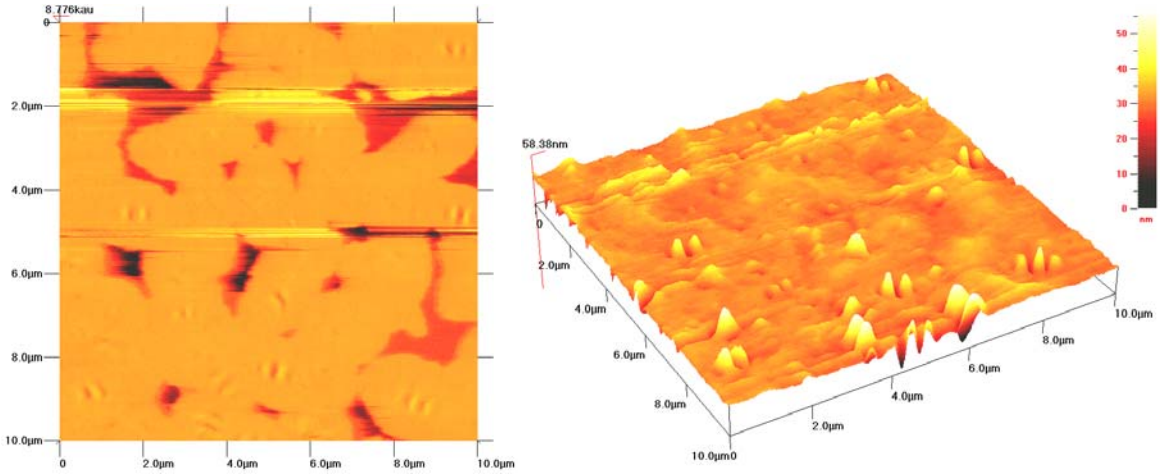


Figure M1b-2.2e. Internal structuring in SHRP core asphalt AAK-1 after heating to 48° C for five additional minutes. Imaged at ambient temperature.

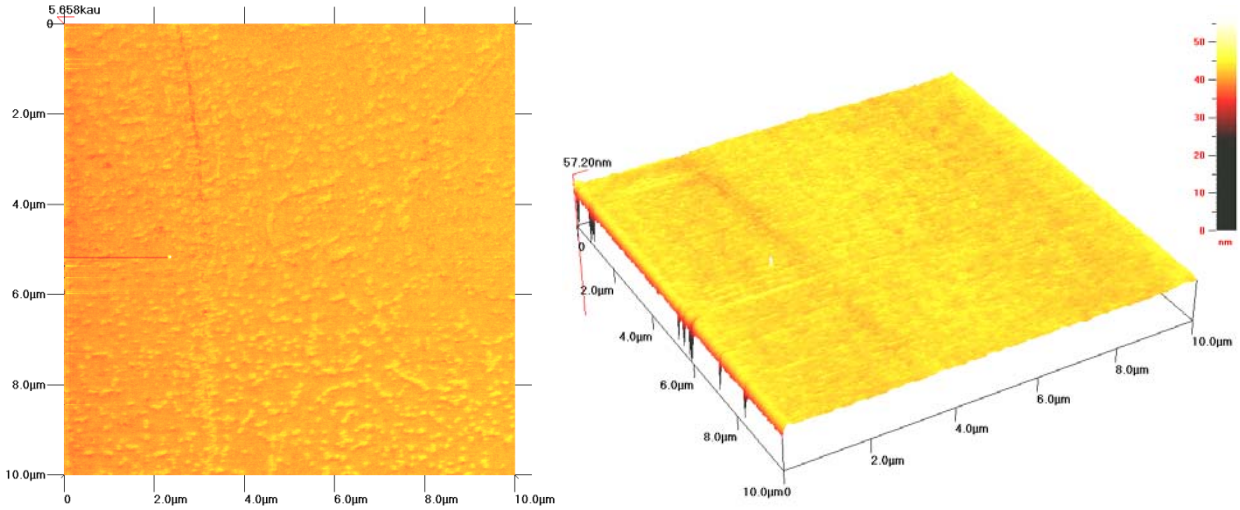


Figure M1b-2.3a. Internal structuring in SHRP core asphalt AAA-1at ambient temperature.

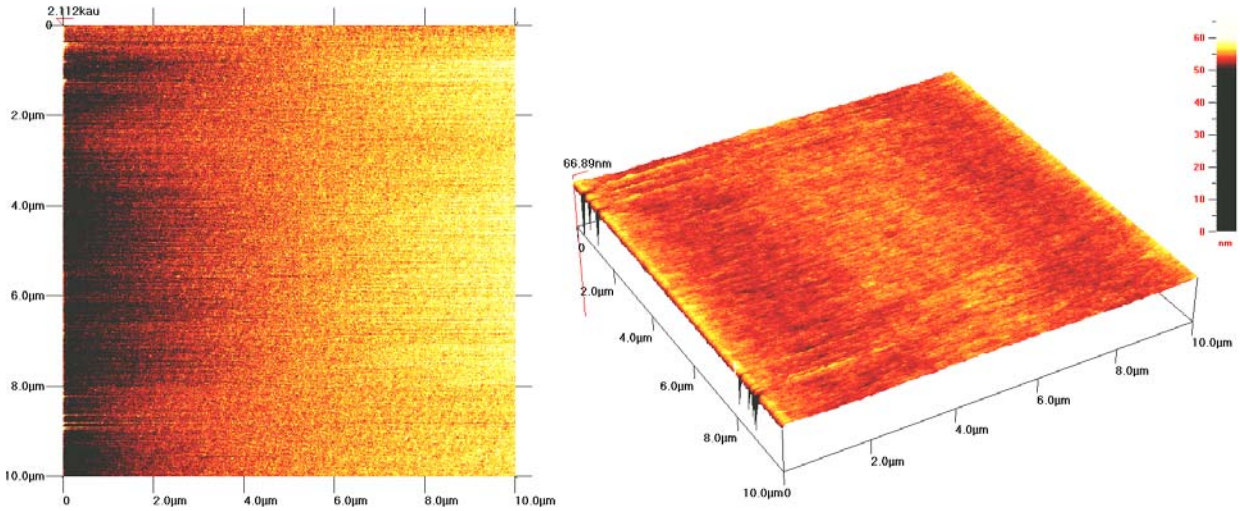


Figure M1b-2.3a. Internal structuring in SHRP core asphalt AAA-1after heating to 48 ° C for five minutes. Imaged at ambient temperature.

Significant Problems, Issues and Potential Impact on Progress

None

Work Planned Next Quarter

Additional work with the newly developed scratch test by AFM nano-lithography is planned for next quarter.

Cited References

Pauli, A. T., R. W. Grimes, A. G. Beemer, T. F. Turner, and J. F. Branthaver, 2011, Morphology of Asphalts, Asphalt Fractions and Model Wax-doped Asphalts Studied by Atomic Force Microscopy. *International Journal of Pavement Engineering* (In Press).

Schmets, A., N. Kringos, T. Pauli, P. Redelius, and T. Scarpas, 2010, On the Existence of Wax-induced Phase Separation in Bitumen. *International Journal of Pavement Engineering*, 11(6), 555–563.

**Work Element M2b: Impact of Moisture Diffusion in Asphalt Mixtures**

***Subtask M2b-1: Measurements of Diffusion in Asphalt Binders and Mixtures (TAMU)***
***Subtask M2b-2: Kinetics of Debonding at the Binder-Aggregate Interface (TAMU)***

Work Done This Quarter

There was no activity this quarter.

Work Planned Next Quarter

We have accomplished significant portions of this work element including measurement of diffusion through binders and fine aggregate matrix. Further work will be conducted if prioritized based on the requirements from other work elements.

**Work Element M2c: Measuring Thin Film Cohesion and Adhesion Using the PATTI Test and the DSR (UWM)**

The remaining activity is reported under Work Element M1a.

**CATEGORY M3: AGGREGATE SURFACE**

**Work Element M3a: Aggregate Surface Characterization (TAMU)**

Work Done This Quarter

This work element was completed and findings were reported in previous quarterly reports. There was no activity this quarter.

## CATEGORY M4: MODELING

### Work Element M4a: Micromechanics Model (TAMU)

Work Done This Quarter

During this quarter we have mainly progressed microstructure modeling of asphalt mixtures with moisture damage through the sequentially coupled moisture diffusion-mechanical analysis. The parametric analyses of the microstructure model incorporated with moisture damage were also conducted by varying primary material characteristics (i.e., diffusion coefficient and degradation model parameters) that affect moisture-dependent fracture behavior of asphalt mixtures.

Simulation results successfully predicted that more moisture diffused into the specimen with increased moisture conditioning time and when a higher value of diffusion coefficient of matrix is involved. As the level of moisture concentration becomes greater, mixtures tend to be more compliant due to the property degradation characteristics.

Subsequent to the moisture transport simulation, three-point bending beam of HMA microstructure was simulated. In the simulation, the material properties found at dry-condition were degraded by incorporating the degradation characteristic function presented in the last quarterly report into the model to predict the damage evolution due to progressive moisture concentration. To conduct the parametric analyses, different values of diffusion coefficients and degradation parameters were attempted to demonstrate the effect of material-specific properties and damage characteristics on the overall mixture performance with moisture damage. Model simulations, as expected, demonstrated that the mixture with a higher value of moisture diffusion coefficient of matrix was more susceptible to moisture damage and consequently, degraded more sensitively than the mixture with lower value of moisture diffusion coefficient of matrix. HMA specimens presented significantly different moisture damage performance with different degradation parameters of matrix phase, although the same value of diffusion coefficient was used. The resulting model simulations and predictions imply that the model can properly account for material-specific performance of moisture damage, damage mechanisms and damage resistance potential of heterogeneous asphalt mixtures.

Significant Problems, Issues and Potential Impact on Progress

None.

Work Planned Next Quarter

In the next quarter we will primarily devote our efforts to develop a final report.

### Work Element M4b: Analytical Fatigue Model for Mixture Design (TAMU)

This work element is addressed under Work Element F2b.

**Work Element M4c: Unified Continuum Model (TAMU)**

Work Done This Quarter

The work done this quarter focused on completing the development of a thermodynamic-based moisture-induced damage model that takes into consideration the effects of moisture diffusion and pore-water pressure that accelerates crack evolution and propagation due to presence of moisture. Both energetic and dissipative processes are clearly distinguished through this thermodynamic framework.

Furthermore, work is accomplished on conducting two-dimensional plane strain micromechanical simulations investigating the effects of combined adhesive and cohesive moisture-induced damage on the overall average response of asphalt mixtures.

Significant Results

None

Significant Problems, Issues and Potential Impact on Progress

None

Work Planned Next Quarter

The next quarter will focus on the experimental calibration and validation of the moisture damage model using the materials from the ARC 2x2 matrix validation plan. Moreover, three-dimensional micromechanical moisture-damage simulations will be started. These simulations can be used to conduct virtual moisture-damage simulation experiments.

**CATEGORY M5: MOISTURE DAMAGE PREDICTION SYSTEM (All, TAMU lead)**

Work on individual components such as test methods and micromechanics models required in the system is complete. The components will be put together in the form of a methodology towards the end of this project.

## TABLE OF DECISION POINTS AND DELIVERABLES FOR MOISTURE DAMAGE

| Name of Deliverable | Type of Deliverable | Description of Deliverable | Original Delivery Date | Revised Delivery Date | Reason for changes in delivery date |
|---|---|---|---|---|---|
| M1a-5: Propose a novel testing protocol (UWM) | Draft Report | Development and Implementation of the Bitumen Bond Strength test for Moisture Damage Characterization | 1/10 | 3/11 | Additional analysis/verification on the BBS test is included: operator sensitivity data, validation with TSR mixture testing and comparison with contact angle measurements |
| | Final Report | Report in 508 format on the use of the Bitumen Bond Strength test for Moisture Damage Characterization | 1/11 | 9/11 | Additional analysis/verification data is included and therefore additional time is required |
| M1b-2: Work of Adhesion at Nano-Scale using AFM | Test Method | A method to determine surface roughness of aggregate and fines based on AFM | 12/30/11 | | N/A |
| M1b-3: Identify mechanisms of competition between water and organic molecules for aggregate surface | Draft Report | Final report documenting the testing protocol and findings of experiments on asphalt-aggregate interactions | 10/31/10 | 10/31/11 | Program activity delayed in order to redirect critical manpower to PANDA development |
| | Final Report | | 4/30/12 | | |
| M1c: Quantifying Moisture Damage Using DMA | AASHTO procedure | AASHTO procedure for preparing Fine Aggregate Matrix (FAM) specimens for the DMA testing | 9/30/10 | Complete | N/A |
| | Draft Report | Use of the method to characterize various mixtures with comparison to field performance | 12/31/10 | | |
| | Final Report | | 3/31/11 | 6/30/11 | Report to be made 508 compliant |
| M2b-1: Measurement of diffusion of water through thin films of asphalt binders and FAM | Draft Report | Mechanism and model for the diffusion of moisture through films of asphalt binder, methods to measure diffusivity in binders and mortars, and the influence of wet-dry cycles on the cumulative moisture induced damage. | 6/30/10 | Complete | |
| | Final Report | | 9/30/11 | 12/31/11 | The dissertation was completed at TAMU and needs editing for 508 format |
| M2b-2: Work of Cohesion at Nano-Scale using AFM | Test Method | A method to determine ductile-brittle properties via AFM measurements | 12/30/11 | | N/A |

| Name of Deliverable | Type of Deliverable | Description of Deliverable | Original Delivery Date | Revised Delivery Date | Reason for changes in delivery date |
|---|---|---|---|---|---|
| M3a: Aggregate Surface Characteristics | Research report | Report on methods and experimental findings and utility of methodology and findings | 6/30/10 | Complete | |
| | Research report | Describes implementation of findings into PANDA and expands experiments to characterization for four aggregates used for validation experiments | 6/30/11 | | |
| M4a: Micro-mechanics Model (TAMU) | Draft Report | Numerical micromechanical model of moisture-induced damage in asphalt mixtures. This report will include the algorithm and modeling method. | Sep-11 | | |
| | Final Report | | Sep-11 | Mar-12 | |
| M4a: Micromechanics Model Development (Moisture Damage) (UNL) | Models and Algorithm | Cohesive zone modeling with moisture damage of asphalt mixtures considering mixture microstructure: modeling methodology, constitutive theory, testing protocols, test data, model simulation/calibration/validation, and user-friendly manuals. | 3/31/11 | No change | N/A |
| | Draft report | | 06/30/11 | | |
| | Final report | | 12/31/11 | | |
| M4a: Lattice Micromechanics Model (NCSU) | Draft Report | Documenting development of lattice micromechanical model | 2/14/12 | | N/A |
| | Final Report | Documenting development of lattice micromechanical model | 8/14/12 | | |
| M4a: Model to Bridge Continuum Damage and Fracture (NCSU) | Draft Report | Documenting development of continuum damage-to-fracture model | N/A | 2/14/12 | N/A |
| | Final Report | Documenting development of continuum damage-to-fracture model | 2/14/12 | 8/14/12 | |
| M4c: Unified Continuum Model (TAMU) | Models and Algorithm | | 6/30/11 | 12/31/11 | Model needs to be updated based on calibration with experimental measurements |
| | Draft Report | Draft Report on the moisture-damage modeling | 9/30/11 | | |
| | Final Report (M5, M4c, F1b-1, F1c, F1d-8, F3c, and V3c) | Report in 508 format that describes a comprehensive and integrated approach to assessing moisture damage on three scales; binder and aggregate components, fine aggregate matrix with DMA and in the full mix – Alternative to more sophisticated PANDA approach | 03/31/12 | 6/30/12 | N/A |

| Name of Deliverable | Type of Deliverable | Description of Deliverable | Original Delivery Date | Revised Delivery Date | Reason for changes in delivery date |
|---|---|---|---|---|---|
| M5: Moisture Damage Prediction System | Protocol | Protocol for implementation of component selection | 6/30/11 | | |
| | Experimental method | Experimental method for measuring moisture damage resistance of full mixture | 9/30/11 | | |
| | Draft Report (M5, M4c, F1b-1, F1c, F1d-8, F3c, and V3c) | Report in 508 format that describes a comprehensive and integrated approach to assessing moisture damage on three scales; binder and aggregate components, fine aggregate matrix with DMA and in the full mix – Alternative to more sophisticated PANDA approach | 12/31/11 | | |
| | Final Report (M5, M4c, F1b-1, F1c, F1d-8, F3c, and V3c) | | 3/31/12 | 6/30/12 | Preparation of a comprehensive report. |

| | Moisture Damage Year 4 | Year 4 (4/10-3/11) | | | | | | | | | | | | Team |
|---|---|---|---|---|---|---|---|---|---|---|---|---|---|---|
| | | 4 | 5 | 6 | 7 | 8 | 9 | 10 | 11 | 12 | 1 | 2 | 3 | |
| **Adhesion** | | | | | | | | | | | | | | |
| **M1a** | **Affinity of Asphalt to Aggregate - Mechanical Tests** | | | | | | | | | | | | | |
| M1a-1 | Select Materials | | | | | | | | | | | | | **UWM** |
| M1a-2 | Conduct modified DSR tests | | | | | | | | | | | | | |
| M1a-3 | Evaluate the moisture damage of asphalt mixtures | P | | | | JP | | | | | P | | | |
| M1a-4 | Correlate moisture damage between DSR and mix tests | | | | | | | | | | | | | |
| M1a-5 | Propose a Novel Testing Protocol | | | | | | | | | | JP | | | |
| M1a-6 | Standard Testing Procedure and Recommendation for Specifications | | | | | | P | | | | | | | |
| **M1b** | **Work of Adhesion** | | | | | | | | | | | | | |
| M1b-1 | Adhesion using Micro calorimeter and SFE | | | | | | | | | | | | | **TAMU** |
| M1b-2 | Evaluating adhesion at nano scale using AFM | | | | | | | | | | | | | **WRI** |
| M1b-3 | Mechanisms of water-organic molecule competition | | | | | | | | | | | | | **TAMU** |
| **M1c** | **Quantifying Moisture Damage Using DMA** | | | | JP | | | | D | | | | F | **TAMU** |
| **Cohesion** | | | | | | | | | | | | | | |
| **M2a** | **Work of Cohesion Based on Surface Energy** | | | | | | | | | | | | | |
| M2a-1 | Methods to determine SFE of saturated binders | | | | | | | | | | | | | **TAMU** |
| M2a-2 | Evaluating cohesion at nano scale using AFM | | | | | | | | | | | | | **WRI** |
| **M2b** | **Impact of Moisture Diffusion in Asphalt** | | | | | | | | | | | | | |
| M2b-1 | Diffusion of moisture through asphalt/mastic films | | | D | | | F | | | | | | | **TAMU** |
| M2b-2 | Kinetics of debonding at binder-aggregate interface | | | | | | | | | | | | | |
| **M2c** | **Thin Film Rheology and Cohesion** | | | | | | | | | | | | | |
| M2c-1 | Evaluate load and deflection measurements using the modified PATTI test | | | | | | | | | | | | | **UWM** |
| M2c-2 | Evaluate effectiveness of the modified PATTI test for Detecting Modification | | | | | | | | | | | | | |
| M2c-3 | Conduct Testing | | | | | | | | | | | | | |
| M2c-4 | Analysis & Interpretation | | | | | | | | | | | | | |
| M2c-5 | Standard Testing Procedure and Recommendation for Specifications | see Subtask M1a-6 | | | | | | | | | | | | |
| **Aggregate Surface** | | | | | | | | | | | | | | |
| **M3a** | **Impact of Surface Structure of Aggregate** | | | | | | | | | | | | | |
| M3a-1 | Aggregate surface characterization | | | JP | | | | | | | | | | **TAMU** |
| **Modeling** | | | | | | | | | | | | | | |
| **M4a** | **Micromechanics model development** | | | | | | JP | | | | | | | **TAMU** |
| **M4b** | **Analytical fatigue model for use during mixture design** | | | | | | | | | | | | | **TAMU** |
| **M4c** | **Unified continuum model** | | | | | | JP | | | DP | | M&A | | **TAMU** |
| **M5** | **Moisture Damage Prediction System** | | | | | | | | | | | | | **ALL** |

**LEGEND**

| **Deliverable codes** | **Deliverable Description** |
|---|---|
| D: Draft Report | Report delivered to FHWA for 3 week review period. |
| F: Final Report | Final report delivered in compliance with FHWA publication standards |
| M&A: Model and algorithm | Mathematical model and sample code |
| SW: Software | Executable software, code and user manual |
| JP: Journal paper | Paper submitted to conference or journal |
| P: Presentation | Presentation for symposium, conference or other |
| DP: Decision Point | Time to make a decision on two parallel paths as to which is most promising to follow through |
| [x] | Indicates completion of deliverable x |

Work planned

Work completed

Parallel topic

| Moisture Damage Year 2 - 5 | | Year 2 (4/08-3/09) | | | | Year 3 (4/09-3/10) | | | | Year 4 (04/10-03/11) | | | | Year 5 (04/11-03/12) | | | | Team |
|---|---|---|---|---|---|---|---|---|---|---|---|---|---|---|---|---|---|---|
| | | Q1 | Q2 | Q3 | Q4 | Q1 | Q2 | Q3 | Q4 | Q1 | Q2 | Q3 | Q4 | Q1 | Q2 | Q3 | Q4 | |
| **Adhesion** | | | | | | | | | | | | | | | | | | |
| **M1a** | **Affinity of Asphalt to Aggregate - Mechanical Tests** | | | | | | | | | | | | | | | | | |
| M1a-1 | Select Materials | | DP | | | | | | | | | | | | | | | UWM |
| M1a-2 | Conduct modified DSR tests | | P | | P | | | | | | | | | | | | | |
| M1a-3 | Evaluate the moisture damage of asphalt mixtures | | | | DP | | P | | | P | JP | | P | | | | | |
| M1a-4 | Correlate moisture damage between DSR and mix tests | | | | | | P | | P | | | | | | | | | |
| M1a-5 | Propose a Novel Testing Protocol | | | | P | | | | P | | | | JP | D | | F | | |
| M1a-6 | Standard Testing Procedure and Recommendation for Specifications | | | | | | | | | | P | | | | | | | |
| **M1b** | **Work of Adhesion** | | | | | | | | | | | | | | | | | |
| M1b-1 | Adhesion using Micro calorimeter and SFE | | | | | | JP | | | | | | | | | | | TAMU |
| M1b-2 | Evaluating adhesion at nano scale using AFM | | | | | | | JP | | | | | | | | | JP, F | WRI |
| M1b-3 | Mechanisms of water-organic molecule competition | | | | JP | | | | | | | | | | | | | TAMU |
| **M1c** | **Quantifying Moisture Damage Using DMA** | | | | | | | | | | JP | D | F | | | | | TAMU |
| **Cohesion** | | | | | | | | | | | | | | | | | | |
| **M2a** | **Work of Cohesion Based on Surface Energy** | | | | | | | | | | | | | | | | | |
| M2a-1 | Methods to determine SFE of saturated binders | | | | | | | | | | | | | | JP | | | TAMU |
| M2a-2 | Evaluating cohesion at nano scale using AFM | | | | | | | JP | | | | | | | | | JP, F | WRI |
| **M2b** | **Impact of Moisture Diffusion in Asphalt** | | | | | | | | | | | | | | | | | |
| M2b-1 | Diffusion of moisture through asphalt/mastic films | | | | | | JP | D | F | D | F | | | | | | | TAMU |
| M2b-2 | Kinetics of debonding at binder-aggregate interface | | | | | | | | | | | | | | | | | |
| **M2c** | **Thin Film Rheology and Cohesion** | | | | | | | | | | | | | | | | | |
| M2c-1 | Evaluate load and deflection measurements using the modified PATTI test | DP | JP | D | F | | | | | | | | | | | | | UWM |
| M2c-2 | Evaluate effectiveness of the modified PATTI test for Detecting Modification | | | D | DP,F | | | | | | | | | | | | | |
| M2c-3 | Conduct Testing | | | | | | JP | | | | | | | | | | | |
| M2c-4 | Analysis & Interpretation | | | | P | | | | D | | | | | | | | | |
| M2c-5 | Standard Testing Procedure and Recommendation for Specifications | | | | | D | | | | see Subtask M1a-6 | | | | | | | | |
| **Aggregate Surface** | | | | | | | | | | | | | | | | | | |
| **M3a** | **Impact of Surface Structure of Aggregate** | | | | | | | | | | | | | | | | | |
| M3a-1 | Aggregate surface characterization | | | | | | | | | JP | | P | | | | | | TAMU |
| **Models** | | | | | | | | | | | | | | | | | | |
| **M4a** | **Micromechanics model development** | | | | JP | | | | JP | | JP | | | D | DP | F, SW | | TAMU |
| **M4b** | **Analytical fatigue model for use during mixture design** | | | | | | | | | | | | | | | M&A,D | F | TAMU |
| **M4c** | **Unified continuum model** | | | | | | | | JP | | JP | DP | M&A | D | DP | F, SW | | TAMU |
| **M5** | **Moisture Damage Prediction System** | | | | | | | | | | | | | | | | | ALL |

**LEGEND**

| **Deliverable codes** | **Deliverable Description** |
|---|---|
| D: Draft Report | Report delivered to FHWA for 3 week review period. |
| F: Final Report | Final report delivered in compliance with FHWA publication standards |
| M&A: Model and algorithm | Mathematical model and sample code |
| SW: Software | Executable software, code and user manual |
| JP: Journal paper | Paper submitted to conference or journal |
| P: Presentation | Presentation for symposium, conference or other |
| DP: Decision Point | Time to make a decision on two parallel paths as to which is most promising to follow througjh |
| [x] | Indicates completion of deliverable x |

Work planned

Work completed

Parallel topic

# PROGRAM AREA: FATIGUE

## CATEGORY F1: MATERIAL AND MIXTURE PROPERTIES

### Work Element F1a: Cohesive and Adhesive Properties (TAMU)

Work Done This Quarter

The final report documenting the results of this task has been completed.

Significant Results

The results demonstrated that a multiplicative relationship exists between the ideal and practical work of fracture. The relationship between these two quantities depends on binder compliance, loading rate, and temperature. This work has validated that the ideal work of fracture, which is calculated from surface energy, is a fundamental property than can be used to rank asphalt-aggregate systems based on their resistance to fracture under dry and wet conditions.

Significant Problems, Issues and Potential Impact on Progress

None

Work Planned Next Quarter

This subtask is completed.

### Work Element F1b: Viscoelastic Properties (Year 1 start)

#### *Subtask F1b-1: Viscoelastic Properties under Cyclic Loading (TAMU)*

Work Done This Quarter

In this quarter we have completed our investigation on the source of nonlinear response in asphalt binders. This study included all potential sources of nonlinear response in asphalt binders. For example, the effect of loading history on the asphalt binders response was investigated by conducting multi-step loading and considering the cross interaction between the load steps. The hysteretic heating under cyclic loading was also investigated by monitoring the temperature of DSR specimens. Furthermore, we investigated the source of the normal force under simple torsion by modeling the test specimen using commercially available finite element software, ABAQUS. The results and analysis were documented in a journal paper titled "Interaction Nonlinearity in Asphalt Binders", which has been accepted for publication in the *Journal of Mechanics of Time-Dependent Materials.* In continuation of this study, we are validating our proposed model under different types of loading including oscillatory and

monotonic. The oscillatory loading tests were conducted at different stress levels and frequencies.

In parallel to this research, we studied different approaches to measure the bulk modulus of asphalt binders, as a time-dependent material property. The poker chip test geometry was selected to carry on the experiment. The test geometry was fabricated and a few preliminary tests were conducted, using Instron ElectroPuls E1000 test instrument.

Significant Results

We developed and employed an experiment design that systematically evaluates the source of nonlinear response in asphalt binders. We have use multi-step loading and measurement of hysteretic heating to demonstrate that the loading history and temperature during cyclic loading, respectively, do not contribute to the nonlinear response. We have also used finite element simulation to demonstrate that the asphalt binder tends to dilate when subjected to shear loading. Comparing the FE simulations and the laboratory measurements, we were able to quantify the magnitude of normal force attributed to the increase in free volume. We have also used Schapery's nonlinear viscoelastic model to quantify the influence of interaction non linearity.

We expect that this understanding of nonlinear response combined with the nonlinear viscoelastic model will significantly improve the accuracy of computational micromechanics model.

Significant Problems, Issues and Potential Impact on Progress

None.

Work Planned Next Quarter

In the next quarter we plan to complete the tests and validation related to the modeling of interaction nonlinearity. We will also conduct the poker-chip tests on asphalt binders to measure the time dependency of bulk modulus. In parallel to laboratory experimentation, we will analyze the data to come up with an appropriate aspect ratio that eliminates the effect of singular point at the edge of the specimen.

***Subtask F1b-2: Separation of Nonlinear Viscoelastic Deformation from Fracture Energy under Repeated and Monotonic Loading (TAMU)***

Work Done This Quarter

The reader is referred to Work Elements F2c and E1a.

Work Planned Next Quarter

The reader is referred to Work Elements F2c and E1a.

**Work Element F1c: Aging**

***Subtask F1c-1: Critical Review of Binder Oxidative Aging and Its Impact on Mixtures (TAMU)***

Work Done This Quarter

No work this quarter.

Significant Results

N/A

Significant Problems, Issues and Potential Impact on Progress

There are no problems or issues.

Work Planned Next Quarter

Review of the literature and work on other research projects is ongoing.

***Subtask F1c-2: Develop Experimental Design (TAMU)***

Work Done This Quarter

No work this quarter.

Significant Results

None.

Significant Problems, Issues and Potential Impact on Progress

The planned experiments using ARC core binders is underway, as well as measurements on mixtures fabricated using other binders.

Work Planned Next Quarter

Measurements of mixture rheology and fatigue continue. Also, rheological measurements of binders extracted and recovered from these mixtures will be made as part of the effort to link binder oxidation to changes in mixture properties.

***Subtask F1c-3: Develop a Transport Model of Binder Oxidation in Pavements (TAMU)***

Work Done This Quarter

*Measurements of Recovered Binder Properties*

Measurements of the WRI test section sites awaits delivery of the field cores.

*Measurements on Oxidation Mechanisms*

Work Done This Quarter

Experiment Phase I on oxidation mechanism study using antioxidants was conducted according to the experiment design in ARC work plan year 5.

Both antioxidants showed little effect on asphalt oxidation rate, the pattern of oxidation (fast-rate plus constant-rate), hardening rate, the pattern of hardening, and the hardening susceptibility. The possible inhibited free radical oxidation mechanism will be investigated to explain the fast-rate plus constant-rate oxidation pattern.

**Analysis of Antioxidant Screening Results**

The results of antioxidant screening test are discussed. The experiment design is detailed in the work plan year 5 submitted to ARC. The base binder is NuStar PG67-22. The following abbreviations are used to represent each antioxidant treatment:

AX1 (1.5% Irganox 1010)
AX3 (3.0% Irganox 1010)
AC1 (1.5% Carbon Black)
AC3 (3.0% Carbon Black)
AS (1.5% Irganox 1010 + 1.5% Carbon Black)

*Effect of antioxidants on oxidation kinetics*

Irganox 1010 is phenolic-type free radical scavenger, and carbon black (Raven 790 from Columbia Chemical Company) is a multifunctional antioxidant that acts as both a free radical scavenger and peroxide decomposer. Both antioxidants were expected to be effective on binder hardening according to literature. However, based on FTIR measurement of carbonyl area data, both antioxidants, applied at different percentages and combined, has little effect of inhibiting or retarding binder oxidation. The kinetics of binder oxidation is the same with or without antioxidant treatment.

Figure F1c-3.1 shows the trend of carbonyl area growth is the same for base binder and treated binders. All treated binders followed the same fast-rate plus constant-rate oxidation pattern as the base binder. This indicates that two possibilities: both fast-rate and constant-rate reactions do not

follow free radical chain reaction pathway, or this reaction pattern is due to inhibited free radical reaction. The second possibility will be proposed later in detail.

The binders treated with Irganox 1010 have greater CA because of the ester group in the chemical structure of Irganox 1010. To make the comparison even clearer, the change or increase of carbonyl area was plotted for each binder, as shown in figure F1c-3.2. Clearly, the rate of oxidation has not been inhibited or retarded by adding antioxidants.

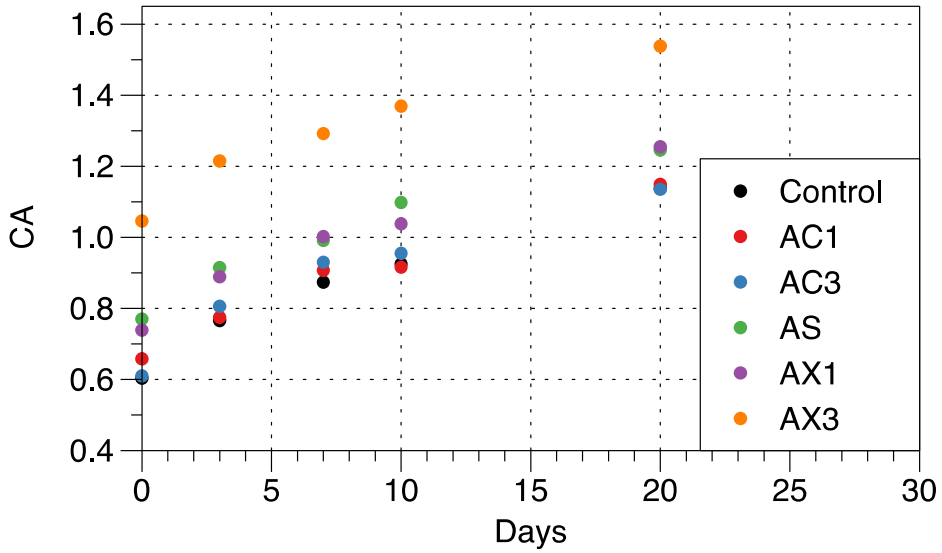


Figure Fc-3.1. The trend of carbonyl area growth is the same for base binder and treated binders.

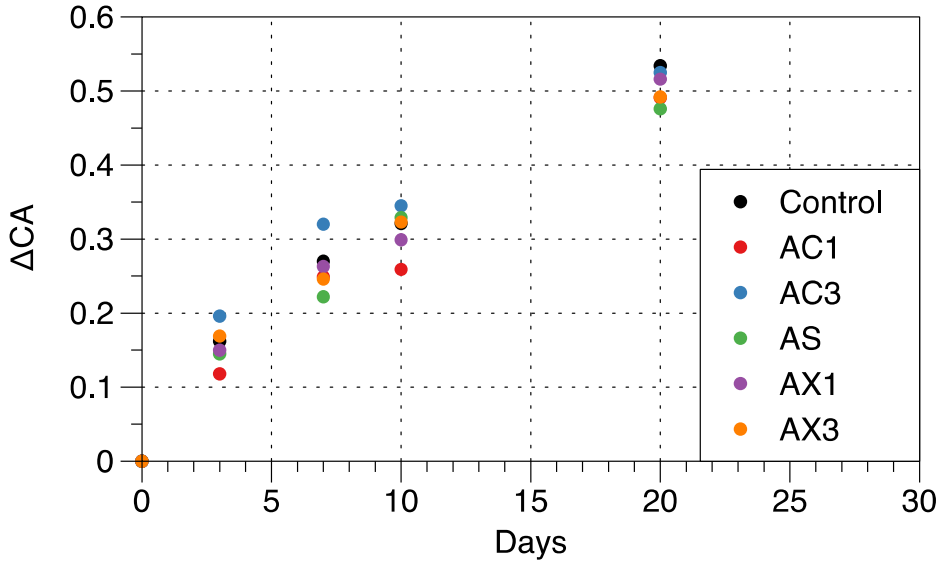


Figure F1c-3.2. The change in carbonyl area with aging time has no significant difference for the base binder and the treated binders.

*Effect of antioxidants on binder hardening and hardening susceptibility*

Although the Irganox 1010 and carbon black were not effective in terms of carbonyl area, it was expected to have some effect on binder hardening based on aging index. Therefore, the 60C low shear rate limiting viscosity was measured to investigate the effect of antioxidants on binder hardening and hardening susceptibility.

Figure F1c-3.3 showed the viscosity with aging time for all binders. While AX3 made binder softer, all other treatments had little effect on viscosity. In terms of hardening rate, all antioxidant treatments are not effective.

Figure F1c-3.4 of viscosity versus carbonyl area gave an idea of the hardening susceptibility. No significant difference in hardening susceptibility was found. However, the softening effect of Irganox 1010 was clear and higher percent of Irganox 1010 makes the binder softer.

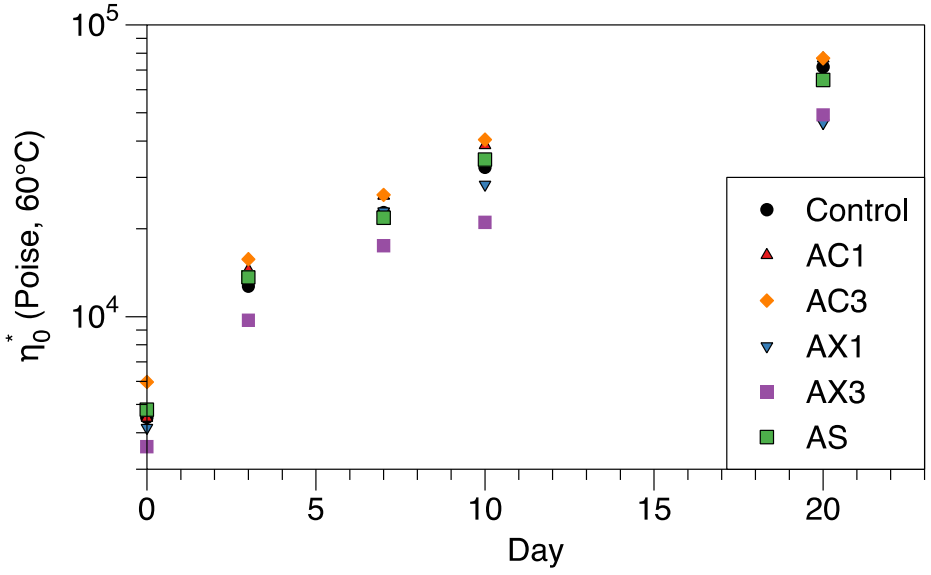


Figure F1c-3.3. Viscosities of base and treated binders at different aging days follow the same trend.

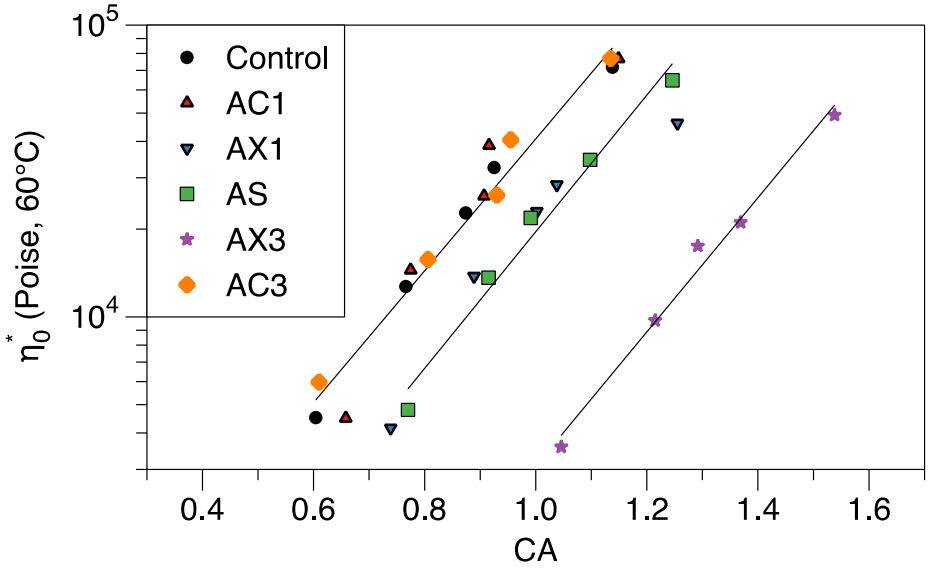


Figure F1c-3.4. The hardening susceptibilities of base and treated binders are the same.

Significant Results

N/A

Significant Problems, Issues and Potential Impact on Progress

There are no problems or issues.

Work Planned Next Quarter

The possible inhibited free radical oxidation mechanism will be investigated to explain the fast-rate plus constant-rate oxidation pattern, as well as the ineffectiveness of antioxidants.

Three ARC binders (NuStar PG67-22, PG76-22 and Valero PG64-16) will be aged in POV according to the experimental design in the previous work plan. Kinetics data will be obtained.

***Subtask F1c-4: The Effects of Binder Aging on Mixture Viscoelastic, Fracture, and Permanent Deformation Properties (TAMU)***

Work Done This Quarter

The reader is referred to Work Elements F1b-2, F2c, and E1a.

Work Planned Next Quarter

The reader is referred to Work Elements F1b-2, F2c, and E1a.

***Subtask F1c-5: Polymer Modified Asphalt Materials (TAMU)***

Work Done This Quarter

The ratios of the limiting viscosity (or DSR function) for the polymer modified binder to the limiting viscosity (or DSR function) for the base binder, are being used to analyze oxidation susceptibility and oxidation kinetics for different polymer modifiers in terms of polymer functional type.

No additional analyses are available this quarter.

Work Planned Next Quarter

This experiment will be continuing throughout the next quarter.

Decreases in this rheological ratio with oxidation at different temperatures will be analyzed for polymer oxidation susceptibility and polymer oxidation kinetics.

**Work Element F1d: Healing (TAMU)**

***Subtask F1d-1: Critical review of the literature***
***Subtask F1d-2: Material selection***
***Subtask F1d-3: Experiment design***
***Subtask F1d-4: Test methods to measure properties related to healing***
***Subtask F1d-5a: Testing of materials and validating healing model***
***Subtask F1d-5b: Thermodynamic model for healing in asphalt binders***

Work Done This Quarter

We have hypothesized overall healing to be due to microscopic wetting and intrinsic strength gain. In the previous quarters we reported a test matrix designed to measure overall healing in different FAM mixes as a function of rest period and level of damage. In the past quarter we have measured overall healing in three different FAM mixes. We reformulated the test matrix by adding a specific validation test procedure to ensure the measured healing function to be artifact free and conducted additional tests according to this new matrix.

We have also completed the development of a procedure that utilizes the AFM to semi-quantitatively measure the micro-rheology of the microstructural domains of different asphalt binders before and after aging. In the previous quarters we had reported these measurements without an absolute force scale. During this quarter we worked on the calibration of the AFM measurements; this allowed us to present these measurements on a more accurate force scale. In addition, because of the high stresses and deformation at the contact between the AFM tip and the binder specimen, the creep response at the tip is not the true creep response of the material. This bias can be corrected using a computational model for the response of the asphalt binder under an AFM tip. In this quarter we started the work on this computational model to back

calculate the true creep curves and micro-rheology of the different domains as identified using the AFM. The true micro-rheology of these domains will ultimately be related to the fatigue cracking and healing potential of the asphalt binders.

Significant Results

We have successfully quantified the overall healing in FAM specimens as a function of rest period as well as level of damage and demonstrated the resultant healing surface to be artifact free by comparing the results from validation tests with results generated by following the original test matrix. Figure F1d.1 illustrates a typical plot from these measurements. In other words, figure F1d.1 allows the user to estimate the expected percentage of healing for a given rest period and damage level immediately preceding the rest period. Completing this experiment design will allow us to measure and validate the healing response of materials as function of its viscoelastic properties and damage level.

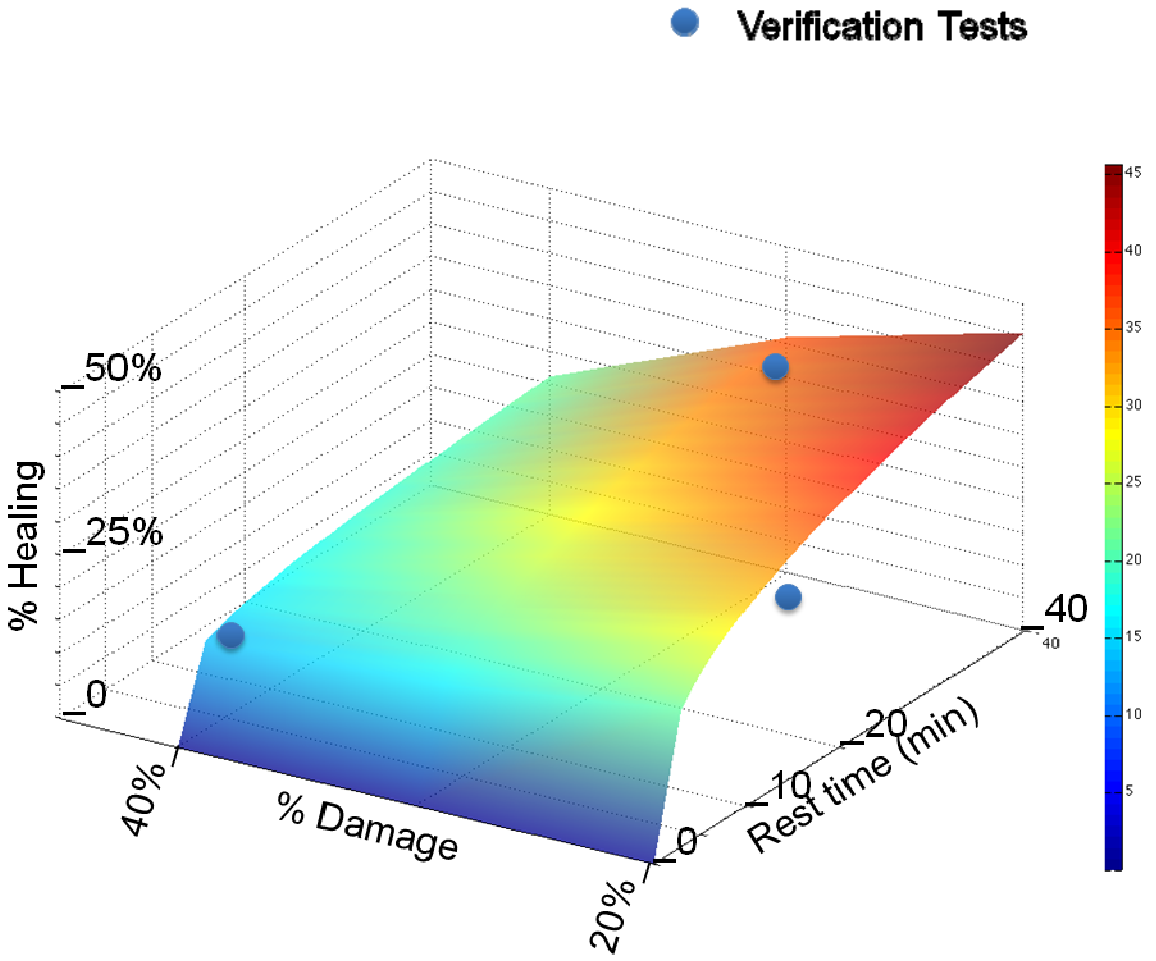


Figure F1d.1. Overall healing in FAM specimens as a function of level of damage as well as rest period.

Significant Problems, Issues and Potential Impact on Progress

None.

Work Planned Next Quarter

We will continue to measure intrinsic healing as well prepare FAM specimens to measure overall healing. Additionally we plan to design and incorporate more validation test protocols in the test matrix to demonstrate the robustness of this procedure.

In addition this, we will continue the measurement and calibration of the micro-rheology of the asphalt binder using a combination of AFM measurements and computational analysis of the tip-surface interaction. We also plan to carry out these measurements on asphalt binders that have been obtained by fractionating and recombining two core binders.

### *Subtask F1d-6: Evaluate Relationship Between Healing and Endurance Limit of Asphalt Binders (UWM)*

Work Done This Quarter

In the past quarter, the research team has continued to evaluate the use of a time sweep with a single long rest period using LTPP binders at different age levels. The procedure is comprised of two steps: (1) a strain-controlled time sweep is run without rest period, and the number of cycles to the specified failure criteria based on a reduction in |G*| is calculated, (2) a time sweep is run at the same amplitude with a rest period inserted at the number of cycles calculated from the no rest case to the desired failure point. In the second step, a small oscillatory load (i.e., $\gamma = 0.01\%$) is applied during the rest period to measure |G*| of the binder during this stage. After the rest period, loading resumes until failure. The stage at which a rest period is applied has been selected as the cycles at which there is 35% reduction in |G*|. The rest period chosen is one hour. A healing index has been defined as the ratio between cycles to 35% reduction in |G*| with rest period (shown as B in figure F1d-6.1) to the cycles without rest period (shown as A in figure F1d-6.1). The concept is depicted in figure F1d-6.1. Test results have demonstrated that the inclusion of a single long rest period leads to a significant recovery in |G*|. It is important to note that after the rest period, damage proceeds, following approximately the same rate as prior to the rest period, thus the benefit of the rest period diminishes quickly. This finding was the basis for the definition of the healing index.

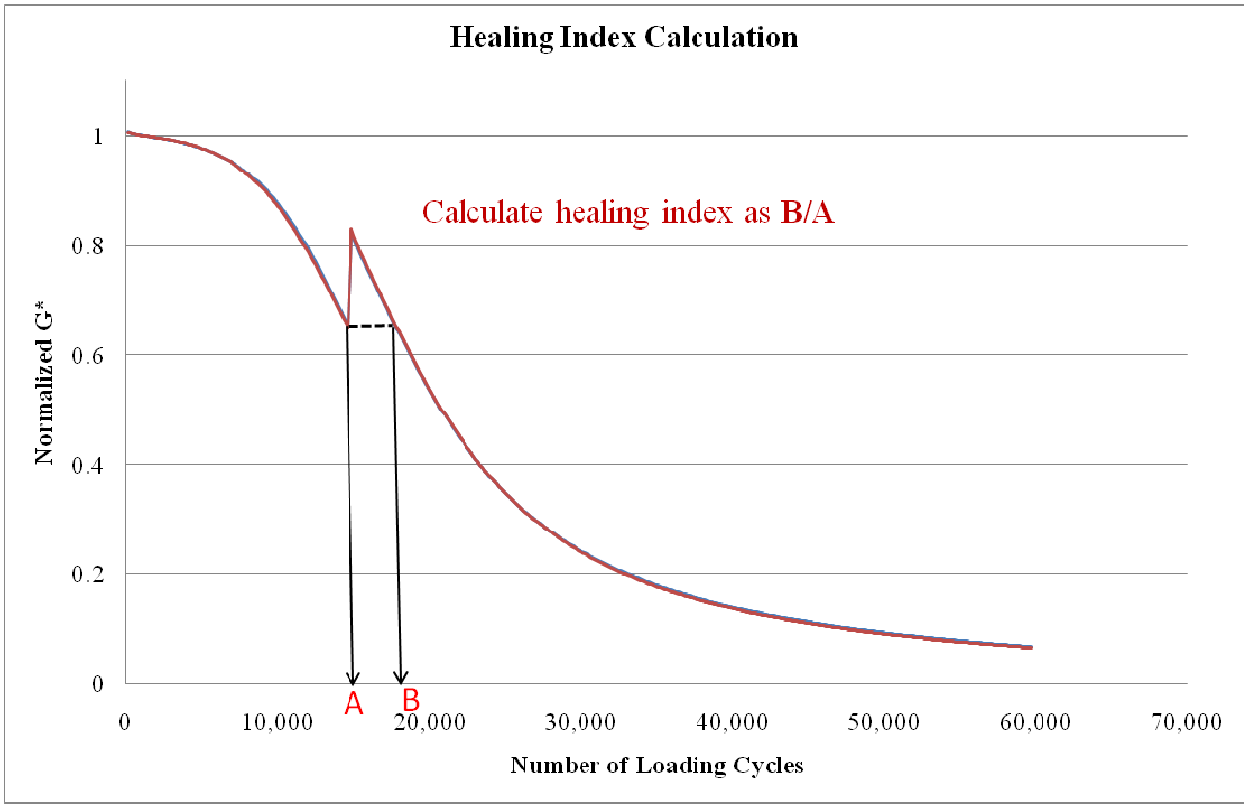


Figure F1d-6.1. Graph. Healing index.

Significant Results

The research team has completed testing four binders at three age levels using the time sweep with rest period inserted at 35% reduction in |G*| and with duration of one hour. It is important to note that some binders were tested at different strain amplitudes to ensure failure occurred in a reasonable time. However, to make a direct comparison among binders' healing indices it would be beneficial to have results at the same strain amplitude. The research team is currently working on testing all binders at a single strain amplitude. Additionally, PAV aged binder 90960 was tested at multiple strain amplitudes, reductions in |G*| prior to rest period insertion, and rest period durations to allow for determining if these factors significantly affect the healing index. Table F1d-6.1 shows the healing index results for the four LTPP binders tested at three different aged conditions. The effect of binder age on the healing index is depicted in figure F1d-6.2.

Trends shown in figure F1d-6.2 indicate that the healing index generally decreases with binder age. Furthermore, results show that the most significant reduction in healing index occurs after RTFO aging, with only marginal effects when further aging with PAV.

Results of PAV aged 90960 in table F1d-6.1 indicate that strain level and reduction in |G*| prior to rest period have marginal effects on the healing index. Results also indicate that increasing the damage level (reduction in |G*| from initial value) prior to rest period could decrease the healing index. Initial testing has also showed longer rest periods significantly increase the healing index.

Note that the healing indices reported fall within a narrow range of values (i.e., 1.04<HI< 1.25). This is not a concern since the variability from sample to sample is significantly lower than the effect of aging (ex. unaged to RTFO) or binder type on the indices.

Table F1d-6.1. Healing index results.

| Binder | Age | Strain (%) | Reduction in \|G*\| Prior to Rest Period (%) | Rest Period Duration (hr) | Healing Index |
|---|---|---|---|---|---|
| 04B903 (PG 70-10) | Unaged | 2 | 35 | 1 | 1.25 |
| | RTFO | 2 | 35 | 1 | 1.11 |
| | PAV | 2 | 35 | 1 | 1.07 |
| 370901 (PG 64-22) | Unaged | 3 | 35 | 1 | 1.21 |
| | RTFO | 3 | 35 | 1 | 1.09 |
| | PAV | 3 | 35 | 1 | 1.06 |
| 370964 (PG 76-22) | Unaged | 5 | 35 | 1 | 1.10 |
| | RTFO | 5 | 35 | 1 | 1.19 |
| | PAV | 5 | 35 | 1 | 1.09 |
| 90960 (PG 58-28) | Unaged | 2 | 35 | 1 | 1.17 |
| | RTFO | 2 | 35 | 1 | 1.06 |
| | PAV | 2 | 35 | 1 | 1.05 |
| | | 3 | 35 | 1 | 1.06 |
| | | 2 | 20 | 1 | 1.07 |
| | | 2 | 35 | 1 | 1.05 |
| | | 2 | 50 | 1 | 1.04 |
| | | 2 | 35 | 3 | 1.07 |
| | | 2 | 50 | 9 | 1.11 |

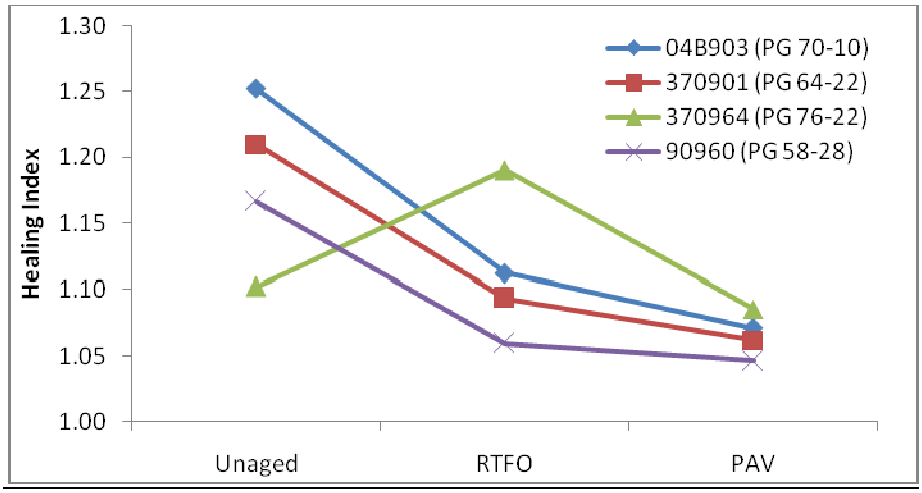


Figure F1d-6.2. Graph. Effect of age on healing index.

Work Planned Next Quarter

The research team will continue evaluating the use of a time sweep with a single long rest period for healing characterization and will investigate a procedure to incorporate healing results in fatigue analysis of asphalt binders. The research team is considering possible modifications to the healing index formulation.

***Subtask F1d-7: Coordinate with Atomic Force Microscopic (AFM) Analysis (WRI)***

Work Done This Quarter

No activity this quarter.

***Subtask F1d-8: Coordinate Form of Healing Parameter with Micromechanics and Continuum Damage Models (TAMU)***

Work Done This Quarter

In this quarter, a novel continuum damage mechanics-based framework is developed to model the micro-damage healing phenomenon in the materials that tend to self-heal. This framework extends the well-known effective configuration in continuum damage mechanics and the concept of the effective stress space to self-healing materials by introducing the healing natural configuration in order to incorporate the micro-damage healing effects. Analytical relations are derived to relate strain tensors and tangent stiffness moduli in the nominal and healing configurations for each postulated transformation hypothesis (i.e. strain, elastic strain energy, and power equivalence hypotheses).

Significant Results

It is shown that the widely-used transformation hypotheses in continuum damage mechanics for transforming stresses, strains, and internal state variables in the damaged material to the effective (undamaged) material lead to loading-path independent degradation in mechanical properties that is physically unsound. These widely-used transformation hypotheses are based on the strain equivalence or energy equivalence hypotheses. However, a new transformation hypothesis in continuum damage mechanics is proposed that leads to loading-path dependent degradations.

Significant Problems, Issues and Potential Impact on Progress

None

Work Planned Next Quarter

The main focus of the coming quarter is on further validation of the micro-damage healing model against the ALF experimental data. Special emphasis will be placed on relating the associated material parameters to fundamental properties (e.g. surface energy, bond strength, length of the healing process zone) based on micro-mechanical arguments.

## CATEGORY F2: TEST METHOD DEVELOPMENT

### Work Element F2a: Binder Tests and Effect of Composition (UWM)

Work Done This Quarter

In this quarter, the research team investigated the effect of filler modification on the fatigue performance of asphalt binders. Three mineral fillers with selected asphalt binders were tested using Elastic Recovery in the Ductility Bath (ER-DB) and DSR (ER-DSR), Linear Amplitude Sweep (LAS), and Multiple Stress Creep and Recovery (MSCR). The asphalt binders selected to be blended with the mineral fillers were: FH neat, FH modified with 4% RSBS and sulfur and FH modified with 1.5%Elvaloy AM and PPA. The mineral fillers selected were: limestone (LS2), dolomite (DS2) and caliches (CA2). The fillers tested have significantly different Rigden voids. The properties of the fillers are presented in table F2a.1. All the mastics were produced by blending the mineral fillers at 28% of volume concentration with the RTFO aged asphalt binder.

Table F2a.1. Filler properties.*

| Code | Rigden Voids (%) | Fineness Modulus | CaO (%) | Methylene Blue Volume | Specific Gravity | Loss On Ignition (%) | Solubility (%) |
|---|---|---|---|---|---|---|---|
| DS2 | 29.4 | 4.73 | 27.00 | 1.82 | 2.70 | 0.35 | 0.7 |
| LS2 | 35.4 | 3.68 | 46.30 | 3.87 | 2.62 | 0.04 | 1.5 |
| CA2 | 45.0 | 5.13 | 40.00 | 10.25 | 2.49 | 1.35 | 1.0 |

* from NCHRP 9-45 (2010)

Significant Results

The relation between elastic recovery in the ductility bath and elastic recovery in the DSR for mastics is shown in figure F2a.1. It can be seen that a very good correlation between ER-DB and ER-DSR exists ($R^2$=0.96). The results also showed that inclusion of mineral fillers reduce elastic recovery of the binder.

The ER-DSR results for different mineral fillers are presented in figure F2a.2. The results pointed out that for the unmodified and RSBS modified binder, the elastic recovery was very similar regardless of the filler type used.

No significant differences in the elastic recovery were observed for the FH +1.5%Elvaloy AM + DS2 and FH +1.5%Elvaloy AM + LS2. The elastic recovery for FH +1.5%Elvaloy AM + CA2 is on average 30% lower than for the FH +1.5%Elvaloy AM + DS2 and FH +1.5%Elvaloy AM + LS2.

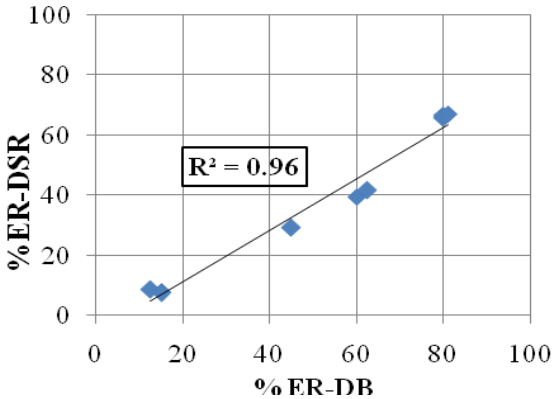


Figure F2a.1. Graph. Correlation between ER-DSR and ER-DB for mastics.

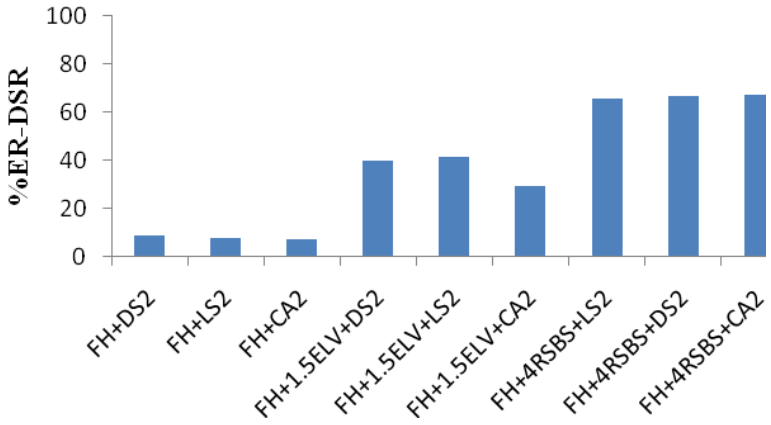


Figure F2a.2. Graph. Mineral filler effect on elastic recovery.

The number of cycles to failure at $\gamma$= 2% estimated from LAS tests of mastics are shown in figure F2a.3. Results indicate that fatigue life decreases with inclusion of mineral fillers. It was also found that mastic fatigue performance is not significantly affected by the Rigden voids.

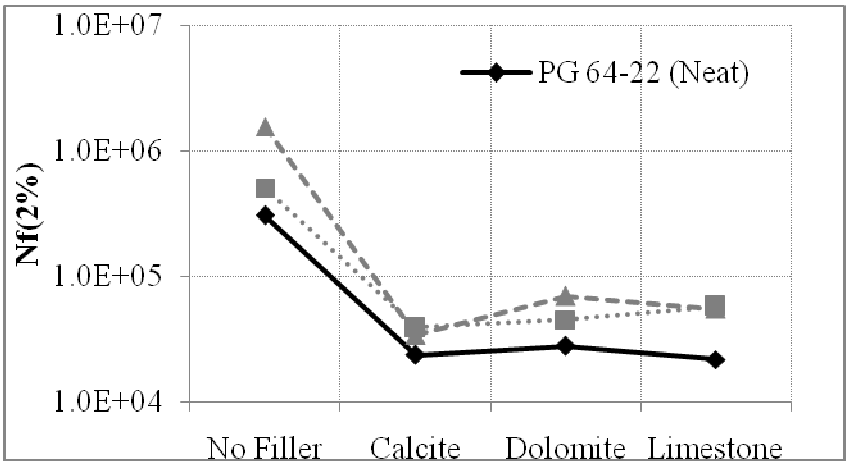


Figure F2a.3. Graph. Number of cycles to failure at 2% strain from LAS.

Work Planned Next Quarter

The research team will work on defining the mechanisms by which modifiers affect fatigue performance of binders. These mechanisms will be used to develop guidelines for selecting modifiers intended to improve fatigue life. The data analysis will focus on rheological properties and damage resistance characterization.

**Work Element F2b: Mastic Testing Protocol (TAMU)**

Work Done This Quarter

This work element is completed and the reader is referred to work element M1c.

**Work Element F2c: Mixture Testing Protocol (TAMU)**

Work Done This Quarter

Two technical presentations were made in the *90th Transportation Research Board (TRB) Annual Meeting* in Washington, D.C., January 2011. The first presentation was entitled "Anisotropic Viscoelastic Properties of Undamaged Asphalt Mixtures" and was made in Section 552 "Testing and Modeling of Asphalt Concrete Mixture". The second presentation, entitled "Microstructure-Based Inherent Anisotropy of Asphalt Mixtures", was made in Workshop 103 "Doctoral Student Research in Asphalt Materials and Mixtures". Both presentations summarized the viscoelastic characterization of anisotropic properties of undamaged asphalt mixtures.

Further investigations have been made in this quarter to characterize the viscoplastic and viscofracture properties of asphalt mixtures. Specifically, the following three achievements are made:

- Experimental protocols are developed to obtain the yield surface parameters in the Perzyna-type viscoplastic strain model of asphalt mixtures as well as the material properties in the Mohr-coulomb yield surface;
- The strain decomposition technique proposed in the last quarter is determined to not only separate the viscoplasticity from the viscoelasticity but also to separate the viscofracture from the viscoelasticity and the viscoplasticity of asphalt mixtures;
- The data analysis tool (DAT) based on Excel and Matlab software is also updated according to the new strain decomposition technique to determine the viscofracture strain in the asphalt mixtures from the experimental data.

Details of the achievements made in this quarter are summarized as follows:

**1) Experimental Protocols for Viscoplastic Yield Surface Parameters Acquisition**

In previous quarterly reports, the yield surface function used in the Perzyna-type viscoplastic strain model is the extended Drucker-Prager model which has three model parameters: slope of yield surface ($\alpha$), intercept of yield surface ($\kappa_0$) and yield stress ratio of extension to compression ($d$). These model parameters are related to material properties in the Mohr-Coulomb yield surface function including cohesion ($C$) and internal friction angle ($\varphi$). Experimental protocols are proposed to determine these model parameters and material properties so that the relationships between them can be verified.

*1.1) Experimental Protocols*

The proposed experiments include three constant strain rate strength tests at different stress conditions: uniaxial compression (UC), triaxial compression (TC) and triaxial extension (TE). For a constant strain rate strength test, the strain is applied following a function of $\varepsilon = \lambda \cdot t$ until the specimen fails, where $\lambda$ is the strain rate which is constant. Table F2c.1 shows the calculations of stress states and model parameters in the three tests, which are employed to obtain the material properties.

*1.2) Yield Stress and Model Parameters Determination*

Table F2c.1 indicates that the yield stresses in the three tests ($\sigma_{UC}^{Y}$, $\sigma_{TC}^{Y}$ and $\sigma_{TE}^{Y}$) are necessary for the calculation of stress variables and model parameters. Generally, the yield stress is determined as a point on the stress-strain curve at which the plastic strain starts to develop and the curve transits from a linear shape to a nonlinear shape. However, no linear part is observed on the stress-strain curve plotted based on the measurements of the constant strain rate strength test, as show in figure F2c.1. Instead, the stress-strain curve in figure F2c.1 illustrates a nonlinear relationship even at a very small strain level. In fact, the nonlinearity in the stress-strain curve exists even for an undamaged linearly viscoelastic material, which is caused by the relaxation of the material. Since the traditional approach of determining the yield stress does not apply to viscoelastic materials like asphalt mixtures, a new analysis method is proposed to effectively and accurately determine the yield stress for viscoelastic materials by using the pseudo strain concept.

Table F2c.1. Stresses and parameters in constant strain rate strength tests.

| **Parameters** | | **Uniaxial Compression** | **Triaxial Compression** | **Triaxial Extension** |
|---|---|---|---|---|
| Stress Variable | Stresses | $\sigma_{11} = \sigma_{UC}^{Y}$<br>$\sigma_{22} = \sigma_{33} = 0$<br>$\sigma_{UC}^{Y}$ =yield uniaxial stress | $\sigma_{11} = \sigma_c + \sigma_{TC}^{Y}$<br>$\sigma_{22} = \sigma_{33} = \sigma_c$<br>$\sigma_{TC}^{Y}$ =yield deviatoric stress;<br>$\sigma_c$ =confining stress. | $\sigma_{11} = 0$<br>$\sigma_{22} = \sigma_{33} = \sigma_{TE}^{Y}$<br>$\sigma_{TE}^{Y}$ =yield confining stress |
| | Principal Stresses | $\begin{bmatrix} \sigma_{UC}^{Y} & 0 & 0 \\ 0 & 0 & 0 \\ 0 & 0 & 0 \end{bmatrix}$ | $\begin{bmatrix} \sigma_c + \sigma_{TC}^{Y} & 0 & 0 \\ 0 & \sigma_c & 0 \\ 0 & 0 & \sigma_c \end{bmatrix}$ | $\begin{bmatrix} \sigma_{TE}^{Y} & 0 & 0 \\ 0 & \sigma_{TE}^{Y} & 0 \\ 0 & 0 & 0 \end{bmatrix}$ |
| | $p = \frac{1}{3}\sigma_{ii}$ | $\frac{1}{3}\sigma_{UC}^{Y}$ | $\sigma_c + \frac{1}{3}\sigma_{TC}^{Y}$ | $\frac{2}{3}\sigma_{TE}^{Y}$ |
| | $q = \sqrt{\frac{3}{2}S_{ij}S_{ji}}$ | $\sigma_{UC}^{Y}$ | $\sigma_{TC}^{Y}$ | $\sigma_{TE}^{Y}$ |
| | $r = \left(\frac{9}{2}S_{ij}S_{jk}S_{ki}\right)^{\frac{1}{3}}$ | $\sigma_{UC}^{Y}$ | $\sigma_{TC}^{Y}$ | $-\sigma_{TE}^{Y}$ |
| | $\tau = \frac{q}{2}\left[1 + \frac{1}{d} + \left(1 - \frac{1}{d}\right)\left(\frac{r}{q}\right)^3\right]$ | $\sigma_{UC}^{Y}$ | $\sigma_{TC}^{Y}$ | $\frac{\sigma_{TE}^{Y}}{d}$ |
| | $\hat{p} = \frac{\sigma_1 + \sigma_2 + \sigma_3}{3}$ | $\frac{1}{3}\sigma_{UC}^{Y}$ | $\sigma_c + \frac{1}{3}\sigma_{TC}^{Y}$ | $\frac{2}{3}\sigma_{TE}^{Y}$ |
| | $\hat{q} = \frac{\sigma_1 - \sigma_3}{3}$ | $\frac{1}{3}\sigma_{UC}^{Y}$ | $\frac{1}{3}\sigma_{TC}^{Y}$ | $\frac{1}{3}\sigma_{TE}^{Y}$ |
| Stress State | $\bar{n} = \frac{2\sigma_2 - \sigma_1 - \sigma_3}{\sigma_1 - \sigma_3}$ | -1 | -1 | 1 |
| | $A = \frac{1}{4}\left(1 + \frac{1}{d}\right)\sqrt{\bar{n}^2 + 3} + \frac{1}{4}\left(1 - \frac{1}{d}\right)\frac{\bar{n}^3 - 9\bar{n}}{\bar{n}^2 + 3}$ | 1 | 1 | $\frac{1}{d}$ |
| Yield Surface Parameter | $d = \frac{3 - \sin\varphi}{3 + \bar{n}\sin\varphi}\sqrt{\frac{\bar{n}^2 + 3}{4}}$ | 1 | 1 | $d = \frac{3 - \sin\varphi}{3 + \sin\varphi}$ |
| | $\alpha = \frac{6A\sin\varphi}{3 + \bar{n}\sin\varphi}$ | $\alpha = \frac{6\sin\varphi}{3 - \sin\varphi}$ | | |
| | $\kappa_0 = \frac{6A \cdot C \cdot \cos\varphi}{3 + \bar{n}\sin\varphi}$ | $\kappa_0 = \frac{6C \cdot \cos\varphi}{3 - \sin\varphi}$ | | |

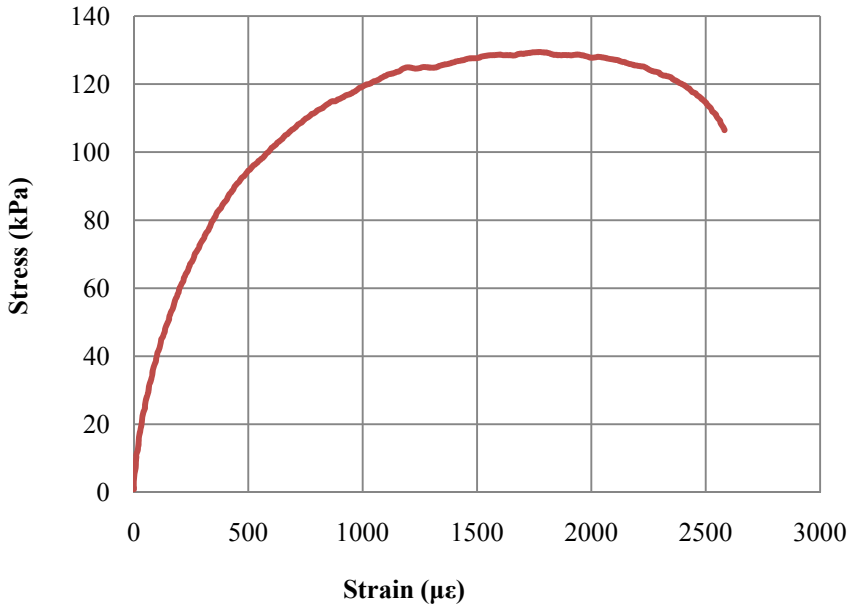


Figure F2c.1. Stress versus strain in a constant strain rate strength test.

First, the creep compliance of the undamaged asphalt mixture is measured by a nondestructive creep test, and the relaxation modulus is estimated from the creep compliance and is modeled using equation F2c.1. Details of the undamaged linear viscoelastic characterization of asphalt mixture are discussed in the last quarterly report.

$$E(t) = E_{\infty} + \sum_{j=1}^{M} E_j \exp\left(-\frac{t}{k_j}\right) \tag{F2c.1}$$

Second, pseudo strain in a constant strain rate strength test is calculated based on its definition and is expressed in equation F2c.2, where $E_R$ = reference modulus. It has been proved that, when $E_R$ equals to Young's modulus, the pseudo strain is the remaining strain after subtracting the viscous strain from the total strain. Thus, the pseudo strain is equivalent to the elastic strain in the nondestructive stage of the test when damages like plasticity and cracking have not been introduced to the specimen yet. Consequently, the pseudo strain should show a linear relationship with the measured stress. When damage starts to develop, the relationship between the measured stress and pseudo strain will become nonlinear, which is caused by either plastic deformation or cracking or both. The equation for the pseudo-strain is:

$$\varepsilon^R(t) = \frac{\lambda}{E_R}\left[E_{\infty} t + \sum_{j=1}^{M} E_j k_j \left(1 - e^{-\frac{t}{k_j}}\right)\right] \tag{F2c.2}$$

Third, the measured stress is plotted against the pseudo strain, as shown in figure F2c.2. The stress-pseudo strain curve in figure F2c.2 has an approximately linear portion that is followed by a nonlinear portion. The yield stress, after which plastic strain develops, is located at the end point of the linear portion of the stress-pseudo strain curve.

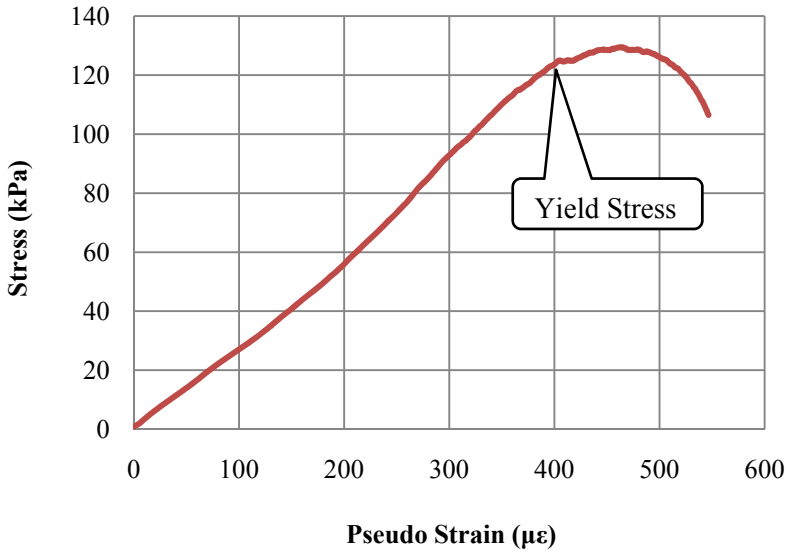


Figure F2c.2. Stress versus pseudo strain in a constant strain rate strength test.

Finally, the yield surface parameters are determined using the equations shown in table F2c.1. The initial yield surface function of the extended Drucker-Prager model is $\tau - \alpha p - \kappa_0 = 0$, in which the parameters $\alpha$ and $\kappa_0$ are determined as the slope and intercept of the $\tau$ versus $p$ curve. The yield stress ratio of extension to compression ($d$) is determined as $d = \tau / (\alpha p + \kappa_0)$ by using the yield stress measured in the triaxial extension test. The yield surface of the Mohr-Coulomb model is expressed as $\hat{q} - \hat{p}\sin\varphi - C \cdot \cos\varphi = 0$, where the parameters cohesion $C$ and internal friction angle $\varphi$ are calculated based on the slope and intercept of the $\hat{q}$ versus $\hat{p}$ curve.

**2) Strain Decompositions of Viscoelasticity, Viscoplasticity and Viscofracture**

In an earlier study conducted in previous quarters, the total strain measured in the compressive dynamic modulus test was initially separated into elastic strain, plastic strain, viscoelastic strain and viscoplastic strain. This way of separating the total strain is appropriate for the primary and secondary deformation stages. For the tertiary stage, the measured total strain has to be decomposed differently since the viscofracture strain occurs when the deformation goes to the tertiary stage in which the permanent deformation increases mainly due to the formation and growth of microcracks. To characterize the fracture properties of the asphalt mixture, the viscofracture strain needs to be separated from the total strain, which will be detailed as follows.

*2.1) Total Strain Fitting Model*

A new total strain fitting model is proposed in equation F2c.3 to characterize the measured total strain not only in primary and secondary stages but also in the tertiary stages of the compressive dynamic modulus test.

$$\begin{cases} \varepsilon^T(t) = \varepsilon_1(t) - \varepsilon_2(t) \\ \varepsilon_1(t) = \varepsilon_0 + \sum_{i=1}^{L} \varepsilon_i \left[ 1 - \exp\left( -\frac{t}{\tau_i} \right) \right] \quad \textit{at least one } \varepsilon_i < 0 \textit{ and one } \tau_i < 0 \\ \varepsilon_2(t) = \varepsilon_N \cos(\omega t - \varphi_N) = \frac{\sigma_0}{\left| E_N^* \right|} \cos(\omega t - \varphi_N) \end{cases} \tag{F2c.3}$$

where $\varepsilon_1$ characterizes the creep part the total strain and $\varepsilon_2$ characterizes the cyclic part of the total strain; $\varepsilon_N$ is the cyclic strain amplitude that varies with load cycles. $\left| E_N^* \right| = \sigma_0 / \varepsilon_N$ is defined as the magnitude of the complex (dynamic) modulus and $\varphi_N$ is the phase angle of the complex (dynamic) modulus. Both $\left| E_N^* \right|$ and $\varphi_N$ are properties of the damaged specimen and are dependent on load cycles.

*2.2) Complex (Dynamic) Modulus and Phase Angle Model of Damaged Specimen*

The dynamic modulus $\left| E_N^* \right|$ and phase angle $\varphi_N$ of damaged specimens are modeled by load cyclic dependent functions that take into account the separation of the total strain into viscoelastic strain, viscoplastic strain and viscofracture strain. The model for $\left| E_N^* \right|$ of the damaged specimen is shown in equation F2c.4, where $A_E$, $B_E$, $C_E$, $D_E$ and $E_E$ are positive fitting parameters. The model for $\varphi_N$ of the damaged specimen is shown in equation F2c.5, where $A_\varphi$, $B_\varphi$, $C_\varphi$, $D_\varphi$ and $E_\varphi$ are also positive fitting parameters. An example of modeling $\left| E_N^* \right|$ and $\varphi_N$ is shown in figure F2c.3, which shows a good fitting between the models and the measured data.

$$\left| E_N^* \right| = A_E \left( 1 - e^{-B_E \cdot N} \right) + C_E \left( 1 - e^{D_E \cdot N} \right) + E_E \tag{F2c.4}$$

$$\varphi_N = A_\varphi \left( e^{-B_\varphi \cdot N} - 1 \right) + C_\varphi \left( e^{D_\varphi \cdot N} - 1 \right) + E_\varphi \tag{F2c.5}$$

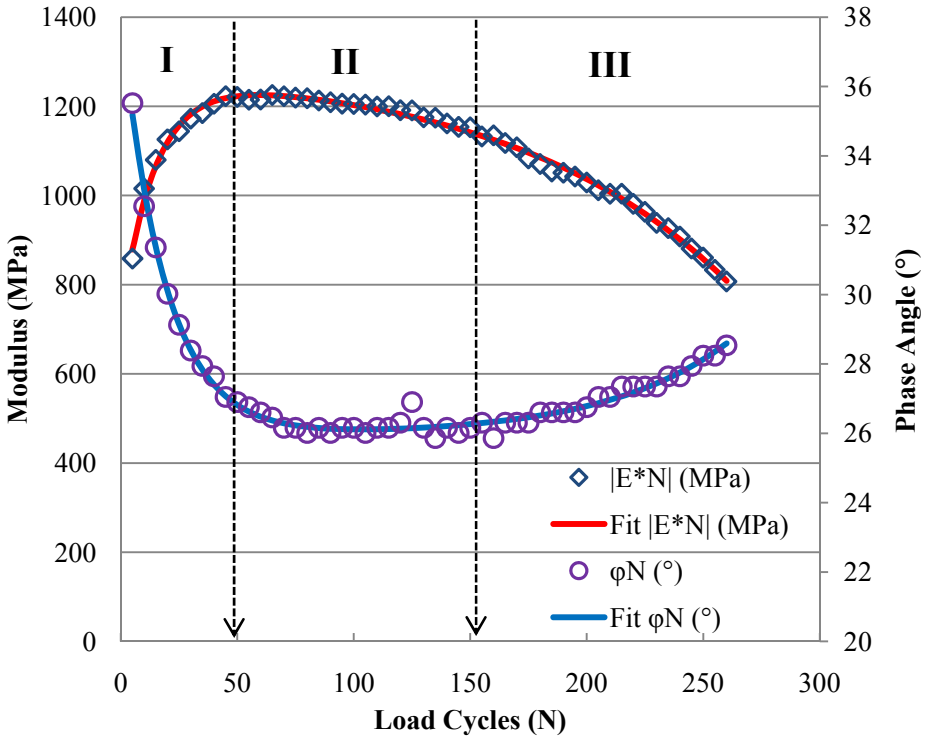


Figure F2c.3. Modeling of damaged dynamic modulus and phase angle.

*2.3) Pseudo Strain Calculation and Strain Decomposition*

The pseudo strain corresponding to the total strain modeled in equation F2c.3 is calculated as shown in equation F2c.6, where $E_R$ = reference modulus.

$$\begin{cases} \varepsilon^R(t) = \varepsilon_1^R(t) - \varepsilon_2^R(t) \\ \varepsilon_1^R(t) = \dfrac{1}{E_R}\left\{ E_\infty \varepsilon_1(t) + \varepsilon_0 \Delta E(t) + \sum_{i=1}^{L}\sum_{j=1}^{M} \dfrac{\varepsilon_i E_j}{\left(1-\tau_i/k_j\right)}\left[ \exp\left(-\dfrac{t}{k_j}\right) - \exp\left(-\dfrac{t}{\tau_i}\right)\right]\right\} \\ \varepsilon_2^R(t) = \dfrac{\sigma_0}{E_R}\dfrac{|E^*|}{|E_N^*|}\cos\left(\omega t - \varphi_N + \phi\right) \end{cases} \quad \text{(F2c.6)}$$

As stated previously, when $E_R$ equals the Young's modulus ($E_0$), the pseudo strain is the remaining strain after subtracting the viscous strain from the total strain. Thus,

$$\varepsilon^T = \varepsilon^e + \varepsilon^{vi} + \varepsilon^p + \varepsilon^{vp} + \varepsilon^{vf} = \varepsilon^R + \varepsilon^{vi} \quad \text{(F2c.7)}$$

where $\varepsilon^T$ = measured total strain; $\varepsilon^e$ = elastic strain; $\varepsilon^{vi}$ = viscous strain; $\varepsilon^p$ = plastic strain; $\varepsilon^{vp}$ = viscoplastic strain; $\varepsilon^{vf}$ = viscofracture strain. The elastic strain $\varepsilon^e$ can always be calculated using stress divided by the Young's modulus, which is shown in equation F2c.8a. The viscous strain $\varepsilon^{vi}$ is obtained from equation F2c.7 and is shown in equation F2c.8b. Since $\varepsilon^{vp}\left(t=0\right)=\varepsilon^{vf}\left(t=0\right)=0$, $\varepsilon^p$ is determined using equation F2c.8c. Since the viscofracture strain due to microcrack growth does not occur until the tertiary stage (Part III), the pseudo strain in the primary and secondary stages ($\varepsilon^R\left(I,II\right)$) only include the elastic strain, plastic strain and viscoplastic strain. As a result, the viscoplastic strain in the primary and secondary stage ($\varepsilon^{vp}\left(I,II\right)$) can be calculated using equation F2c.8d. Equation F2c.8e is the Tseng-Lytton model which is employed to fit $\varepsilon^{vp}\left(I,II\right)$ and then to predict the viscoplastic strain ($\varepsilon^{vp}$) during the entire deformation process including the primary, secondary and tertiary stages. Finally, the viscofracture strain ($\varepsilon^{vf}$) can be computed using equation F2c.8f with rearranging equation F2c.7. Thus the strain decomposition is accomplished by a complete separation of each strain component.

$$\varepsilon^e = \sigma / E_0 \tag{F2c.8a}$$

$$\varepsilon^{vi} = \varepsilon^T - \varepsilon^R \tag{F2c.8b}$$

$$\varepsilon^p = \varepsilon^R\left(t=0\right) - \varepsilon^e \tag{F2c.8c}$$

$$\varepsilon^{vp}\left(I,II\right) = \varepsilon^R\left(I,II\right) - \left(\varepsilon^e + \varepsilon^p\right) \tag{F2c.8d}$$

$$\varepsilon^{vp} = \varepsilon_\infty^{vp} \exp\left[-\left(\rho/N\right)^\lambda\right] \tag{F2c.8e}$$

$$\varepsilon^{vf} = \varepsilon^R - \left(\varepsilon^e + \varepsilon^p\right) - \varepsilon^{vp} \tag{F2c.8f}$$

An example is given in figure F2c.4 to show the strain decomposition for an asphalt mixture in a compressive dynamic modulus test. It is found that elastic and plastic strain are time-independent and the viscous strain shows three stage changes and has a large proportion of the total strain. To clearly show the viscoplastic strain and viscofracture strain, figure F2c.4 is magnified and shown in figure F2c.5 which illustrates that the viscoplastic strain has a power curve and that the viscofracture strain declines very quickly to zero and remains constant until the tertiary stage in which the viscofracture strain increases rapidly. The declination of the viscofracture strain in the first several load cycles is believed to be caused by the closure of the air voids in the asphalt mixture under a compressive load. The increasing viscofracture strain in the tertiary stage is similar to a typical crack growth curve, which can be implemented to acquire the viscofracture properties of the asphalt mixture in compression. Another direct application of the viscofracture strain curve is to obtain the flow number that is the number of load cycles at which the viscofracture strain, when departing from zero, starts to increase.

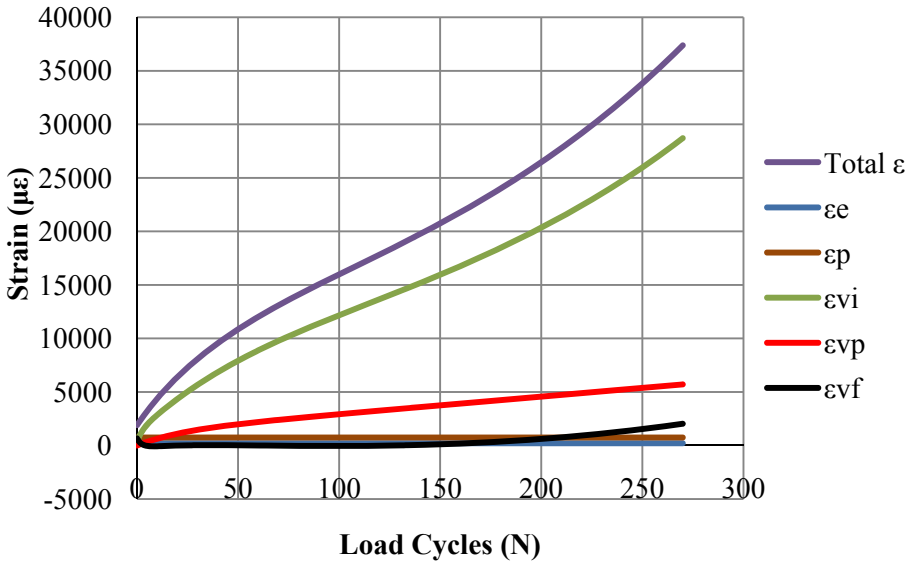


Figure F2c.4. Strain decomposition in dynamic modulus test.

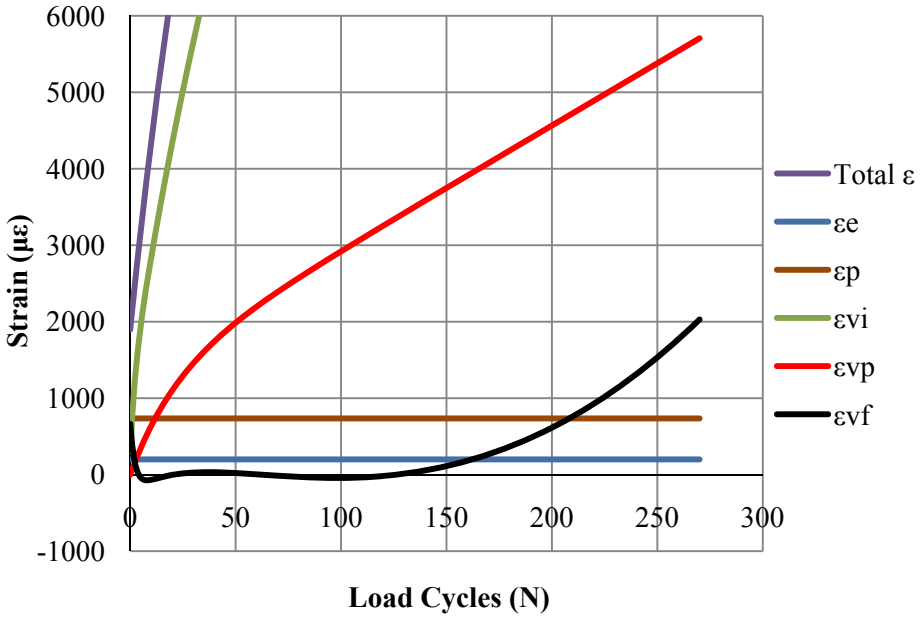


Figure F2c.5. Magnified figure F2c.4 to show viscoplastic and viscofracture strains.

**3) Data Analysis Tool (DAT) Updates**

The data analysis tool (DAT) programmed in Excel and Matlab in previous quarters is updated to take into account the viscofracture strain in the following aspects:

a) A brief instruction of using the DAT is provided for new users;

b) An initial value assignment modulus is programmed into all regression models in the DAT to eliminate the non-convergent errors;

c) Models of total strain, damaged dynamic modulus and phase angle in equations F2c.3-F2c.5 are programmed in the DAT to take into account the deformation in all three stages: primary, secondary and tertiary during the dynamic modulus test; and

d) Strain decomposition calculation is modified based on equations F2c.8 to conduct the strain decomposition of viscoelastic strain, viscoplastic strain and viscofracture strain.

Significant Results

The viscoplastic and viscofracture properties of asphalt mixtures are further investigated and two primary accomplishments are obtained. One of the accomplishments is that experimental protocols are proposed including three constant strain rate strength tests in uniaxial compressive, triaxial compressive and triaxial extensive stress conditions to acquire the yield surface parameters in the Perzyna-type viscoplastic model and the material properties in the Mohr-Coulomb yield surface, in which the initial yield stress of viscoelastic material such as an asphalt mixture is effectively and accurately determined by employing the pseudo strain concept. Another accomplishment is that, by modeling the total strain, the dynamic modulus and phase angle of the damaged specimen during the whole deformation stage, the strain is successfully decomposed to not only separate the viscoplasticity from the viscoelasticity but also to separate the viscofracture from the viscoelasticity and the viscoplasticity in the asphalt mixture. The data analysis tool (DAT) based on Excel and Matlab software is also updated according to the new strain decomposition technique. The separated viscoplastic strain and viscofracture strain can be used to characterize the viscoplastic and viscofracture properties of the asphalt mixture, respectively.

Significant Problems, Issues and Potential Impact on Progress

None.

Work Planned in Next Quarter

- More constant strain rate strength tests according to the proposed testing protocol will be conducted to obtain the yield surface of asphalt mixtures that vary in the volumetric properties, material properties and aging conditions; and
- New fracture mechanical models will be proposed based on the viscofracture strain to characterize the viscoelastic fracture in the asphalt mixtures including the estimation of the anisotropic damage density and crack growth associated with the permanent deformation in an asphalt pavement.

**Work Element F2d: Structural Characterization of Micromechanical Properties in Bitumen using Atomic Force Microscopy (TAMU)**

Work Done This Quarter

Tomography is carried out as needed on specimens that are used in developments of aging, healing and unified models. The reader is referred to work element F1c-3. The success in using the AFM and nano-indentation to determine microstructural properties of asphalt binders has been included in previous quarterly reports and a summary is also provided on pages 47 – 51 of the Year 5 work plan and will not be repeated here. However, it is instructive to briefly summarize the results of the nano-indentation experiments. For this work we have found:

1. We achieve repeatable and statistically significantly different stiffness, adhesive and elastic/plastic behavior among the various distinctive phases of the asphalt binder as they appear from the AFM and reasonable creep responses that are significantly different among the heterogeneous domains.
2. A protocol has been developed for the nano-indentation experiments can successfully measure these properties.
3. These microstructural properties change significantly with aging. See figures F2d.2 and F2d.3 in the Year 5 work plan.
4. The analysis is sensitive to the asphalt binder evaluated as demonstrated by analysis if asphalt binders AAB, AAD, and ABD (unaged and aged).
5. The steps involved in the "fingerprinting" of the binders with the AFM nano-indentation protocol are:
    a. Thin-film sample preparation and AFM equipment calibration.
    b. Mapping of topography and phase-separated regions.
    c. Nano-indentation creep testing.
    d. Analysis of measurements and characterization of physical, microstructural properties.

Significant Results

It is significant that engineering properties can be successfully extracted from nano-indentation experiments with the promise that refinement of these measurement in year 5 can lead to yet more meaningful viscoelastic-viscoplastic characterization of asphalt binder properties.

Significant Problems, Issues and Potential Impact on Progress

None.

Work Planned Next Quarter

The following work will begin next quarter and continue in Year 5.

1. Obtain additional information regarding asphalt microstructural properties (confirm whether the observed phases are a surface or bulk phenomenon) by using spin-echo, small angle neutron scattering (in collaboration with TU Delft).
2. Obtain chemical map of each asphalt binder using x-ray beam line with the University of Saskatchewan's synchrotron and by using functionalized AFM tips to map different carbonyl groups.
3. Convert creep measurements to viscoelastic-viscoplastic properties.
4. Investigate surface mechanics effects.
5. Extract individual components from asphalt binders studied using size-exclusion chromatography and synthesize different asphalt binders (in collaboration with WRI).
6. Validate relationship between chemical composition and microstructural properties.

Tomography will be carried out as needed for the models development.

**Work Element F2e: Verification of the Relationship between DSR Binder Fatigue Tests and Mixture Fatigue Performance (UWM)**

Work Done This Quarter

The research team tested mastics using the linear amplitude sweep (LAS) protocol. The results were used to determine if the LAS test is applicable to mastics and to determine the effect of mineral fillers on binder fatigue resistance. The binder used for mastic preparation was a neat PG 64-22, and the three fillers used are known to have properties that vary significantly, as shown in table F2e.1. The fillers were blended with the binder at four different volumetric concentrations: 0%, 10%, 27%, and 40%. Filler volume concentration is known to significantly affect the stiffening of fillers on binders (Faheem 2009). Thus, it was speculated that filler volume concentration would also impact the fatigue resistance of binders.

Table F2e.1. Fillers properties.

| Filler | Rigden Voids (%) | Fineness Modulus | CaO (%) | Methylene Blue Value | Specific Gravity |
|---|---|---|---|---|---|
| Dolomite | 42.8 | 5.07 | 26 | 2.79 | 2.59 |
| Granite | 38.3 | 4.26 | 4.7 | 2.81 | 2.62 |
| Limestone | 35.4 | 3.68 | 46.3 | 3.87 | 2.62 |

Significant Results

The response of the mastic with the dolomite filler is depicted in figure F2e.1. The trends clearly show that the mastics become stiffer as the volumetric concentration of filler increases and that the peak shear stress is reached at a lower strain for mastics as filler volume fraction is increased.

Beyond the peak, shear stresses decrease most rapidly for higher filler concentrations. These experimental results appear to indicate that fatigue performance decreases with increasing volume fraction of filler.

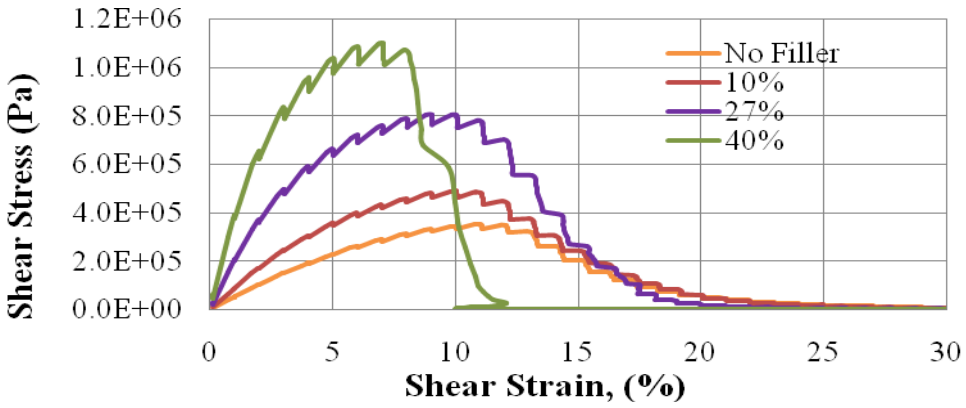


Figure F2e.1. Graph. Shear stress response of mastics.

Figure F2e.2 shows the number of cycles to failure at 2.5% strain determined from Viscoelastic Continuum Damage (VECD) analysis for all fillers and volume concentrations tested. The trends shown indicate that increasing filler volume fraction decreases fatigue life of the binder significantly, while filler type does not appear to have a significant impact on fatigue results.

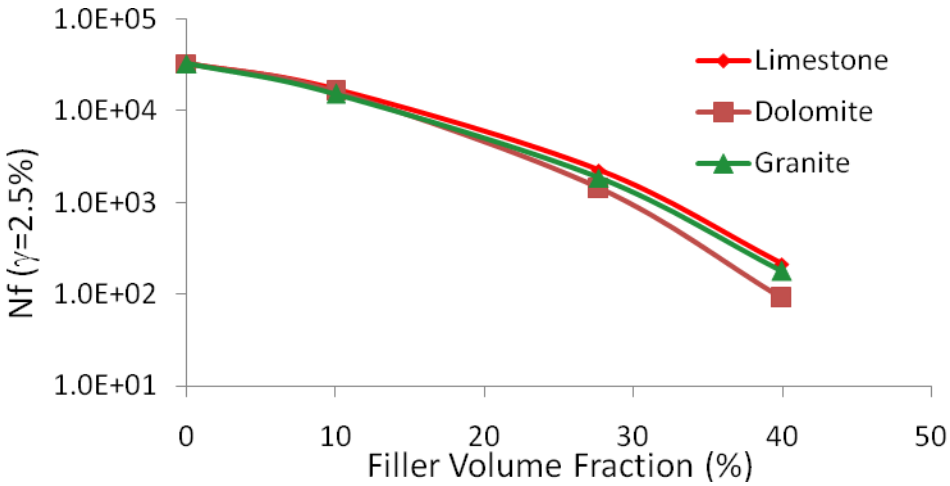


Figure F2e.2. Graph. Effect of filler type and volume fraction on fatigue life predictions using VECD analysis.

Results of LAS analysis were verified by conducting strain controlled time sweeps at 2% applied strain. Fatigue lives were calculated directly from time sweep data and correlated to LAS results. The correlation between measured fatigue lives from time sweep results and predicted fatigue

lives determined from VECD analysis of LAS results is shown in figure F2e.3. A moderate correlation is observed between LAS and Time Sweep results, which indicates that the two procedures could produce similar ranking.

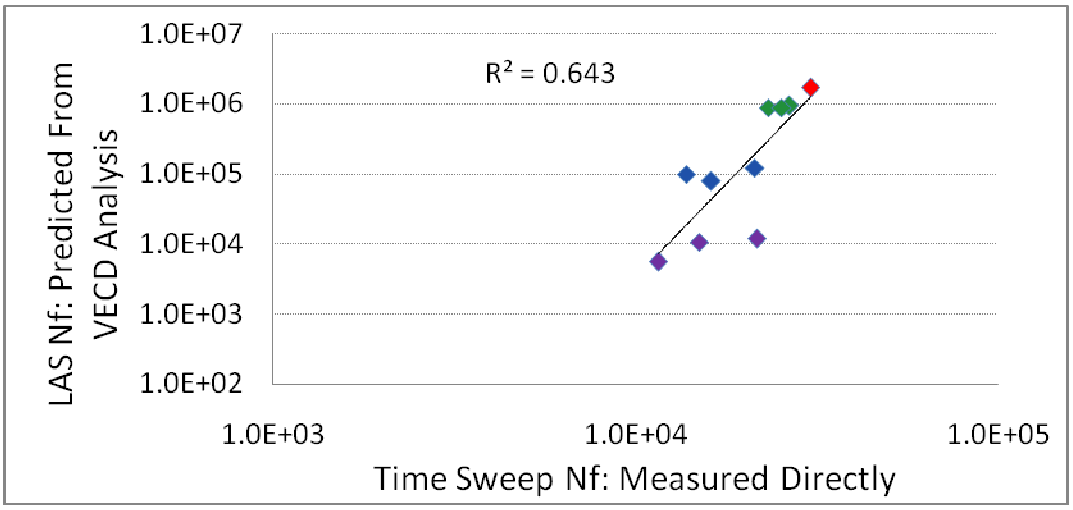


Figure Fe2.3. Graph. Correlation between LAS predicted fatigue life and fatigue life directly measured from time sweep.

Note that both procedures show increasing filler volumetric concentration decreases fatigue life. The research team believes that the LAS procedure in combination with VECD analysis is capable of characterizing the fatigue damage resistance of mastics.

It is also worth noting that the trends in results agree with observations in metal matrix composites (MMC). Research on MMCs, which are particulate composites with a metal matrix, has demonstrated increasing volume fraction decreases fatigue life under strain controlled loading. Under stress controlled loading, however, MMCs typically show increased fatigue life with increasing volume fraction. No clear explanation for these trends exists. However, researchers have hypothesized this phenomenon is observed because a much higher stress is required to reach a given strain for a material with higher volume fraction of particulates. This stress is much closer to the ultimate strength of the material than the stresses required to reach the given strain for lower volume fractions (Allison et al. 1993).

Work Planned Next Quarter

The team will conduct fatigue testing of asphalt mixtures using the Indirect Tensile Test. The LAS procedure will be used for fatigue characterization of the binders used for asphalt mixture preparation and a comparison between binder and mixture fatigue performance will be conducted. Additionally, the research team will test mastics using stress controlled time sweeps to determine if trends match MMC literature.

Cited References

Allison, J. E., and J. W. Jones, 1993, in *Fundamentals of Metal Matrix Composites*, S. Suresh, A. Mortensen, and A. Needleman, eds., Butterworth-Heinemann, Stoneham, MA.

Faheem, A., 2009, Modeling of Asphalt Mastic in Terms of Filler-Bitumen Interaction, PhD Dissertation, Department of Civil and Environmental Engineering, University of Wisconsin-Madison.

## CATEGORY F3: MODELING

### Work Element F3a: Asphalt Microstructural Model

Work Done This Quarter

#### *Subtask F3a-1. ab initio Theories, Molecular Mechanics/Dynamics and Density Functional Theory Simulations of Asphalt Molecular Structure Interactions (URI)*

Recent proposed asphaltene structures published by Mullins (2010) were found during initial simulations (during prior quarters of this project) to contain bonding patterns that result in high internal energies and thus low probabilities of occurring in practice. The high energies correspond to aromatic rings that are forced to be non-planar due to repulsive intramolecular forces. A manuscript was completed that demonstrates using quantum mechanics calculations how these energies can be attributed to Flory's "pentane effect": torsion angles that appear to be locally favorable instead lead to position overlaps for atoms separated by 6 bonds. Modifications to asphaltene structure were proposed that alleviate these effects and restore planar aromatic rings. An example is shown in the figure below. The manuscript was submitted to the journal *Energy & Fuels* immediately after the end of the quarter.

Molecular dynamics simulations were conducted of a next-generation model asphalt that is representative of SHRP AAA-1. See subtask F3a-3 below.

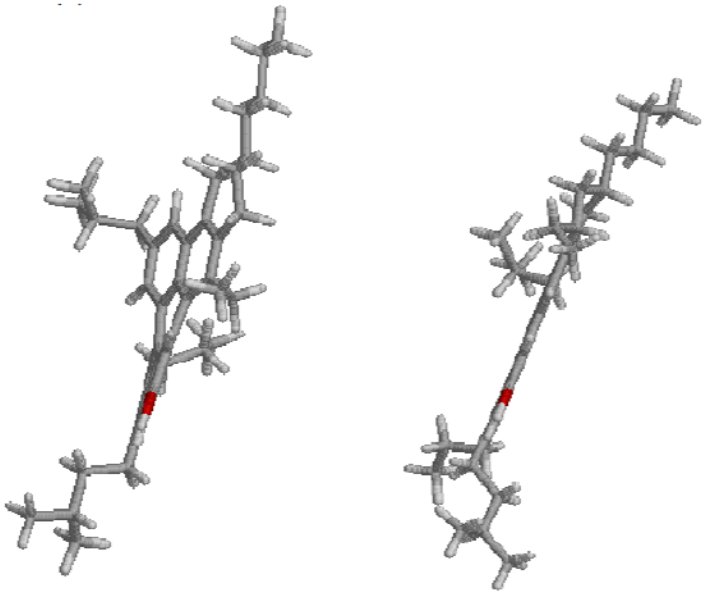

Figure: Images from molecular simulations that focus on the fused aromatic rings within an asphaltene (left) using a bonding geometry proposed by Mullins (2010) and (right) using alterations in side chain position that alleviate bonding conflicts and restore planar aromatic rings (Li and Greenfield 2011).

Significant Problems, Issues and Potential Impact on Progress

The challenges for balancing sulfur content with aromatic vs. aliphatic carbon content, as described in the December 2010 quarterly report, remain. The molecular dynamics simulations for the next-generation AAA-1 system were performed using the model composition with 3.6% sulfur (compared to 5.5% reported from experiments in the literature) and 39.5% aromatic carbon (compared to 28.1% reported from experiments in the literature). Increasing the sulfur concentration further would increase the aromatic carbon content, and vice versa.

Work Planned Next Quarter

Data analysis and manuscripts will be completed on a spontaneous wax formation event in a molecular simulation and on unique attributes of asphaltene chemistry that have been recognized through quantum mechanics calculations and molecular simulations. This work was delayed from the prior quarter in order to focus efforts on completing the manuscript about high energy asphaltene configuration and on conducting and analyzing the AAA-1 molecular simulations.

Analysis of equilibrium and dynamics properties for the AAA-1 system will be completed, and manuscripts that describe its composition and properties will be prepared for publication. Molecular simulations will be initiated for the model AAK-1 bitumen systems.

***Subtask F3a-2. Develop algorithms and methods for directly linking molecular simulation outputs and phase field inputs (URI, NIST, VT)***

Nothing to report.

***Sub-subtask F3a-2.1. Collect information on available models and numerical methods suitable for phase field modeling (VT-WRI)***

This sub-subtask includes a comprehensive literature, identification of promising theories and identification of corresponding numerical tools.

Work Done

This sub-subtask was completed in last quarter. Major achievements include a comprehensive literature, identification of promising theory and identification of corresponding numerical tool.

Significant Problems, Issues and Potential Impact on Progress

None

Work Planned Next Quarter

NA

***Sub-subtask F3a-2.2. Phase-field parameter determination (VT-WRI)***

This sub-subtask focuses on identification of model parameters, identification of parameter characterization methods, and performing parameter determination.

Work Done

This sub-subtask was almost completed in last quarter. Major achievements include identification of model parameters, and identification of parameter characterization methods for phase separation and cracking initiation problems.

Significant Problems, Issues and Potential Impact on Progress

None

Work Planned Next Quarter

The work will focus on performing tests to determine parameters for the selected asphalt binders.

***Sub-subtask F3a-2.3. Numerical solution of the phase-field equations (VT-WRI)***

This sub-subtask focuses on developing numerical algorithms, computer code and methods for visualizing the computational results.

Work Done

Two different methods are currently being developed, one using the Finite Difference Method to be implemented on Matlab for small scale and 2D problems; and the other using the Finite Element Method to be implemented on ABAQUS for 3D and large scale problems.

Significant Problems, Issues and Potential Impact on Progress

The Cahn-Hilliard equation that governs the phase-field parameter is a $4^{th}$ order equation. This poses stringent limitations on the time steps in numerical simulations and severely affects the computational time.

Work Planned Next Quarter

Development of the codes for implementing a general phase-field theory on Matlab and ABAQUS. The experience in the 2D code will help us to select optimal numerical methods and programming language for the large scale 3D simulations. Due to the high (4th) order of derivatives in the phase-field equations, an efficient spectral method may be used for 3D problems with periodic boundary conditions.

***Sub-subtask F3a-2.4. Application of diffuse interface modeling to asphalt microstructure evolution (VT-WRI)***

This sub-subtask includes development of a diffuse interface model, modeling the phase distribution due to heating/re-solidification, and modeling of inter-phase diffusion.

Work Done

A diffuse interface model was identified and being adapted for application to asphalt binder.

Significant Problems, Issues and Potential Impact on Progress

None

Work Planned Next Quarter

The future work will mainly focus on deriving the equations and numerical implementation algorithms, and applying the theory to modeling the phase distribution due to heating/re-solidification, and inter-phase diffusion. The effect of external shear on the evolution of microstructures will also be investigated.

***Sub-subtask F3a-2.5. Develop phase field models for characterizing asphalt emulsion and phase separation processes (VT-WRI)***

This sub-subtask includes formulating bulk and gradient energy theory, modeling of emulsification process, and modeling of phase separation.

Work Done

A diffuse interface model was identified. The simplest Cahn-Hilliard model will be used as a start.

Significant Problems, Issues and Potential Impact on Progress

None

Work Planned Next Quarter

To enable the modeling of emulsification and phase separation process, a theoretical framework needs to be developed. A 2D code (either Matlab, C/Fortran, or commercial software) on the simplest Cahn-Hilliard model will be developed. This code can simulate different scenarios of phase separation, namely nucleation and spinodal decomposition. The 2D code will enable the use of different types of free energies to assess the free energy and binder property relationship. Modeling of fluid flow will be enabled for computing the shear property of the mixture. The 2D code will be extended to three components to model the asphaltene, wax, and resin in the mixture. Finally, the code will be finally extended to 3D cases.

***Sub-subtask F3a-2.6. Phase-field modeling for fatigue cracking and self-healing processes(VT-WRI)***

This sub-subtask focuses on the development of mesoscale cracking initiation, propagation and arrest criteria, modeling of self-healing process, and performing experimental verification.

Work Done

No significant achievements for this quarter.

Significant Problems, Issues and Potential Impact on Progress

None

Work Planned Next Quarter

The next quarter will develop mechanisms to link the density change to the cracking process using the phase field theory. Self-healing process will be modeled at the atomistic scale and up scaled to mesoscale. The theory for phase-field modeling of the self-healing process, which is still undeveloped, will be further explored.

***Subtask F3a-3. Obtain temperature-dependent dynamics results for model asphalts that represent asphalts of different crude oil sources (URI)***

Molecular dynamics simulations for different temperatures were used to equilibrate molecule positions and orientations in the next-generation AAA-1 system and to perform dynamics calculations. Note that the molecule choices have been revised compared to the prior model of AAA-1 (Zhang and Greenfield 2008) in response to concerns about molecule size.

Results were being finalized towards the end of the quarter. Two preliminary results are shown below. First, the overall density calculated in the simulations is closer than prior models to the true density of SHRP asphalt AAA-1. The improved agreement can be attributed to more accurate choices of model compounds in terms of molecular weight and polarity. Second, the higher molecular weights lead to longer relaxation times. The results in the figure for the current model (upper blue lines with open circle and triangles) illustrate that relaxations occur much more slowly in this system than in the prior AAA-1 model or in an earlier 3-component model asphalt. This suggests a higher viscosity as a function of temperature.

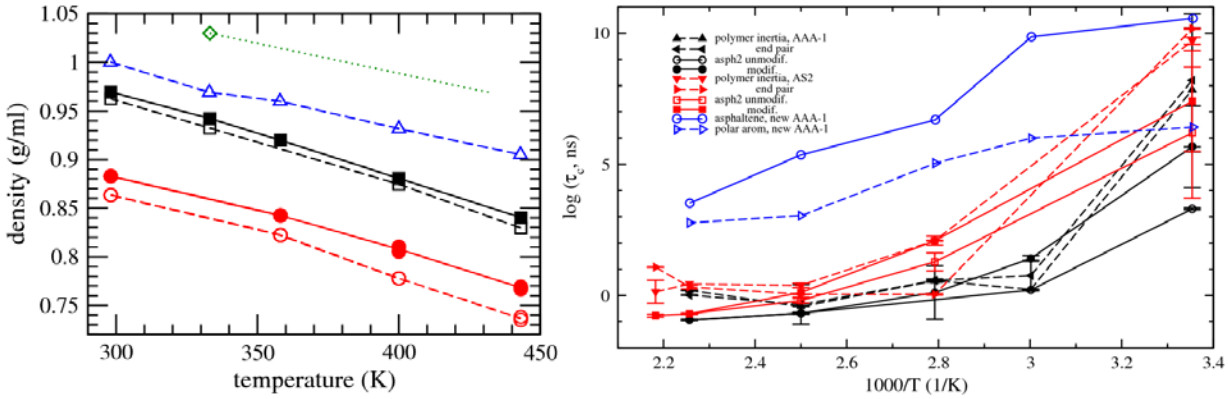


Figure: results from molecular dynamics simulations on next-generation model asphalt AAA-1. **(Left)** Density results (blue with triangles) indicate better agreement with experiment (green diamond) than for the prior AAA-1 model (black squares, Zhang and Greenfield, 2008) or an older 3-component model asphalt (red circles, Zhang and Greenfield, 2007a). The slope of the experimental data (dotted green line) is obtained from the experimental thermal expansion coefficient. **(Right)** Rotational relaxation time for the next-generation model (blue) compared to results for the prior AAA-1 model (black) and 3-component model (red) (Zhang and Greenfield, 2007b, 2010).

***Subtask F3a-4. Simulate changes in asphalt dynamics after inducing representations of chemical and/or physical changes to a model asphalt (URI)***

Nothing to report.

***Subtask F3a-5. Molecular mechanics simulations of asphalt-aggregate interfaces (VT)***

This subtask focuses on modeling of binder-aggregate compatibility, the interface shear behavior, the interface tensile behavior, and moisture damage using molecular dynamics.

Work Done This Quarter

The methodology has been developed to simulate the asphalt-aggregate interface behavior using MD code LAMMPS. The asphalt binder is modeled using an average molecular structure and aggregates are modeled as a crystal structure. The moisture damage effect is modeled by placing a water molecule between the aggregate and binder molecules.

Significant Problems, Issues and Potential Impact on Progress

None

Work Planned Next Quarter

The major work in next quarter will focus on applying the methods developed for evaluating the aggregate-binder compatibility, the shear and tensile strength between the aggregate and binder, and assessing the major influencing factors to moisture damage.

***Subtask F3a-6. Modeling of fatigue behavior at atomic scale (VT, NIST)***

This subtask includes atomistic scale exploration of fatigue mechanism, nano pore creation process, modeling of fatigue in coupled physical-mechanical factors, modeling of stiffness reduction at macro scale, and modeling of binder-mastic-mixture fatigue relationship.

Work Done This Quarter

The newly developed fatigue test for binder and mastics is modeled using a Finite Element Method (FEM) with an elastoplastic model (Wang, 2010). Major components (binder and aggregates) of asphalt mixture are modeled using different constitutive models. The aggregates and fillers are modeled as linear elastic. The asphalt binder is modeled as elasto-plastic. In the mesh generation of asphalt mastic and mixture specimens, 2D x-ray scanned images are used to reconstruct the 3D internal structure. The elements belonging to different components are identified and assigned different material properties. An assumption is made that fatigue damage only happened in asphalt binder but not in aggregates and fillers. The hardening behavior of the asphalt binder at low temperature is described using a combined isotropic/kinematic hardening model developed by Lemaitre and Chaboche (1990). The model consists of two components: a nonlinear kinematic hardening component, which describes the translation of the yield surface in stress space through the backstress; and an isotropic hardening component, which describes the change of the equivalent stress defining the size of the yield surface as a function of plastic deformation. The elastic modulus of the asphalt binder is measured using direct tension test at a desired temperature. The parameters of the kinematic and isotropic hardening model are determined using the first half cycle data of the fatigue test for asphalt binder. To address the

fatigue damage caused by cyclic loading, or the stiffness decrease during fatigue process, a damage model proposed by Darveaux (1997) was adopted. The parameter analysis of the model is conducted and calibrated by comparing the fatigue simulation results and fatigue test results. To avoid the extremely high computational cost during the fatigue simulation, direct cyclic analysis is used to obtain the response of the structure after a large number of loadings.

Significant Problems, Issues and Potential Impact on Progress

None

Work Planned Next Quarter

The next quarter will focus on associating the nano pore creation process with fatigue mechanism, and the relationship between the modulus reduction and damage mechanisms in a view using fundamental mechanics.

Cited References

Darveaux, R., 2000, Effect of Simulation Methodology on Solder Joint Crack Growth Correlation. *Proc.* 50th Electronic Components and Technology Conference, 2000, 1048-1058.

Lemaitre, J., and J. L., Chaboche, 1990, *Mechanics of Solid Materials*. Cambridge University Press, Cambridge, UK.

Wang, D., 2011, A Micro-scale Method to Associate the Fatigue Properties of Asphalt Binder, Mastic and Mixture. Dissertation, Doctor of Philosophy in Civil and Environmental Engineering.

***Subtask F3a-7. Modeling of moisture damage (VT)***

This subtask focuses on investigating the moisture damage mechanisms at atomistic scale, void structure and mesoscale damage due to excess pore water pressure, and binder-mastics-mixture moisture damage using a multiscale approach.

Work Done This Quarter

The excess pore water induced damage to asphalt mixture is modeled using a poroelasticity model based on mixture theory formulations implemented on FEM code ABAQUS. Different influencing factors including elasticity modulus, loading magnitude, boundary conditions, permeability and vehicle speeds have been assessed.

Significant Problems, Issues and Potential Impact on Progress

None

Work Planned Next Quarter

The next quarter will focus on the modeling of moisture damage mechanisms at atomistic scale for asphalt binder.

***Subtask F3a-8. ab initio Calculations of Asphalt Molecular Structures and Correlation to Experimental Physico-Chemical Properties of SHRP Asphalts (WRI-TUDelft)***

Work Done This Quarter

*Entropy Production in Damage/Healing Processes*

A thermodynamic model of damage-healing of asphalt binder has been derived based on non-equilibrium thermodynamic principles and studied by nano-lithography with atomic force microscopy.

*Fracture-Healing Reaction Kinetics*

Phase-field expressions which describe both damage and healing processes may be exploited to derive an expression for the kinetic rate process of damage-healing based on self-ordering non-equilibrium thermodynamics, (Nicolis and Prigogine 1977). Damage-self-healing in asphalt is defined here as a thermally activated rate process, described by the net free energy functional.

Efforts are presently underway to run finite element simulations of damage-healing processes based on the theoretical approach developed here.

*Experimental Approach:*

Asphalt thin films, 3 to 4 micron in thickness, were spin-cast from solution, thermally annealed, then rapidly freeze fractured in liquid nitrogen. Films were imaged with an optical microscope and atomic force microscopy. Rates and efficiencies of change in morphology, in terms of healing of freeze-fracture induces cracking, over time as a function of asphalt crude source were studied for several SHRP asphalts.

Figure F3a-8.1 depicts a series of optical microscope images of asphalt AAG-1, photographed before and each day after freeze-fracturing for a total of 10 days, for sample storage at ambient conditions (~25°C). Figures F3a-8.2 and F3a-8.3 also depict AAG-1, directly after freeze-fracturing (LEFT), and (RIGHT) after 10 days storage at ambient conditions (~25°C), and after 30 days storage at ambient conditions (~7.6°C), as depicted in F3a-8.3 (RIGHT).

Figure F3a-8.1. AAG-1, photographed before and each day after freeze-fracturing for a total of 10 days, storage at ambient conditions (~25°C).

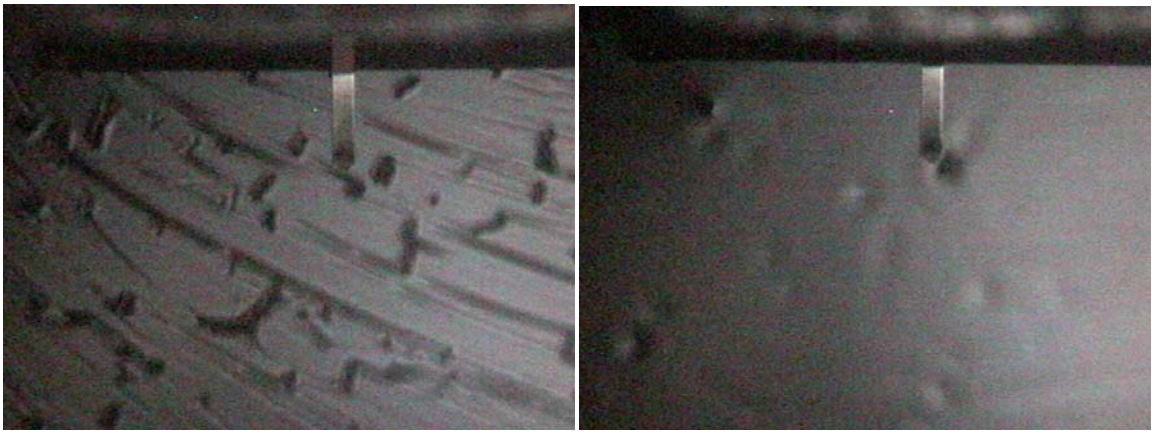

Figure F3a-8.2. AAG-1, photographed directly after freeze-fracturing (LEFT), and (RIGHT) after 10 days storage at ambient conditions (~25°C).

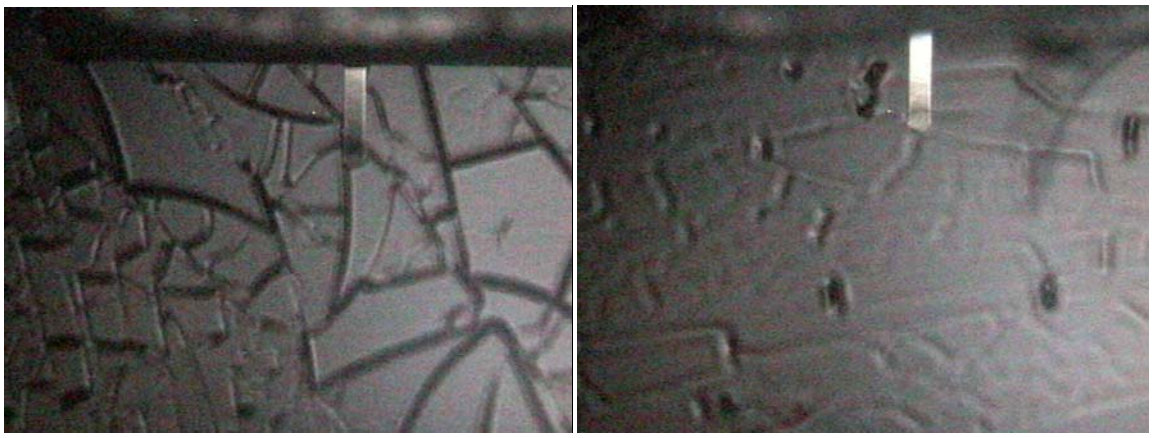

Figure F3a-8.3. AAG-1, photographed directly after freeze-fracturing (LEFT), and (RIGHT) after 30 days storage at ambient conditions (~7.6°C).

Similar sets of images are depicted for SHRP asphalts AAA-1, figures F3a-8.4 & 5, and AAD-1, figures F3a-8.6 & 7. Of the three asphalts considered here, asphalt AAG-1 appears to heal most efficiently. These findings are in agreement with findings reported by Little et al. (1998, 1999); Kim et al. (2001); Williams et al. (2001); Lytton et al. (2001), which observed that asphalt test specimens in cyclic loading experiments, (conducted by dynamical mechanical analysis (DMA), regained strength when rest periods were introduced during the testing protocol as compared with the same number of load cycles subjected to a test sample where rest periods were not introduced.

Figure F3a-8.4. AAA-1, photographed directly after freeze-fracturing (LEFT), and (RIGHT) after 10 days storage at ambient conditions (~25°C).

Figure F3a-8.5. AAA-1, photographed directly after freeze-fracturing (LEFT), and (RIGHT) after 30 days storage at ambient conditions (~7.6°C).

Figure F3a-8.6. AAD-1, photographed directly after freeze-fracturing (LEFT), and (RIGHT) after 10 days storage at ambient conditions (~25°C).

Figure F3a-8.7. AAD-1, photographed directly after freeze-fracturing (LEFT), and (RIGHT) after 30 days storage at ambient conditions (~7.6°C).

*Interpretation of Results:*

Thermally activated rate processes of damage/self-healing processes in asphalt (freeze-fractured thin films for example) described by the free energy functional, could be defined by activation energies $E_a^+$ and $E_a^-$, with pre-exponential factors $\xi^+$ and $\xi_-$ which may serve to rank asphalts in terms of stored energy to do work in either damage or healing processes.

The estimated percent change in morphology at two temperatures, as depicted in figure F3a-8.2 to F3a-8.7 are listed in table F3a-8.1. Activation energies of healing are calculated from rate constants and temperatures. AAG-1 has the lowest activation energy and appears to heal most efficiently. Asphalts AAA-1 and AAD-1 have the highest values in $E_a$, and thus appear to heal less efficiently compared to AAG-1. It is worth noting that both asphalts AAA-1 and AAD-1 are much less viscous compared to AAG-1, yet, AAG-1 is the best healer of these three asphalts, suggesting that other mechanism than flow may be involved in the healing process considered here. Overall values in $E_a$ are observed to be low. Additional studies will be considered to help interpret the results discussed here.

Table F3a-8.1. Estimated percent change in morphology to restored state and healing rate constants, $k^+ = \varphi_j \left( \partial \varphi_j / \partial t \right)$ at two temperatures, and activation energies of healing.

| Asphalt | %ΔMorphology $\partial \varphi_j$ (25°C) 10-days | %ΔMorphology $\partial \varphi_j$ (7.6°C) 30-days |
|---|---|---|
| AAA-1 | 100% | 30 |
| AAD-1 | 80 | 30 |
| AAG-1 | 90 | 50 |

| Asphalt | $k^+$(25°C)(%$^2$/day) | $k^+$(7.6°C) (%$^2$/day) | $E_a$ (kJ/mol) |
|---|---|---|---|
| AAA-1 | (1/10)*1=.1 | (.3/30)*1=.01 | -3.6 |
| AAD-1 | (.8/10)*1=.08 | (.3/30)*1=.01 | -2.8 |
| AAG-1 | (.9/10)*1=.09 | (.5/10)*1=.05 | -1.6 |

Significant Problems, Issues and Potential Impact on Progress

None

Work Planned Next Quarter

The present theory will be employed to interpret scratch testing by AFM nano-lithography in cooperation with Subtask M2a-2.

References

Kim, Y. R., Lee, H.-H., and D. N. Little, 2001, *Microdamage Healing in Asphalt and Asphalt Concrete, Volume IV: A Viscoelastic Continuum Damage Fatigue Model of Asphalt Concrete with Microdamage Healing*, Publication No. FHWA-RD-98-144. U. S. Department of Transportation, Federal Highway Administration, McLean, VA.

Kyu, T., Mehta, R. and Chin, H-W., 2000. Spatiotemporal Growth of Faceted and Curved Single Crystals. *Phys. Rev. E.,* 61 (4), 4161-4170.

Little, D. N., R. L. Lytton, and D. Williams, 1998, "Propagation and Healing of Microcracks in Asphalt Concrete and their Contributions to Fatigue," in *Asphalt Science and Technology*, Usmani, A., Editor, Marcel Dekker, Inc., New York, p. 149-195.

Little, D. N., R. L. Lytton, D. Williams, and Y. R. Kim, 1999, Analysis of the Mechanism of Microdamage Healing Based on Application of Micromechanics First Principles of Fracture and Healing. *Journal of the Association of Asphalt Paving Technologists*, 68: 501-542.

Lytton, R. L., C. W. Chen and D. N. Little, 2001, *Microdamage Healing in Asphalt and Asphalt Concrete, Volume III: A Micromechanics Fracture and Healing Model for Asphalt Concrete*, FHWA-RD-98-143. Federal Highway Administration, U. S. Department of Transportation, McLean, VA.

Mehta, R., W Keawwattana, and T. Kyu, 2004a, Growth Dynamics of Isotactic Polypropylene Single Crystals During Isothermal Crystallization from a Miscible Polymeric Solvent. *J. Chem. Phys*., 120 (8), 4024-4031.

Mehta, R., W. Keawwattana, A. L. Guenthner, and T. Kyu, 2004b, Role of Curvature Elasticity in Sectorization and Ripple Formation During Melt Crystallization of Polymer Single Crystals. *Phys. Rev. E.,* 69, 061802.

Mullins, O. C., 2010, The Modified Yen Model. *Energy Fuels*, 24, 2179-2207.

Nicolis, G., and I. Prigogine, 1977, *Self-Organization in Nonequilibrium Systems: From Dissipative Structures to Order through Fluctuations*. John Wiley & Sons, Inc., New York.

Williams, D., D. N. Little, R. L. Lytton, Y. R. Kim, and Y. Kim, 2001, *Microdamage Healing in Asphalt and Asphalt Concrete, Volume II: Laboratory and Field Testing to Assess and Evaluate Microdamage and Microdamage Healing*, Publication No. FHWA-RD-98-142, U. S. Department of Transportation, Federal Highway Administration, McLean, VA.

Xu, H., R. Matkar, and T. Kyu, 2005, Phase-field Modeling on Morphological Landscape of Isotactic Polystyrene Single Crystals. *Phys. Rev. E.,* 72, 011804.

Zhang, L., and M. L. Greenfield, 2007, Analyzing Properties of Model Asphalts using Molecular Simulation. *Energy Fuels*, 21, 1712-1716.

Zhang, L., and M. L. Greenfield, 2007, Relaxation Time, Diffusion, and Viscosity Analysis of Model Asphalt Systems using Molecular Simulation. *J. Chem. Phys.*, 127, 194502.

Zhang, L., and M. L. Greenfield, 2008, Effects of Polymer Modification on Properties and Microstructure of Model Asphalt Systems. *Energy Fuels*, 22, 3363-3375.

Zhang, L., and M. L. Greenfield, 2010, Rotational Relaxation Times of Individual Compounds within Simulations of Molecular Asphalt Models. *J. Chem. Phys.*, 132, 184502.

**Work Element F3b: Micromechanics Model**

***Subtask F3b-1: Model Development (TAMU, NCSU, UNL)***

Work Done This Quarter

*Cohesive Zone Model*

During this quarter we have mainly progressed towards the following activities:

- We have improved the cohesive zone model, which has been developed in the form of User ELement (UEL) codes, to account for the effects of damage accumulation during subcritical cyclic loading. This is considered a significant feature to model fatigue damage and failure. The irreversible constitutive relation in the cohesive zone model is represented in such a way that unloading and subsequent reloading follow the same path on the bilinear traction-separation curve.
- We have also tested the cohesive zone model for general HMA microstructure where cohesive zone elements are randomly embedded to simulate realistic mixed-mode crack growth. Parametric analyses of the microstructure model incorporated with cohesive zone fracture were conducted by varying key fracture properties (i.e., cohesive strength, fracture energy, and a ratio of mode I fracture energy to mode II fracture energy).

The new implementation of the irreversibility into the current cohesive zone model has been verified by testing a simple uniaxial bar where a cohesive element is placed between two volumetric elements. A saw-tooth cyclic loading history with increasing amplitude was applied to the uniaxial bar to simulate progressive fatigue damage. Simulation results were in good agreement with analytical solutions. Both numerical and analytical results identically presented that reloading followed the same path of last unloading curve when the unloading-reloading cycle is within the subcritical region.

For the parametric analyses of the cohesive zone model implemented, three-point bending beam testing of a HMA microstructure (aggregate particles surrounded by asphalt matrix phase) was simulated. Different sets of fracture properties of matrix phase were attempted to demonstrate the effect of material-specific properties and fracture characteristics on the overall HMA mixture performance. Simulation results presented that overall HMA performance is quite sensitively governed by material-specific characteristics such as the fracture properties of asphalt matrix

phase. It clearly implies that the cohesive zone fracture engine can properly model material-dependent fracture performance and resistance potential of heterogeneous asphalt mixtures.

*Lattice Micromechanical Model*

Based on the research during the previous quarters, it is evident that shape of air voids plays an important role in the viscoelastic properties of the asphalt specimens. Efforts to capture realistic shapes have begun in the previous quarter. Image processing techniques have been applied to X-ray tomography images obtained from the study of Kutay et al. (2010) to extract the shape of air voids, resulting in black and white images with black areas representing the air voids.

The efforts in current quarter have been focused on studying the shapes extracted from processed X-ray images. Several images from different cores have been processed and it is found that different air voids have different shape characteristics and size distributions. The shapes of several air void particles have been analyzed to extract detailed shape parameters. The lower order parameters (such as dimension, orientation, aspect ratio) were found to be insufficient to fully describe the shape of the air voids.

After an extensive study, as expected, it is found that the air void shape is strongly dependent on the surrounding aggregate structure. Consistent with this finding, a preliminary virtual fabrication algorithm has been developed to generate air voids, given the specific aggregate microstructure. A sample result from this algorithm is given in figure F3b-1.1. Subsequent work will focus on finding better parameters for the algorithm to make the shapes more realistic and, more importantly, accurately capture the effect of air voids on stiffness reduction.

*Continuum Damage to Fracture*

The phase angle change during the cyclic loading has been investigated for better understanding of localization and fracture mechanism. In a typical cyclic test of asphalt concrete, the phase angle usually experiences increasing first and then followed by a drop. The “drop” point has been widely taken as the onset of localization in experimental analyses. A quantitative analysis has been done for the increasing part, and it is concluded that this increase is due to both temperature change and damage. Subsequent work will focus on understanding the drop of phase angle.

In parallel to the above study, the nonlocal computational framework is being enhanced to incorporate viscoelastic continuum damage.

Significant Problems, Issues and Potential Impact on Progress

None.

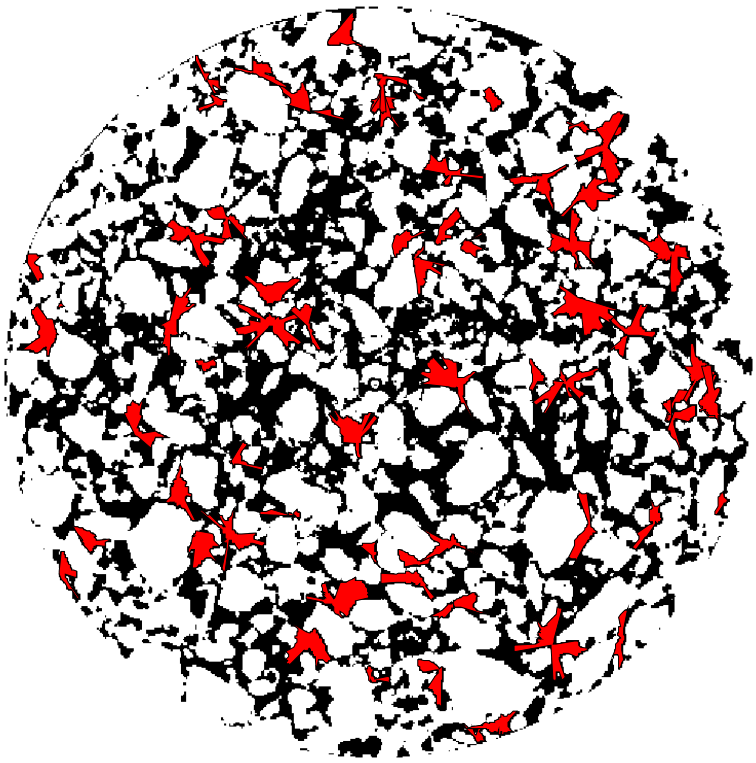

Figure F3b-1.1. Virtually fabricated air voids on a real microstructure from Kutay et al. (2010).

Work Planned Next Quarter

*Cohesive Zone Model*

- In the next quarter we will primarily devote our efforts to model validation and a final report.

*Lattice Micromechanical Model*

- Refining the shapes of the air voids generated using the new algorithm.
- Evaluating the stiffness using the realistic virtually fabricated microstructure.

*Continuum Damage to Fracture*

- Further investigation of the phase angle drop and understanding of localization.
- Incorporate the VECD model into nonlocal computational framework.

Cited Reference

Kutay, M. Emin, Hande I. Ozturk, and Nelson Gibson, "3D Micromechanical Simulation of Compaction of Hot Mix Asphalt Using Real Aggregate Shapes Obtained from X-ray CT". *Proc.*, Pavements and Materials: Characterization and Modeling Symposium at EMI, 2010.

### *Subtask F3b-2: Account for Material Microstructure and Fundamental Material Properties (TAMU)*

Work Done This Quarter

The reader is referred to work elements F1c and F1d.

## Work Element F3c: Development of Unified Continuum Model (TAMU)

Work Done This Quarter

See M4c for details on the progress in the development of the continuum-based moisture-induced damage mode. Also see F1d-8 on the development of the continuum-based micro-damage healing model. We have completed the calibration and validation of the nonlinear viscoelastic and viscoplastic constitutive models in PANDA using the ALF laboratory data from NCState based on the compression data under different temperatures. The data included tension/compression dynamic modulus test at different temperatures and frequencies, compression creep-recovery tests under different confinements and stress loading conditions. Moreover, a systematic procedure has been developed for calibrating the viscodamage constitutive model based on ALF tension data.

Significant Results

We finalized the method to obtain the model parameters and demonstrated the ability of the model to describe the results of compression and extension tests at various testing conditions.

Significant Problems, Issues and Potential Impact on Progress

The process of obtaining the model parameters for the extension tests was more time consuming than we originally planned. Therefore, we fell slightly behind on conducting simulations of the structural response of the ALF sections.

Work Planned Next Quarter

The focus of the coming quarter is on calibrating the viscodamage model based on the extension cyclic tests and uniaxial monotonic tensile tests. Furthermore, we will continue examining several methods that have been used in the past in the simulations of fatigue tests. The objective is to determine if these methods can be used to reduce the time needed to apply loads in the

structural finite element model. We will also conduct simulations to validate the model against the structural response of the various sections of the ALF experiment.

**Continuum-based Model for Aging**

Work Done This Quarter

This task was temporarily suspended in this quarter and resources were diverted to the task on the validation of PANDA against the ALF rutting tests. We expect to resume work on this task as soon as we complete the validation of PANDA against the ALF data.

Significant Results

There are no significant results for this quarter.

Significant Problems, Issues and Potential Impact on Progress

Although this task is temporarily suspended, we expect to resume the task in near future as soon we have the aging data from the ARC 2x2 asphalt mixture testing.

Work Planned Next Quarter

We expect to resume work on this task as outlined in the fifth year work plan.

## TABLE OF DECISION POINTS AND DELIVERABLES FOR FATIGUE

| Name of Deliverable | Type of Deliverable | Description of Deliverable | Original Delivery Date | Revised Delivery Date | Reason for changes in delivery date |
|---|---|---|---|---|---|
| F1a: Cohesive and Adhesive Properties (TAMU) | Draft Report | Draft Report on Cohesive and Adhesive Properties, 508 compliant | 11/11 | N/A | N/A |
| | Final Report | | 6/30/12 | | |
| F1b-1: Nonlinear viscoelastic response under cyclic loading (TAMU) | Models and Algorithm | A constitutive model that accounts for the nonlinearity and three - dimensional stress state of the material including a method to obtain model constants for asphalt binders. | 3/31/09<br>6/30/10<br>12/31/11 | 3/31/12 | It is more efficient and informative if the three different final reports, models and algorithms are consolidated into a single final report. The work at UT Austin that will make up the final report is 60% complete. |
| | Draft report | | 12/31/08<br>12/31/11 | | |
| | Final report | | 6/30/08<br>3/31/12 | 6/30/12 | |
| F1b-2: Viscoelastic properties under monotonic loading (TAMU) | Draft Report | Documentation of PANDA Models and Validation Including the Method for Analysis of Viscoelastic Properties | 11/11 | N/A | N/A |
| | Final Report (M5, M4c, F1b-1, F1c, F1d-8, F3c, and V3c) | | 3/12 | N/A | N/A |
| F1c: Aging (Unified Continuum Model for Aging) | Draft Report | Draft Report on the aging modeling | 03/12 | N/A | N/A |
| | Final Report (M5, M4c, F1b-1, F1c, F1d-8, F3c, and V3c) | | 3/31/12 | 6/30/12 | |
| F1c-2. Experimental Design | Report | Experimental Design Report | 1/09 | Complete | N/A |

| Name of Deliverable | Type of Deliverable | Description of Deliverable | Original Delivery Date | Revised Delivery Date | Reason for changes in delivery date |
|---|---|---|---|---|---|
| F1d – 1,2,3,4,5a,5b,8: Healing (TAMU) | Models and Algorithm | A mathematical model for self-healing at the micron scale, partial validation of this model, measurement of properties related to this model, measurement of overall healing as a function of damage and rest period, and micro to nano scale evaluation of properties that influence fracture and self-healing | 06/30/11 | 3/31/12 | It is more efficient and informative if the different final reports, models and algorithms are consolidated into a single final report. The final report is based on two theses: the thesis from Texas A&M University is complete and work for the thesis from UT Austin is 70% complete. |
| | Draft report | | 06/30/10<br>06/30/11<br>12/31/11 | | |
| F1d-6: Evaluate relationship between healing and endurance limit of asphalt binders (UWM) | Draft Report | Report summarizing major findings for evaluation of healing of binders by means of cyclic testing with rest periods | 12/11 | N/A | N/A |
| | Final Report | Final report in 508 format on healing characterization of binders and its relation to fatigue performance | 1/12 | 6/12 | Final report submission date moved back to allow at least 6 months between draft and final report submission. |
| F1d-8: Coordinate Form of Healing Parameter with Micromechanics and Continuum Damage Models (TAMU) | Draft Report (M5, M4c, F1b-1, F1c, F1d-8, F3c, and V3c) | Draft Report on the self-healing modeling | 12/11 | | |
| | Final Report (M5, M4c, F1b-1, F1c, F1d-8, F3c, and V3c) | Report on the self-healing modeling | 3/12 | 6/12 | |

| Name of Deliverable | Type of Deliverable | Description of Deliverable | Original Delivery Date | Revised Delivery Date | Reason for changes in delivery date |
|---|---|---|---|---|---|
| F2a-5: Analyze data and propose mechanisms (UWM) | Draft Report | Report summarizing major findings for the effect of modification on asphalt binder performance at high and intermediate temperatures. | 10/11 | N/A | N/A |
| | Final Report | Report in 508 format summarizing major findings for the effect of modification on asphalt binder performance at high and intermediate temperatures | 1/12 | 4/12 | Final report submission date moved back to allow at least 6 months between draft and final report submission. |
| F2d: Structural Characterization of Micromechanical Properties in Bitumen using Atomic Force Microscopy | Protocol for Measuring Viscoelastic Properties Using AFM | Protocol for preparing samples and taking measurements in AASHTO format – Protocol development complete, AASHTO format planned for 5/30/11 | 7/31/10 | N/A | N/A |
| | Evaluation of Impact of Aging and Moisture Conditioning | Complete | 12/15/10 | N/A | N/A |
| | Final Research Report | | 2/28/12 | N/A | N/A |
| F2e-2: Selection of Testing Protocols (UWM) | Draft Report | Report on the development and implementation of the Binder Yield Energy (BYET) test and the Linear Amplitude Sweep Test (LAS) | 4/09 | Complete | N/A |
| | Final Report | | 7/09 | | |
| | Draft Report | | 4/10 | | |
| | Final Report | | 7/10 | | |
| F2e-4: Verification of Surrogate Fatigue Test (UWM) | Draft Report | Correspond to reports in F2e-2 | 10/10 | Complete | N/A |
| | Final Report | | 1/11 | | |
| F2e-6: Recommendations for Use in Unified Fatigue Damage Model (UWM) | Draft Report | Report summarizing major findings for each subtask. The report includes: evaluation of correlations between binder and mixture fatigue performance, comparison between binder fatigue testing procedures, verification/validation of LAS test | 11/11 | N/A | N/A |
| | Final Report | Final report in 508 format on the development and implementation of the Linear Amplitude Sweep (LAS) Test. It includes the latest AASHTO standard. | 1/12 | 5/12 | Final report submission date moved back to allow at least 6 months between draft and final report submission. |

| Name of Deliverable | Type of Deliverable | Description of Deliverable | Original Delivery Date | Revised Delivery Date | Reason for changes in delivery date |
|---|---|---|---|---|---|
| F3b-1: Micromechanics Model Development (Fatigue) | Models and Algorithm | Cohesive zone fracture modeling of asphalt mixtures considering inelasticity, nonlinearity, rate-dependent fracture, and mixture microstructure: modeling methodology, constitutive theory, testing protocols, test data, model simulation/calibration/validation, user element (UEL) codes in ABAQUS, and user-friendly manuals.<br>Multiscale modeling of asphaltic mixtures and pavements: modeling methodology, constitutive theory, and parametric analyses of the model. | 3/31/11 | No change | N/A |
| | Draft report | | 06/30/11 | 9/30/11 | A little more time is necessary for model validation with lab testing. |
| | Final report | | 12/31/11 | No change | N/A |
| F3c: Development of Unified Continuum Model | PANDA Workshop | Workshop on PANDA Models and Validation Results | 8/11 | N/A | N/A |
| | Draft Report | Documentation of PANDA Models and Validation | 11/11 | N/A | N/A |
| | Final Report | | 3/12 | 6/30/12 | N/A |
| | UMAT Material | PANDA Implemented in Abaqus | 3/12 | N/A | N/A |

| | Fatigue Year 4 | Year 4 (4/10-3/11) | | | | | | | | | | | | Team |
|---|---|---|---|---|---|---|---|---|---|---|---|---|---|---|
| | | 4 | 5 | 6 | 7 | 8 | 9 | 10 | 11 | 12 | 1 | 2 | 3 | |
| **Material Properties** | | | | | | | | | | | | | | |
| **F1a** | **Cohesive and Adhesive Properties** | | | | | | | | | | | | | |
| F1a-1 | Critical review of literature | | | | | | | | | | | | | TAMU |
| F1a-2 | Develop experiment design | | | | | | | | | | | | | |
| F1a-3 | Thermodynamic work of adhesion and cohesion | | | | | | | | | | | | | |
| F1a-4 | Mechanical work of adhesion and cohesion | | | D | | | F | | | | | | | |
| F1a-5 | Evaluate acid-base scale for surface energy calculations | | | | | | | | | | | | | |
| **F1b** | **Viscoelastic Properties** | | | | | | | | | | | | | |
| F1b-1 | Separation of nonlinear viscoelastic deformation from fracture energy under cyclic loading | | | M&A,F,JP | | | JP | | | | | | | TAMU |
| F1b-2 | Separation of nonlinear viscoelastic deformation from fracture energy under monotonic loading | | | | | | | | | | | | JP | |
| **F1c** | **Aging** | | | | | | | | | | | | | |
| F1c-1 | Critical review of binder oxidative aging and its impact on mixtures | | | | | | | | | | | | | TAMU |
| F1c-2 | Develop experiment design | | | | | | | | | | | | | |
| F1c-3 | Develop transport model for binder oxidation in pavements | | | | P | | | | | JP | P, JP | | | |
| F1c-4 | Effect of binder aging on properties and performance | | | | | | | | | | P, JP | | | |
| F1c-5 | Polymer modified asphalt materials | | | | P | | | | | | | | | |
| **F1d** | **Healing** | | | | | | | | | | | | | |
| F1d-1 | Critical review of literature | | | | | | | | | | | | | TAMU |
| F1d-2 | Select materials with targeted properties | | | | | | | | | | | | | TAMU |
| F1d-3 | Develop experiment design | | | | | | | | | | | | | TAMU |
| F1d-4 | Test methods to determine properties relevant to healing | | | D | | | F | | | | | | | TAMU |
| F1d-5 | Testing of materials | | | | | | JP | | | | | | | TAMU |
| F1d-6 | Evaluate relationship between healing and endurance limit of asphalt binders | | | | | | JP | | | | P | | | UWM |
| F1d-7 | Coordinate with AFM analysis | JP | | | | | | | | | | | | WRI |
| F1d-8 | Coordinate form of healing parameter with micromechanics and continuum damage models | | | | | | | | | | | | | TAMU |
| **Test Methods** | | | | | | | | | | | | | | |
| **F2a** | **Binder tests and effect of composition** | | | | | | | | | | | | | |
| F2a-1 | Analyze Existing Fatigue Data on PMA | | | | | | | | | | | | | UWM |
| F2a-2 | Select Virgin Binders and Modifiers and Prepare Modified Binder | | | | | | | | | | | | | |
| F2a-3 | Laboratory Aging Procedures | | | | | | | | | | | | | |
| F2a-4 | Collect Fatigue Test Data | | | | | JP | | | | | DP, P | | JP | |
| F2a-5 | Analyze data and propose mechanisms | | | | | | | | | P | | | | |
| **F2b** | **Mastic testing protocol** | | | | | | | | | | | | | |
| F2b-1 | Develop specimen preparation procedures | | | | F | | | | | | | | | TAMU |
| F2b-2 | Document test and analysis procedures in AASHTO format | | | | F | | | | | | | | | |
| **F2c** | **Mixture testing protocol** | | | | | | | | | | | | | |
| **F2d** | **Tomography and microstructural characterization** | | | | | | | | | | | | | |
| F2d-1 | Micro scale physicochemical and morphological changes in asphalt binders | | | | | | | | | | | | JP | TAMU |
| **F2e** | **Verify relationship between DSR binder fatigue tests and mixture fatigue performance** | | | | | | | | | | | | | |
| F2e-1 | Evaluate Binder Fatigue Correlation to Mixture Fatigue Data | | | | | | | | | | | | | UWM |
| F2e-2 | Selection of Testing Protocols | | D | | F | | | | | | | | | |
| F2e-3 | Binder and Mixture Fatigue Testing | | | | | | | | | | | | | |
| F2e-4 | Verification of Surrogate Fatigue Test | | | | | | | D | | | F, DP | | | |
| F2e-5 | Interpretation and Modeling of Data | | | | JP | | | | | | | | M&A | |
| F2e-6 | Recommendations for Use in Unified Fatigue Damage Model | | | | | | | | | | P | | | |
| **Models** | | | | | | | | | | | | | | |
| **F3a** | **Asphalt microstructural model** | | | | | | | | | | | | | WRI |
| **F3b** | **Micromechanics model** | | | | | | | | | | | | | |
| F3b-1 | Model development | | | | JP | | | | | | P | | | TAMU |
| F3b-2 | Account for material microstructure and fundamental material properties | | | | | | | | | | | | | |
| **F3c** | **Develop unified continuum model** | | | | | | | | | | | | | |
| F3c-1 | Analytical fatigue model for mixture design | | | | | | | | | | | | | TAMU |
| F3c-2 | Unified continuum model | | | | | | | | | JP | | M&A | | |
| F3c-3 | Multi-scale modeling | | | | | | | | JP | | | | M&A | |
| | Lattice Model | | DP | | DP,JP | | | | | | | | | NCSU |
| | Continuum Damage to Fracture | | | DP | | | | JP | | | | | | |

**LEGEND**

| **Deliverable codes** | **Deliverable Description** |
|---|---|
| D: Draft Report | Report delivered to FHWA for 3 week review period. |
| F: Final Report | Final report delivered in compliance with FHWA publication standards |
| M&A: Model and algorithm | Mathematical model and sample code |
| SW: Software | Executable software, code and user manual |
| JP: Journal paper | Paper submitted to conference or journal |
| P: Presentation | Presentation for symposium, conference or other |
| DP: Decision Point | Time to make a decision on two parallel paths as to which is most promising to follow througjh |
| [x] | Indicates completion of deliverable x |

Work planned

Work completed

Parallel topic

| | Fatigue Year 2 - 5 | Year 2 (4/08-3/09) | | | | Year 3 (4/09-3/10) | | | | Year 4 (04/10-03/11) | | | | Year 5 (04/11-03/12) | | | | Team |
|---|---|---|---|---|---|---|---|---|---|---|---|---|---|---|---|---|---|---|
| | | Q1 | Q2 | Q3 | Q4 | Q1 | Q2 | Q3 | Q4 | Q1 | Q2 | Q3 | Q4 | Q1 | Q2 | Q3 | Q4 | |
| **Material Properties** | | | | | | | | | | | | | | | | | | |
| **F1a** | **Cohesive and Adhesive Properties** | | | | | | | | | | | | | | | | | |
| F1a-1 | Critical review of literature | | | JP | | | | | | | | | | | | | | TAMU |
| F1a-2 | Develop experiment design | | | | | | | | | | | | | | | | | |
| F1a-3 | Thermodynamic work of adhesion and cohesion | | | | | | | | | | | | | | | | | |
| F1a-4 | Mechanical work of adhesion and cohesion | | | | | | JP | | | D | F | | | | | | | |
| F1a-5 | Evaluate acid-base scale for surface energy calculations | | | | | | | | | | | | | | JP | | | |
| **F1b** | **Viscoelastic Properties** | | | | | | | | | | | | | | | | | |
| F1b-1 | Separation of nonlinear viscoelastic deformation from fracture energy under cyclic loading | | | D,JP | M&A | | | | JP | &A,F,J | JP | | P | | JP,M&A,D | | F | TAMU |
| F1b-2 | Separation of nonlinear viscoelastic deformation from fracture energy under monotonic loading | | | JP | M&A | | | | JP | | | | JP | | JP,M&A,D | | F | |
| **F1c** | **Aging** | | | | | | | | | | | | | | | | | |
| F1c-1 | Critical review of binder oxidative aging and its impact on mixtures | | | | | | | | | | | | | | | | | TAMU |
| F1c-2 | Develop experiment design | | | D | | F | | | | | | | | | | | | |
| F1c-3 | Develop transport model for binder oxidation in pavements | | P | | P, JP | | P | | P, JP | | P(2), JP | JP(2) | | | | D, M&A | F | |
| F1c-4 | Effect of binder aging on properties and performance | | | | JP, P | | JP | D | F | | | | | | JP | D | F | TAMU |
| F1c-5 | Polymer modified asphalt materials | | | | | | P | | | | P | | | | | D | F | |
| **F1d** | **Healing** | | | | | | | | | | | | | | | | | |
| F1d-1 | Critical review of literature | | | | | | | | | | | | | | | | | TAMU |
| F1d-2 | Select materials with targeted properties | | | | | | | | | | | | | | | | | TAMU |
| F1d-3 | Develop experiment design | | | | | | | | | | | | | | | | | TAMU |
| F1d-4 | Test methods to determine properties relevant to healing | | | JP | | | | | JP | D | F | | | | | | | TAMU |
| F1d-5 | Testing of materials | | | | | | JP | | | | JP | | | M&A,D | JP, F | | | TAMU |
| F1d-6 | Evaluate relationship between healing and endurance limit of asphalt binders | DP | | | | DP | JP | DP | | | JP | | P | | JP | D | F | UWM |
| F1d-7 | Coordinate with AFM analysis | | | | | | | | | JP | | | | | | | | WRI |
| F1d-8 | Coordinate form of healing parameter with micromechanics and continuum damage models | | | | | | | | | | | | | | | JP,D | F | TAMU |
| **Test Methods** | | | | | | | | | | | | | | | | | | |
| **F2a** | **Binder tests and effect of composition** | | | | | | | | | | | | | | | | | |
| F2a-1 | Analyze Existing Fatigue Data on PMA | | DP | | | | | | | | | | | | | | | UWM |
| F2a-2 | Select Virgin Binders and Modifiers and Prepare Modified Binder | | DP | | | | | | | | | | | | | | | |
| F2a-3 | Laboratory Aging Procedures | | | | | | | | | | | | | | | | | |
| F2a-4 | Collect Fatigue Test Data | | P | | JP | | P | | P | | | P, DP, JP | | | | | | |
| F2a-5 | Analyze data and propose mechanisms | | | | P | | | P | | | | P | | | P | D | F | |
| **F2b** | **Mastic testing protocol** | | | | | | | | | | | | | | | | | |
| F2b-1 | Develop specimen preparation procedures | | D | | | | | | | | F | | | | | | | TAMU |
| F2b-2 | Document test and analysis procedures in AASHTO format | | D | | | | | | | | F | | | | | | | |
| **F2c** | **Mixture testing protocol** | | D, JP | | P, JP | JP | P | P | JP | P | P | JP | P(3), JP | | | | | |
| **F2d** | **Tomography and microstructural characterization** | | | | | | | | | | | | | | | | | |
| F2d-1 | Micro scale physicochemical and morphological changes in asphalt binders | | | | | | JP | | | | | JP | | | | | | TAMU |
| **F2e** | **Verify relationship between DSR binder fatigue tests and mixture fatigue performance** | | | | | | | | | | | | | | | | | |
| F2e-1 | Evaluate Binder Fatigue Correlation to Mixture Fatigue Data | | | | | | | | | | | | | | | | | UWM |
| F2e-2 | Selection of Testing Protocols | | | | | DP, D | F | | | D | F | | | | | | | |
| F2e-3 | Binder and Mixture Fatigue Testing | | | | | | | | | | | | | | | | | |
| F2e-4 | Verification of Surrogate Fatigue Test | | | | | | | | | | | D | F, DP | | | | | |
| F2e-5 | Interpretation and Modeling of Data | | JP | | P | | JP | | P | | JP | | M&A | | | | | |
| F2e-6 | Recommendations for Use in Unified Fatigue Damage Model | | | | | | | | | | | | P | | | D | F | |
| **Models** | | | | | | | | | | | | | | | | | | |
| **F3a** | **Asphalt microstructural model** | | | | | | | JP | | | | | | | | M&A | F | WRI |
| **F3b** | **Micromechanics model** | | | | | | | | | | | | | | | | | |
| F3b-1 | Model development | | | | JP | | | | JP | | JP | | M&A | D | DP | F, SW | | TAMU |
| F3b-2 | Account for material microstructure and fundamental material properties | | | | | | | | | | | | | D | | F | | |
| **F3c** | **Develop unified continuum model** | | | | | | | | | | | | | | | | | |
| F3c-1 | Analytical fatigue model for mixture design | | | | | | | | | | | | | | M&A,D | | F | TAMU |
| F3c-2 | Unified continuum model | | | JP | | | | JP | | | | JP | M&A | D | DP | F, SW | | |
| F3c-3 | Multi-scale modeling | | | | | | | | | | | JP | M&A | D | | F | | |
| | Lattice Model | | | | | | | | | DP | DP, JP | | | | | | | NCSU |
| | Continuum Damage to Fracture | | | | | | | | | DP | | JP | | | | | | |

**LEGEND**

| Deliverable codes | Deliverable Description |
|---|---|
| D: Draft Report | Report delivered to FHWA for 3 week review period. |
| F: Final Report | Final report delivered in compliance with FHWA publication standards |
| M&A: Model and algorithm | Mathematical model and sample code |
| SW: Software | Executable software, code and user manual |
| JP: Journal paper | Paper submitted to conference or journal |
| P: Presentation | Presentation for symposium, conference or other |
| DP: Decision Point | Time to make a decision on two parallel paths as to which is most promising to follow througjh |
| [x] | Indicates completion of deliverable x |

Work planned

Work completed

Parallel topic

# PROGRAM AREA: ENGINEERED MATERIALS

## CATEGORY E1: MODELING

### Work element E1a: Analytical and Micro-mechanics Models for Mechanical Behavior of Mixtures (TAMU)

Work Done This Quarter

Three technical presentations were made at the *90th Transportation Research Board (TRB) Annual Meeting* in Washington, D.C., January 2011. These presentations were: 1) "Distribution of Crack Size in Asphalt Mixtures"; 2) "Anisotropic Viscoelastic Characterization of Undamaged Asphalt Mixtures in Compression"; and 3) "Microstructure-Based Inherent Anisotropy of Asphalt Mixtures." A technical paper entitled "Distribution of Crack Size in Asphalt Mixtures" has been accepted for publication in *Transportation Research Record: Journal of the Transportation Research Board*.

Progress is made in this quarter on three topics including healing properties of asphalt mixtures, modulus gradient in aged field cores of asphalt pavements and moisture susceptibility of fine asphalt mixtures (FAM).

**1. Healing Properties of Asphalt Mixtures**

The concept of internal stress was proposed in previous quarters to study the healing properties of asphalt mixtures. The internal stress is the driving force of the recovery of asphalt mixtures and is directly related to the healing process that accompanies the recovery process. The theoretical internal stress was calculated based on the viscoelastic theory in previous quarters and the calculation process was documented in the last quarterly report. A revised creep and recovery test is proposed in this quarter to measure the internal stress. This test is a modified normal creep and recovery test with several step-loading stages in the recovery phase. The internal stress measured from the revised creep and recovery test is then simulated to determine the recovery properties of undamaged asphalt mixtures that serve as the reference state of the healing process.

In the proposed test protocol, the internal stress is firstly obtained at a series of time points. Then a mathematical fitting model is used to simulate the curve of internal stress versus time. An appropriate fitting model for the internal stress curve can be an exponential function or power law function. The exponential function is proposed in equation E1a.1:

$$\sigma_i(t) = \sigma_1 e^{-\frac{t}{\eta_1}} + \sigma_2 e^{-\frac{t}{\eta_2}} \qquad \text{(E1a.1)}$$

where $t$ is time (sec); $\sigma_i(t)$ is the internal stress (kPa); and $\sigma_1$, $\sigma_2$, $\eta_1$, and $\eta_2$ are fitting parameters. The power law function is given in equation E1a.2:

$$\sigma_i(t) = dt^e + f \tag{E1a.2}$$

where $d$, $e$, and $f$ are fitting parameters. The software Matlab is used to fit the measured internal stress curve with both functions presented above, as shown in figure E1a.1, which also presents the theoretical internal stress calculated in the last quarter. The R-squared value of the exponential model is 0.9999, while the R-squared value of the power law model is 0.9987. The high R-squared values of both fitting models demonstrate the goodness of the model fit. However, figure E1a.1 shows that the exponential model better matches the theoretical internal stress curve, while the power law model deviates from the theoretical internal stress curve after approximately 100 seconds. In addition, the internal stress should vanish after a sufficient time period since the viscoelastic deformation will completely recover eventually. As a result, the exponential model is more appropriate for the internal stress.

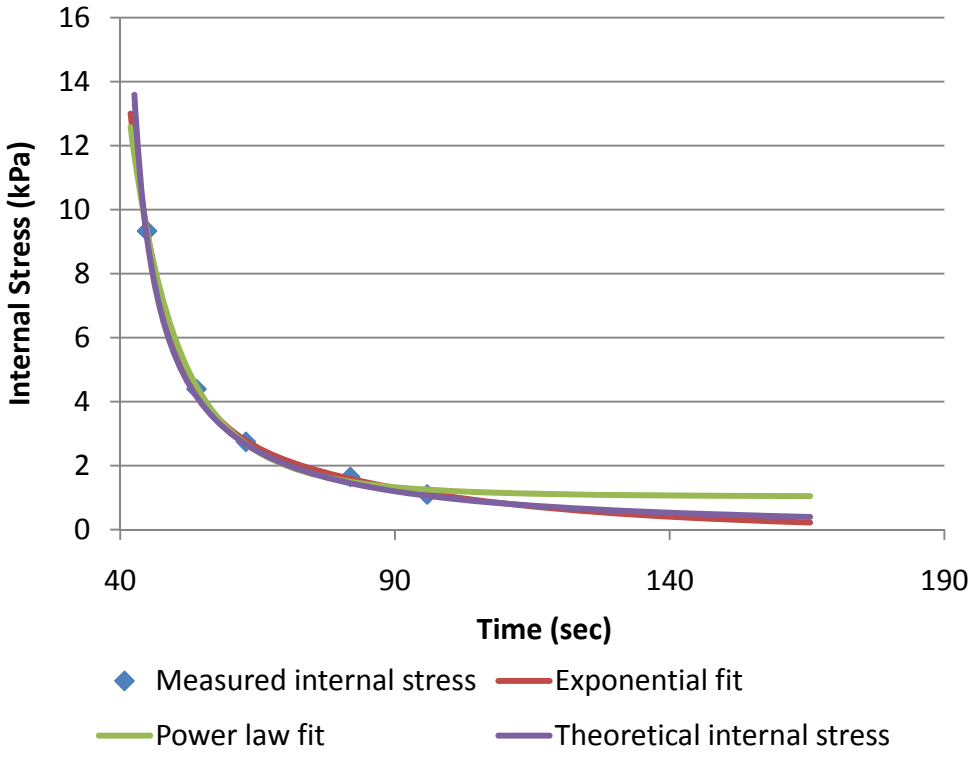


Figure E1a.1. Measured and fitted internal stress of asphalt mixture specimen.

The determined internal stress is used to characterize the recovery property of the undamaged asphalt mixture in terms of the recovery modulus, which is defined as the ratio of the internal stress to the residual strain as shown in equation E1a.3:

$$R(t) = \frac{\sigma_i(t)}{\varepsilon_r(t)} \tag{E1a.3}$$

in which $\sigma_i(t)$ is the internal stress determined using equation E1a.1; and $\varepsilon_r(t)$ is the residual strain modeled with the following function:

$$\varepsilon_r(t) = \varepsilon_{0,r} + \varepsilon_{1,r} e^{-\frac{t}{\gamma_r}} \quad \text{(E1a.4)}$$

where $\varepsilon_{0,r}$, $\varepsilon_{1,r}$, and $\gamma_r$ are fitting parameters for the residual strain. The recovery moduli of the asphalt mixture specimen in the nondestructive test and in the destructive test are plotted in figure E1a.2. The recovery modulus determined at various load levels remains the same at any specific time point provided the load level is nondestructive (or below the fatigue limit). For example, the recovery modulus curves with 20 lb, 30 lb and 40 lb load levels overlap each other, which indicates that all three load levels are nondestructive to the specimen. In contrast, when raising the load level to the destructive level of 400 lb, the measured recovery modulus is different from that with the nondestructive load at a given time point, as shown in figure E1a.2. The recovery modulus in the nondestructive test does not change with the increase of loading levels as long as the asphalt mixture is not damaged. However, the recovery modulus becomes different in the damaged asphalt mixture specimen because of the healing that occurs in the recovery phase. The recovery of an undamaged asphalt mixture is controlled by the asphalt binder, which is a natural recovery process dependent only on the material itself. However, the recovery of damaged asphalt mixtures is a mixed process that is controlled by the asphalt binder and the healing process. The interruption of the natural recovery process is due to the existence of interfacial forces of attraction, or surface energy between two crack surfaces (Schapery 1989). This concept is illustrated in figure E1a.3. The internal stress in the bulk of the material is provided by the asphalt binder, driving the recovery of the asphalt mixture. The interface bonding stress on the crack surfaces comes from the interfacial forces of attraction, driving the closure of the crack. The two separated crack surfaces gradually become closed by the action of the bonding stress to produce surface-to-surface contact. The combined effect of the internal stress provided by the asphalt binder and the bonding stress on crack surfaces is shown by a change in the stress-strain relationship, i.e. a changed recovery modulus. The measurement of the internal stress can be done in about 3 minutes.

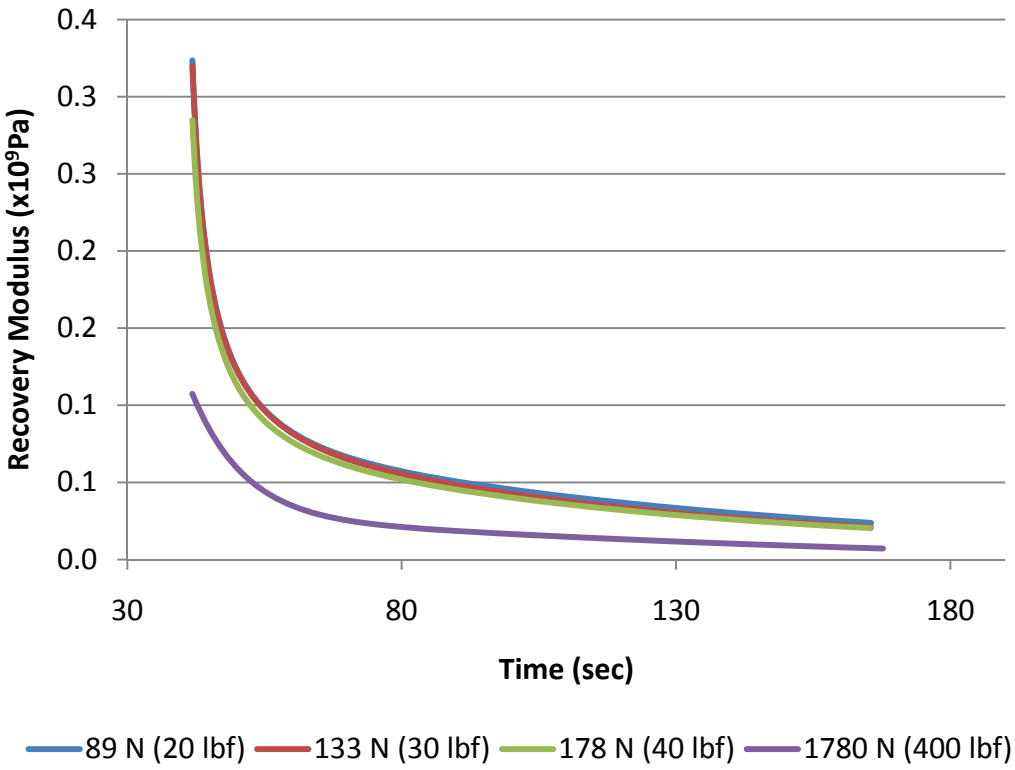


Figure E1a.2. Recovery modulus of asphalt mixture in the nondestructive tests (89 N, 133N, and 178 N) and destructive test (1780 N).

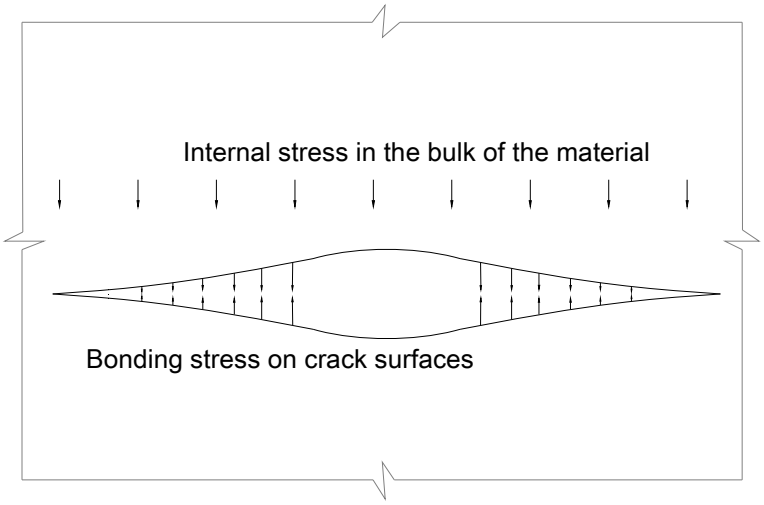


Figure E1a.3. Stresses in recovery of damaged asphalt mixtures.

## 2. Modulus Gradient in Field Cores of Asphalt Pavements

The determination of the modulus gradient in aged field cores of asphalt pavements was detailed in previous quarterly reports. In order to verify the results of laboratory tests, the direct tension

test is simulated using the commercial finite element software ABAQUS in this quarter. Figure E1a.4 shows the loading and boundary conditions of the finite element model. The upper surface at which the load is applied is not allowed to move laterally since the loading frame that is attached to the upper end cap moves in a rigid sleeve that prevents the specimen from any lateral movement or rotation in the direct tension test. In the mean time, the lower end cap is fixed with a pin support that allows rotation only but not lateral movement. To simulate the rigid end caps on the top and bottom of the specimen, the nodes on both ends are tied to a reference point that forces these nodes to remain in the same plane during the deformation.

Under a monotonically increasing direct tensile load, the central part of the specimen tends to displace laterally. This lateral movement is caused by the induced moments in the specimen because of the modulus gradient. The servo-controlled loading machine corrects this movement at its feedback frequency resulting in an oscillation of the sample. Since both the actual machine loading and subsequent feedback response are sinusoidal, a sinusoidal model in the form of equation E1a.5 is used to simulate both the actual machine displacement and the feedback rate effect on the displacement tests. The displacement magnitude is the same as the displacement of the upper end cap in the actual test.

$$d(t) = a.t + b.\sin(c.t) \tag{E1a.5}$$

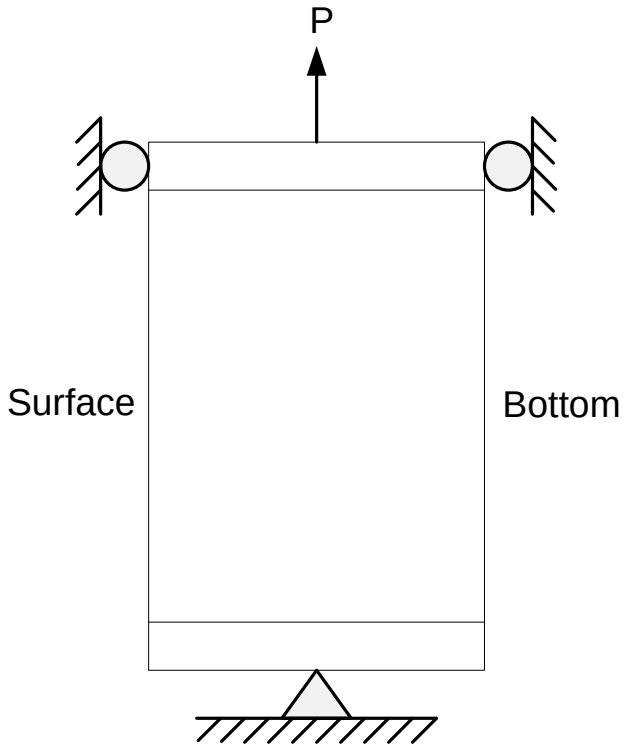


Figure E1a.4. Boundary conditions of the finite element model.

To simulate the stiffness gradient with pavement depth in the aged field core specimen, the original model for the specimen is partitioned into 8 subsections. Different viscoelastic moduli are assigned to each section to create the stiffness gradient with depth. The Poisson's ratio is assumed to be the same in all subsections. The viscoelastic properties of the specimen are defined using the Prony series as shown in equation E1a.6.

$$G(\tau) = G_{\infty} + \sum_{i=1}^{n} G_i e^{-\frac{\tau}{\tau_i}} \qquad \text{(E1a.6)}$$

where $G_{\infty}$ is the long term complex modulus and $\tau_i$ is the relaxation time. The long term complex modulus was assumed to be zero in this model. The relaxation time parameters of the Prony series are measured from lab-mixed-lab-compacted (LMLC) specimens and are assumed to be the same for all subsections. The magnitudes of the complex moduli of subsections are obtained from the stiffness gradient analysis of the field core specimen using the aforementioned procedure. The material properties of the model are listed in table E1a.1.

The viscoelastic analysis module in ABAQUS is used to analyze the model with viscoelastic properties. The modeling results of ABAQUS match well with the results of the direct tension test on the aged field core specimen, which confirms the accurate measurement of the direct tension test on the field core specimens. Figure E1a.5 illustrates the measured strain and modeled strains at the top (pavement surface) and bottom (of the pavement layer) of the specimen. There are some differences between the actual test response and the numerical model outputs, which may be due to the assumptions of the material properties in the finite element model, the specimen misalignment and the assumed smooth feedback rate function. Figure E1a.6 presents the maximum principal stress contours and the deformed shape of the specimen at the end of the test. As shown in figure E1a.6, the bottom of the specimen rotates because it is allowed to do so by the pin support, and there is stress concentration near the upper corner of the stiffer side. The finite element model uses a 2 Hz feedback rate.

Table E1a.1. Material properties in the finite element model.

| Section | Elastic Modulus (MPa) | Poisson's Ratio | Prony series' $G_i$ | Prony series' $\tau_i$ |
|---|---|---|---|---|
| 1 | 7046 | 0.3 | 0.37 | 6.75 |
| 2 | 6316 | 0.3 | 0.37 | 6.75 |
| 3 | 5578 | 0.3 | 0.37 | 6.75 |
| 4 | 4847 | 0.3 | 0.37 | 6.75 |
| 5 | 4116 | 0.3 | 0.37 | 6.75 |
| 6 | 3378 | 0.3 | 0.37 | 6.75 |
| 7 | 2648 | 0.3 | 0.37 | 6.75 |
| 8 | 1910 | 0.3 | 0.37 | 6.75 |

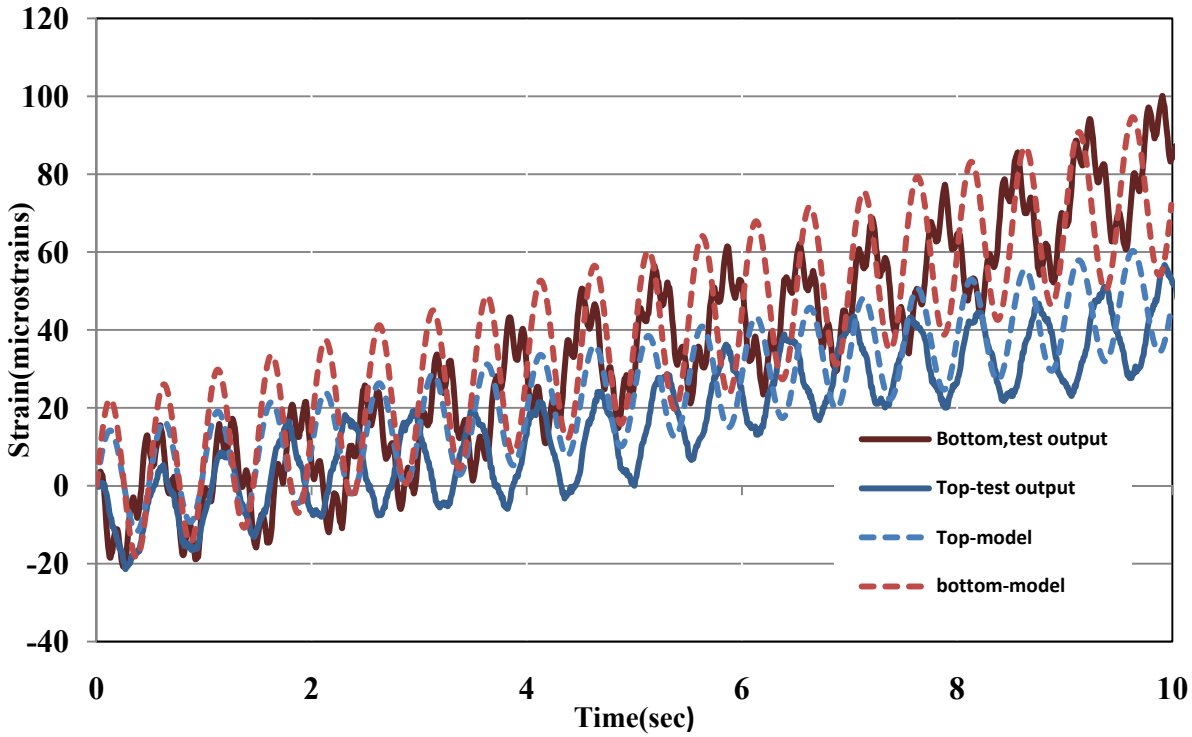


Figure E1a.5. Finite element model outputs vs. actual test results.

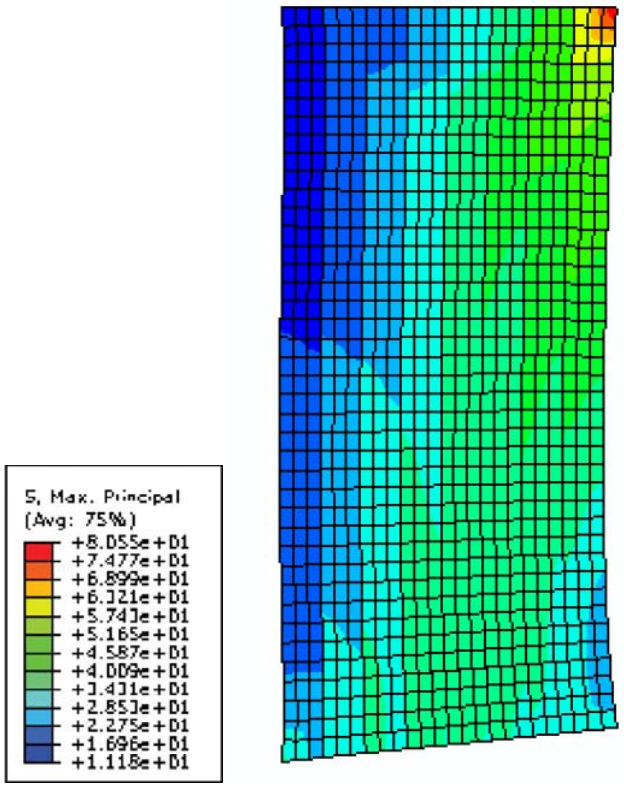


Figure E1a.6. Final deformed shape and principal stress contours.

Based on the comparison between the test results and the finite element modeling results, further modifications are performed on the calculation procedure of the stiffness gradient. The results of the modified calculation procedure show that the asphalt mixture ages severely near the surface for the first few months after construction and that the aging extends to deeper layers below the surface with time. Figure E1a.7 shows the stiffness gradient transition in an asphalt layer from 3-month aging to 20-month aging after construction. The two aged field cores used in this analysis were extracted from US 277 in Texas in the wheel path from the same section.

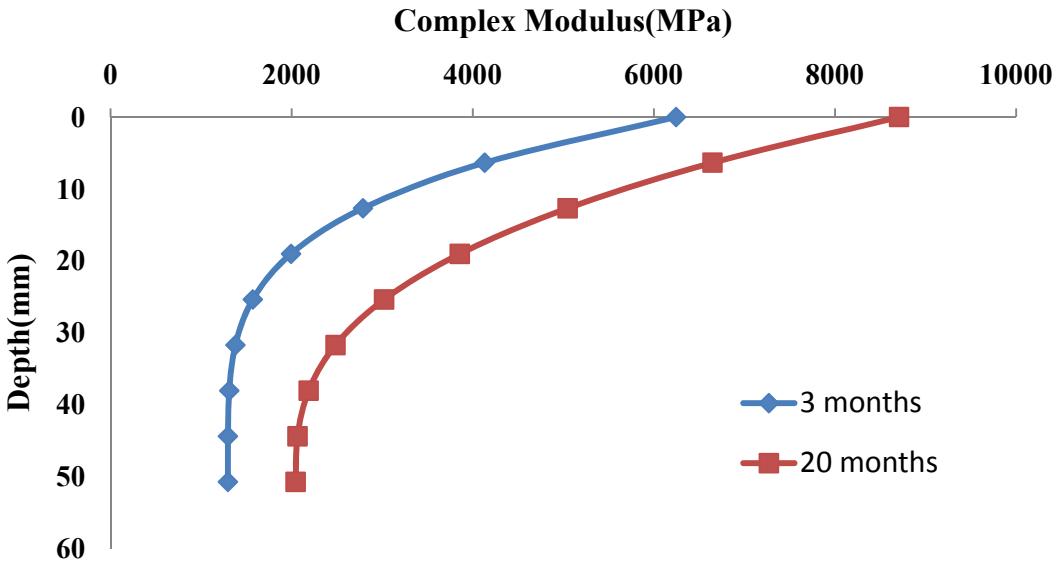


Figure E1a.7. Stiffness gradient for the US277RWP-1-2 and 2-3 at 10°C.

### 3. Moisture Susceptibility of Fine Asphalt Mixtures

The fine asphalt mixtures (FAMs) that were conditioned at different levels of relative humidity (RH) in previous quarters are tested using the controlled-stress repeated direct tension (RDT) test in this quarter. The crack growth of each specimen is calculated based on the RDT test results and is shown in figure E1a.8.

It can be clearly observed in figure E1a.8 that the crack growth rate of specimen AAD1 which was conditioned at 100% RH is greater than that of specimen AAD36, which was conditioned at 50% RH. Specimen AAD2 which was conditioned at 0% RH has the smallest crack growth rate.

For the specimens that are conditioned at the same RH level and that have approximately the same level of air void content, the crack growth rate tends to be at the same scale. As illustrated in figure E1a.9, the crack growth rates are in the same order for specimens AAD7, AAD32 and AAD27, which are conditioned at 50% RH, and the corresponding air void contents are 2.6%, 2.4% and 2.5%, respectively.

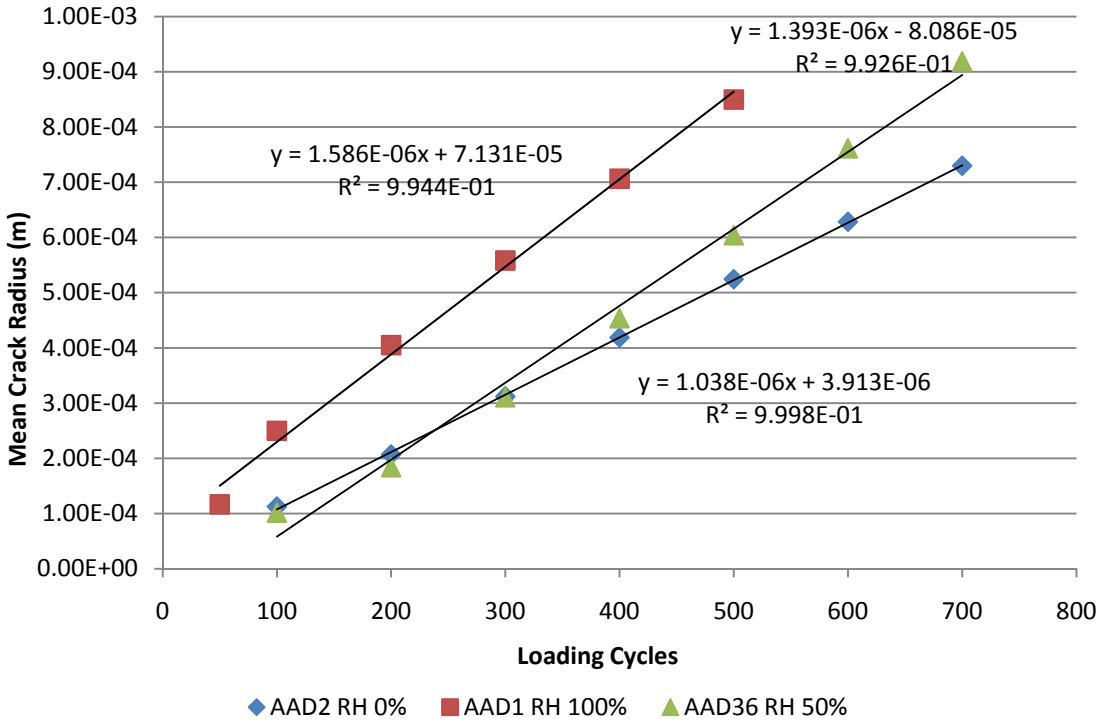


Figure E1a.8. Crack growth rate for specimens conditioned at different RH.

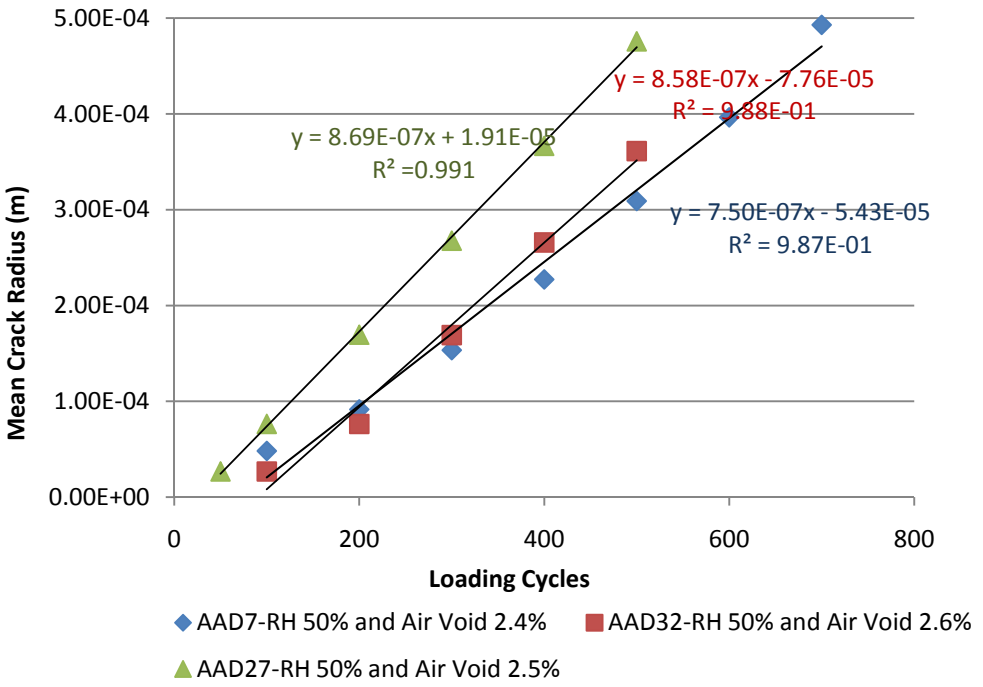


Figure E1a.9. Crack growth rate for specimens conditioned at same RH.

The method used to obtain undamaged FAM properties has been revised in this quarter. In the previous analysis, the undamaged material properties of FAM were obtained by applying a low stress level with a stress amplitude of 88 kPa and then use the measured modulus and phase angle from phase II, which corresponds to the leveling phase shown in figure E1a.10. Phase I stiffening was observed even when a high stress level with a magnitude of 320 kPa was applied. Because of this, in the future, the properties of undamaged FAMs will be determined at the same stress level rather than from a different applied stress level.

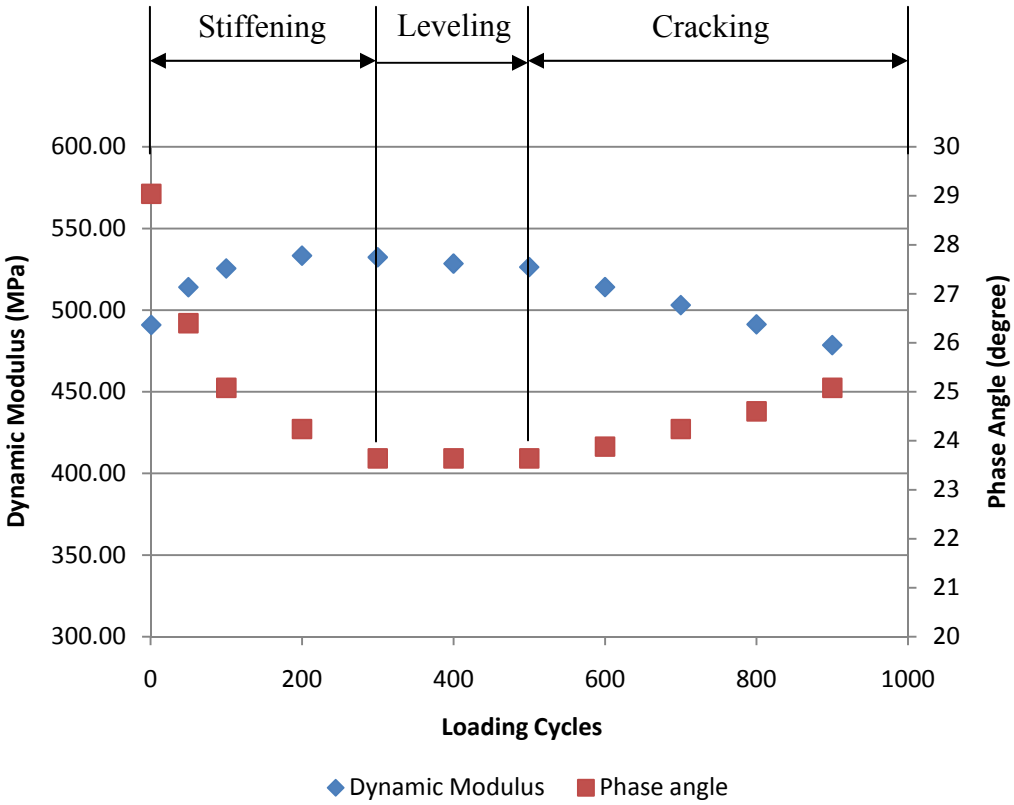


Figure E1a.10. Assembly of aggregates in FAM specimen in RDT test.

Significant Results

In order to use the internal stress to study the healing process of damaged asphalt mixtures, an appropriate internal stress curve versus time should be obtained first. This is achieved by fitting a proper function to the measured internal stress from the revised creep and recovery test. It is found that an exponential function is the best in not only fitting the measured internal stress well but also in conforming to the actual material behavior in the recovery phase. The internal stress calculated by this exponential function can be used to describe the recovery behavior of asphalt mixtures.

The recovery behavior of asphalt mixtures can be described by a recovery modulus, which is defined as the ratio of the internal stress to the residual strain which is the measured strain in the recovery phase. The recovery modulus of undamaged asphalt mixtures does not change with the increase of loading levels, indicating that it is a material property that only depends on the material itself. The recovery of undamaged asphalt mixtures is thus a natural process that is controlled by the asphalt binder. However, the recovery modulus of damaged asphalt mixtures becomes different because healing occurs in the recovery phase. The recovery of damaged asphalt mixtures is a mixed process that has a combined effect from the internal stress provided by the asphalt binder and the interface bonding stress on crack surfaces. The fact of this difference between the recovery of undamaged asphalt mixtures and that of damaged asphalt mixtures provides a new perspective on characterizing the healing process.

Significant Problems, Issues and Potential Impact on Progress

The interface bonding stress is the cause of the crack closure in the healing process. Schapery (1989) used it to determine the rate of crack closure, but the derivation is based on linear viscoelastic material, which is not suitable for damaged asphalt mixtures. Even though the bonding stress cannot be used in a direct way, understanding of this concept is important. It provides an insight into the internal stress in the damaged asphalt mixture in the recovery phase, which will further facilitate the application of the energy balance approach which was developed in the E1a Work Element to quantify healing.

Work Planned Next Quarter

The next step to study healing following the work presented here is to make use of the difference between the recovery of undamaged asphalt mixtures and that of damaged asphalt mixtures to quantify healing. The energy balance approach developed in previous quarters will be used to construct energy balance equations to determine the cracking damage in the creep phase and the extent of healing in the recovery phase.

The gradient stiffness analysis should be correlated with the mixture compositional characteristics such as air void distribution, binder content and binder rheological characteristics. To achieve this goal the binder chemical and mechanical test results from the same cores are needed to be studied together with the stiffness gradient calculations.

There will be more FAM analysis results for AAD specimens conditioned at 25% and 75% relative humidity, and the AAM specimen's analysis will also be available in next quarter.

Cited Reference

Schapery, R. A., 1989, On the Mechanics of Crack Closing and Bonding in Linear Viscoelastic Media. *International Journal of Fracture*, 39: 163-189.

**Work element E1b: Binder Damage Resistance Characterization (DRC) (UWM)**

***Subtask E1b-1: Rutting of Asphalt Binders***

Work Done This Quarter

Work completed during this quarter included testing Repeated Creep and Recovery (RCR) and Multiple Stress Creep and Recovery (MSCR) of mastics of neat binder. Testing matrix included two replicates of each test type at temperatures of 46, 58, and 70°C and stress level of 100 and 3200 Pa for MSCR, and 100, 3200, and 10000 Pa for RCR. Limestone and Granite mineral fillers at 0.63 filler to binder mass ratios were used for preparation of mastics. Testing of modified binder mastics are still in progress.

Significant Results

MSCR and RCR testing of neat binder mastics at all temperatures and stress levels using both fillers were completed. A summary of the MSCR test results for the neat binder mastics can be seen in figure E1b-1.1.

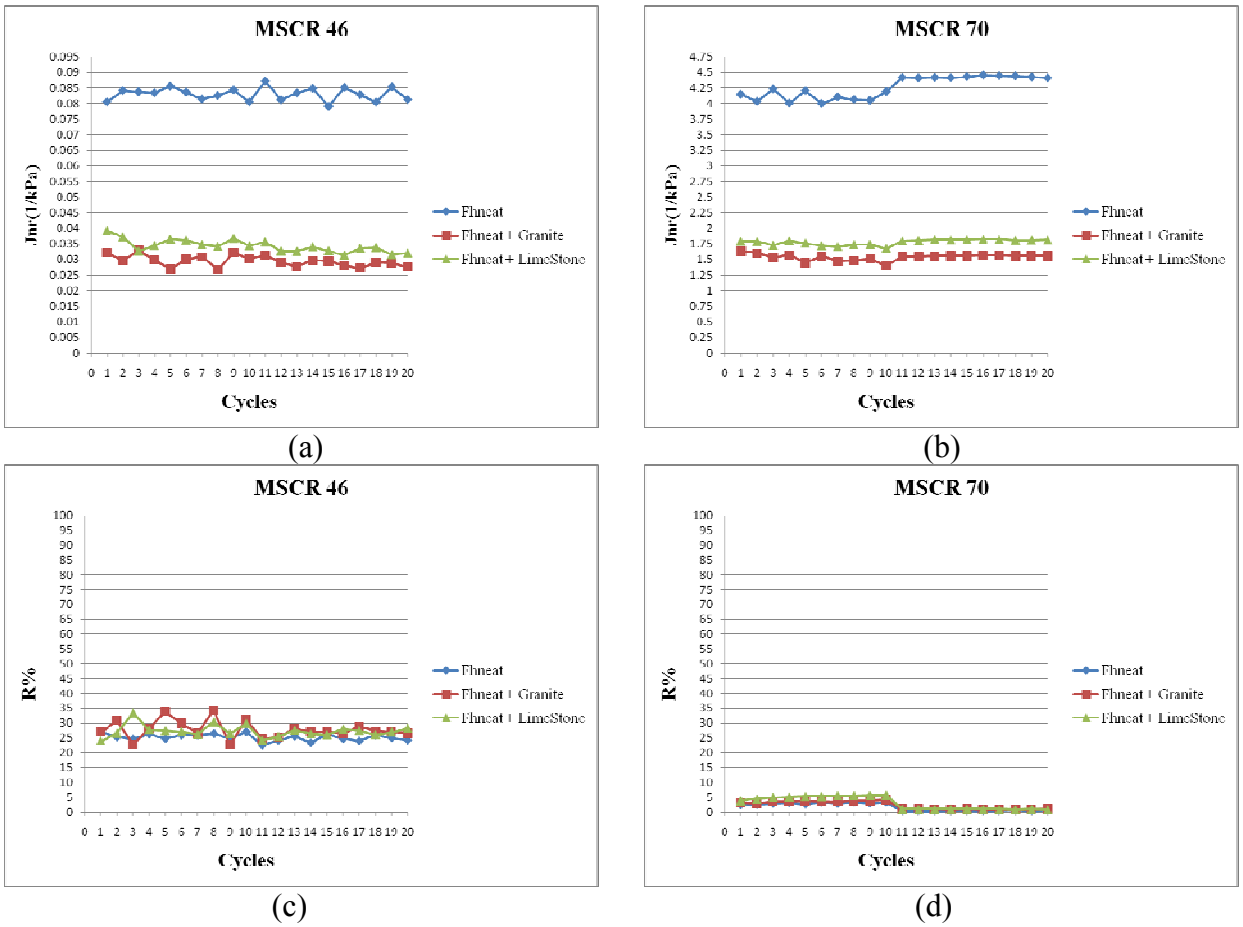


Figure E1b-1.1. MSCR results for mastic with neat binder.

Figure E1b-1.1 shows that Jnr of neat binder mastics are less than half of the neat base binder for both stress levels and at the three test temperatures. As the temperature is increased from 46 $^{o}$C to 58 $^{o}$C and then 70 $^{o}$C, Jnr at 3200 Pa decreases from about 0.075 $kPa^{-1}$ to 0.75 $kPa^{-1}$ and then 4.5 $kPa^{-1}$, respectively, a 60 fold decrease over the tested temperature span. As for percent recovery, the results show that there is practically no difference between the neat binder and neat mastic %R values at any of the testing temperatures. However, as the temperature is increased from 46 $^{o}$C to 58 $^{o}$C and then 70 $^{o}$C, percent recovery at 3200 Pa is reduced from about 30% to 7% and then about 3%, a 10 fold decrease over the tested temperature span.

The above data shows clear relationship between the binder and mastics creep response. It was found that the neat binder mastics can be modeled using the same model that was used for the binder, with different values for the constant parameters. It is expected that the same model can be applied to the modified binder mastics as well.

Furthermore, the binder and mastic data are being analyzed to investigate potential correlation with mixtures rutting properties. Preliminary results suggest that there is some correlation between binder properties and mixture properties. Further investigation of the effect is needed. In addition, image analysis conducted on cut sections of laboratory compacted samples were analyzed to quantify internal structure parameters including aggregate orientation, contact points, and contact branches.

MSCR data for the binders studied in this research revealed that some fluctuations can be observed in the Jnr and R% values from the first to the last cycles at each stress level. These fluctuations usually diminish as the testing goes toward the last cycles, as if the material gets conditioned to a steady situation. To quantify this observation the average Jnr values of each binder at each stress level and temperature was calculated once for all 10 cycles and then for the last 5 cycles. Figure E1b-1.2(a) and (b) show the percent change between the 10-cycle and last 5-cycle values of Jnr and R%. The data shown in these figures correspond to 4 binders (one neat and 3 modified), 3 temperatures (46, 58 and 70 $^{o}$C), and 2 stress levels (100 and 3200 Pa), that is a total of 24 data points. Each data point in these figures represents the average of two replicate tests.

Results show that for the most part, the percent change for both Jnr and R% are less than 10 percent. However, based on the analysis of other binders tested with different DSR machines and different analysis software, it can be concluded that calculating the Jnr and R% values based on the average of the last 5 cycles provides more repeatable values.

Another activity in this quarter was the completion of the binder modeling based on the model presented in the 2008 Q3 report. All binders (neat and modified) were fitted at both stress levels at the 3 test temperatures. Results show very good agreement between the accumulated strain predicted by the model as compared to the MSCR test results on the binders (figure E1b-1.3).

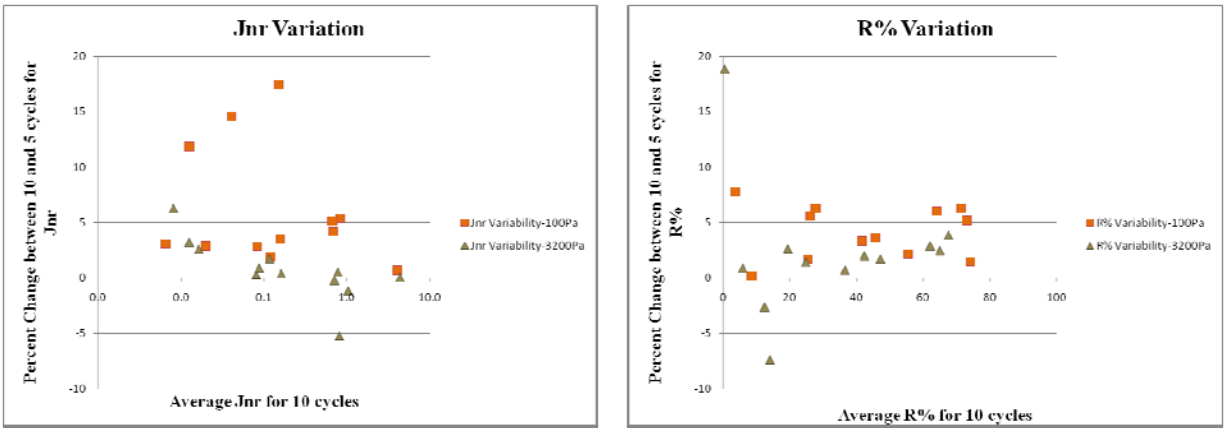


(a) Jnr Variations (b) Percent Recovery Variations

Figure E1b-1.2. All binder MSCR results.

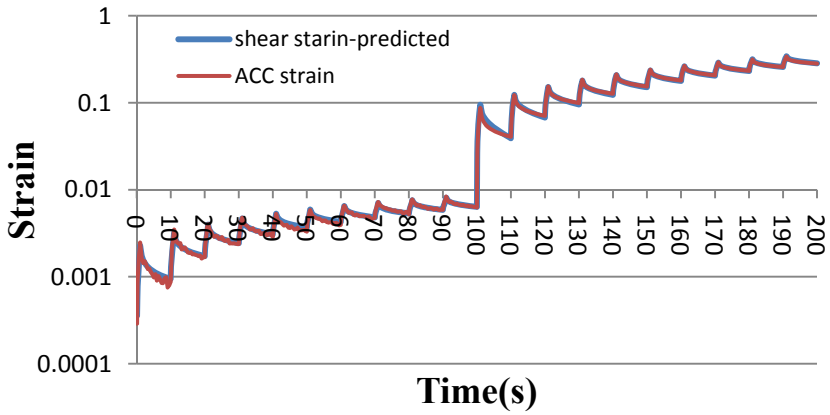


Figure E1b-1.3. Summary of binder modeling using MSCR data.

Significant Problems, Issues and Potential Impact on Progress

None.

Work Planned Next Quarter

Work for next quarter will focus on the following tasks:

- Complete RCR and MSCR testing of mastic with modified binders.
- Continue analysis of mastic data.
- Continue modeling of mastic data.
- Modify the imaging software to measure contact branches.

- Develop an aggregate structure (gradation) that simplifies that image analysis and enhance our understanding of mix behavior.
- Investigate the relationship between binder, mastic, and mixture.

***Subtask E1b-2: Feasibility of Determining Rheological and Fracture Properties of Asphalt Binders and Mastics using Simple Indentation Tests***

Work Done This Quarter

The indentation procedure was updated to eliminate repeatability issues due to the vibrations caused by engaging the spindle locking mechanism. The new procedure takes advantage of the high precision deflection acquisition system by detecting the slightest change in deflection as the indenter makes contact with the sample surface. This enables the operator to zero the deflection reading at that point while minimizing the impact of dynamic loading due to erroneous zeroing. The new procedure was shown to improve repeatability for the test matrix carried out. Also, efforts were made toward optimization of sample geometry using experimental data and finite elements modeling results. The modeling was done for sample geometries with varying depth and radius. The modeling results were found to agree well with experimental results.

Significant Results

The test matrix shown in table E1b-2.1 was completed to determine the optimum indentation test geometry. Note that all tests were conducted at room temperature.

Table E1b-2.1. Experimental matrix for optimization of indentation sample size.

| Sample container diameter (mm) | Sample depth (mm) | Replicates |
|---|---|---|
| 97 | 17 | 5 |
| | 34 | 5 |
| | 51 | 5 |
| 54.5 | 30 | 4 |
| 75 | | 3 |
| 97 | | 15* |
| 165 | | 3 |
| 250 | | 5 |

*Three samples were used to evaluate the effect of indenter position on results.

Figure E1b-2.1 shows the indenter peak deflection for samples of different depths. It can be seen that as the depth increases the peak deformation increases at a decreasing rate. It may be inferred from the trend that beyond a certain depth the effect of sample depth becomes negligible.

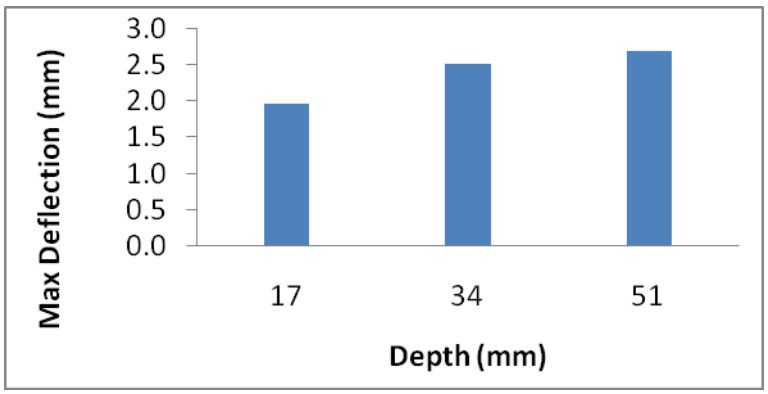


Figure E1b-2.1. Graph. Peak deflection for different container depths.

To optimize the sample geometry, tests were performed on samples with varying diameters (figure E1b-2.2). Results showed that sample diameter has a significant effect on deflection. Note that this effect persists to relatively high diameters. Therefore, it is necessary to optimize sample diameter to minimize boundary effects while keeping the sample dimensions reasonable. The research team found that to reduce the boundary affect a sample with $\phi$= 140 mm may be used.

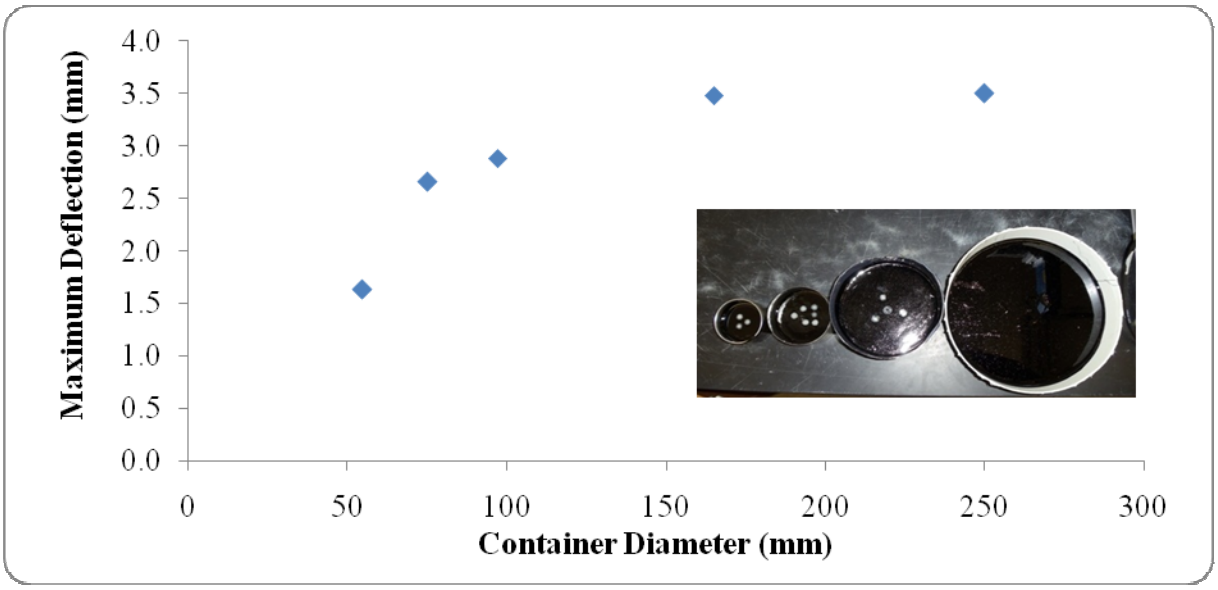


Figure E1b-2.2. Graph. Effect of container diameter on maximum deflection.

The effect of consecutive testing on the same sample was explored by first testing three identical samples with the indenter centered on the sample surface. Then, tests were conducted at three different locations on the surface of the sample. The averages of the centered and un-centered test results were compared. The results showed that the difference in deflection of the centered

tests and the average of the following consecutive tests is significant. However, the effect of test temperature, binder stiffness and other mechanical and chemical factors must also be considered before generalization.

Figure E1b-2.3 shows typical creep and recovery test results. This figure highlights the good repeatability of the new indenter test procedure.

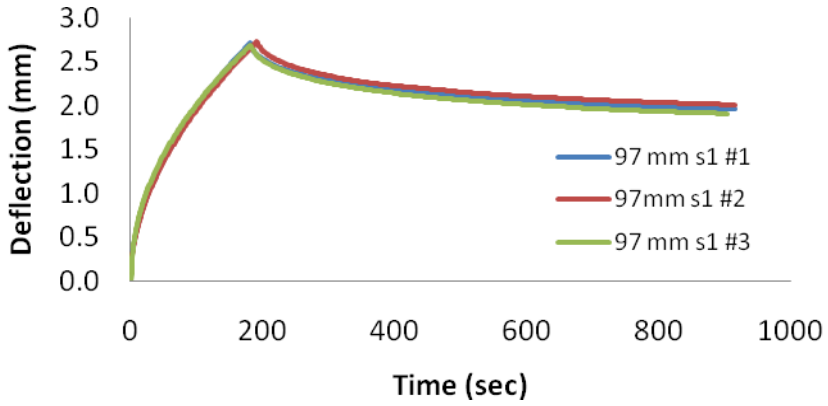


Figure E1b-2.3. Graph. Repeatability of creep and recovery indentation test results

Greater flexibility in tested geometries and loading conditions motivated the research team to use ABAQUS for the geometry optimization process. Finite element simulations of the indentation test for different sample geometries were analyzed. It was observed that for 5% error in maximum deflection, a minimum depth of 70 mm must be used. Furthermore, the model was run for different diameters at a constant depth. The results showed that the optimum diameter for which the error is limited to a maximum of 5% is 150 mm.

The results of indentation experiments and FEM modeling are in agreement. However, the resulting optimum geometry would result in relatively large samples, reducing the practicality of the test. Therefore, further research will focus on producing correction factors for smaller sample sizes to account for boundary effects.

Work Planned Next Quarter

Work next quarter will focus on the following tasks:

- Developing a temperature control system for the indenter to enable testing at varying temperatures.
- Comparing the results of indentation tests with DSR creep and recovery test results to establish relationships, as well as gain valuable material input for FE modeling.

## Work Element E1c: Warm and Cold Mixes

### *Subtask E1c-1: Warm Mixes (UWM)*

Work Done This Quarter

The research team developed a plan for the evaluation of the lubricity test. This includes establishing repeatability and determining the effects of testing parameters including testing speed, testing temperature, and normal force. Modifications to the lubricity procedure were made in an effort to improve controlling normal force and measurement of torque during testing. Specifically, the reference point used to set the "zero gap" of the testing apparatus and the delay time for data sampling were modified. Under the work plan, the lubricity test will be conducted at the compaction temperature (CT) CT-30°C and CT-50°C. For unmodified binders, mixing and compaction temperatures were determined using AASHTO 312 (Viscosity). For modified binders, two procedures have been selected, the Phase Angle Method proposed in NCHRP Report 648 and the Zero Shear Viscosity method proposed in NCHRP Report 459.

Efforts related to the evaluation of the effects of WMA additives and reduced aging temperatures on asphalt binder and mixture performance focused on the evaluation of appropriate binder aging methods and methods to estimate allowable temperature reductions to prevent significant reductions in performance. The RTFO aging method depends on both temperature and viscosity to short term age the binder in the laboratory, thus the contribution of reduced temperature to the decrease in performance at lower aging temperatures is still not specifically quantified. To isolate viscosity and temperature, the materials used in the study that has been published in the AAPT 2011 paper have been short term aged using the TFOT method. Testing and analysis will be conducted in the next quarter. The paper accepted by the Association of Asphalt Paving Technologists was presented on March 30$^{th}$ at the annual meeting in Tampa, FL.

Collaborative efforts continued with the University of Nevada-Reno on moisture damage testing. Mix designs from the materials shipped from WI were verified, appropriate HMA and WMA mixing and compaction temperatures were determined, and WMA additive mixing procedures were recommended. Bitumen bond strength testing at UW Madison remains 50% complete; preparation of aggregate plates from the Reno aggregate is underway. The research team is unaware of any WisDOT WMA field projects that were constructed in the 2010 season, thus no progress has been made on this element. The research team will discuss opportunities for research and testing on 2011 construction projects in the next quarter.

Significant Results

The modified lubricity procedure significantly improved the repeatability of the test method. Results for testing of a single replicate at a normal force of 25N and four testing speeds ranging from 5RPM – 50RPM are provided in figure E1c-1.1.

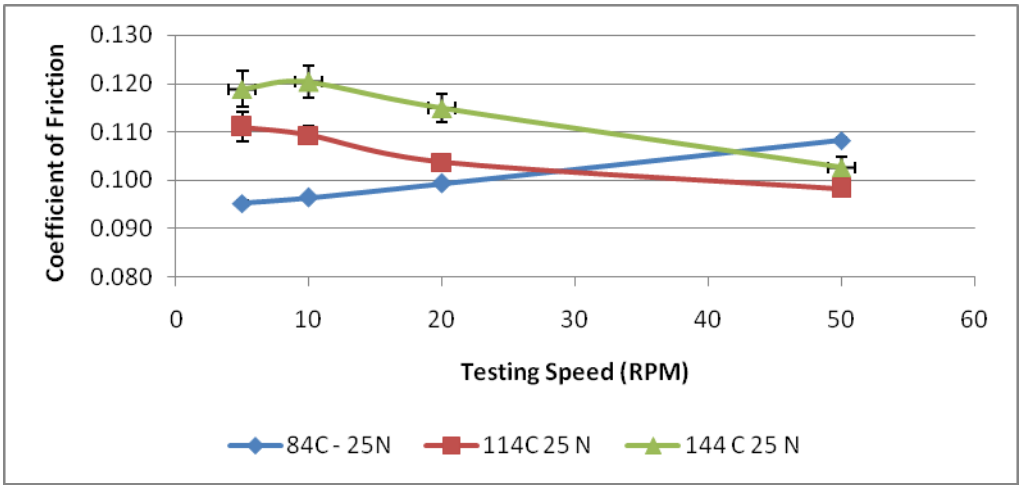


Figure E1c-1.1. Coefficient of friction vs. testing speed at 25 N – PG 64-22.

The error bars included in figure E1c-1.1 demonstrate the repeatability of the test method. The values of coefficient of friction ranged between 0.095 – 0.12, however the consistency of the measurements indicate the sensitivity of the device to testing speed and temperature. Further testing is needed to evaluate these results.

Work related to examining the impacts of the reduced WMA production temperatures and the presence of WMA additives on performance was continued this quarter. The aging index is used to evaluate sensitivity to aging and is defined as the ratio of the SuperPave rutting parameter ($G^*/\sin\delta$) after short term aging in the RTFO at standard conditions to that of the un-aged binder. The impacts of different WMA additive types on the binder aging index from two asphalt sources are provided in figure E1c-1.2.

Comparison of the WMA modified binders to the control for each asphalt source indicates that the aging index is influenced by both asphalt binder source and WMA additive type. Based on existing literature, sensitivity of the aging index to asphalt source was expected. Variation in aging index with WMA additive type implies that both aging temperature and WMA additive type must be considered to properly estimate allowable reductions in production temperature.

The procedure to estimate allowable production temperature reductions was simplified Examination of the data generated from the FHWA aging study and the data collected during this research indicates that for aging indices greater than 1.5 the power law describing the relationship between aging index and sensitivity of binder performance to aging temperature previously used can be replaced with a linear trend-line. This linear relationship can be divided by a user defined reduction in asphalt binder performance grade to estimate the associated allowable reduction in production temperature. Results are provided in figure E1c-1.3.

The results presented in figure E1c-1.3 can be used as a design tool to determine the potential impacts of a specific WMA production temperature on performance. Aging indices provided in figure E1c.1.2 range from 1.5 to 3.0. To limit reduction in performance to ½ PG grade (-3°C),

the maximum reduction in production temperatures for the low and high aging indices are approximately 40°C and 30°C, respectively. Applying a similar procedure for a reduction in performance of a full PG grade (-6°C) yields maximum temperature reductions of 75°C and 50°C, respectively.

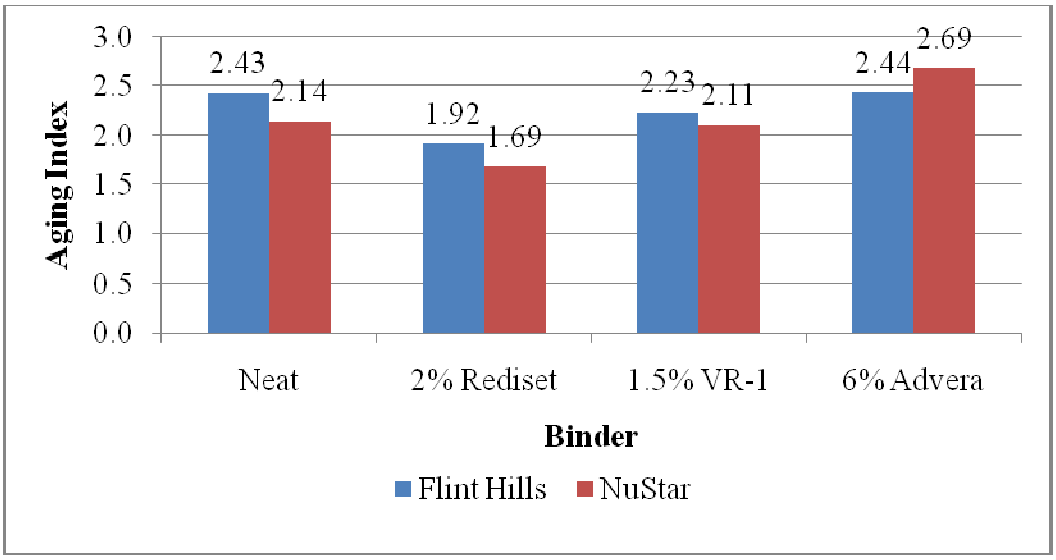


Figure E1c-1.2. Summary of aging index for various WMA additives.

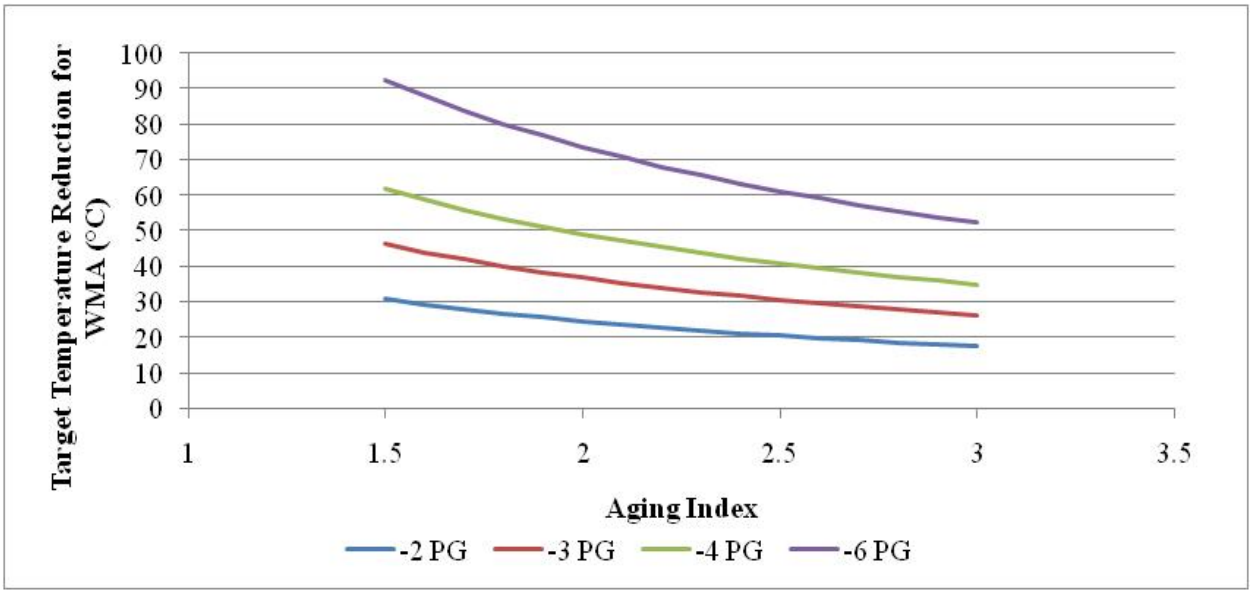


Figure E1c-1.3. Allowable temperature reductions for a user defined change in PG grade.

Significant Problems, Issues and Potential Impact on Progress

Asphalt lubricity testing and validation of the RTFO procedure were delayed due to a break down in testing equipment. It is anticipated the machine used to conduct the tests will be available by mid-April.

Work Planned Next Quarter

*Lubricity Testing*

The experiment to establish the repeatability and the sensitivity to testing parameters will be conducted. Based on the results, a final procedure will be developed and four WMA additives at three concentrations will be evaluated.

*Development of Mixing and Compaction Guidelines for WMA*

Evaluation of three candidate test methods to determine appropriate mixing and compaction temperatures for modified binders with WMA additives will continue. Testing temperatures will be applied to lubricity testing, viscosity, and mixture workability testing.

*Impacts of Reduced Aging on Performance*

Use of the RTFO to evaluate material sensitivity to aging temperature will be validated through comparison to TFOT aged materials. An appropriate aging procedure that isolates the effect of temperature will be selected and evaluation of conventional and WMA binders will commence. Mixture performance testing will be planned and executed to evaluate various mixture performance measures.

*Moisture Damage*
Complete BBS testing matrix and coordinate with Reno to discuss results of mixture testing.

Cited References

None

***Subtask E1c-2: Improvement of Emulsions' Characterization and Mixture Design for Cold Bitumen Applications (UWM)***

Work Done This Quarter

Work was conducted both in the areas of rheological characterization of emulsion residue properties and designing a work plan for cold mix asphalt. For emulsion residues, DSR testing at intermediate temperatures was conducted on recovered residue and PAV aged residues to measure fatigue and estimate low temperature properties. Low temperature properties were estimated using inter-conversion from oscillation testing to creep testing to estimate BBR properties based on DSR master curves from testing at 5°C, 10°C, and 15°C. Fatigue resistance

was evaluated using the Linear Amplitude Sweep (LAS) Test conducted at the IT PG grade of the base binder (19°C). Parameters measured during testing were used to model fatigue life as a function of strain level. Due to the thin emulsion films used for chip seals, the analysis focused on comparison of fatigue performance at high levels of strain.

This quarter, preliminary literature review of different mix design procedures for dense-graded cold mixes was carried out. Various documents, publications, ASTM standards and design manuals including the Asphalt Institute manual for cold asphalt mixes, OPTEL report, and the French's bitumen emulsion manual book were reviewed. The results of the literature review revealed that the most commonly used methods for cold mix design are mainly modified versions of either the standard Hveem (ASTM D1560 or AASHTO T 246 and T247) or Marshall (ASTM D 6926/7 of AASHTO T 245) test methods. In addition, the literature also revealed work has been dedicated to developing performance based mix design methods for cold mixes. In this case, an approach similar to the Superpave mix design method is used, whereby the SuperPave gyratory compactor is used to compact mix samples.

Significant Findings

The LAS test demonstrated an ability to differentiate between emulsion residue based on chemistries, types of modification, and the effect of aging. In general, PAV aging increases fatigue life relative to the recovered residue; however the magnitude of the increase varies for different emulsion types. One emulsion does not follow this trend, the HFRS-2. These results were not unexpected as fuel oil was added to the HFRS-2 prior to construction, resulting in a softer residue. The residue testing framework selected in this study demonstrated an ability to identify this behavior in both HT and LT testing. The strain of 5% was selected based on the testing results and potential application of the LAS test to characterize emulsion residues for chip seals. Further research is needed to evaluate if this strain level is similar to strains experienced in the field.

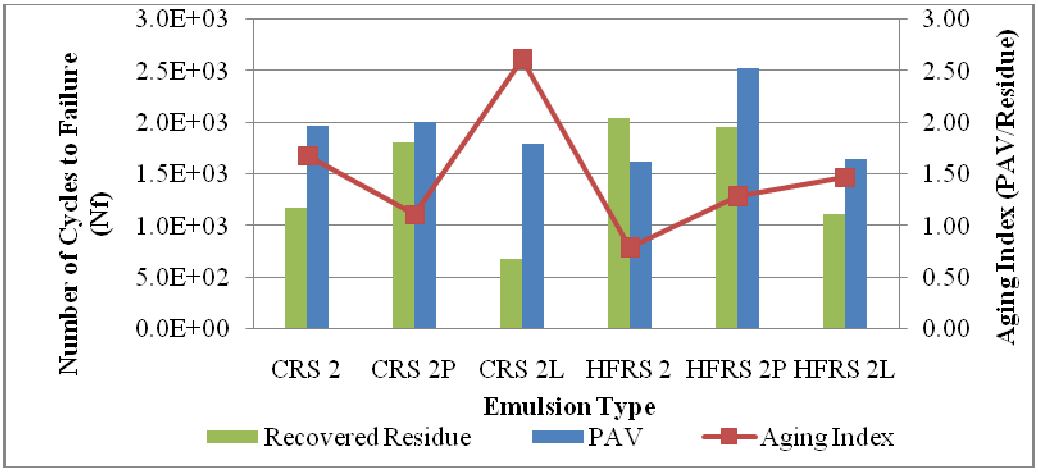


Figure E1c-2.1. Predicted cycles to failure (γ=5%) for various emulsion residues.

The impacts of aging for each emulsion are demonstrated by the red line in figure E1c-1. The aging index has been defined as the ratio of cycles to failure of the PAV material to the recovered residue. An aging index greater than one indicates improved fatigue life due to aging. The results indicate that most emulsion residues exhibit aging indices between 1.0 and 1.5, the exception being the CRS-2L, which demonstrates a significant improvement in fatigue life with aging (aging index more than 2.5).

Master curves were developed for the CRS series emulsions and inter-conversion was conducted to convert the DSR data to estimated BBR properties, S(60) and m(60), at -12°C and -18°C using values of the complex modulus (G*) and phase angle (δ) at specific frequencies. The estimated S(60) and m(60) were used to determine the LT continuous grade for each material. Results are provided in figure E1c-2.2

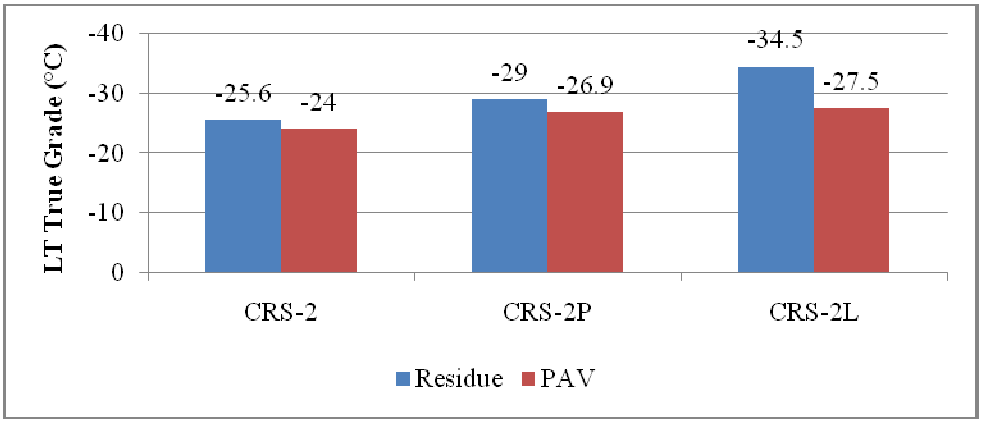


Figure E1c-2.2. Summary of low temperature continuous grade for CRS series emulsions – estimated from DSR testing at intermediate temperatures.

The base binder used in the emulsions had a low temperature grade of -28°C. Results indicate that the PAV aged emulsion residues were unable to meet the performance of the base binder. The effect of PAV aging varied by emulsion type, with reductions in LT continuous grade temperatures ranging from -1.6°C to -7°C. Initial results indicate that the test method has potential for evaluation of emulsion properties.

A literature review was conducted to define the emulsion and aggregate properties that impact cold mix design and performance. Aggregate properties reported in the literature to affect the performance of cold mixes are given in table E1c-2.1. These properties are addition to the standard quality tests required for hot mix asphalt mixes. Emulsion properties that mainly affect the performance of cold mixes are given in table E1c-2.2. The properties listed are also in addition to the traditional quality test for asphalt emulsions specified in the ASTM D244.

Table E1c-2.1. Aggregate properties important for cold emulsion mixes.

| Property | Description | Test method |
|---|---|---|
| Dust content (Gradation) | High dust content results in "balling" of the mix, and in absorption of moisture from the mix which result dry mixes | Sand Equivalent test (ASTM D 2940 or D3515<br>Methylene Blue Test (ASTM C837 – 09) |
| Reactivity (Ability to cause pH increase) | Highly reactive aggregates can cause premature breaking and coalescence of "pH sensitive" emulsions and can affect proper coating of the aggregate; workability; cohesion development of the mix; and its ultimate mechanical properties. | LCPC Method (OPTEL Report)<br>The test method exposes the aggregate dust to acidified pure water or the emulsion it's self, and measures increase in pH over time. |
| Moisture Content | Moisture content affects the ability of the emulsion to coat aggregate. If too dry, aggregate will absorb water from the emulsion. This cause premature breaking of the emulsion before it could uniformly coat the aggregate. | Visual inspection of mix samples prepared at varying moisture content to asses coating. |

Table E1c-2.2. Emulsion properties important for cold mixes.

| Property | Description | Test method |
|---|---|---|
| PSD | Particle size distribution of emulsions affects the uniformity of coating | Laser Diffraction analysis using the Frauhnhoffer or Mie model |
| Residual Emulsifier | An excess emulsifier is desired to control the breaking rate of the emulsion. However, too much residual emulsifier can lead to formation of a double layer around the aggregate, which has a negative effect on the coating of the aggregate. | Color (norms NF T 73-320/NF T 73-258 or ISO 2871-2) or titration of emulsion water obtained from centrifugal test. |
| pH | Some emulsions are pH sensitive. The interaction between the emulsion and some aggregates used for road construction result in increase in pH. This has destabilizing effect on the emulsion, and results in fast increase in mix stiffness | LCPC Method (OPTEL Report, 2002)<br>This test method exposes the aggregate dust to acidified pure water or the emulsion it's self, and measures increase in pH over time. |
| Viscosity | An emulsion with higher viscosity is able to prevent the mix from fast coalescence, which could result in premature breaking. | Method for measuring asphalt emulsion viscosity exists (Saybolt Furol or rotational viscometer). |

For this project, the modified Superpave Gyratory Compactor (suitable for cold mix) will be used. The modified SGC is designed to dissipate the water into a built-in-container. A review of publications that uses the SGC for cold mixes has revealed that there are no clear and standard guidelines for major mix design issues including the number of gyrations, curing and maturation period, time to leave the sample before it can be removed from the SGC, and the tests to be used to determine the optimum emulsion rate. Therefore, the initial part of the cold mix project will focus mainly on these issues.

Significant Problems, Issues and Potential Impact on Progress

A new gyratory compactor with modified molds for cold mixes has been procured. Thus, the cold mix project is expected to make significant progress in the next quarter.

Work Planned Next Quarter

Planned work for performance evaluation of emulsion residues includes completion of data analysis, evaluation of field performance, and preparation of the draft final report. The six emulsions used in this research were sampled from chip seal projects constructed in fall of 2010. The data set includes one emulsion, HFRS-2, that significantly differed from the other materials evaluated. The projects will be surveyed visually to identify differences in performance. Other methods of performance evaluation will also be investigated. If possible, materials will be sampled from the field for validation testing. All laboratory data has been collected for this portion of the study. Data will be summarized and work will begin in preparing the draft final report. The anticipated completion date for the report is 9/30/2011.

A preliminary research plan for the cold mix project has been drafted. It can be summarized as follows:

- Aggregate gradation selection and asphalt emulsions selection (based on aggregate characteristics, properties of the emulsion and emulsion rheology).
- Evaluating aggregate coating.
- Evaluating criteria for workability.
- Establish the compaction and curing procedure for mix samples
- Establish mechanical testing for cold mixes

A preliminary experimental plan for the project has been assembled in which the following factors are to be considered: aggregate type, aggregate gradation, emulsion type, emulsion content, and number of gyrations. Some of these work elements will be continued throughout the following quarter.

## CATEGORY E2: DESIGN GUIDANCE

### Work element E2a: Comparison of Modification Techniques (UWM)

Work Done This Quarter

To take advantage of mixture testing for validation of effect of modifiers on mixture performance, the research team added four binders typically used in Europe in the experimental plan: B50-70 Coruna, B50/70 Puertollano, BC 50-70, and BM-3c –Puertollano. While binder testing is performed at the University of Wisconsin-Madison, mixture testing is currently being conducted at Universitat Politecnica de Catalunya (UPC)-Spain. Binder testing includes $G^*/\sin\delta$

(i.e., original, RTFO, and PAV material), Linear Amplitude Sweep (LAS) on RTFO and PAV materials at 5°C and 20°C, Single Edge Notched Bending (SENB) on RTFO aged material at -15°C, -5°C and 5°C and glass transition temperatures ($T_g$). The collaboration will allow an early comparison of binder and mixture performance for validation of tests and effect of modifiers.

Significant Results

The G*/sinδ and the true grade temperatures for original and RTFO aged binder are shown in table E2a.1.

Table E2a.1. True grading for Spanish binders.

| | **B50-70 Coruna** | **B50-70 Puertollano** | **BM-3c Puertollano** | **BC 50-70** |
|---|---|---|---|---|
| **Original binder** | | | | |
| G*/sinδ @ 64°C,kPa | 1.64 | 1.62 | | |
| G*/sinδ @ 70°C,kPa | 0.8 | 0.79 | 2.02 | |
| G*/sinδ @ 76°C,kPa | | | 1.18 | 1.11 |
| G*/sinδ @ 82°C,kPa | | | 0.69 | 0.6 |
| **Pass/ Fail Temp** | **68.2** | **68.1** | **77.9** | **77.0** |
| **RTFO Residue** | | | | |
| G*/sinδ @ 70°C,kPa | 2.92 | 2.88 | | |
| G*/sinδ @ 76°C,kPa | 1.43 | 1.38 | 2.73 | 3.36 |
| G*/sinδ @ 82°C,kPa | | | 1.57 | 1.82 |
| **Pass/ Fail Temp** | **72.4** | **72.2** | **78.3** | **80.1** |
| **PAV Residue** | | | | |
| Stiffness @ -12°C, MPa | 228 | 247 | 124 | 179 |
| m-value @ -12°C, MPa | 0.263 | 0.278 | 0.338 | 0.269 |
| Stiffness @ -18°C, MPa | 325 | 390 | 254 | 287 |
| m-value @ -18°C, MPa | 0.269 | 0.250 | 0.291 | 0.289 |

The SENB results with the error bars are shown in figure E2a.1. It can be seen that the BC50-70 and BM-3c Puertollano binders have higher fracture energy for all temperatures in comparison to the B50-70 binders.

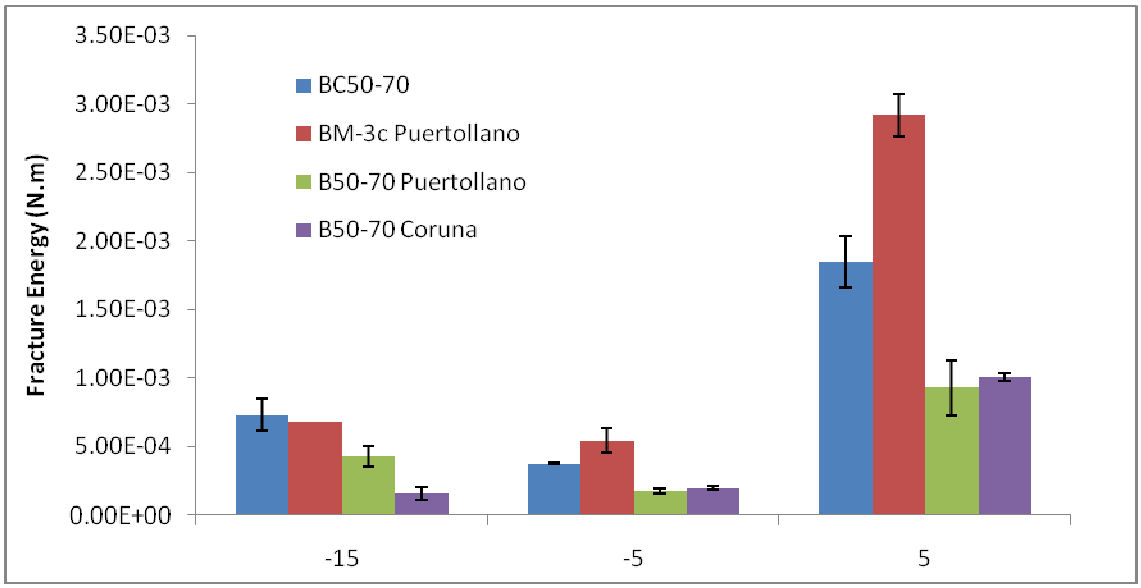


Figure E2a.1. Graph. SENB results for Spanish binders.

An example of the LAS stress vs. strain curve for RTFO and PAV material at 5°C and 20°C is shown in figure E2a.2. It can be seen that after aging, the LAS response changed significantly. Generally, shear stresses in PAV binders are greater than in RTFO binders.

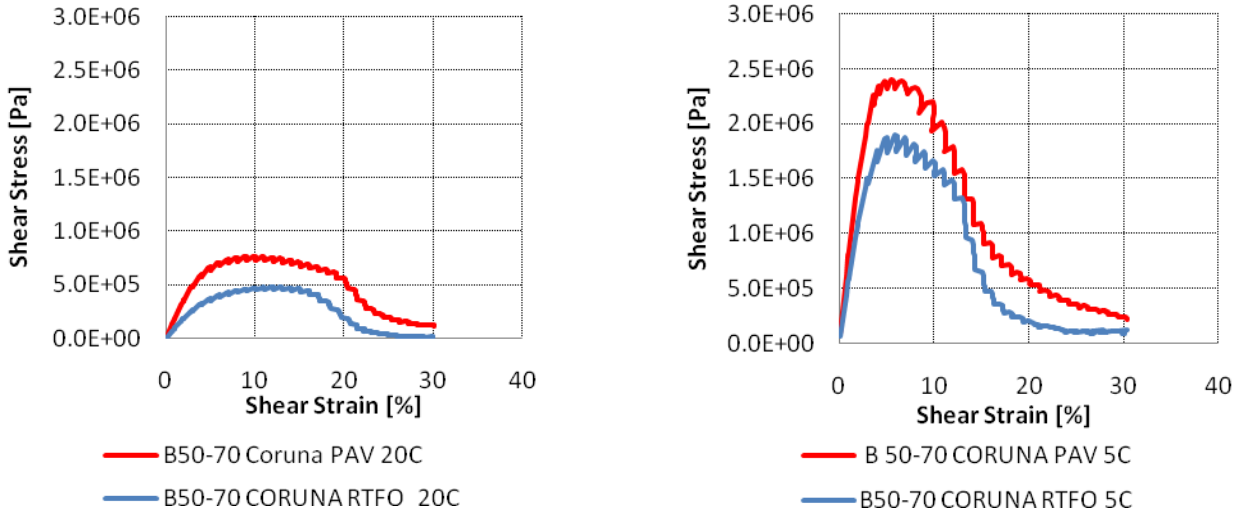


Figure E2a.2. Graph. LAS stress versus strain curve at 20°C ( left) and 5°C (right).

The numbers of cycles to failure at 2.5% strain for the RTFO and PAV materials at 20°C are shown in figure E2a.3. The results indicate that for these set of binders and strain level, aging improve the fatigue performance. Also, for RTFO aging, the four binders have very similar

response. After PAV aging, the binder B50-70 Coruna has significantly better fatigue performance than the other materials.

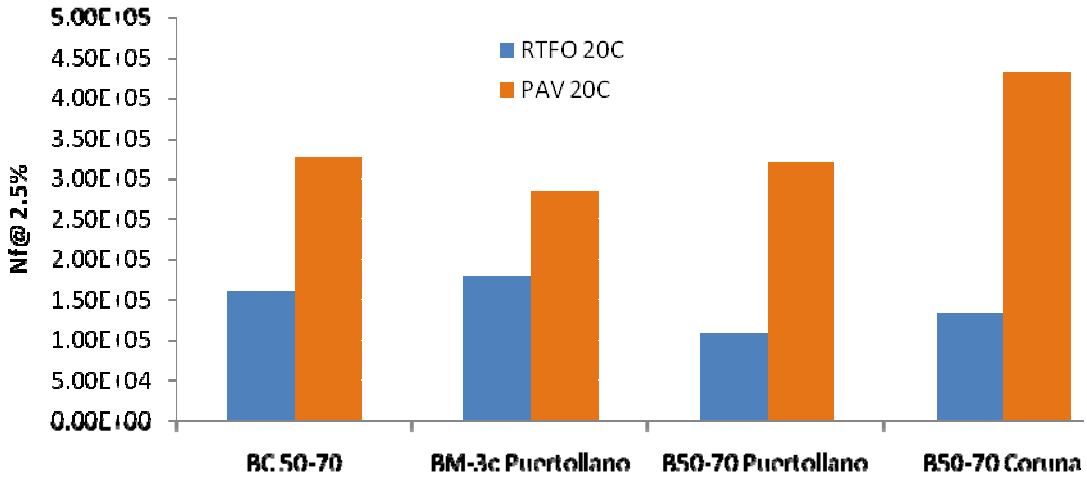


Figure E2a.3. Graph. Number of cycles to failure at 20°C and 2.5% strain after RTFO and PAV.

Work Planned Next Quarter

Next quarter, the research team will focus on completing the test matrix for Bitumen Bond Strength (BBS) tests and glass transition measurements. Based on the testing results from this work element, the team will develop a model to help estimate the level of binder modification needed and provide a costing index.

**Work element E2b: Design System for HMA Containing a High Percentage of RAP Materials (UNR)**

Work Done This Quarter

This work element is a joint project between University of Nevada, Reno and University of Wisconsin–Madison. Work was focused on three main topics:

- The proposed analysis procedure for estimating blended binder properties based on binder replacement percentages were applied to additional mixture binder extraction sample. This was done in attempt to justify the validity of the proposed procedure in estimating blended binder properties.
- It has been identified that workability testing of high percentage RAP mixes remains a critical concern within this project. As such, a testing procedure has been proposed for viscosity of mortars and initial testing has begun in the Dynamic Shear Rheometer.

- Coordination with work element E2d (Thermal Cracking in Asphalt Mixtures) continues and is identified as the final research objective in work element E2b. A proposed testing procedure for estimating effect of RAP binders on cracking using RAP mortars has been identified using the Single Edged Notched Bending (SENB) apparatus. Initial results are promising.

In subtask E2b-2, samples of RAP stockpiles in Iowa, California, and South Carolina have been extracted using a toluene/ethanol mixture as well as with cyclohexane. Characterization using the Asphaltene Determinator, as well as rheological measurements, has been completed and indicate some potential differences in the materials extracted with cyclohexane versus the toluene/ethanol extracted binders. Blends of ARC core asphalts BI 0001 and BI 0002 and the extracted RAP binders from Palmdale California at ratios of 15 and 50% are underway. The prepared blends will be investigated using Automated Flocculation Titrimetry (AFT), Asphaltene Determinator, and rheology.

Under subtask E2d-3, "Develop a Mix Design Procedure," the requested materials for both projects in UTAH have been received. The experimentation has begun for mixing Method A and Method B. To gauge the differences between the mixing methods certain characteristics and properties are being measured. These include monitoring the temperature during the mixing process, subjecting them to different short-term aging levels, measuring the binder properties, measuring volumetric properties and conducting dynamic modulus (E*) testing. To ultimately compare the separate methods with the field mixed lab-compacted mixtures all the same testing is conducted on those samples. The material being tested in the first phase of this project was obtained from projects constructed in Utah. It was a ½" HMA with 25 % RAP with a 58-34 virgin asphalt binder.

Under subtask E2b-5, the fatigue testing of the asphalt mixtures from Manitoba PTH8 has started.

Significant Results

Blended binders chemically extracted from additional mixes containing a known weight percentage of reclaimed material (RAP) and fresh binder grade were tested. The results where compared with the estimated properties of the blended binders using the proposed mortar testing of select RAP mixed with fresh binders.

Figures E2b.1a and E2b.1b summarize the results of this comparison utilizing four unique RAP sources and two fresh binder grades. The true low temperature grades estimated from the extraction data, and those estimated from the analysis procedure, for the PG 64-22 fresh binder (figure E2b.1a) are within 6°C for the mixtures containing 15 percent and 25 percent RAP. Two of the four RAP sources demonstrated less than a 3°C continuous grade difference in this range of RAP inclusion. It should be noted that as the weight percentage of RAP is increased, the difference in low temperature continuous grade between the proposed analysis procedure and the extracted binder increased, reaching almost 9°C for one RAP source at 40% RAP binder.

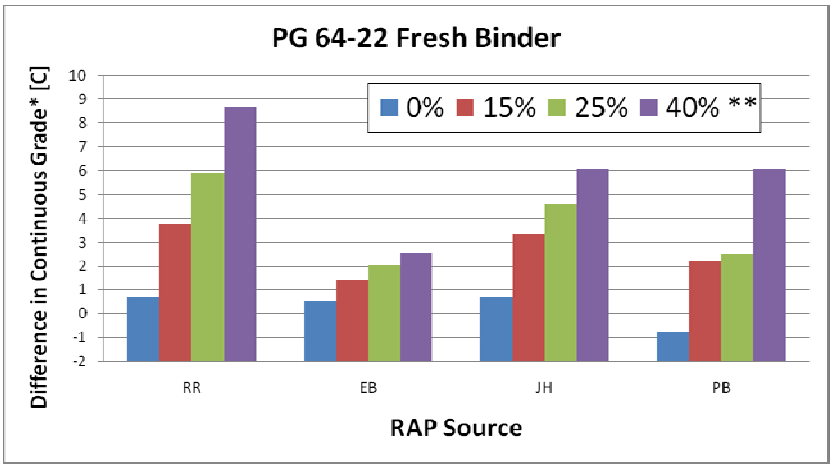


(a)

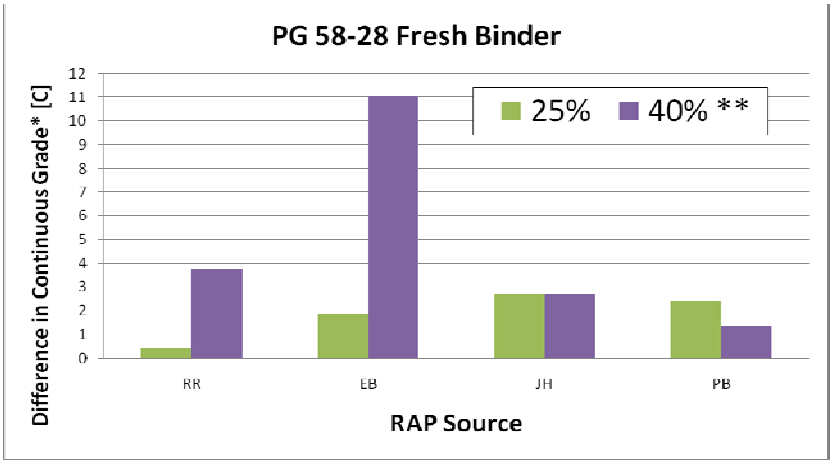


(b)

Figure E2b.1. Difference in low temperature continuous grade estimates for fresh binder PG 64-22 (a) and PG 58-28 (b).*Difference in continuous grade is calculated as the proposed mortar procedure estimate minus the extracted binder continuous grade estimate.
**Weight percentage of RAP in mixture.

Similarly, the low temperature continuous grade estimates between the extraction data and analysis procedure for the PG 58-28 fresh binder (figure E2b.1b) were within 3°C up to 25 percent RAP by weight of mixture. Similar to the PG 64-22 binder, increasing the RAP content of the mixture for this binder show higher difference between continuous grade estimates, up to nearly 11°C for one RAP source. This trend is not the same for all RAP sources using the PG 58-28 binder as one source, PB source demonstrates the opposite effect, while another source, JH, showed nearly no difference in estimates. It should be noted that mixes containing 0 percent and 15 percent RAP were not completed for the PG 58-28 fresh binder.

As mentioned in the previous progress report, the difference in estimates could be due the problem of solvent left in extracted binders, unsuccessful removal of the layer of binder adsorbed to aggregate, or compatibility of the RAP and virgin binders. An example supporting these

claims can be seen in the data. In some cases increasing the weight percentage of RAP in the mixtures corresponded to a counterintuitive *decrease* in low temperature continuous grade. Addition of RAP materials in a mixture is expected to increase the low temperature continuous grade, not decrease it. This discrepancy is demonstrated in table E2b.1 for one RAP source. As well, the continuous grade change associated with increasing the RAP percentage of the mixture from 0 percent to 15 percent corresponds to a change in continuous grade of only 0.1°C, which seems unlikely. Finally, note that the continuous grade of the extracted PG 64-22 binder at 0 percent RAP does not pass the -22 grade by nearly 2°C. If the differences are found to not be the result of residual solvent, it may be an example of a change in compatibility. The effect of compatibility of the RAP binder and virgin binder may become more significant at higher RAP levels. WRI is investigating the significance of compatibility of RAP and virgin binder in subtask E2b-2.

Table E2b.1. Low temperature RAP mixture extraction data.

| RAP [%][1] | Fresh Binder | RAP Source | Extracted Binder Continuous Grade, °C |
|---|---|---|---|
| 0% | PG 64-22 | PB | -20.6 |
| 15% | PG 64-22 | PB | -20.5 |
| 25% | PG 64-22 | PB | -18.6 |
| 40% | PG 64-22 | PB | -19.1 |
| 25% | PG 58-28 | PB | -26.3 |
| 40% | PG 58-28 | PB | -21.3 |

[1]Weight percentage of RAP in mixture

Workability testing following the proposed material preparation (mortar) procedure has begun and is planned as the next major research objective for this work element. The trial procedure selected for analysis is the Steady Flow Procedure in the Dynamic Shear Rheometer, which is outlined in the NCHRP Report 648 Mixing and Compaction Temperatures of Asphalt Binders in Hot Mix Asphalt. The first step will be to identify the temperature – viscosity profile of the mortars using a constant shear rate. Plotting an identified shear stress versus temperature will allow for the extrapolation of the mixing and compaction temperatures required for the RAP mixture. It should be noted that the Steady Flow Procedure is designed for binder testing and may require adjustments for testing the mortar materials. Sample geometry may also be modified if necessary; similar to what was discovered in the verification testing previously tested.

Under subtask E2d-3, three distinct laboratory mixing methods to incorporate the RAP material are being evaluated:

> Method A: All materials, including RAP, are heated to the appropriate mixing temperature for the virgin binder grade.
>
> Method B: Virgin aggregates are superheated according to NAPA's guidelines with the RAP added at the ambient temperature in the dry condition.

Method C: Virgin aggregates are superheated according to NAPA's guidelines with the RAP added at the ambient temperature in the wet condition.

Monitoring the temperature throughout the mixing process was done using an infrared temperature gun. The plots of the temperatures versus the time can be seen in figures E2b.2 and E2b.3. The timer was started just as the aggregate was removed from the oven, which creates the delay in readings at the beginning of the plots. It was found that the aggregate and RAP needed at least 15-30 seconds for heat transfer to start occurring throughout the mix so temperature readings are started in that range after the sample has begun mixing. The mixing temperature for Method A was 313°F while the virgin aggregate used in Method B was superheated to 379°F. It is interesting to note that while in Method B the temperature near the beginning of mixing was in some cases 20°F higher than Method A, both methods resulted in nearly the same temperature at the completion of mixing of 285 – 290 °F. So superheating the virgin aggregate was effective in transferring heat to the RAP, but at the expense of the extra energy required to heat the materials.

When conducting the volumetric analysis the times and temperatures for mixing and aging were monitored closely. For both Methods A and B the maximum specific gravity (Gmm) was performed for using three different absorption times: 0, 2, and 4 hours. Each increase in absorption time yielded a slightly larger Gmm value. The complete volumetric analysis is summarized in table E2b.2. In figure E2b.4, the relationship between absorption time and the maximum specific gravity is displayed.

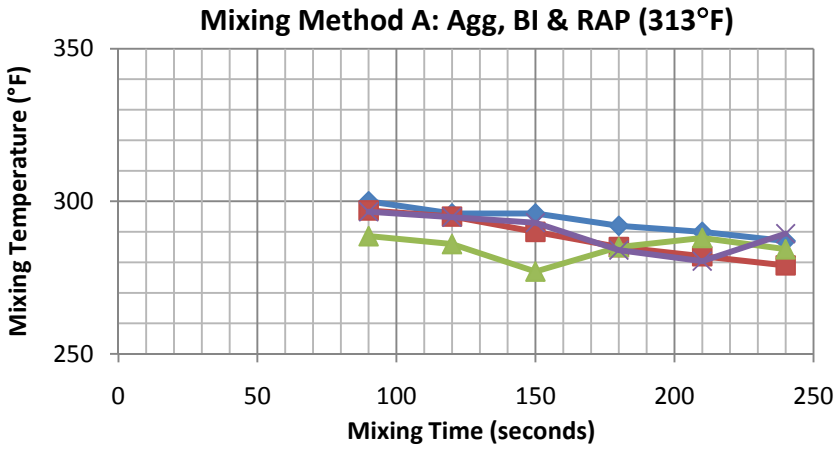


Figure E2b.2. Monitoring mixing temperature of Method A.

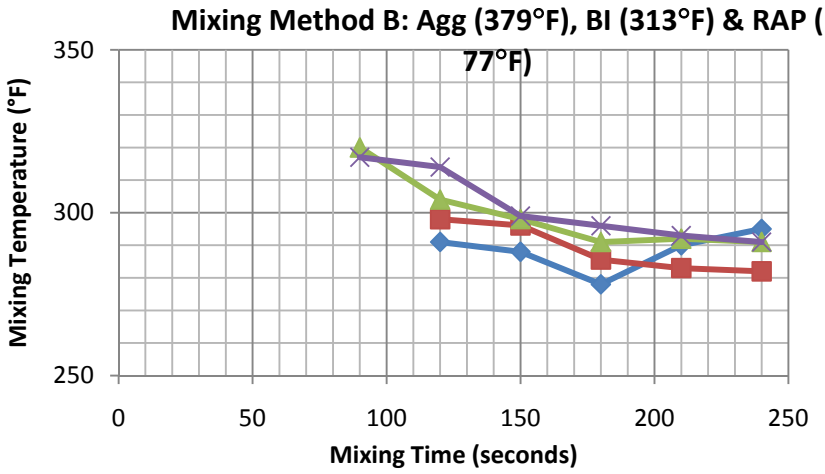


Figure E2b.3. Monitoring mixing temperature of Method B.

Table E2b.2. Summary of volumetric properties.

| Mix | Property | | | | | | | | | | |
|---|---|---|---|---|---|---|---|---|---|---|---|
| | Gmb | | | | Gmm | | | | Va (%) | VMA (%) | VFA (%) |
| | Sample Reheat | STO aging of loose mix at 284 F (hrs) | Rep | Mean | Sample Reheat | STO aging of loose mix at 284 F (hrs) | Rep | Mean | | | |
| Field | 2.5 hrs at 275F | 0.5 | 2.42 | 2.41 | 2.5 hrs at 275F | 0 | 2.49 | 2.484 | 2.85 | 14.1 | 79.8 |
| | | | 2.41 | | | | 2.48 | | | | |
| | 3 hrs at 275F | 2 | 2.41 | 2.40 | 3 hrs at 275F | 0.5 | 2.49 | 2.491 | 3.82 | 14.7 | 74.1 |
| | | | 2.39 | | | | 2.49 | | | | |
| Method A | N/A* | 2 | 2.38 | 2.38 | N/A* | 0 | 2.50 | 2.494 | 4.66 | 15.4 | 69.7 |
| | | | 2.37 | | | | 2.49 | | | | |
| | N/A* | 2 | 2.38 | 2.38 | N/A* | 2 | 2.51 | 2.510 | 5.25 | 15.4 | 65.8 |
| | | | 2.37 | | | | 2.51 | | | | |
| | N/A* | 2 | 2.38 | 2.38 | N/A* | 4 | 2.52 | 2.514 | 5.42 | 15.4 | 64.7 |
| | | | 2.37 | | | | 2.51 | | | | |
| Method B | N/A* | 2 | 2.39 | 2.38 | N/A* | 0 | 2.49 | 2.497 | 4.54 | 15.1 | 70.1 |
| | | | 2.38 | | | | 2.50 | | | | |
| | N/A* | 2 | 2.39 | 2.38 | N/A* | 2 | 2.50 | 2.505 | 4.83 | 15.1 | 68.1 |
| | | | 2.38 | | | | 2.51 | | | | |
| | N/A* | 2 | 2.39 | 2.38 | N/A* | 4 | 2.51 | 2.514 | 5.16 | 15.1 | 65.9 |
| | | | 2.38 | | | | 2.51 | | | | |

* N/A denotes not applicable

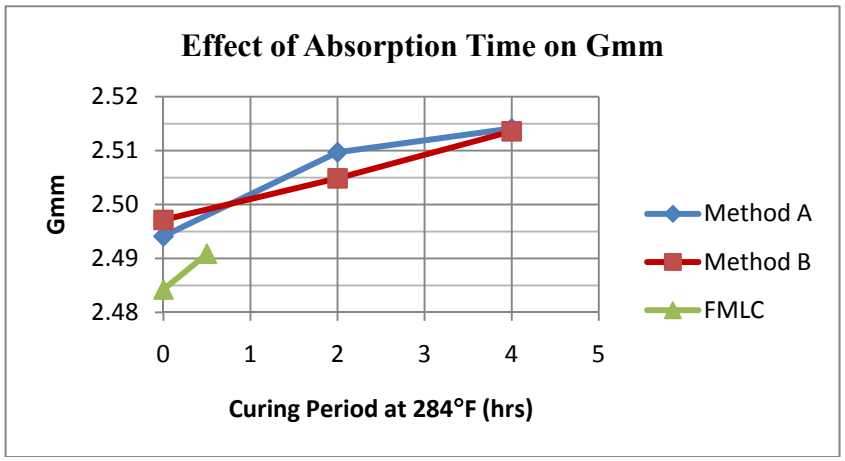


Figure E2b.4. Gmm versus plot of absorption time.

As can be seen in the summary table the air voids and the maximum specific gravity for the laboratory created samples was larger than the values for the field mix lab compacted samples. The mix design values for this particular mix were air voids of 3.6%, a Gmm of 2.492 and a VMA of 14.5. So the FMLC samples most closely represent the mix design values. Method B has volumetric properties most simulating those of the field samples, but there are still some differences.

A short-term aging analysis is also being conducted to determine which level of aging will most closely represent the actual aging that occurs in the field. After each aging level is complete the binder from the sample is extracted and recovered so it can be graded. The extraction is done using a solution mix of 85% toluene and 15% ethanol. The asphalt binder is then recovered using the RotoVap recovery apparatus. A small portion of the asphalt is set aside for carbonyl testing. The results for the carbonyl testing are not yet available. The remaining asphalt binder is graded in accordance with AASHTO procedures using the Dynamic Shear Rheometer and the Bending Beam Rheometer. A summary of the extracted binder properties is shown is table E2b.3. Table E2b.4 summarizes the increases in temperatures after short-term aging for each method. For each method the performance grade increased after short-term aging as would be expected. The field mixes have the largest increase because those have the longest additional aging time. Examining the results for Methods A and B they appear to be very similar with field mixes. Method A have a slightly larger increase in the high grade while Method B had a slightly larger increase for the low and intermediate grades.

Figure E2b.5 presents a graphical representation of the extracted binder performance grades. It is important to note that Methods A and B produced asphalt binders that have nearly identical properties to those of the field mix when considering no additional short-term aging (0hr). So at this point the mixing method does not affect the performance grade of the asphalt immediately after mixing.

Table E2b.3. Summary of recovered binder grading.

| Binder | STO Aging of loose mix @ 284°F | True High Grade | True Intermediate Grade | Low Temperature Characteristics | | | | | True Low Grade | PG Grade |
|---|---|---|---|---|---|---|---|---|---|---|
| | | Temp, °C | Temp, °C | Criteria | Temp, °C | Δ T, °C | Controlling | | Temp, °C | Temp, °C |
| Original | N/A* | 65 | 11.8 | Stiffness | -23.8 | 0.7 | Stiffness | -23.8 | -33.8 | 64 - 28 |
| | | | | m-value | -24.5 | | | | | |
| Field | 0 | 71.5 | 18.9 | Stiffness | -20.5 | 3.4 | m-value | -17.0 | -27.0 | 70 - 22 |
| | | | | m-value | -17.0 | | | | | |
| | 4 | 76.7 | 22.0 | Stiffness | -19.4 | 6.5 | m-value | -12.9 | -22.9 | 76 - 22 |
| | | | | m-value | -12.9 | | | | | |
| Method A | 0 | 68.7 | 17.3 | Stiffness | -21.2 | 2.9 | m-value | -18.3 | -28.3 | 64 - 28 |
| | | | | m-value | -18.3 | | | | | |
| | 2 | 73 | 18.1 | Stiffness | -20.5 | 3.1 | m-value | -17.4 | -27.4 | 70 - 22 |
| | | | | m-value | -17.4 | | | | | |
| Method B | 0 | 70.1 | 17.3 | Stiffness | -20.8 | 1.8 | m-value | -19.0 | -29.0 | 70 - 28 |
| | | | | m-value | -19.0 | | | | | |
| | 2 | 72.7 | 19.2 | Stiffness | -20.4 | 2.9 | m-value | -17.5 | -27.5 | 70 - 22 |
| | | | | m-value | -17.5 | | | | | |
| Lab Blend | N/A* | 71.3 | 16.3 | Stiffness | -21.5 | 2.1 | m-value | -19.4 | -29.4 | 70 - 28 |
| | | | | m-value | -19.4 | | | | | |
| Rap | 0 | 89 | 33.4 | Stiffness | -10.6 | 8.7 | m-value | -2.0 | -12.0 | 88 - 12 |
| | | | | m-value | -2.0 | | | | | |

Table E2b.4. Summary of increase in recovered binder grading after short-term aging.

| Binder | High Grade | Low Grade | Intermediate Temp |
|---|---|---|---|
| Field | 5.2 | 4.1 | 3.1 |
| Method A | 4.3 | 0.9 | 0.8 |
| Method B | 2.6 | 1.5 | 1.9 |

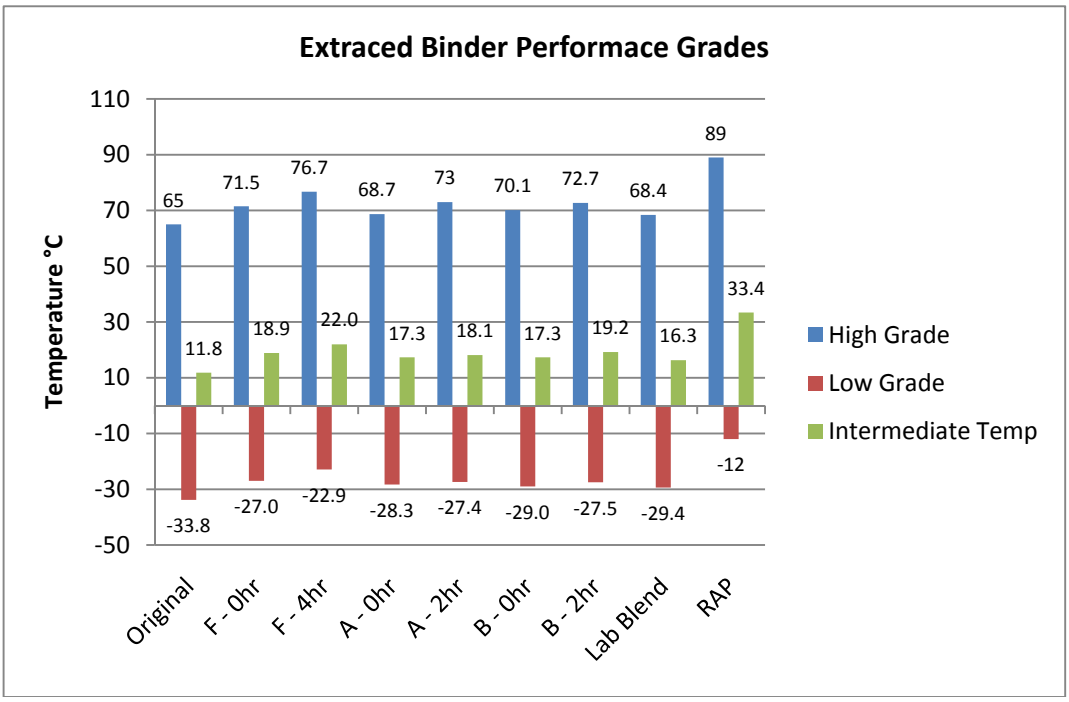


Figure E2b.5. Representation of recovered asphalt binder grades.

Significant Problems, Issues and Potential Impact on Progress

None

Work Planned Next Quarter

The workability testing described above is considered to be the highest priority for this work element and will be explored in depth for the next progress report. Although no additional fracture testing (SENB) has been completed as of this report time, the apparatus and testing procedure has been finalized and testing will resume once a work plan is completed.

Work will continue on the fatigue testing of the Manitoba PTH8 RAP project.

In subtask E2b-2, after completion of the analyses of the blends using the California RAP, blends will be prepared with the extracted Iowa RAP binder for analysis by AFT, AD and rheology.

Under subtask E2b-3, all work previously completed for the I-215 material will be repeated for the newly received material for the second project from Utah. Once information is received concerning the field adjustments due to moisture within the RAP; testing following Method C will commence. Additionally dynamic modulus testing will start to determine the effect of both the mixing method and the short-term aging time on the stiffness of the lab created mixes.

**Work element E2c: Critically Designed HMA Mixtures (UNR)**

Work Done This Quarter

Work continued to evaluate the applicability of the recommended deviator and confining stresses for the flow number test. As part of the FHWA FN task group, materials from FLDOT, NCDOT, TxDOT, Wisconsin, NCAT and Granite (West California) have been received. In this quarter, mix designs for FLDOT, NCDOT, TxDOT and NCAT have been verified and adjusted to meet the Superpave requirements. In addition, each gradation source has been verified in the laboratory. Figure E2c.1 shows the blend gradations of the mixtures that have been verified. The figure shows that the mixtures cover a wide range of gradations. The dynamic modulus of the verified mixtures has been conducted at 7, 4 and 2% air void content.

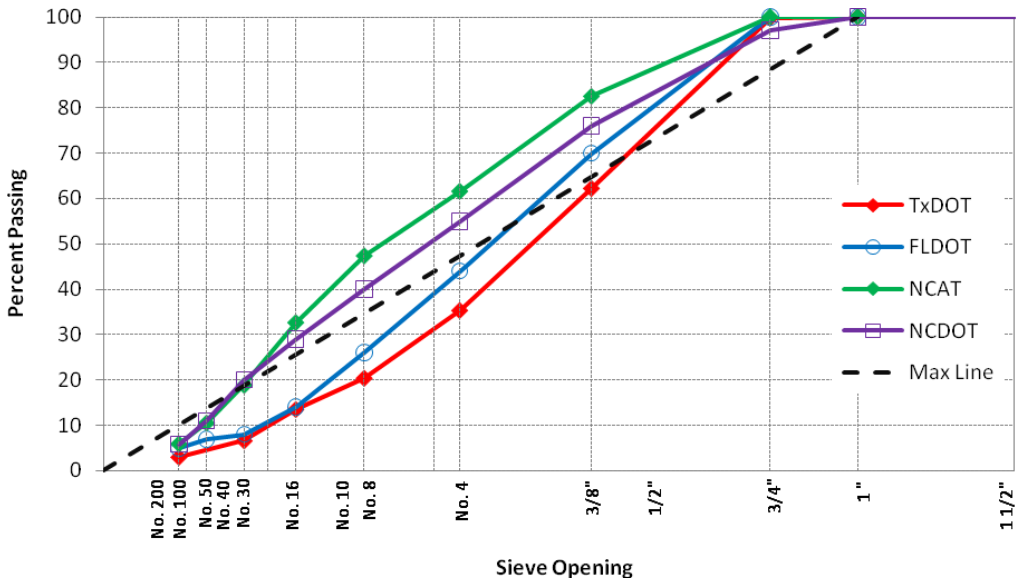


Figure E2c.1. Blend gradations.

The work on converting the pulse duration in time domain for a given pavement response into frequency domain continued to be investigated using the Fast Fourier Transformation (FFT). The concept of predominant frequency(ies), $f_p$, to predict all components of the pavement responses was verified for different pavement structures and conditions. The frequencies for the asphalt sub-layers as proposed by the MEPDG procedure were determined and compared to the predominant frequencies determined by the FFT analysis.

Significant Results

The dynamic modulus of the FLDOT, NCDOT, TxDOT and NCAT mixes are shown in figures E2c.2 to E2c.5, respectively.

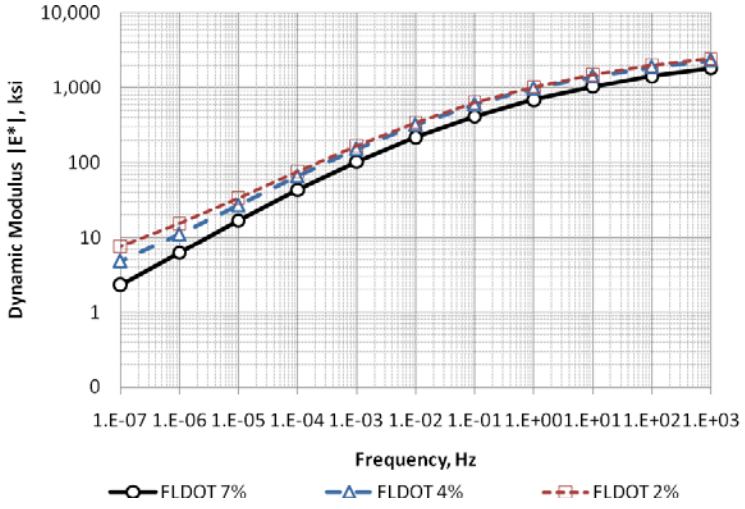


Figure E2c.2. Dynamic modulus at 20°C for FLDOT.

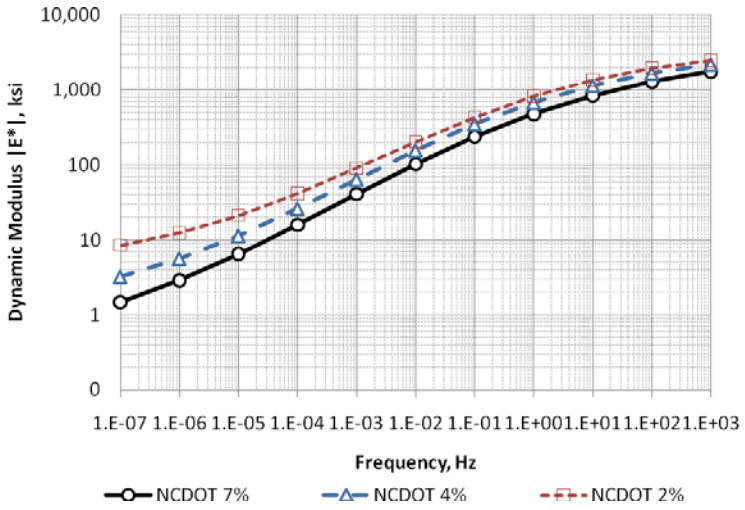


Figure E2c.3. Dynamic modulus at 20°C for NCDOT.

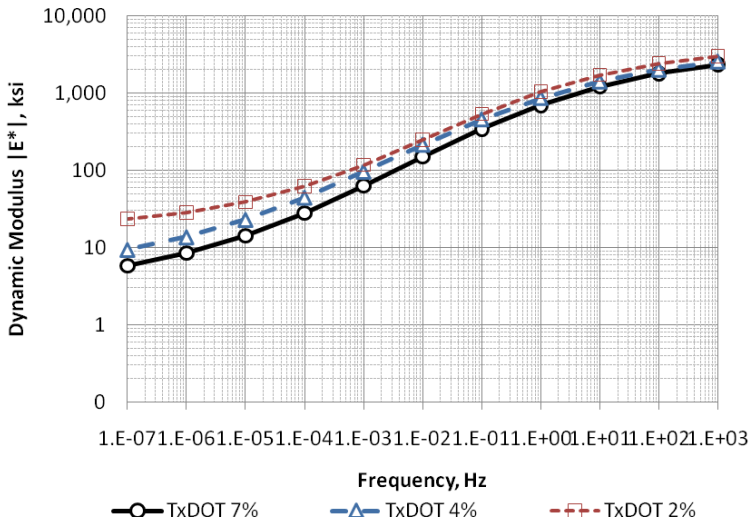


Figure E2c.4. Dynamic modulus at 20°C for TxDOT.

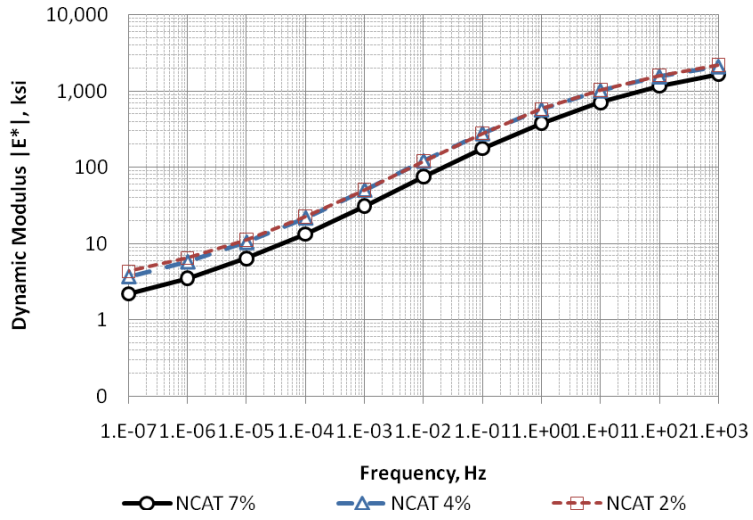


Figure E2c.5. Dynamic modulus at 20°C for NCAT.

Significant Problems, Issues and Potential Impact on Progress

The write-ups for the figures and tables captions have delayed the submission of the subtask E2c.1 report for review.

Work Planned for Next Quarter

Continue the evaluation of the various mixtures according to the Flow Number Task Force experimental plan.

Complete the tables and figures write-ups for the report.

Continue the work on the evaluation of the predominant frequencies and present the findings at the 2011 annual meeting for the AFD80 committee in Washington D.C.

**Work element E2d: Thermal Cracking Resistant Mixes for Intermountain States (UNR & UWM)**

Work Done This Quarter

This work element is a joint project between University of Nevada Reno and University of Wisconsin–Madison. Under subtask E2d.1.a, probability functions are currently being fitted for pavement temperature distributions for the various sections using a statistical analysis software called SAS® 9.2. The data will provide details of the overall characteristics of pavement temperatures in the field sections. Hopefully this will provide further insight on how each section compare to each other. Particularly, if there are any differences in pavement temperature profiles for sections within and outside the intermountain region.

Under subtask E2d.3.a, some carbonyl measurements have been received from Texas A&M University and data is being analyzed at UNR for hardening susceptibility and reaction kinetics.

The TSRST experiment at UNR is ongoing. Particularly, the effect of cooling rate on low-temperature characteristics of cylindrical asphalt mixtures is still under investigation. However, a few refinements of the TSRST test and equipment are currently being investigated which has caused some delay in this research effort.

In this quarter, the research team started efforts on finite element modeling of thermal stress buildup in asphalt mixtures. High resolution scans of asphalt mixture slices were prepared and converted to binary images using MATLAB. The binary images were then mapped into a 2-dimensional solid model in ABAQUS for analysis. Initial runs have been able to capture the stress buildup in the aggregate-binder interface as temperature decreased due to differences in the coefficients of thermal expansion/contraction.

As part of efforts on standardizing the Tg-TSRST test procedure, the device was renamed to the Asphalt Thermal Cracking Analyzer (ATCA). Modifications were made to the end plates and gluing procedure to prevent occasional adhesion failures in the restrained beam. The changes have successfully eliminated these problems. With these changes the device was deemed sufficiently ready for a complete experimental testing matrix on beams prepared from MnROAD materials. The samples will be simultaneously tested in restrained conditions (for measuring stress build up) and unrestrained conditions (for measuring coefficient of contraction and glass

transition). Observations of isothermal stress buildup and contraction during ATCA testing, as reported in the previous quarterly reports, prompted the group to investigate the effect of isothermal conditioning on the fracture properties and stress buildup of the mixtures. Data collected last quarter indicate the need for careful examination of such effects.

Under subtasks E2d.3.b and E2d.3.c, with all of the E*-compression testing completed, the extraction and recovery for the asphalt binders is underway. To date 88% of the samples have been extracted and recovered. Nearly 45% of the Carbonyl Area (CA) measurements have been completed for this subtask. Further samples are in the process of being tested. Progress continues with the determination of the low shear viscosity (LSV) and binder master curve measurements. Nearly 25% of that testing has been completed from this subtask.

The Thermal Stressed Restrained Specimen Test (TSRST) specimens are all mixed and compacted and are currently going through their aging durations. Few samples have been tested, as the final testing procedure is being finalized under work element E2d-3. However, all of the 0, 3, and 6 month aged samples have been cut and prepared for testing, along with the majority of 9 month samples.

Along with the TSRST preparation, samples for the coefficient of thermal expansion, CTE, have also been prepared and are undergoing their respective aging as well. The first of the CTE samples are being cut and prepared to send to the University of Wisconsin for testing.

Under subtask E2d-4, a numerical procedure was developed to determine the relaxation modulus ($E_R$) from the stress-build curve as measured by the TSRST test. An algorithm was written in MATLAB that would allow, numerically, to find $E_R$ for any shape of stress build-up.

Significant Results

Under subtask E2d.3.a, hardening susceptibility and reaction kinetics have been prepared for one of the binder types (PG64-22+3%SBS). Results are shown in figures E2d.1, E2d.2 and E2d.3. These plots and relationships will be valuable input to the pavement oxidation model.

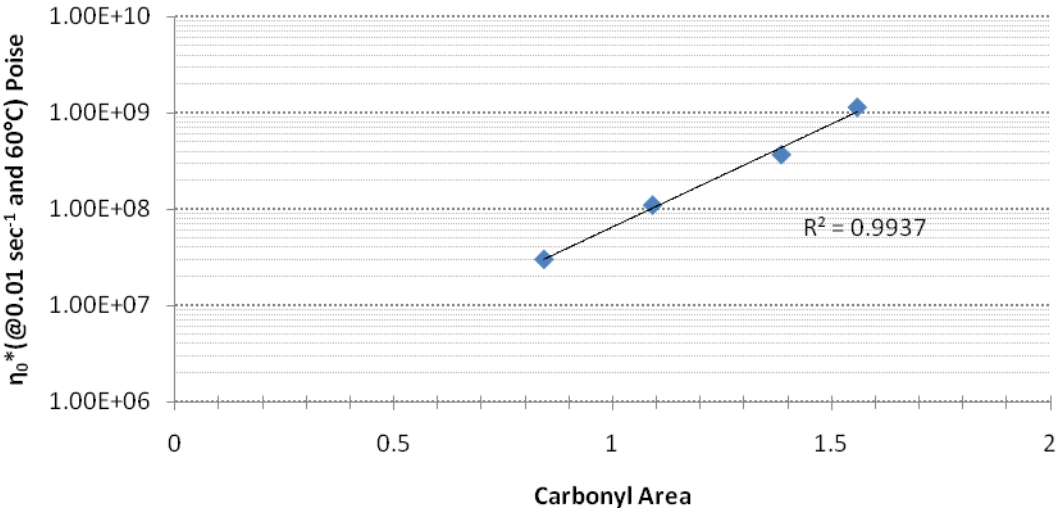


Figure E2d.1. Zero shear viscosity vs. carbonyl area for PG64-22+3%SBS aged at 85°C to determine hardening susceptibility.

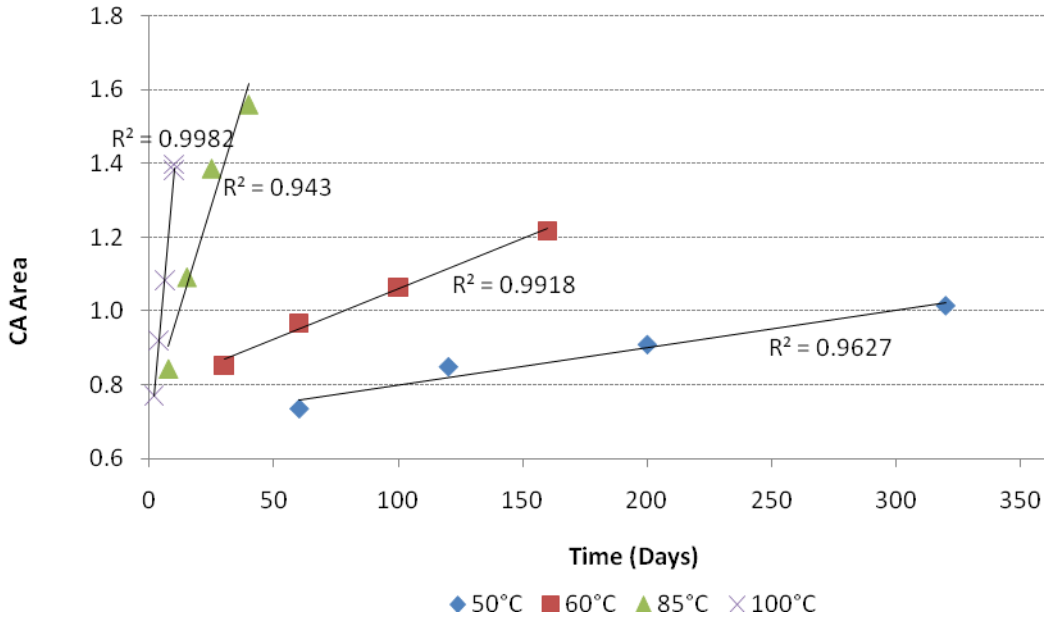


Figure E2d.2. Carbonyl area as a function of time for PG64-22+3%SBS binder aged at various temperatures.

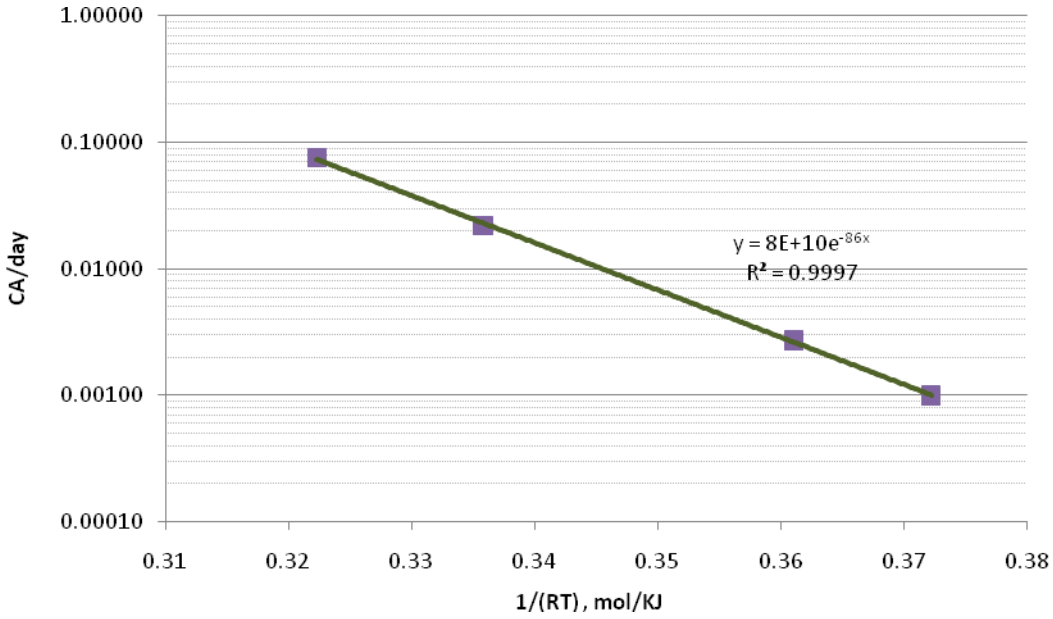


Figure E2d.3. Carbonyl growth.

Significant progress has been made in the E*-Tension testing procedure at UNR. The software and hardware upgrades have been installed. The testing protocol has been established and validation testing is taking place prior to the actual experimental matrix samples. The procedure has been fairly well validated in compression, with efforts now being put into the tension testing mode.

The DSR issues at UNR that hindered testing previously have been resolved and production testing of the binders is underway.

Results from the ATCA were analyzed and used to calculate relevant low temperature material properties, most notably, the relaxation modulus. The relaxation modulus convolution integral was solved numerically. Both sides of the equation were differentiated with time to eliminate the integral. Thermal stress (i.e., restrained beam) and strain (i.e., unrestrained beam) data was differentiated by calculating the point by point slope of these variables and inputted into the equation, which was subsequently solved to achieve the relaxation modulus. An example of ATCA results and the calculated relaxation modulus curve are shown in figure E2d.4.

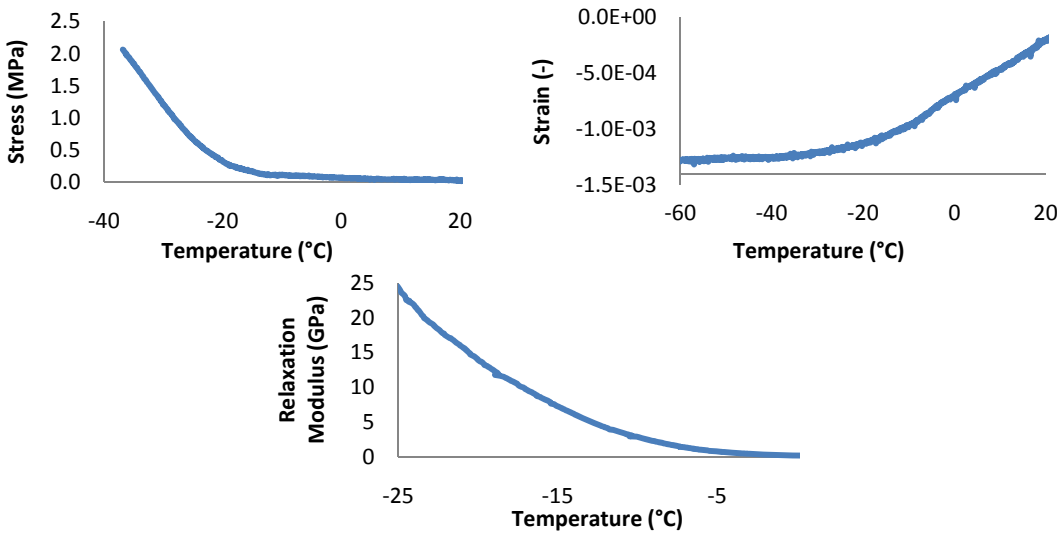


Figure E2d.4. Graph. TCAA results and calculated relaxation modulus curve.

The change in stress buildup and fracture properties with isothermal conditioning investigated in this quarter prompted more testing of effect of isothermal conditioning on binder properties. Figure E2d.5 depicts results of testing five binders from MnROAD sections after 0.5 and 72 hr of conditioning at their glass transition temperature ($T_g$). It can be seen that a 37% average increase in stiffness was observed, as indicated by the slope of the P-u curve after conditioning. The fracture toughness also increased for all binder tested after conditioning; however, the effect on fracture energy was not clear. Fracture energy increased for the 2 unmodified binders (i.e., MnROAD Cell 20 and NY), while decreasing for the 3 modified binders. This decrease is explained by the relative loss of deformation at fracture with conditioning time. In other words, the increase in load at fracture is offset by reduction in deformation at break for the unmodified binders.

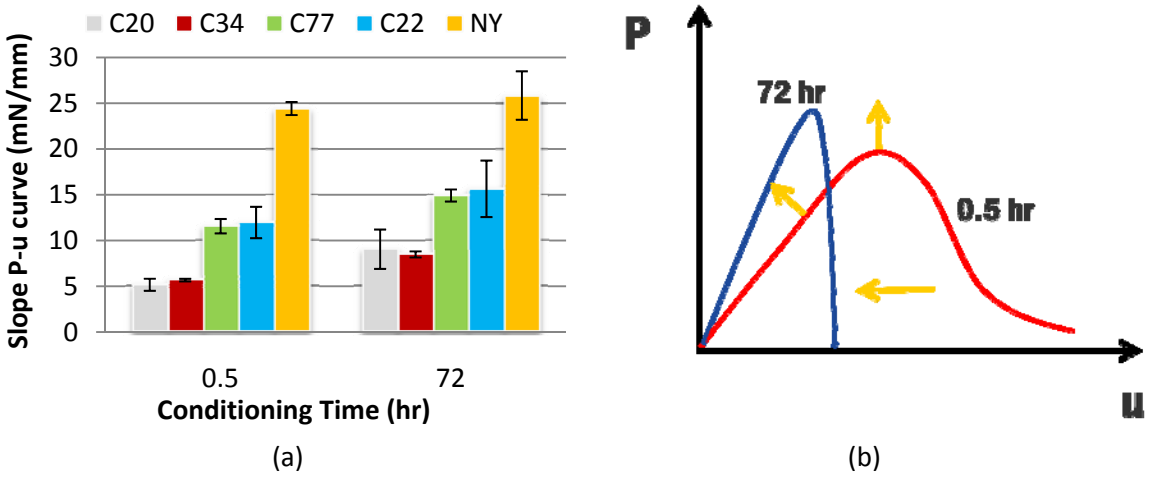


Figure E2d.5. Graph. (a) Slope of P-u curve before and after isothermal conditioning at $T_g$. (b) Schematic of general trend observed after conditioning.

Thermal stresses were calculated from BBR creep tests run after 1 and 72 hr of conditioning to determine the effect of physical hardening on thermal stress build-up. Figure E2d.6 shows the thermal stress calculated at T=-30°C for both cases of isothermal conditioning.

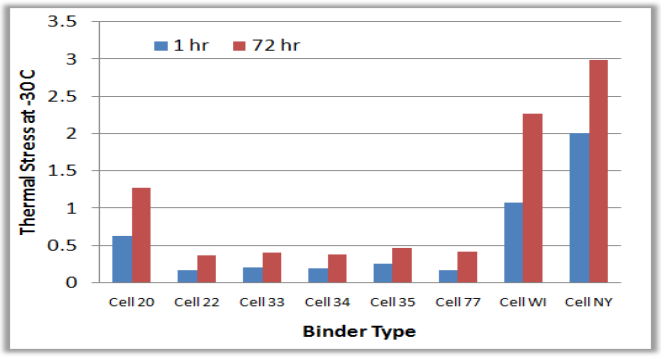


| Cell No. | 1 hr Rank | 72 hrs Rank |
|---|---|---|
| Cell 20 | 6 | 6 |
| **Cell 22** | **2** | **1** |
| **Cell 33** | **4** | **3** |
| **Cell 34** | **3** | **2** |
| Cell 35 | 5 | 5 |
| **Cell 77** | **1** | **4** |
| Cell WI | 7 | 7 |
| Cell NY | 8 | 8 |

Figure E2d.6. Graph. Effect of 72 hr isothermal conditioning on ranking of binders (by least stress buildup at -30°C).

It can be seen that physical hardening has increased the amount of stress build-up very significantly. Figure E2d.6 indicates that physical hardening caused the ranking of the top four performers before conditioning to change after 72 hr of conditioning. These results indicate that the effect of physical hardening and isothermal conditioning on thermal stress build-up needs to be further investigated.

The team also worked on establishing the relationship between binder fracture properties predicted by the Single Edge Notch Bending test (SENB) and mixture fracture properties estimated by the Semi Circular Bending (SCB) and the Disc Compact Tension (DCT) tests. Comparisons were made based on testing of MnROAD materials. SCB and DCT mixture testing was conducted by the University of Minnesota and the University of Illinois at Urbana-Champaign, respectively. Overall it is observed that a relatively good relationship between the SENB and the SCB results exists. Comparison of the test results between the SENB and the DCT, as well as between the SCB and the DCT did not yield any apparent correlation. This can be explained by the significantly higher loading rates in the DCT compared to the SCB and SENB, both which use a similar loading rate.

Significant Problems, Issues and Potential Impact on Progress

A few refinements of the TSRST test and equipment at UNR are currently being investigated which has caused some delay in this research effort. Once adjustments are made, this research effort will progress and will continue looking into the effect of binary cooling rates on TSRST results.

Work Planned Next Quarter

Continue the experiment to evaluate the aging characteristics (oxidation and hardening kinetics) of asphalt binders when aged in forced convection (horizontal airflow) ovens.

The research team will focus on theoretical calculation and prediction of thermal stress buildup and relaxation, as observed using the ATCA. Efforts on thermal cyclic modeling will also continue based on finite element simulations. AASTO draft standard specifications will be prepared for both the SENB and the ATCA.

Continue to evaluate the effect of cooling rate on TSRST results using the proposed cylindrical test geometry.

Under subtasks E2d.3.b and E2d.3.c, the main focus early in the next quarter will be continue to increase the amount of completed testing and begin the analysis of the results. All of the extraction/recovery testing is expected to be completed within the next quarter, with only 30 planned extractions left to be completed in this subtask. The final validation for E*-tension protocol is expected to be finalized and production testing should be underway. The development of the binder master curves and LSV measurements are expected to proceed with little difficulty. Testing on the TSRST samples are also expected to get underway as the exact testing conditions are determined.

The research team is planning on having in April a two-day meeting at UNR with Dr. Charles Glover from Texas A&M to discuss the temperature and oxidation models and how to incorporate them into the viscoelastic finite element tool (VE2D).

**Work element E2e: Design Guidance for Fatigue and Rut Resistance Mixtures (AAT)**

Work Done This Quarter

*Hirsch Model Refinements*

Laboratory work continued this quarter on the experiments to refine the Hirsch model. Three experiments were planned to improve the Hirsch model: (1) curing time experiment, (2) limiting modulus experiment, and (3) stress dependency experiment. Each of these experiments addresses a specific aspect of the Hirsch model and dynamic modulus testing. The curing time experiment addresses whether specimen aging significantly affects measured dynamic modulus values. The limiting modulus experiment address whether the limiting minimum modulus is a HMA is significantly affected by the modulus of the aggregate used in the mixture. Finally, the stress dependency experiment addresses the effect of stress level on the limiting minimum modulus of HMA.

Sufficient material for seven of the eight aggregates included the Hirsch model experiments have now been procured. The last remaining aggregate is a soft limestone from Florida. Specimens for 4 of the aggregates have been fabricated and testing is proceeding with these specimens.

*Resistivity Model Refinements*

The objective of this work is to refine the rutting model developed in NCHRP Projects 9-25 and 9-31 to better address modified binders by using data from the multiple stress creep recovery tests to characterize the binders. A final experimental design for the resistivity model refinements was developed based on the aggregates selected for the Hirsch model refinement. It includes nine binders with high temperature grade ranging from PG 58 to PG 82. Five of the binders are polymer modified, one is air blown, and three are neat. Eighteen mixtures will be tested. A total of 34 binder/mixture/temperature combinations will be used in the testing.

The binders and aggregates for this experiment were procured last quarter. This quarter the binder modulus, phase angle, and multiple stress creep recovery data required by the experimental design was measured.

*Fatigue Model Refinements*

Further work on continuum damage fatigue modeling was performed this quarter. The full report and additional data on the ALF II experiment was received from Nelson Gibson of the FHWA. This data allowed an intensive analysis of both ALF I and ALF II fatigue data which produced exceptional results.

A variety of approaches were taken in the analysis. Some of the factors considered are listed below:

- X-coordinate for calculating strains: at tire edge, 1 cm outside tire edge, various other distances from edge of tire.

- Z-coordinate (depth) for calculating strains: surface, 1 cm, and various other depths.
- Point of failure/crack initiation: cycles at first observed crack and cycles to 25 m total cracking.
- Variables for predicting critical C value: mix modulus, binder modulus, mix phase angle, binder phase angle, pavement thickness, in-place voids, design voids, difference between in-place and design voids (an indicator of compaction effectiveness), VMA, VBE, VFA, and various mixture and fracture parameters given in the ALF II report.

Eventually, an excellent model was developed, which used pavement strains that are calculated at 3.5 × tire radii at 1 cm below the surface. The loading frequency used was based upon a wavelength equal to 4 times the average tire radius. The point of failure was defined as cycles to 25 m total cracking. The model for predicting the critical C value was as follows:

$$Logit = 8.384 - 0.112\delta + 0.00962T - 0.2237\varepsilon_f + 0.072VTM_{in-place} - 0.317VMA \quad \text{(E2e.1)}$$

Where:

$Logit$ = logistic transform of the critical C value

$$= \ln\left(\frac{C_{critical}}{1 - C_{ciritical}}\right)$$

$\delta$ = phase angle of mix, in tension/compression or flexural loading, estimated from Hirsch model and empirical equation given in NCHRP Report 567 for converting modulus in dynamic compression to modulus in tension/compression or flexure

$T$ = pavement thickness, in cm

$\varepsilon_f$ = binder failure strain from direct tension test (%), estimated at m-value of 0.300 from bending beam rheometer test data

$VTM_{in\text{-}place}$ = in-place air voids, %

$VMA$ = design voids in the mineral aggregate, %

All predictors in this model were highly significant; p-values were 0.000 for four of the predictors, and 0.047 for in-place voids. The $r^2$ value for this model, adjusted for degrees of freedom, was 98.7 %. This leads to the following equation for $C_{critical}$:

$$C_{critical} = \frac{\exp\left(8.384 - 0.112\delta + 0.00962T - 0.2237\varepsilon_f + 0.072VTM_{in-place} - 0.317VMA\right)}{1 + \exp\left(8.384 - 0.112\delta + 0.00962T - 0.2237\varepsilon_f + 0.072VTM_{in-place} - 0.317VMA\right)} \quad \text{(E2e.2)}$$

Figure E2e.1 shows the predicted and observed values for $C_{critical}$. Figure E2e.2 shows predicted and observed cycles to 25 m cracking, calculated from predicted values of $C_{critical}$, and predicted values of $K_1$, $K_2$ and $\alpha$, using the models presented in last quarter's progress report. The accuracy of the predicted values are excellent for a pavement fatigue model; the standard error is 33 %.

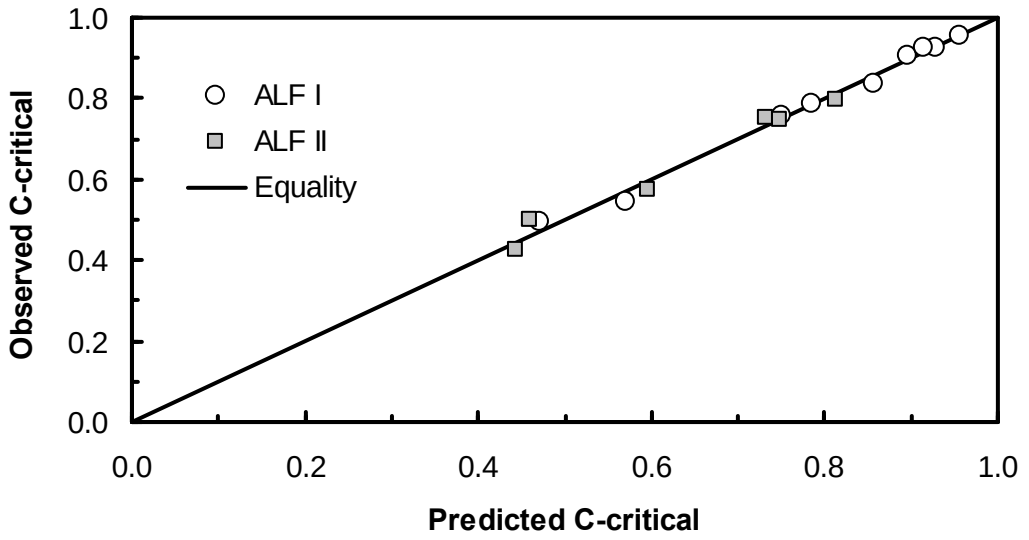


Figure E2e.1. Predicted and observed values of critical for ALF I and ALF II fatigue experiments.

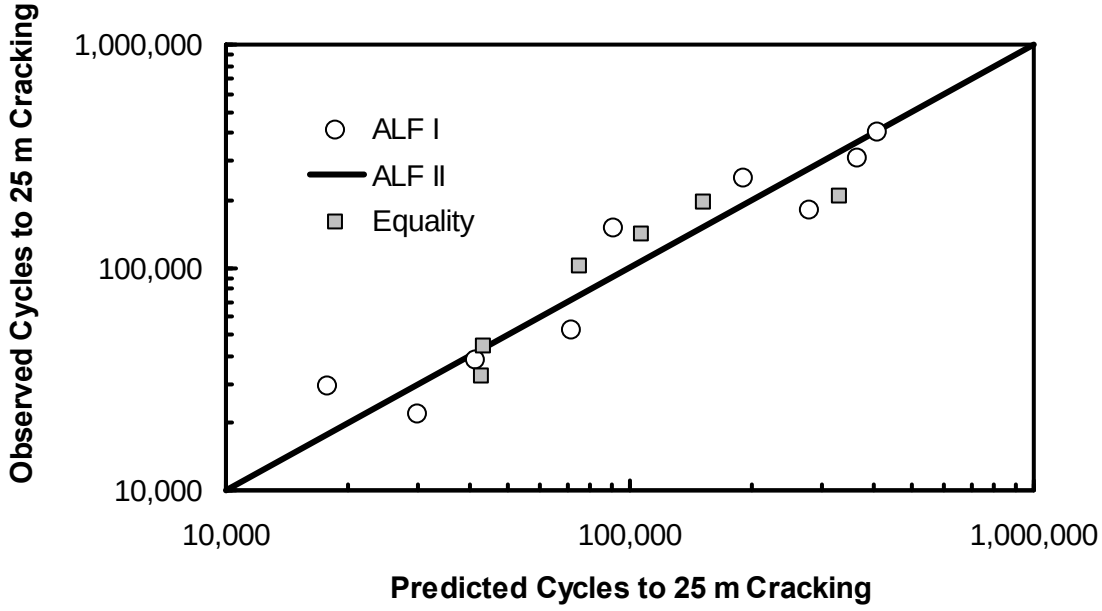


Figure E2e.2. Predicted and observed cycles to 25 m total cracking for ALF I and ALF II fatigue experiments.

A few comments are in order considering the proposed model. The modulus used in calculating the pavement strains was a tension/compression modulus, estimated from the Hirsch predicted dynamic compression modulus, using an equation given in NCHRP Report 567. In initial models, an indicator variable had to be used to differentiate the behavior of ALF I and ALF II data. However, as the model evolved and improved, the indicator variable was no longer needed. Critical to elimination of the indicator variable was inclusion of the failure strain from the direct tension test. It must be emphasized that this parameter is the failure strain at the temperature where m = 0.30, as estimated from bending beam rheometer (BBR) data. The failure strain must be estimated at some rheological reference point because it is so dependent on binder stiffness; by calculating the strain at m=0.30, the effect of binder stiffness is removed and the parameter becomes a good indicator of overall failure behavior. Various other fracture parameters were tried as predictors but this performed the best. Furthermore, direct tension and BBR data were available for both ALF I and ALF II binders, whereas for the other fracture parameters data was only available for ALF II binders.

Although there are a relatively large number of predictors in the model (five), the $r^2$ value of 99.4 % has been adjusted for the degrees of freedom, and all parameters are highly significant, so the likelihood that the model is over-parameterized is very small. Furthermore, all of the parameters make sense from an engineering perspective, with the possible exception of pavement thickness. The parameters affect fatigue life in the following ways:

- As phase angle increases, fatigue life increases
- As pavement thickness increases, fatigue life decreases
- As failure strain increases, fatigue life increases
- As in-place voids increase, fatigue life decreases
- As VMA increases, fatigue life increases

It is not clear why fatigue life should decrease with increasing thickness, although a quick review of literature on top-down cracking suggests that this may be consistent with some field observations. It is also possible that this parameter is perhaps accounting for some bias in the layered elastic analysis. It is also possible that including thickness as a predictor helps account for damage that occurs at other locations through other mechanisms, other than simply tension a relatively large distance away from the tire. The effect of tire thickness on top-down cracking bears further study.

It must be emphasized that the model described here and in the last quarterly report is based entirely on mixture composition, binder properties and pavement structure—no measured mixture properties were used. This model is potentially extremely useful in pavement design, in that it can be applied early in the design stages without mixture testing. It can also be applied to low volume roads, where mixture testing is not practical. The only data required that is not routinely available is the binder failure strain, but this test is an optional/standard test and is relatively easy to perform. It is likely that in cases where unmodified binders are used, a typical value for failure strain can be used while still maintaining good accuracy.

Work Planned Next Quarter

Laboratory work will proceed for the Hirsch model, resistivity model, and continuum damage fatigue model refinements. Analysis of the data from these experiments will proceed concurrently with the laboratory testing.

The effect of pavement thickness on top-down cracking as reported in the literature will be studied, to determine if in fact top-down cracking tends to increase with increasing pavement thickness. A more in-depth sensitivity analysis will be performed, to evaluate the effects of various parameters on top-down cracking. Two papers on this topic will be compiled for publication. If possible, other data on top-down cracking will be located and used to verify the model.

Significant Problems, Issues and Potential Impact on Progress

The laboratory experiments in this Work Element are behind schedule. Materials have been procured and laboratory work has been initiated. These experiments will be completed during 2011.

## TABLE OF DECISION POINTS AND DELIVERABLES FOR ENGINEERED MATERIALS

| Name of Deliverable | Type of Deliverable | Description of Deliverable | Original Delivery Date | Revised Delivery Date | Reason for changes in delivery date |
|---|---|---|---|---|---|
| E1a- Model and Algorithm (TAMU) | Model and Algorithm | The model and algorithm for testing and analysis of damaged asphalt mixtures in tension | | 09/01/11 | |
| E1a- Continuum Damage Permanent Deformation Analysis for Asphalt Mixtures (TAMU) | Final Report | Ph.D. dissertation at TAMU that describes the viscoplastic mechanism for permanent deformation of the asphalt mixtures and provides the testing protocols and analysis methods to acquire the input parameters of the PANDA program. | 12/31/2010 | 12/31/2011 | Time is needed to make the product compatible with the PANDA program |
| E1a- Develop a RDT DMA Testing Protocol (TAMU) | Technology Transfer | This new testing protocol is stress controlled repeated tension testing method and will be used to replace the previous torsional DMA testing method | 08/15/2010 | 02/15/2011 | New DMA Machine Arrive Late |
| E1a- Standardize Testing Procedure for Specifications (TAMU) | AASHTO Specification | Develop a Standard Specification to use as a comparative test to evaluate fracture properties, healing and moisture damage of FAM | 4/30/11 | 09/30/2011 | Expanded scope |
| E1a- Develop a New DMA Testing Protocol for Compression (TAMU) | AASHTO Specification | Develop a Standardized testing method to use as a comparative test to evaluate compressive properties of FAM | | 09/15/2011 | |
| E1b1-5: Standard Testing Procedure and Recommendation for Specifications (UWM) | Draft Report | Report on final conclusions and proposed procedures and specifications | 7/11 | N/A | N/A |
| | Final Report | | 1/12 | 3/12 | Final report submission date moved back to allow at least 6 months between draft and final report submission. |
| E1b-2i. Literature review (UWM) | Draft Report | Review of previous work on indentation and closed formed solution to the indentation problem. | 7/09 | Complete | N/A |
| E1b-2iii. Preliminary testing and correlation of results (UWM) | Draft Report | The use of indentation test for characterization of asphalt binders. | 1/10 | Complete | N/A |

| Name of Deliverable | Type of Deliverable | Description of Deliverable | Original Delivery Date | Revised Delivery Date | Reason for changes in delivery date |
|---|---|---|---|---|---|
| E1b-2iv. Feasibility of using indentation tests for fracture and rheological properties (UWM) | Draft Report | Report on Finite element simulations of the indentation test and correlations with DSR results. | 1/11 | 10/11 | Postponed due to significant delays in receiving the modified test setup from the machine shop. |
| | Final Report | | 4/11 | 4/12 | |
| E1c-1ii. Effects of Warm Mix Additives on Mixture Workability and Stability (UWM) | Draft Report | Report of reviewed relevant literature and studies (to be combined with final report) | 10/08 | Complete | N/A |
| | Final Report | | 1/09 | | N/A |
| | Draft Report | Impacts of WMA Additives on Asphalt Binder Performance and Mixture Workability | 4/11 | 10/11 | N/A |
| | Final Report | | 1/12 | 4/12 | N/A |
| E1c-1v. Field Evaluation of Mix Design Procedures and Performance Recommendations (UWM) | Draft Report | Report on WMA Field Evaluation of Mix Design Procedures and Performance | 10/11 | N/A | N/A |
| | Final Report | | 1/12 | 4/12 | Final report submission date moved back to allow at least 6 months between draft and final report submission. |
| E1c-2: Improvement of Emulsions' Characterization and Mixture Design for Cold Bitumen Applications | Practice | Mix design method for cold-in-place recycling (CIR) that is consistent with the Superpave technology and that can be used to define the optimum combination of moisture content and emulsion content. | 12/11 | N/A | N/A |
| | Practice | Mix design method for cold mix asphalt (CMA) that is consistent with the Superpave technology and that can be used to define the optimum combination of moisture content and emulsion content. | 03/12 | N/A | N/A |
| E1c-2i: Review of Literature and Standards (UWM) | Draft Report | Review of Literature and Standards that will be combined with the final draft reports (to be combined with E1c-2vii and E1c-2ix final reports) | 7/08 | Complete | N/A |
| | Final Report | | 10/08 | | |
| | Draft Report | | 4/09 | | |
| | Draft Report | | 7/09 | | |
| | Draft Report | | 1/10 | | |
| E1c-2iii: Identify Tests and Develop Experimental Plan (UWM) | Draft Report | Reports outlining the required tests and experimental plan for the study (to be combined with E1c-2vii and E1c-2ix final reports) | 4/09 | Complete | N/A |
| | Draft Report | | 10/09 | | N/A |
| E1c-2v. Conduct Testing Plan (UWM) | Draft Report | Report on the results and analysis of tests run in accordance to test plan (to be combined with E1c-2vii and E1c-2ix final reports) | 10/09 | Complete | N/A |

| Name of Deliverable | Type of Deliverable | Description of Deliverable | Original Delivery Date | Revised Delivery Date | Reason for changes in delivery date |
|---|---|---|---|---|---|
| E1c-2vii. Validate Guidelines (UWM) | Draft Report | Draft report of the performance and Rheological and Bond Properties of Emulsions (to be combined with E1c-2vii final report) | 7/09 | 9/11 | N/A |
| | Final Report | Final report of the performance and Rheological and Bond Properties of Emulsions | 4/11 | 4/12 | Final report submission date moved back to allow at least 6 months between draft and final report submission. |
| E1c-2ix. Develop CMA Performance Guidelines (UWM) | Draft Report | Draft and final report of the performance guidelines of Cold Mix asphalt pavements | 10/11 | N/A | N/A |
| | Final Report | | 1/12 | 4/12 | Final report submission date moved back to allow at least 6 months between draft and final report submission. |
| E2a-4: Write asphalt modification guideline/report on modifier impact over binder properties (UWM) | Draft Report | Report summarizing effect of modification on low, intermediate, and high temperature performance of asphalt binders. It includes guidelines for modification and cost index for different modification types | 10/11 | N/A | N/A |
| | Final Report | Report in 508 format that addresses comments/concerns from Draft Report | 1/12 | 4/12 | Final report submission date moved back to allow at least 6 months between draft and final report submission. |

| Name of Deliverable | Type of Deliverable | Description of Deliverable | Original Delivery Date | Revised Delivery Date | Reason for changes in delivery date |
|---|---|---|---|---|---|
| E2b-1: Develop a System to Evaluate the Properties of RAP Materials (UNR with UWM input) | Draft Report | Report on Test Method to Quantify the Effect of RAP and RAS on Blended Binder Properties without Binder Extraction (To be combined with E2b1-b draft and final reports) (UWM input) | 4/09 | Complete | N/A |
| | Final Report | | 4/09 | | N/A |
| | Practice | Recommend the most effective methods for extracting RAP aggregates based on their impact on the various properties of the RAP aggregates and the volumetric calculations for the Superpave mix design. | 12/10 | 04/11 | Additional testing and verifications were required for some of the reported data |
| | Draft report | Report on the developed testing and analysis procedure system to estimate the RAP binder properties from binder and mortar testing including fracture results. | 10/11 | N/A | N/A |
| | Final report | | 04/12 | N/A | N/A |
| E2b-1.b: Develop a System to Evaluate the Properties of the RAP Binder (UWM) | Draft Report | Report on the developed testing and analysis procedure system to estimate the RAP binder properties from binder and mortar testing including fracture results. | 10/11 | N/A | N/A |
| | Final Report | | 1/12 | 4/12 | Final report submission date moved back to allow at least 6 months between draft and final report submission. |
| E2b-3: Develop a Mix Design Procedure | Draft report | Report summarizing the laboratory mixing experiment. | 02/12 | N/A | N/A |
| | Final report | | 08/12 | N/A | N/A |
| E2b-4: Impact of RAP Materials on Performance of Mixtures And E2b-5: Field Trials | Draft report | Report summarizing the laboratory and field performance of field mixtures. | 02/12 | N/A | N/A |
| | Final report | | 08/12 | N/A | N/A |
| E2c-2: Conduct Mixtures Evaluations | Draft report | Approach to identify critical conditions of HMA mixtures | 09/11 | N/A | N/A |
| | Final report | | 03/12 | N/A | N/A |
| E2c-3: Develop a Simple Test | Draft report | Report summarizing the evaluation of mixtures from the Flow Number Task Force group. | 11/11 | N/A | N/A |
| | Final report | | 05/12 | N/A | N/A |
| E2c-4: Develop Standard Test Procedure | Practice | Recommended practice to identify the critical condition of an HMA mix at the mix design stage to avoid accelerated rutting failures of HMA pavements. | 12/11 | N/A | N/A |

| Name of Deliverable | Type of Deliverable | Description of Deliverable | Original Delivery Date | Revised Delivery Date | Reason for changes in delivery date |
|---|---|---|---|---|---|
| E2c-5: Evaluate the Impact of Mix Characteristics | Draft report | Report summarizing the impact of mixture characteristics on the critical condition of the HMA mixes | 02/12 | N/A | N/A |
| | Final report | | 08/12 | N/A | N/A |
| E2d-2: Identify the Causes of the Thermal Cracking | Draft report | Report summarizes the testing and findings for materials from LTPP sections. | 12/11 | N/A | N/A |
| | Final report | | 06/12 | N/A | N/A |
| E2d-3: Identify an Evaluation and Testing System (UNR with UWM input) | Draft report | Low Temperature Cracking Characterization of Asphalt Binders by Means of the Single-Edge Notch Bending (SENB) Test (UWM input) | 04/11 | N/A | N/A |
| | Final report | | 10/11 | N/A | N/A |
| E2d-4: Modeling and validation of the Developed System (UNR with UWM input) | Draft report | Thermal cracking characterization of mixtures by means of the unified Tg-TSRST device. (UWM input) | 10/11 | N/A | N/A |
| | Final report | | 04/12 | 4/12 | Final report submission date moved back to allow at least 6 months between draft and final report submission. |
| | Model | Model that can effectively simulate the long-term properties of HMA mixtures in the intermountain region and assess the impact of such properties on the resistance of HMA mixtures to thermal cracking. | 03/12 | N/A | N/A |
| E2d-5: Develop a Standard (UNR with UWM input) | Draft standard | Draft standards for the use of the SENB, binder Tg and the Tg-TSRST device. (UWM input) | 10/11 | N/A | N/A |
| | Final standard | | 01/12 | 4/12 | Final report submission date moved back to allow at least 6 months between draft and final report submission. |
| | Draft standard | Draft standard for the use of the TSRST with cylindrical specimens compacted using the SGC. | 03/11 | 09/11 | Delayed due to issues with specimens breaking at the edge. |
| | Final standard | | 01/12 | N/A | N/A |

| **Engineered Materials Year 4** | Year 4 (4/2010-3/2011) | | | | | | | | | | | | Team |
|---|---|---|---|---|---|---|---|---|---|---|---|---|---|
| | 4 | 5 | 6 | 7 | 8 | 9 | 10 | 11 | 12 | 1 | 2 | 3 | |
| **(1) High Performance Asphalt Materials** | | | | | | | | | | | | | |
| E1a: Analytical and Micro-mechanics Models for Mechanical behavior of mixtures | | | | | | | | | | | | | TAMU |
| E1a-1: Analytical Micromechanical Models of Binder Properties | | | | P | | | | | | | | | |
| E1a-2: Analytical Micromechanical Models of Modified Mastic Systems | | | | P | | | | | | | | | |
| E1a-3: Analytical Models of Mechanical Properties of Asphalt Mixtures | | | | P, JP | | JP (2) | | JP (2) | | P(2) | | | |
| E1a-4: Analytical Model of Asphalt Mixture Response and Damage | | | | | | | | | | P, JP | | | |
| E1b: Binder Damage Resistance Characterization | | | | | | | | | | | | | UWM |
| E1b-1: Rutting of Asphalt Binders | | | | | | | | | | | | | |
| E1b-1-1: Literature review | | | | | | | | | | | | | |
| E1b1-2: Select Materials & Develop Work Plan | | | | | | | | | | | | | |
| E1b1-3: Conduct Testing | DP | | | | | | | | | | | | |
| E1b1-4: Analysis & Interpretation | | | | | | | | | | | | | |
| E1b1-5: Standard Testing Procedure and Recommendation for Specifications | | | | | P | | | | | | DP | | |
| E1b-2: Feasibility of determining rheological and fracture properties of asphalt binders and mastics using simple indentation tests (modified title) | | | | | | | | | | | | | UWM |
| E1b-2i. Literature Review | | | | | | | | | | | | | |
| E1b-2ii. Proposed SuperPave testing modifications | | | | | | | | | | | | | |
| E1b-2iii. Preliminary testing and correlation of results | | | | | | JP | | | | | | | |
| E1b-2iv. Feasibility of using indentation tests for fracture and rheological properties | | | | | | | | | | P | | D | |
| E2a: Comparison of Modification Techniques | | | | | | | | | | | | | UWM |
| E2a-1: Identify modification targets and material suppliers | | | | | | | | | | | | | |
| E2a-2: Test material properties | | | | | | | | | | P | | | |
| E2a-3: Develop model to estimate level of modification needed and cost index | | | | | | | | | | | | | |
| E2a-4: Write asphalt modification guideline/report on modifier impact over binder properties | | | | | JP | | | | | | | | |
| E2c: Critically Designed HMA Mixtures | | | | | | | | | | | | | UNR |
| E2c-1: Identify the Critical Conditions | | | | | | | | | | | | | |
| E2c-2: Conduct Mixtures Evaluations | | | | | | | | | | JP | | | |
| E2c-3: Develop a Simple Test | | | | | | | | | | | | | |
| E2c-4: Develop Standard Test Procedure | | | | | | | | | | | | | |
| E2c-5: Evaluate the Impact of Mix Characteristics | | | | | | | | | | | | | |
| E2d: Thermal Cracking Resistant Mixes for Intermountain States | | | | | | | | | | | | | UWM/UNR |
| E2d-1: Identify Field Sections | | | | | | | | | | | | | |
| E2d-2: Identify the Causes of the Thermal Cracking | | | | | | | | | | | | | |
| E2d-3: Identify an Evaluation and Testing System | | | | | JP | | | | | P | | | |
| E2d-4: Modeling and Validation of the Developed System | | | | | JP | | | | | | P | | |
| E2d-5: Develop a Standard | | | | | | | | | | | | | |
| E2e: Design Guidance for Fatigue and Rut Resistance Mixtures | | | | | | | | | | | | | AAT |
| E2e-1: Identify Model Improvements | | | | | | | | | | | | | |
| E2e-2: Design and Execute Laboratory Testing Program | | | | | | | | | | | | | |
| E2e-3: Perform Engineering and Statistical Analysis to Refine Models | | | | | | | | | | | | | |
| E2e-4: Validate Refined Models | | | | | | | | | | | | | |
| E2e-5: Prepare Design Guidance | | | | | | | | | | | | | |
| **(2) Green Asphalt Materials** | | | | | | | | | | | | | |
| E2b: Design System for HMA Containing a High Percentage of RAP Material | | | | | | | | | | | | | UNR |
| E2b-1: Develop a System to Evaluate the Properties of RAP Materials | | P | | | JP | | | | P | | | | |
| E2b-2: Compatibility of RAP and Virgin Binders | | | | | | | | | | | | | |
| E2b-3: Develop a Mix Design Procedure | | | | | | | | | D | | | | |
| E2b-4: Impact of RAP Materials on Performance of Mixtures | | | | | | | | | | | | | |
| E2b-5: Field Trials | | | | | JP | | | | | | | | |
| E1c: Warm and Cold Mixes | | | | | | | | | | | | | UWM |
| E1c-1: Warm Mixes | | | | | | | | | | | | | |
| E1c-1i: Effects of Warm Mix Additives on Rheological Properties of Binders | | | | | | | | | | | | | |
| E1c-1ii. Effects of Warm Mix Additives on Mixture Workability and Stability | | | | | JP | | | | | | | | |
| E1c-1iii. Mixture Performance Testing | | DP, P | | | | | | | | | | | |
| E1c-1iv. Develop Revised Mix Design Procedures | | | | | | | | | | | | | |
| E1c-1v. Field Evaluation of Mix Design Procedures and Performance Recommendations | | | | | | | | | | | | | |
| E1c-2: Improvement of Emulsions' Characterization and Mixture Design for Cold Bitumen Applications | | | | | | | | | | | | | UWM/UNR |
| E1c-2i: Review of Literature and Standards | | | | | | | D | | | | | | |
| E1c-2ii: Creation of Advisory Group | | | | | | | | | | | | | |
| E1c-2iii: Identify Tests and Develop Experimental Plan | D | | | | | | | | | | | | |
| E1c-2iv. Develop Material Library and Collect Materials. | | | | | | | | | | | | | |
| E1c-2-v. Conduct Testing Plan | | | | | JP | | | | | P | | | |
| E1c-2-vi. Develop Performance Selection Guidelines | | | | | JP | | | | | P | | | |
| E1c-2-vii. Validate Performance Guidelines | | | | | | | | | | | | | |
| E1c-2-viii. Develop CMA Mix Design Guidelines | | | | | | | | | | | | | |
| E1c-2ix. Develop CMA Performance Guidelines | | | | | | | | | | | | | |

**Deliverable codes**
D: Draft Report
F: Final Report
M&A: Model and algorithm
SW: Software
JP: Journal paper
P: Presentation
DP: Decision Point

**Deliverable Description**
Report delivered to FHWA for 3 week review period.
Final report delivered in compliance with FHWA publication standards
Mathematical model and sample code
Executable software, code and user manual
Paper submitted to conference or journal
Presentation for symposium, conference or other
Time to make a decision on two parallel paths as to which is most promising to follow through

Work planned
Work completed
Parallel topic

| Engineered Materials Year 2 - 5 | Year 2 (4/08-3/09) | | | | Year 3 (4/09-3/10) | | | | Year 4 (04/10-03/11) | | | | Year 5 (04/11-03/12) | | | | Team |
|---|---|---|---|---|---|---|---|---|---|---|---|---|---|---|---|---|---|
| | Q1 | Q2 | Q3 | Q4 | Q1 | Q2 | Q3 | Q4 | Q1 | Q2 | Q3 | Q4 | Q1 | Q2 | Q3 | Q4 | |
| **(1) High Performance Asphalt Materials** | | | | | | | | | | | | | | | | | |
| E1a: Analytical and Micro-mechanics Models for Mechanical behavior of mixtures | | | | | | | | | | | | | | | | | TAMU |
| E1a-1: Analytical Micromechanical Models of Binder Properties | | | | P, JP | JP | P | P | JP | | P | | | P | JP | D, JP | F | |
| E1a-2: Analytical Micromechanical Models of Modified Mastic Systems | | | | P, JP | JP | P | P | | | P | | | P | JP | D | F, SW, M&A | |
| E1a-3: Analytical Models of Mechanical Properties of Asphalt Mixtures | P | P,JP | | P, JP | JP | P | P | M&A | | P, JP(3) | JP (2) | P(2) | P | JP(2) | D, JP | F, SW, M&A | |
| E1a-4: Analytical Model of Asphalt Mixture Response and Damage | | | | P, JP | JP | P | P | | | | | P, JP | P | | D | F, SW, M&A | |
| E1b: Binder Damage Resistance Characterization | | | | | | | | | | | | | | | | | UWM |
| E1b-1: Rutting of Asphalt Binders | | | | | | | | | | | | | | | | | |
| E1b-1-1: Literature review | | | | | | | | | | | | | | | | | |
| E1b1-2: Select Materials & Develop Work Plan | DP, P | | P | | | | | | | | | | | | | | |
| E1b1-3: Conduct Testing | | | P | | | JP | | P | DP | | | | | | | | |
| E1b1-4: Analysis & Interpretation | | JP | P | JP | | JP | | P | | | | | JP | | | | |
| E1b1-5: Standard Testing Procedure and Recommendation for Specifications | | | | | | | | | | P | | DP | P | D | JP | F | |
| E1b-2: Feasibility of Determining rheological and fracture properties of asphalt binders and mastics using simple indentation tests (modified title) | | | | | | | | | | | | | | | | | |
| E1b-2i. Literature Review | | | | | | D | | | | | | | | | | | |
| E1b-2ii. Proposed SuperPave testing modifications or new testing devices | | | | | | P | | | | | | | | | | | |
| E1b-2iii. Preliminary testing and correlation of results | | | | | | | | D | | JP | | | JP | | | | |
| E1b-2iv. Feasibility of using indentation tests for fracture and rheological properties | | | | | | JP | | P | | | | P, D | | | D | F | |
| E2a: Comparison of Modification Techniques | | | | | | | | | | | | | | | | | UWM |
| E2a-1: Identify modification targets and material suppliers | | | | DP | | DP | | | | | | | | | | | |
| E2a-2: Test material properties | | | | | | | | P | | | | P | | | | | |
| E2a-3: Develop model to estimate level of modification needed and cost index | | | | | | | | | | | | | | | | | |
| E2a-4: Write asphalt modification guideline/report on modifier impact over binder properties | | | | | | | | | | JP | | | | | D | F | |
| E2c: Critically Designed HMA Mixtures | | | | | | | | | | | | | | | | | UNR |
| E2c-1: Identify the Critical Conditions | | JP | | D, F | | JP | D | F | | | | | | | | | |
| E2c-2: Conduct Mixtures Evaluations | | | | | | | | D | | | | JP | | | | | |
| E2c-3: Develop a Simple Test | | | | | | | | | | | | | D, F | JP | | | |
| E2c-4: Develop Standard Test Procedure | | | | | | | | | | | | | D, F | | | | |
| E2c-5: Evaluate the Impact of Mix Characteristics | | | | | | | | | | | | | | | | D, F | |
| E2d: Thermal Cracking Resistant Mixes for Intermountain States | | | | | | | | | | | | | | | | | UWM/UNR |
| E2d-1: Identify Field Sections | | | D, F | D, F | D | F | | | | | | | | | | | |
| E2d-2: Identify the Causes of the Thermal Cracking | | | | | | | | | | | | | | | | | |
| E2d-3: Identify an Evaluation and Testing System | | | | | DP | JP | DP, D | | | JP | | JP, P | JP | | | | |
| E2d-4: Modeling and Validation of the Developed System | | | | | | | | | | JP | | P | | | | D, F | |
| E2d-5: Develop a Standard | | | | | | | | | | | | | | | | D, F | |
| E2e: Design Guidance for Fatigue and Rut Resistance Mixtures | | | | | | | | | | | | | | | | | AAT |
| E2e-1: Identify Model Improvements | | | | | | | | | | | | | | | | | |
| E2e-2: Design and Execute Laboratory Testing Program | | | | | | | | | | | | | | | | | |
| E2e-3: Perform Engineering and Statistical Analysis to Refine Models | | | | | | | | | | | | | | P, D, F | | | |
| E2e-4: Validate Refined Models | | | | | | | | | | | | | | JP | | | |
| E2e-5: Prepare Design Guidance | | | | | | | | | | | | | | | M&A | P,D,F | |
| **(2) Green Asphalt Materials** | | | | | | | | | | | | | | | | | |
| E2b: Design System for HMA Containing a High Percentage of RAP Material | | | | | | | | | | | | | | | | | UNR |
| E2b-1: Develop a System to Evaluate the Properties of RAP Materials | | JP | | P | D | D, F | D | | P | JP | P | | | | | | |
| E2b-2: Compatibility of RAP and Virgin Binders | | | | | | | | | | | | | | D, F | JP | | |
| E2b-3: Develop a Mix Design Procedure | | | | | | | | D | | | D | | | D, F | JP | | |
| E2b-4: Impact of RAP Materials on Performance of Mixtures | | | | | | | | | | | | | | | | D, F | |
| E2b-5: Field Trials | | | | | | | | | | JP | | | | | | D, F | |
| E1c: Warm and Cold Mixes | | | | | | | | | | | | | | | | | |
| E1c-1: Warm Mixes | | | | | | | | | | | | | | | | | |
| E1c-1i: Effects of Warm Mix Additives on Rheological Properties of | | | | | | | | | | | | | | | | | UWM |
| E1c-1ii. Effects of Warm Mix Additives on Mixture Workability and Stability | | P | D | F,DP | | | | | | JP | | | | D | F | | UWM |
| E1c-1iii. Mixture Performance Testing | | | | | | JP | | P, DP | DP, P | | | | | | | | UW/UNR |
| E1c-1iv. Develop Revised Mix Design Procedures | | | | | | | | | | | | | | | | | UW/UNR |
| E1c-1v. Field Evaluation of Mix Design Procedures and Performance Recommendations | | | | | | | | | | | | | | | D | F | UW/UNR |
| E1c-2: Improvement of Emulsions' Characterization and Mixture Design for Cold Bitumen Applications | | | | | | | | | | | | | | | | | UWM |
| E1c-2i: Review of Literature and Standards | | JP, P, D | F | | D1 | D3 | | D6 | | | | | | | | | |
| E1c-2ii: Creation of Advisory Group | | | | | | | | | | | | | | | | | |
| E1c-2ii: Identify Tests and Develop Experimental Plan | | | | P, DP | D1 | | D4 | | | | | | | | | | |
| E1c-2iv. Develop Material Library and Collect Materials. | | | | | | | | | | | | | | | | | |
| E1c-2v. Conduct Testing Plan | | | | | | JP | D5 | P | | JP | | P | | | | | |
| E1c-2vi. Develop Performance Selection Guidelines | | | | | | | | | | JP | | P | D | F | | | |
| E1c-2vii. Validate Guidelines | | | | | | D2 | | | | | | | | | | F | |
| E1c-2viii. Develop CMA Mix Design Procedure | | | | | | | | | | | | | | | | | |
| E1c-2ix. Develop CMA Performance Guidelines | | | | | | | | | | | | | | JP | D | F | |

**Deliverable codes**
D: Draft Report
F: Final Report
M&A: Model and algorithm
SW: Software
JP: Journal paper
P: Presentation
DP: Decision Point

**Deliverable Description**
Report delivered to FHWA for 3 week review period.
Final report delivered in compliance with FHWA publication standards
Mathematical model and sample code
Executable software, code and user manual
Paper submitted to conference or journal
Presentation for symposium, conference or other
Time to make a decision on two parallel paths as to which is most promising to follow through

Work planned
Work completed
Parallel topic
Delayed

# PROGRAM AREA: VEHICLE-PAVEMENT INTERACTION

## CATEGORY VP1: WORKSHOP

### Work element VP1a: Workshop on Super-Single Tires (UNR)

This work element is complete.

## CATEGORY VP2: DESIGN GUIDANCE

### Work element VP2a: Mixture Design to Enhance Safety and Reduce Noise of HMA (UWM)

Work Done This Quarter

Efforts this quarter focused on calibrating the stationary laser profilometer (SLP) using common materials with known profiles, and streamlining related data analysis templates using predetermined frequency input data. Researchers selected several calibration surfaces with varying dominant wavelengths for the calibration study. Data analysis methods followed the International Organization for Standardization (ISO) 13473 series of standard specifications and the American Society of Testing and Materials (ASTM) E1845 specification for standard practice. These standards allow for characterization of pavement texture based on surface profiles, in terms of spectral distribution and mean profile depth (MPD). Researchers worked with equipment manufacturers to resolve a few problematic software and hardware issues.

After calibrating and troubleshooting, the SLP device was used to collect profile data from Superpave gyratory compactor (SGC) samples and field cores taken from field sections located throughout Wisconsin. For these measurements, relevant control variables including measuring rate, laser frequency, and horizontal measuring distance were selected based on manufacturer's recommendations and experience. Important response variables recorded include MPD, root mean square (RMS) depth, and spectral distribution of surface texture. These variables were selected based on collaboration with international experts. These parameters are used by various experts as means to evaluate noise and friction characteristics of pavement surfaces.

Significant Results

Figure VP2a.1 depicts portions of the analysis templates used in this work element. In this figure, the template allows input of raw profile amplitude and displacement data obtained from the SLP. This data is transformed based on the device's horizontal and vertical resolution before inverting the profile and removing dropouts. The conditioned data serves as an input for MPD calculations and spectral distribution analysis.

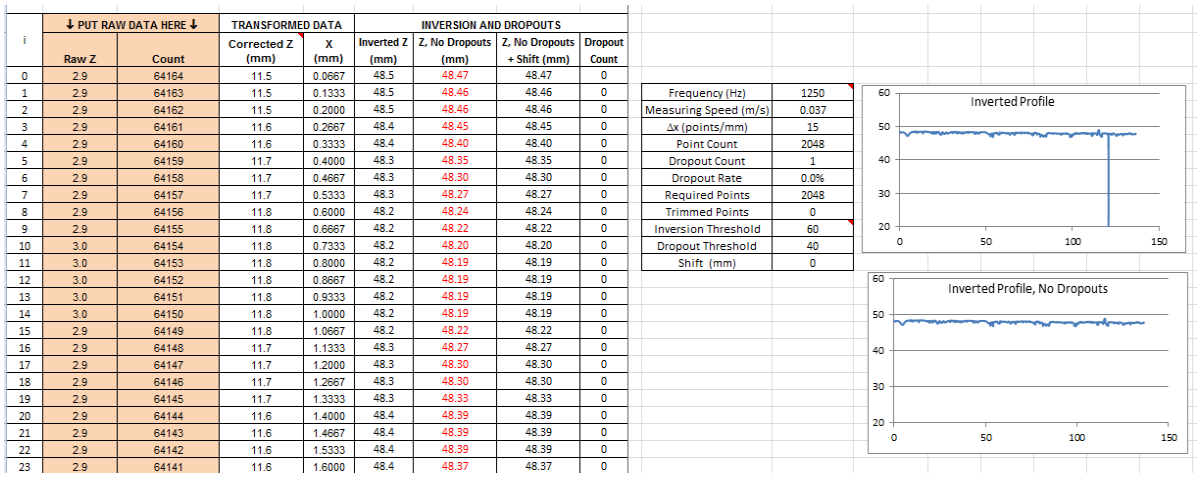

| i | ↓ PUT RAW DATA HERE ↓ | | TRANSFORMED DATA | | INVERSION AND DROPOUTS | | | |
|---|---|---|---|---|---|---|---|---|
| | Raw Z | Count | Corrected Z (mm) | X (mm) | Inverted Z (mm) | Z, No Dropouts (mm) | Z, No Dropouts + Shift (mm) | Dropout Count |
| 0 | 2.9 | 64164 | 11.5 | 0.0667 | 48.5 | 48.47 | 48.47 | 0 |
| 1 | 2.9 | 64163 | 11.5 | 0.1333 | 48.5 | 48.46 | 48.46 | 0 |
| 2 | 2.9 | 64162 | 11.5 | 0.2000 | 48.5 | 48.46 | 48.46 | 0 |
| 3 | 2.9 | 64161 | 11.6 | 0.2667 | 48.4 | 48.45 | 48.45 | 0 |
| 4 | 2.9 | 64160 | 11.6 | 0.3333 | 48.4 | 48.40 | 48.40 | 0 |
| 5 | 2.9 | 64159 | 11.7 | 0.4000 | 48.3 | 48.35 | 48.35 | 0 |
| 6 | 2.9 | 64158 | 11.7 | 0.4667 | 48.3 | 48.30 | 48.30 | 0 |
| 7 | 2.9 | 64157 | 11.7 | 0.5333 | 48.3 | 48.27 | 48.27 | 0 |
| 8 | 2.9 | 64156 | 11.8 | 0.6000 | 48.2 | 48.24 | 48.24 | 0 |
| 9 | 2.9 | 64155 | 11.8 | 0.6667 | 48.2 | 48.22 | 48.22 | 0 |
| 10 | 3.0 | 64154 | 11.8 | 0.7333 | 48.2 | 48.20 | 48.20 | 0 |
| 11 | 3.0 | 64153 | 11.8 | 0.8000 | 48.2 | 48.19 | 48.19 | 0 |
| 12 | 3.0 | 64152 | 11.8 | 0.8667 | 48.2 | 48.19 | 48.19 | 0 |
| 13 | 3.0 | 64151 | 11.8 | 0.9333 | 48.2 | 48.19 | 48.19 | 0 |
| 14 | 3.0 | 64150 | 11.8 | 1.0000 | 48.2 | 48.19 | 48.19 | 0 |
| 15 | 2.9 | 64149 | 11.8 | 1.0667 | 48.2 | 48.22 | 48.22 | 0 |
| 16 | 2.9 | 64148 | 11.7 | 1.1333 | 48.3 | 48.27 | 48.27 | 0 |
| 17 | 2.9 | 64147 | 11.7 | 1.2000 | 48.3 | 48.30 | 48.30 | 0 |
| 18 | 2.9 | 64146 | 11.7 | 1.2667 | 48.3 | 48.30 | 48.30 | 0 |
| 19 | 2.9 | 64145 | 11.7 | 1.3333 | 48.3 | 48.33 | 48.33 | 0 |
| 20 | 2.9 | 64144 | 11.6 | 1.4000 | 48.4 | 48.39 | 48.39 | 0 |
| 21 | 2.9 | 64143 | 11.6 | 1.4667 | 48.4 | 48.39 | 48.39 | 0 |
| 22 | 2.9 | 64142 | 11.6 | 1.5333 | 48.4 | 48.39 | 48.39 | 0 |
| 23 | 2.9 | 64141 | 11.6 | 1.6000 | 48.4 | 48.37 | 48.37 | 0 |

| | |
|---|---|
| Frequency (Hz) | 1250 |
| Measuring Speed (m/s) | 0.037 |
| Δx (points/mm) | 15 |
| Point Count | 2048 |
| Dropout Count | 1 |
| Dropout Rate | 0.0% |
| Required Points | 2048 |
| Trimmed Points | 0 |
| Inversion Threshold | 60 |
| Dropout Threshold | 40 |
| Shift (mm) | 0 |



Figure VP2a.1. Data conditioning template for spectral analysis and MPD calculations.

Calculation of the texture spectrum is considered the most complicated process in this analysis. Slope and offset suppression are applied to the conditioned data per standard recommendation. A windowing algorithm prepares the data set for analysis using Discrete Fourier Transform (DFT) methods. Texture spectrum parameters and MPD values are the primary outputs for this method. These parameters have been applied successfully by Professor M. Losa of the University of Pisa in models to optimize noise (Losa et al. 2005). Such characteristics may also be compared to field data obtained from the Circular Track Meter (CTM) and Dynamic Friction Tester (DFT) to develop friction models. At the end of this quarter more than 50 smaples from various projects in Wisconsin have been scanned and analyzed. The comparions of the spectrum and MPD of the surafces of gyratory samples with the surfaces of the cores taken from the same project immediately after construction have started, and will continue next quarter.

## Significant Problems, Issues and Potential Impact on Progress

No significant problems were encountered this quarter. The delays encountered due to software and hardware issues of the SLP will be addressed by expediting the testing next quarter. One more graduate student and a visiting Scholar have been assigned to the work element to insure rapid progress.

## Work Planned Next Quarter

Activities planned in the next quarter include:

- Standardizing an analysis package for field measurements to allow efficient field testing of sampled field sections.
- Examining mixture characteristics such as nominal maximum aggregate size, aggregate gradation type and aggregate type as potential factors that impact surface texture characteristics of the mix.

- Calculating IFI (International Friction Index) values for laboratory samples measured using the SLP and BPT (British Pendulum Tester) for comparison to IFI values obtained using DFT and CTM devices in the field.
- Beginning to develop guidelines to optimize noise reduction, safety, and user costs.

Cited References

ASTM, Standard Practice for Calculating Pavement Macrotexture Mean Profile Depth, Standard No. E1845, *American Society for Testing and Materials,* West Conshohocken, PA, 2009.

ISO, Characterization of Pavement Texture by Use of Surface Profiles – Part 1: Determination of Mean Profile Depth, Standard No. 13473-1, *International Organization for Standardization*, 2004.

ISO, Characterization of Pavement Texture by Use of Surface Profiles – Part 2: Terminology and Basic Requirements Related to Pavement Texture Profile Analysis, Standard No. 13473-2, *International Organization for Standardization*, 2002.

ISO, Characterization of Pavement Texture by Use of Surface Profiles – Part 3: Specification and Classification of Profilometers, Standard No. 13473-3, *International Organization for Standardization*, 2004.

ISO, Characterization of Pavement Texture by Use of Surface Profiles – Part 4: Spectral Analysis of Texture Profiles, Standard No. 13473-4, *International Organization for Standardization*, 2008.

ISO, Characterization of Pavement Texture by Use of Surface Profiles – Part 5: Determination of Megatexture, Standard No. 13473-5, *International Organization for Standardization*, 2009.

Losa, M., P. Leandri, and R. Bacci, 2005, Rolling Noise Prediction Models Based on Pavement Surface Characteristics. *Road Materials and Pavement Design*.

## CATEGORY VP3: MODELING

### Work element VP3a: Pavement Response Model to Dynamic Loads (UNR)

Work Done This Quarter

Continued the work on the *3D-Move Analysis* software to make it a menu-driven software. A graphical display for the measured nun-uniform contact stress distributions and tire imprints was developed during the last quarter. Work is still undergoing to integrate MEPDG and VESYS performance models in 3D-Move. The minimum necessary (critical) locations throughout the pavement structure were implemented for pavement performance evaluation. A new graphical display was developed for pavement responses.

Using the 3D-Move model, the research team evaluated the impact of interpolation and extrapolation of the stress distributions at the tire-pavement interface from the currently available measurements on the calculated response and estimated performance of two HMA pavements.

Assisted user's with issues ranging from usage questions, concepts clarifications, and bugs. A detailed example for Option F was created and posted on the forum. The 3D-Move Analysis software developing team worked on fixing the reported bugs.

Significant Results

There are as many as six loading types available in the 3D-Move Analysis. Some of them are uniform contact stress distribution loading and some are non-uniform contact stress distribution loading. Loading options used in 3D-Move are:

1. Option A - Pre-Defined: Uniform contact stress distributions over circle, ellipse or rectangle tire imprint
2. Option B - User-Selected: Uniform contact stress distributions over circle ,ellipse or rectangle tire imprint
3. Option C - User-Selected: Non-uniform contact stress distributions over non-uniform tire imprint
4. Option D - User-Selected: Uniform pressure over circle, ellipse or rectangle tire imprint or Non-uniform contact stress distributions over non-uniform tire imprint
5. Option E - User-Selected: Uniform contact stress distributions over circle, ellipse or rectangle tire imprint for off-highway vehicles
6. Option F - User-Defined: Non-uniform contact stress distributions over non-uniform tire imprint over non-uniform tire imprint for any vehicle

The Options C, D and F are non-uniform contact stress distributions over non-uniform tire imprint. These distributions and tire imprint data are selected from the database generated by Vehicle-Road Surface Pressure Transducer Array (VRSPTA) and Kistler MODULAS devices. The pre-existing version of 3D-Move has already the Option C and it is shown in figure VP3a.1. As shown in this figure, user can select the loading for the tire type, tire pressure and tire loading. However, a user is not aware about the extent of the tire imprint and contact stress distribution over the tire imprint. Since tire imprint and corresponding contact stress distribution are major factors in the selection of the response points for performance analysis, a graphical display of such data is important.

Figure VP3a.2 shows the modified input window for the Option C. As shown at the top of the figure, 3D Stress Distribution and Tire Imprint tabs are now included. When 3D Stress Distribution tab is clicked, the 3D contact stress plot for the selected tire and plan view of tire imprint will be displayed (figure VP3a.3). Both plots are drawn to the same color code scheme so that user can easily identify the maximum stress locations. These plots will change dynamically according to selection of tire in the previous window (figure VP3a.2). Additionally,

the tire type, tire pressure and tire loading that are appropriate for the plots are also shown in figure VP3a.3 at the bottom. This means that user does not need to go back and forth to see the selections made in the previous window. Figure VP3a.4 shows the tire imprint for the selected tire. This plot can be used to zero in on the locations of the response points, where 3D-Move responses are to be computed.

All the charts were drawn using Microsoft Excel and converted into picture format and subsequently incorporated in the program. Every time a user selects the tire from the window shown in figure VP3a.2, the program will select the appropriate graphical display for the selected tire from a pre-assembled picture gallery. Therefore, as of now, graphical displays are not available for tire loads that are different from those reported by VRSPTA and Kistler MODULUS.

To compliment the performance analysis feature in 3D-MOVE, a traffic input widow has been created and integrated into the software (figure VP3a.5). This window primarily counts the number of design axle repetitions along with corresponding variables (factors) and growth functions. It is designed to accommodate up to four seasons or periods for traffic analysis.

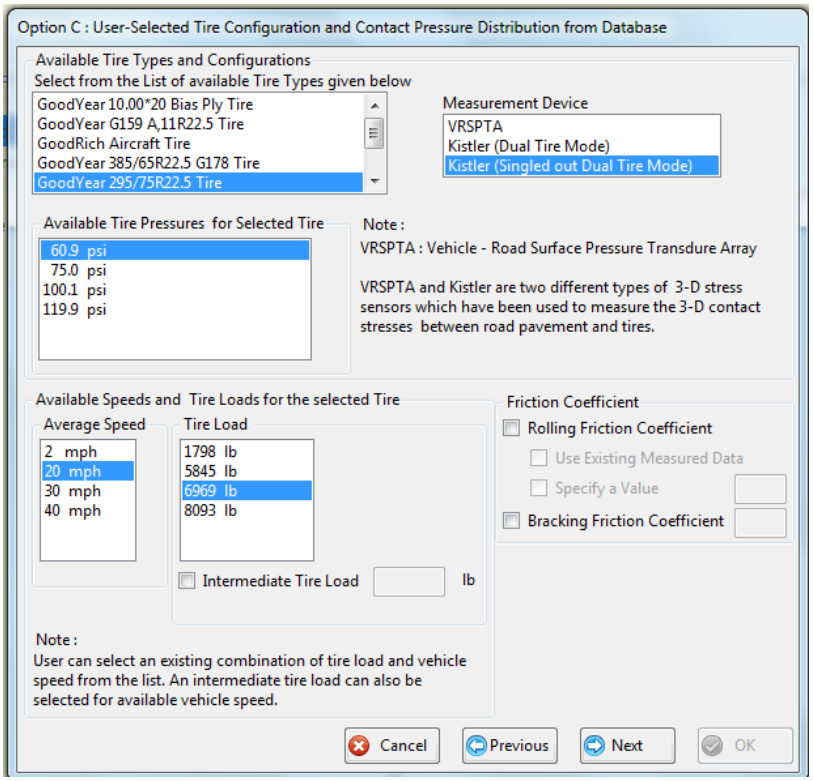


Figure VP3a.1. Pre-existing input window for Option C.

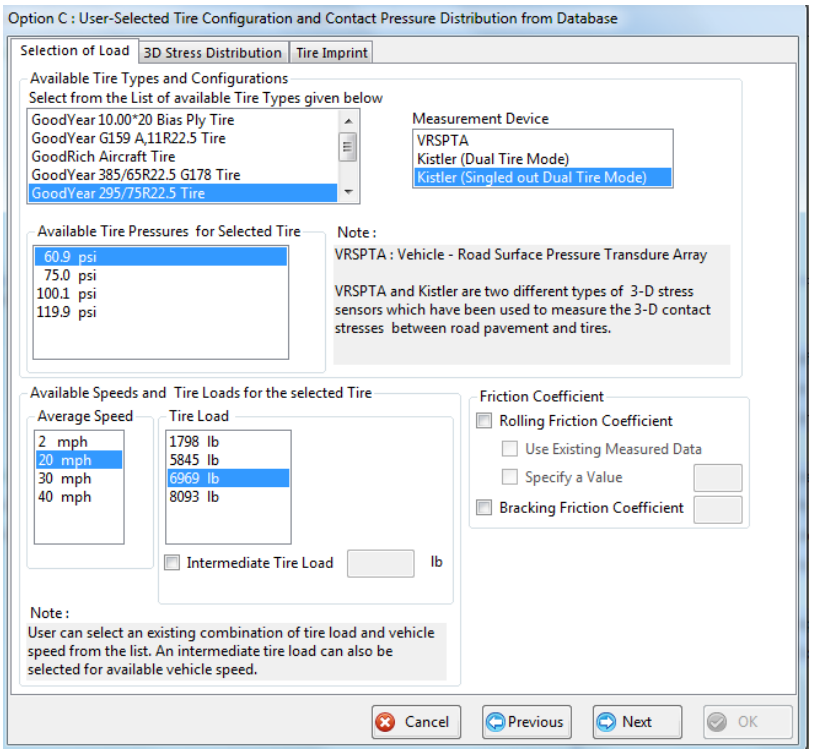


Figure VP3a.2. Modified input window for Option C.

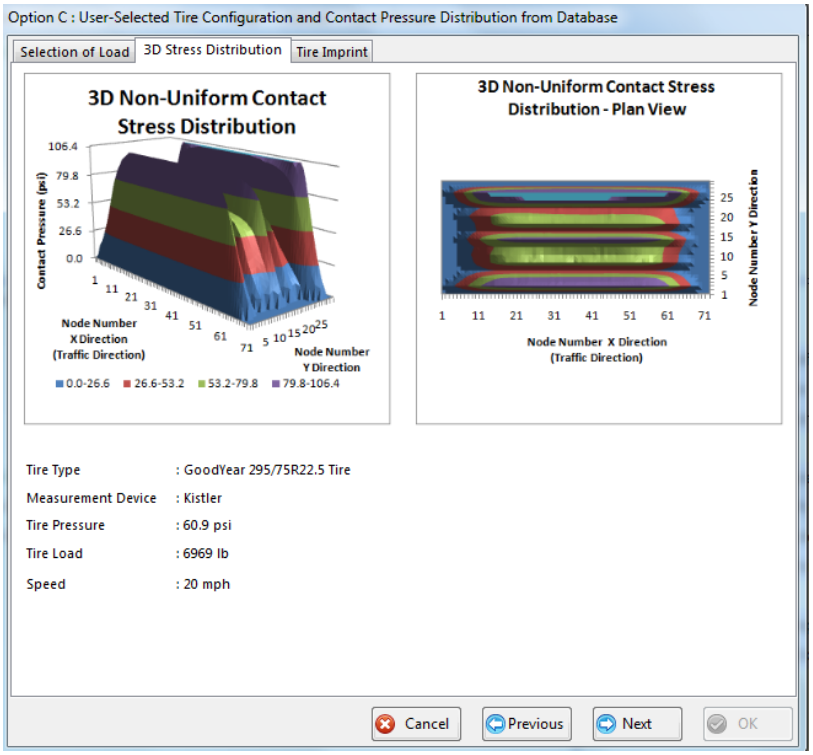


Figure VP3a.3. Stress distribution and tire imprint window.

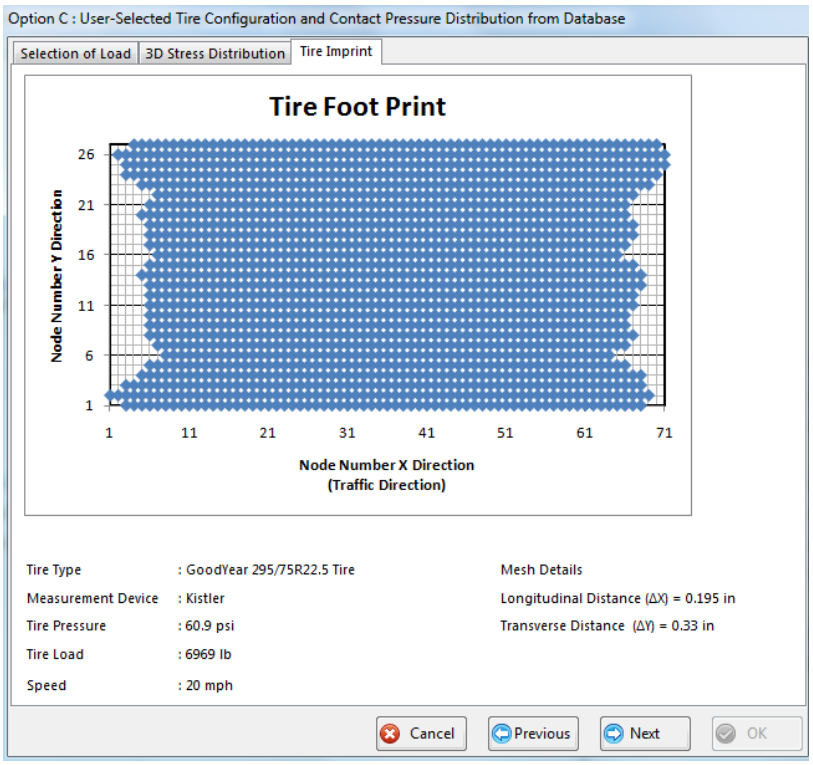


Figure VP3a.4. Graphical display of tire imprint.

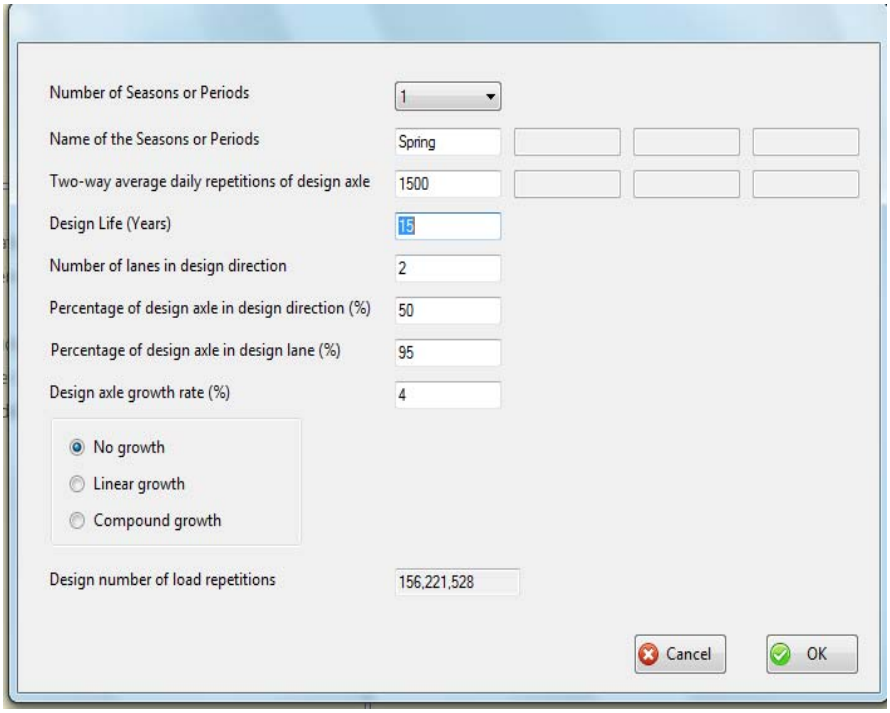


Figure VP3a.5. Traffic input window.

The critical locations for pavement evaluation were implemented to optimize the run time of the software with the performance analysis option. Figure VP3a.6 shows the automatically generated response points. Pre-defined points are displayed with green color background in the individual response point's window. The user added points are categorized into two groups. The first group, which is colored in dark blue, consists of the set of points entered at similar depths to the pre-defined points and will be considered in the performance analysis; whereas, the second group, which is colored in light blue, consists of the set of points entered at different depths than the pre-defined points and will not be considered in the performance analysis.

A graphical display tab for the pavement response points was also created in addition to individual and array response points (figure VP3a.7). This special tab comprises various features to view the pavement structure. It is capable of viewing only individual response points or only array points or both at the same time. Also response points could be looked at in XZ or YZ planes. These planes could be viewed at certain offset distance from the axes that are available in a drop down list. The entire pavement with all created layers and response points will be shown by default; however each layer could be zoomed out by entering the required depth by user. Additionally, the existing layers could be removed or added depending on the interest of layers and the location of response points. Furthermore, when the mouse pointer is held over a response point, it pops up the coordinate of that point.

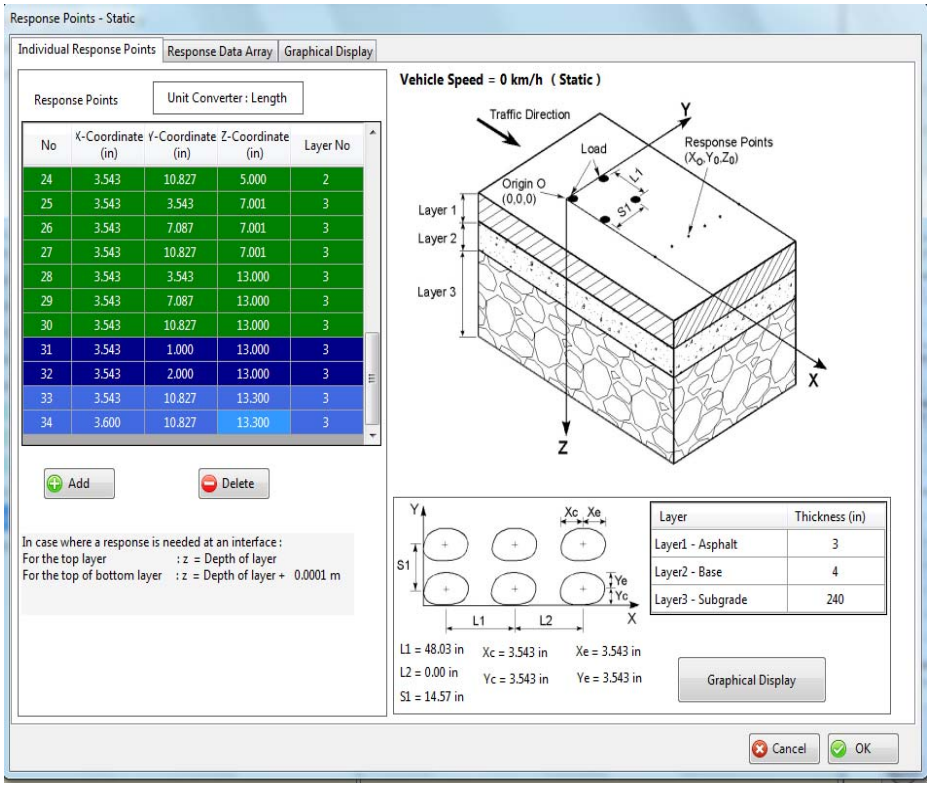


Figure VP3a.6. Individual response points window.

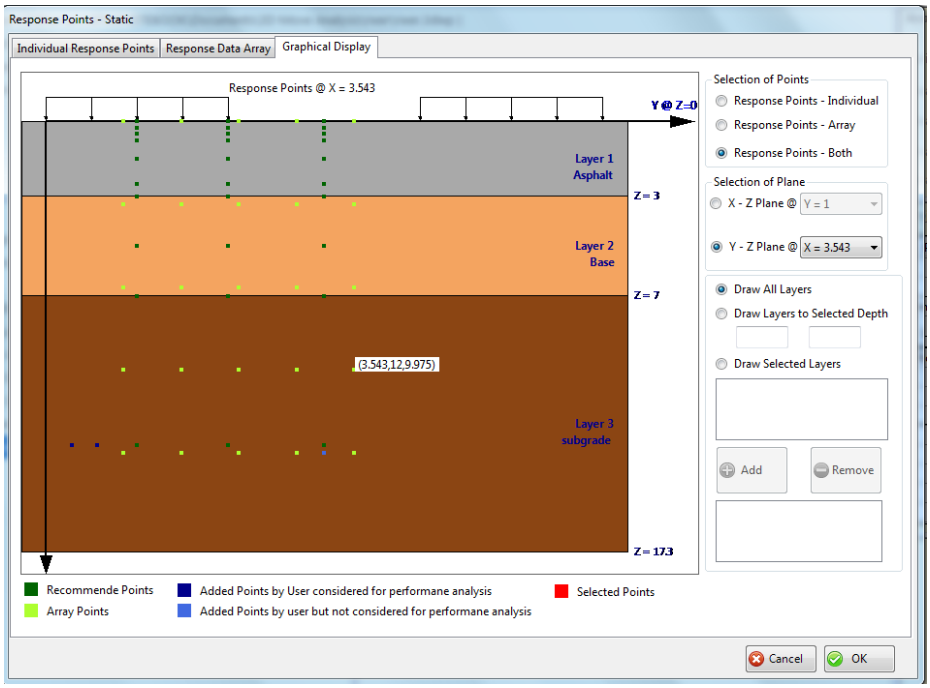


Figure VP3a.7. Graphical display tab for response point's window.

The impact of interpolation and extrapolation of the stress distributions from the currently available measurements on the responses of two HMA pavements was evaluated and completed. The calculated pavement responses were used in the mix-specific rutting and fatigue models to predict the performance of the HMA pavements. The analyses of the pavement responses and performance data indicated that stress distributions interpolated from distributions measured under two load levels that are significantly apart such as the 4.5 and 30 kN leads to significant variations in the stress distributions and the estimated performance of the HMA pavements. Interpolation and/or extrapolation of the stress distributions from distributions measured at two load levels that are not significantly apart such as the 30 and 36 kN leads to close estimation of the stress distributions and close estimation of the performance of the HMA pavements.

Significant Problems, Issues and Potential Impact on Progress

The 3D-Move Analysis verification plan was postponed until the release of the version 2.0 of the software that will have the various new features and address the various bugs.

Work Planned Next Quarter

Continue working on the 3D-Move model to make it a menu-driven software. Continue working on the performance evaluation subroutine. Continue to solve any issues and bugs that users may encounter.

## TABLE OF DECISION POINTS AND DELIVERABLES FOR VEHICLE-PAVEMENT INTERACTION

| Name of Deliverable | Type of Deliverable | Description of Deliverable | Original Delivery Date | Revised Delivery Date | Reason for Changes in Delivery Date |
|---|---|---|---|---|---|
| VP2a-4: Run parametric studies on tire-pavement noise and skid response (UWM) | Draft Report | Draft report on proposed design guideline for noise reduction, durability, safety and costs | 1/10 | 10/11 | Software issues with the KUNDT tube for noise measurements. In addition, the laser spot size and variability necessitated a system re-design. |
| VP2a-7: Proposed optimal guideline for design to include noise reduction, durability, safety and costs (UWM) | Final Report | Final report on proposed design guideline for noise reduction, durability, safety and costs | 1/12 | 4/12 | Final report submission date moved back to allow at least 6 months between draft and final report submission. |
| VP3a-4: Overall Model | Software | Release of version 2.0 of the 3D-Move pavement response model | 06/11 | N/A | N/A |
| | Draft report | Summarizing *3D-Move Analysis* software | 12/11 | N/A | N/A |
| | Final report | | 06/12 | N/A | N/A |
| | Software | Release of final version of the 3D-Move pavement response model | 03/12 | N/A | N/A |

| Vehicle-Pavement Interaction Year 4 | Year 4 (4/2010-3/2011) | | | | | | | | | | | | Team |
|---|---|---|---|---|---|---|---|---|---|---|---|---|---|
| | 4 | 5 | 6 | 7 | 8 | 9 | 10 | 11 | 12 | 1 | 2 | 3 | |
| **(1) Workshop** | | | | | | | | | | | | | |
| VP1a: Workshop on Super-Single Tires | | | | | | | | | | | | | UNR |
| **(2) Design Guidance** | | | | | | | | | | | | | |
| VP2a: Mixture Design to Enhance Safety and Reduce Noise of HMA | | | | | | | | | | | | | UWM |
| VP2a-1: Evaluate common physical and mechanical properties of asphalt mixtures with enhanced frictional skid characteristics | | | | | | | | | | | | | |
| VP2a-2: Evaluate pavement macro- and micro-textures and their relation to tire and pavement noise-generation mechanisms | | | | | | | | | | | | | |
| VP2a-3: Develop a laboratory testing protocol for the rapid evaluation of the macroand micro-texture of pavements | | | | | | | | | | | | | |
| VP2a-4: Run parametric studies on tire-pavement noise and skid response | | | | | JP | | | | | | | | |
| VP2a-5: Establish collaboration with established national laboratories specialized in transportation noise measurements. Gather expertise on measurements and analysis | | | | | | | | | | | | | |
| VP2a-6: Model and correlate acoustic response of tested tire-pavement systems | | | | | JP | P | | | | | | | |
| VP2a-7: Proposed optimal guideline for design to include noise reduction, durability, safety and costs | | | | | | | | | | | | P | |
| **(3) Pavement Response Model Based on Dynamic Analyses** | | | | | | | | | | | | | |
| VP3a: Pavement Response Model to Dynamic Loads | | | | | | | | | | | | | UNR |
| VP3a-1: Dynamic Loads | | | | | | | | | | | | | |
| VP3a-2: Stress Distribution at the Tire-Pavement Interface | | | | | | | | | | | | | |
| VP3a-3: Pavement Response Model | | | | | | | | | JP | | | | |
| VP3a-4: Overall Model | | | | | | | | | SW | | | | |

| Deliverable codes | Deliverable Description |
|---|---|
| D: Draft Report | Report delivered to FHWA for 3 week review period. |
| F: Final Report | Final report delivered in compliance with FHWA publication standards |
| M&A: Model and algorithm | Mathematical model and sample code |
| SW: Software | Executable software, code and user manual |
| JP: Journal paper | Paper submitted to conference or journal |
| P: Presentation | Presentation for symposium, conference or other |
| DP: Decision Point | Time to make a decision on two parallel paths as to which is most promising to follow througjh |

Work planned
Work completed
Parallel topic

| Vehicle-Pavement Interaction Years 2 - 5 | Year 2 (4/08-3/09) | | | | Year 3 (4/09-3/10) | | | | Year 4 (04/10-03/11) | | | | Year 5 (04/11-03/12) | | | | Team |
|---|---|---|---|---|---|---|---|---|---|---|---|---|---|---|---|---|---|
| | Q1 | Q2 | Q3 | Q4 | Q1 | Q2 | Q3 | Q4 | Q1 | Q2 | Q3 | Q4 | Q1 | Q2 | Q3 | Q4 | |
| **(1) Workshop** | | | | | | | | | | | | | | | | | |
| VP1a: Workshop on Super-Single Tires | | | | | | | | | | | | | | | | | UNR |
| **(2) Design Guidance** | | | | | | | | | | | | | | | | | |
| VP2a: Mixture Design to Enhance Safety and Reduce Noise of HMA | | | | | | | | | | | | | | | | | UWM |
| VP2a-1: Evaluate common physical and mechanical properties of asphalt mixtures with enhanced frictional skid characteristics | | | | DP | | | | | | | | | | | | | |
| VP2a-2: Evaluate pavement macro- and micro-textures and their relation to tire and pavement noise-generation mechanisms | | | | DP | | | | | | | | | | | | | |
| VP2a-3: Develop a laboratory testing protocol for the rapid evaluation of the macroand micro-texture of pavements | | M&A | | | | | | | | | | | P | | | | |
| VP2a-4: Run parametric studies on tire-pavement noise and skid response | | | | | | JP | | D | | JP | | | | | | | |
| VP2a-5: Establish collaboration with established national laboratories specialized in transportation noise measurements. Gather expertise on measurements and analysis | | | | | | | | | | | | | | | | | |
| VP2a-6: Model and correlate acoustic response of tested tire-pavement systems | | | | | | | | | | JP, P | | | | JP, P | | | |
| VP2a-7: Proposed optimal guideline for design to include noise reduction, durability, safety and costs | | | | | | | | | | | | P | | P | D | F | |
| **(3) Pavement Response Model Based on Dynamic Analyses** | | | | | | | | | | | | | | | | | |
| VP3a: Pavement Response Model to Dynamic Loads | | | | | | | | | | | | | | | | | UNR |
| VP3a-1: Dynamic Loads | | | JP | | | | | | | | | | | | | | |
| VP3a- 2: Stress Distribution at the Tire-Pavement Interface | | | | | | | | | | | | | | | | | |
| VP3a-3: Pavement Response Model | | | | | | SW, v. β | | | | | JP | | | | | | |
| VP3a-4: Overall Model | | | | | | | | | | | SW | | SW | | D | F, SW | |

**Deliverable codes**

D: Draft Report
F: Final Report
M&A: Model and algorithm
SW: Software
JP: Journal paper
P: Presentation
DP: Decision Point

**Deliverable Description**

Report delivered to FHWA for 3 week review period.
Final report delivered in compliance with FHWA publication standards
Mathematical model and sample code
Executable software, code and user manual
Paper submitted to conference or journal
Presentation for symposium, conference or other
Time to make a decision on two parallel paths as to which is most promising to follow througjh

Work planned
Work completed
Parallel topic

# PROGRAM AREA: VALIDATION

## CATEGORY V1: FIELD VALIDATION

### Work element V1a: Use and Monitoring of Warm Mix Asphalt Sections (WRI)

Work Done This Quarter

No monitoring activity during the last quarter.

Significant Results

None.

Significant Problems, Issues and Potential Impact on Progress

None.

Work Planned Next Quarter

No WMA pavement site monitoring is planned for the second quarter of 2011.

### Work element V1b: Construction and Monitoring of Additional Comparative Pavement Validation Sites (WRI)

Work Done This Quarter

No monitoring activity during the last quarter.

Significant Results

None.

Significant Problems, Issues and Potential Impact on Progress

None.

Work Planned Next Quarter

It is planned to monitor the Kansas comparative pavement site in May 2011.

## CATEGORY V2: ACCELERATED PAVEMENT TESTING

### Work element V2a: Accelerated Pavement Testing including Scale Model Load Simulation on Small Test Track

Work Done This Quarter

No activity this quarter. This work element was included in order to accommodate any accelerated testing that may occur during the project.

Significant Results

None.

Significant Problems, Issues and Potential Impact on Progress

None.

Work Planned Next Quarter

No accelerated (field) testing is planned.

### Work element V2b: Construction of Validation Sections at the Pecos Research & Testing Center

This work element is included to indicate that this may be a possibility for accelerated pavement testing for ARC research because it is a facility in the TAMU system.

## CATEGORY V3: R&D VALIDATION

### Work element V3a: Continual Assessment of Specifications (UWM)

Work Done This Quarter

The research team focused efforts on analyzing data collected from the Western Cooperative Test Group (WCTG) round-robin binder testing to determine sources of variability in Performance-Graded Plus (PG+) test methods and specifications. Of these PG+ tests, the Multiple Stress Creep and Recovery (MSCR) test method continues to show the most potential for being widely implemented, though issues remain with calculation and analysis methods. In an effort to gain insight into the sources of variability, researchers updated online test reporting forms to gain additional information about Dynamic Shear Rheometer (DSR) manufacturer, model, cooling system, and method of calculation.

Significant Results

A statistical analysis of eight Western Cooperative Test Group (WCTG) binders revealed high variability for parameters reported in the MSCR test (figure V3a.1). Out of approximately 70 labs participating in the study, about 30 labs consistently contribute MSCR test data on a monthly basis. The parameters under investigation included non-recoverable creep compliance (Jnr) at stress levels of 0.1 kPa and 3.2 kPa, percent recovery at each of these stress levels, and percent difference in Jnr. Note that some laboratories reported Jnr values at stress levels of 10kPa. Researchers observed several issues in reported results. These issues include: not dividing calculated Jnr values by the correct stress level, reporting inconsistent Jnr values (e.g., negative values and incorrect units), using incorrect formulas for calculations of percent recovery and percent difference in Jnr, and reverse reporting of Jnr and % Recovery.

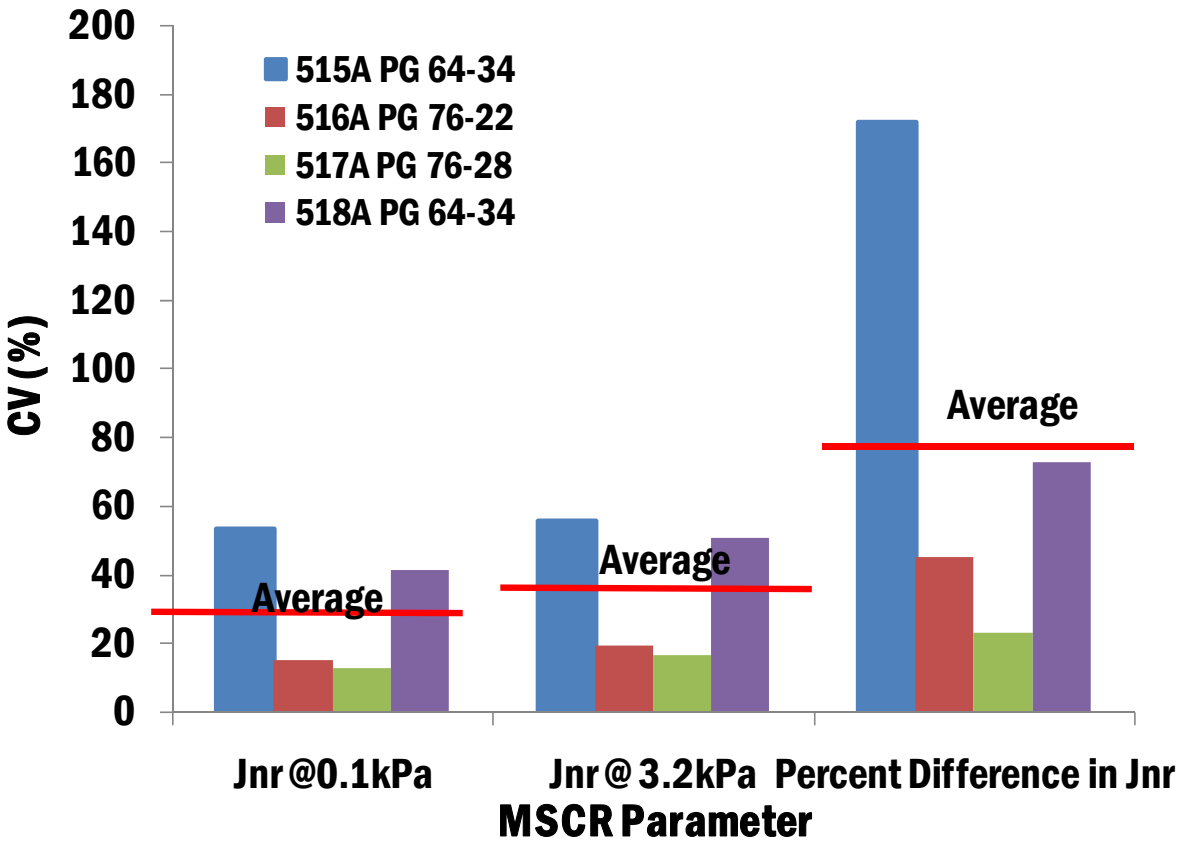


Figure V3a.1. Graph. Coefficient of variation (CV) for MSCR parameters.

Figure V3a.2 shows the effect of stress level on the variation of Jnr. It can be seen that the coefficient of variation increases when the stress level increases, especially when changing the stress level from 3.2 kPa to 10 kPa.

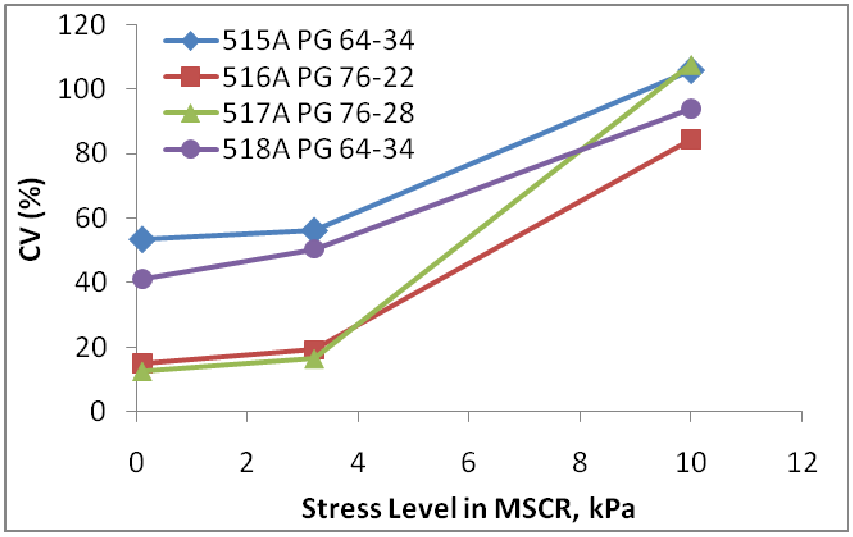


Figure V3a.2. Graph. Effect of stress level on coefficient of variation for $J_{nr}$.

In an attempt to identify sources of variation in the MSCR test, the research team investigated the possibility of different aging methods as major source of variation in MSCR results. Figure V3a.3 shows the coefficient of variation for G*/Sin δ for the unaged, RTFO and PAV aged binders. The coefficient of variation for G*/Sin δ after RTFO and PAV are reasonably low and show consistency among laboratories.

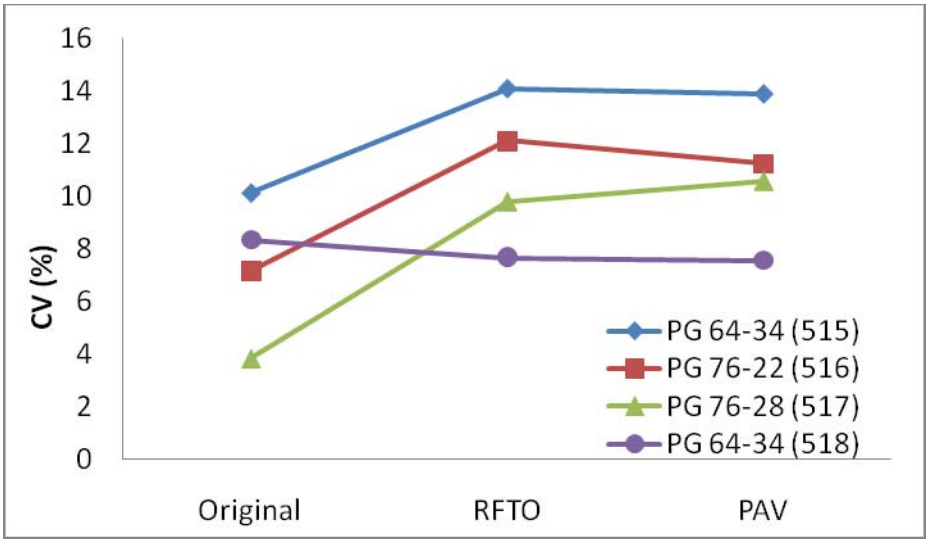


Figure V3a.3. Graph. Effect of aging on coefficient of variation for G*/Sin δ.

Significant Problems, Issues and Potential Impact on Progress

Mixture samples were not tested over the last quarter due to a motherboard failure in the mixture testing machine. The issue has been resolved, and the work is expected to continue in the next quarter. Efforts will be doubled to ensure work element progress is not delayed.

Work Planned Next Quarter

The following activities are planned for the next quarter:

- Researchers will present results from the V3a data analysis at the **WCTG Annual Meeting**.
- **Mixture testing** will continue and focus on dynamic modulus, fatigue and flow number.
- **Binder testing** will continue through the next quarter on a monthly basis.
- **Conference calls** will continue monthly with the WCTG.

**Work element V3b: Validation of the MEPDG Asphalt Materials Models Using New MEPDG Sites and Selected LTPP Sites (UNR, UWM)**

***Subtask V3b-1: Design and Build Sections (Start Year 1, Year 2, and Year 3)***

***Subtask V3b-2: Additional Testing (Start Year 2, Year 3, and Year 4)***

Work Done This Quarter

None

Significant Results

None

Significant Problems, Issues and Potential Impact on Progress

Only two agencies have committed to the construction of MEPDG sites: the Washoe RTC in northern Nevada in 2008, The South Dakota DOT in 2009/2010. The researchers are facing significant hesitation from the DOTs to use the MEPDG to design and construct HMA pavements. The level of this work element has been reduced.

Work Planned Next Quarter

None

***Subtask V3b-3: Select LTPP Sections (Start Year 1 thru Year 5)***

Work Done This Quarter

In this quarter, the research team collected thermal cracking and rutting field performance for 26 binders from the LTPP program. The thermal cracking and rutting field measurements for the LTPP binders will be used in validation efforts and are presented in table V3b-3.1 and table V3b-3.2, respectively.

Table V3b-3.1. Thermal cracking performance for LTPP binders.

| Agency | Exp. No | SHRP ID | Climate Zone | Location | | Freeze Index (C-days) | No. of Transverse cracks per section | Year |
|---|---|---|---|---|---|---|---|---|
| | | | | Lat | Long | | | |
| CT | 9A | 90902 | WF | 41.57 | -72.29 | 323.8 | 14 | 2007 |
| NC | 9A | 370901 | WN | 35.54 | -79.17 | 42.7 | 30 | 2007 |
| NC | 9A | 370902 | WN | 35.54 | -79.17 | 42.7 | 50 | 2007 |
| NC | 9A | 370903 | WN | 35.54 | -79.17 | 43.7 | 15 | 2008 |
| NC | 9A | 370962 | WN | 35.54 | -79.17 | 43.7 | 1 | 2004 |
| WI | 9 | 550903 | WF | 44.10 | -90.53 | 833.4 | 20 | 2007 |
| CT | 9A | 90960 | WF | 41.57 | -72.29 | 323.8 | 2 | 2007 |
| CT | 9A | 90961 | WF | 41.57 | -72.29 | 323.8 | 3 | 2007 |
| FL | 9A | 120902 | WN | 30.26 | -82.48 | 1.2 | 30 | 2006 |
| CT | 9A | 90962 | WF | 41.57 | -72.29 | 323.8 | 2 | 2007 |
| CT | 9A | 90903 | WF | 41.57 | -72.29 | 323.8 | 8 | 2007 |
| PQ | A9 | 89a902 | WN | 48.43 | -71.36 | 1569.6 | 11 | 2007 |
| PQ | A9 | 89a901 | WN | 48.43 | -71.36 | 1569.6 | 6 | 2007 |
| NJ | 9A | 340902 | WF | 40.18 | -74.56 | 182.6 | 10 | 2007 |
| NC | 9A | 370963 | WN | 35.54 | -79.17 | 43.7 | 1 | 2004 |
| NM | 9 | 350903 | DN | 32.20 | -108.25 | 9.5 | 0 | 2003 |
| NC | 9A | 370965 | WN | 35.54 | -79.17 | 43.7 | 1 | 2004 |
| NM | 9 | 350902 | DN | 32.20 | -108.25 | 9.5 | 1 | 2003 |
| NJ | 9A | 340901 | WF | 40.18 | -74.56 | 182.6 | 13 | 2007 |
| NC | 9A | 370964 | WN | 35.54 | -79.17 | 43.7 | 4 | 2004 |
| NE | 9 | 310902 | DF | 40.30 | -99.83 | - | 1 | 2002 |
| NC | 9A | 370960 | WN | 35.54 | -79.17 | 43.7 | 9 | 2004 |
| NE | 9 | 310903 | DF | 40.30 | -99.83 | 349.4 | 0 | 2002 |
| NJ | 9A | 340961 | WF | 40.18 | -74.56 | 182.6 | 28 | 2007 |
| AZ | 9A | 04b901 | DN | 33.44 | -112.58 | 0.0 | 140 | 2004 |
| AZ | 9A | 04b903 | DN | 33.44 | -112.58 | 0.0 | 5 | 2005 |

DF = dry-freeze. WN = wet-nonfreeze. WF = wet-freeze. DN = dry-nonfreeze.

Table V3b-3.1. Rutting performance for LTPP binders.

| Agency | Exp. No | SHRP ID | Climate Zone | Location | | Max Wheelpath Rut Depth, mm | Year |
|---|---|---|---|---|---|---|---|
| | | | | Lat | Long | | |
| CT | 9A | 90902 | WF | 41.57 | -72.29 | 3.2 | 2007 |
| NC | 9A | 370901 | WN | 35.54 | -79.17 | 7.3 | 2008 |
| NC | 9A | 370902 | WN | 35.54 | -79.17 | 7.0 | 2008 |
| NC | 9A | 370903 | WN | 35.54 | -79.17 | 7.0 | 2008 |
| NC | 9A | 370962 | WN | 35.54 | -79.17 | 4.9 | 2006 |
| WI | 9 | 550903 | WF | 44.10 | -90.53 | 8.7 | 2007 |
| CT | 9A | 90960 | WF | 41.57 | -72.29 | 2.5 | 2007 |
| CT | 9A | 90961 | WF | 41.57 | -72.29 | 5.3 | 2007 |
| FL | 9A | 120902 | WN | 30.26 | -82.48 | 9.0 | 2007 |
| CT | 9A | 90962 | WF | 41.57 | -72.29 | 2.2 | 2007 |
| CT | 9A | 90903 | WF | 41.57 | -72.29 | 8.4 | 2007 |
| PQ | A9 | 89a902 | WN | 48.43 | -71.36 | 12.5 | 2007 |
| PQ | A9 | 89a901 | WN | 48.43 | -71.36 | 14.0 | 2007 |
| NJ | 9A | 340902 | WF | 40.18 | -74.56 | 5.5 | 2007 |
| NC | 9A | 370963 | WN | 35.54 | -79.17 | 3.4 | 2003 |
| NM | 9 | 350903 | DN | 32.20 | -108.25 | 3.0 | 2004 |
| NC | 9A | 370965 | WN | 35.54 | -79.17 | 2.9 | 2003 |
| NM | 9 | 350902 | DN | 32.20 | -108.25 | 4.2 | 2003 |
| NJ | 9A | 340901 | WF | 40.18 | -74.56 | 13.8 | 2007 |
| NC | 9A | 370964 | WN | 35.54 | -79.17 | 5.0 | 2003 |
| NE | 9 | 310902 | DF | 40.30 | -99.83 | 6.5 | 2001 |
| NC | 9A | 370960 | WN | 35.54 | -79.17 | 4.0 | 2003 |
| NE | 9 | 310903 | DF | 40.30 | -99.83 | 4.8 | 2002 |
| NJ | 9A | 340961 | WF | 40.18 | -74.56 | 6.5 | 2007 |
| AZ | 9A | 04b901 | DN | 33.44 | -112.58 | 7.3 | 2004 |
| AZ | 9A | 04b903 | DN | 33.44 | -112.58 | 7.3 | 2004 |

DF = dry-freeze. WN = wet-nonfreeze. WF = wet-freeze. DN = dry-nonfreeze.

Significant Results

Low temperature cracking and rutting field performance for 26 LTPP binders were collected. This information will be used for validation of technologies developed in other work elements.

Work Planned Next Quarter

The research team will perform SENB tests on the LTPP binders and will establish correlations between field performance and laboratory results for validation of the SENB procedure.

Furthermore, experimental protocols developed in rutting work element will be used in LTPP binders, and comparison to rutting field performance will be established as well.

***Subtask V3b-5: Review and Revisions of Materials Models (Start Year 2, Year 3, Year 4, and Year 5)***

The reader is referred to subtask V3b-1.

***Subtask V3b-6: Evaluate the Impact of Moisture and Aging (Start Year 3, Year 4, and Year 5)***

The reader is referred to subtask V3b-1.

**Work Element V3c: Validation of PANDA (TAMU)**

Work Done this Quarter

Please refer to the details presented in work elements M4c, F1d-8, and F3c. These work elements outline what has already been accomplished in validating the constitutive models that are implemented in PANDA as well as the validation work that will be carried out in the coming quarter.

We have developed the experimental setup that will be used to carry out the ARC 2x2 matrix validation plan. The experimental setup allows measuring radial and axial deformation under compression loading at different confining stresses and temperatures. The extension tests will be carried out at North Carolina State University.

Significant Results

See the significant results sections in work elements M4c, F1d-8, and F3c.

Significant Problems, Issues and Potential Impact on Progress

See the significant results sections in work elements M4c, F1d-8, and F3c.

Work Planned Next Quarter

Focus will be placed on validation of PANDA using the ARC 2x2 matrix validation plan and on the structural simulations of the ALF sections.

**Work Element V3d: Engineered Properties Testing Plan (TAMU)**

Work Done this Quarter

The work completed this quarter relates to work described in Work Elements F2c and E1a.

Work Planned Next Quarter

Please refer to Work Elements F2c and E1a.

## TABLE OF DECISION POINTS AND DELIVERABLES FOR VALIDATION

| Name of Deliverable | Type of Deliverable | Description of Deliverable | Original Delivery Date | Revised Delivery Date | Reason for changes in delivery date |
|---|---|---|---|---|---|
| V3a-1: Evaluation of the PG-Plus practices and the motivations for selecting the "plus" tests. (UWM) | Draft Report | Detailed analysis of PG and PG+ tests | 10/08 | 9/11 | Extended time was needed to start the joint effort between Western Cooperative Test Group (WCTG), the Rocky Mountain Asphalt User-Produce Group (RMAUPG), and UW-Madison which is generating data from PG and PG+ tests run in more than 40 different laboratories. |
| | Final Report | Report on 508 format on benefits of PG+ and new ARC tests in comparison to PG tests. Repeatability of PG+ and newly developed ARC procedures | 12/08 | 3/12 | |
| V3a-2: Detailed analysis of all PG-Plus tests being proposed or in use today, documentation of benefits and costs of these tests, and comparison with new tests (UWM) | Draft Report | Refer to Draft Report for V3a-1 | 4/09 | 9/11 | |
| V3a-4: Development of specification criteria for new tests based on field evaluation of construction and performance (UWM) | Draft Report | Refer to Draft Report for V3a-1 | 7/09 | 9/11 | Refer to Draft Report for V3a-1 |
| V3a-5: Interviews and surveys for soliciting feedback on binder tests and specifications (UWM) | Draft Report | Report summarizing collaboration between Western Cooperative Test Group (WCTG), the Rocky Mountain Asphalt User-Produce Group (RMAUPG) and UW-Madison | 12/11 | N/A | N/A |
| | Final Report | Report in 508 format on Development and maintenance of database for evaluation of PG, PG+, and new ARC tests. | 1/12 | 6/12 | Final report submission date moved back to allow at least 6 months between draft and final report submission. |

| Name of Deliverable | Type of Deliverable | Description of Deliverable | Original Delivery Date | Revised Delivery Date | Reason for changes in delivery date |
|---|---|---|---|---|---|
| V3b-3: Select LTPP Sites to Validate New Binder Testing Procedures (UWM) | Draft Report | Report summarizing characterization of LTPP binders by means of the Linear Amplitude Sweep (LAS), Single Edge-Notch Beam (SENB) and Bitumen Bond Strength (BBS) tests. | 12/11 | N/A | N/A |
| | Final Report | Final report in 508 format on validation/verification of fatigue, thermal cracking, and moisture damage procedures using LTPP binders. | 1/12 | 6/12 | Final report submission date moved back to allow at least 6 months between draft and final report submission. |
| V3c: Validation of PANDA (TAMU) | PANDA Workshop | Workshop on PANDA Models and Validation Results | 8/11 | N/A | N/A |
| | Draft Report | Documentation of PANDA Models and Validation | 11/11 | N/A | N/A |
| | Final Report (M5, M4c, F1b-1, F1c, F1d-8, F3c, and V3c) | Documentation of PANDA Models and Validation | 3/12 | 6/30/12 | N/A |
| | UMAT Material | PANDA Implemented in Abaqus | 3/12 | N/A | N/A |
| | Software | Standalone Software to support the use of and future utility and flexibility of PANDA | 3/12 | N/A | N/A |

| Validation Year 4 | Year 4 (4/2010-3/2011) | | | | | | | | | | | | Team |
|---|---|---|---|---|---|---|---|---|---|---|---|---|---|
| | 4 | 5 | 6 | 7 | 8 | 9 | 10 | 11 | 12 | 1 | 2 | 3 | |
| **(1) Field Validation** | | | | | | | | | | | | | |
| V1a: Use and Monitoring of Warm Mix Asphalt Sections | | | | | | | | | | | | | WRI |
| V1b: Construction and Monitoring of additional Comparative Pavement Validation sites | | | | | | | | | | | | | WRI |
| **(2) Accelerated Pavement Testing** | | | | | | | | | | | | | |
| V2a: Accelerated Pavement Testing including Scale Model Load Simulation on small test track (This work element will include all accelerated pavement testing) | | | | | | | | | | | | | WRI |
| V2b: Construction of validation sections at the Pecos Research & Testing Center | | | | | | | | | | | | | WRI |
| **(3) R&D Validation** | | | | | | | | | | | | | |
| V3a: Continual Assessment of Specification | | | | | | | | | | | | | UWM |
| V3a-1: Evaluation of the PG-Plus practices and the motivations for selecting the "plus" tests. | | | | | | | P | | | | | | |
| V3a-2: Detailed analysis of all PG-Plus tests being proposed or in use today, documentation of benefits and costs of these tests, and comparison with new tests | | | | | | | | | | | | | |
| V3a-3: Development of protocols for new binder tests and database for properties measured | | | | P | | | | | | | | | |
| V3a-4: Development of specification criteria for new tests based on field evaluation of construction and performance | | | P | | | | | | | | JP | | |
| V3a-5: Interviews and surveys for soliciting feedback on binder tests and specifications | | P | | | | | | | | | | | |
| V3b: Validation of the MEPDG Asphalt Materials Models and Early Verification of Technologies Developed by ARC using new MEPDG Sites and Selected LTPP sites | | | | | | | | | | | | | UNR/UWM/ WRI |
| V3b-1: Design and Build Sections | | | | | | | | | | | | | UNR |
| V3b-2: Additional Testing (if needed) | | | | | | | | | | | | | |
| V3b-3: Select LTPP Sites to Validate New Binder Testing Procedures | | | | DP | JP | | | | | P | | | UWM |
| V3b-4: Testing of Extracted Binders from LTPP Sections | | | | | | | | | | | | | |
| V3b-5: Review and Revisions of Materials Models | | | | | | | | | | | | | |
| V3b-6: Evaluate the Impact of Moisture and Aging | | | | | | | | | | | | | |
| V3c: Validation of PANDA | | | | | | | | | | | | | TAMU |
| V3d: Engineered Properties Testing Plan | | | | P | JP(2) | P | | | JP | P(3), JP | | | TAMU |

**Deliverable codes**

D: Draft Report
F: Final Report
M&A: Model and algorithm
SW: Software
JP: Journal paper
P: Presentation
DP: Decision Point

**Deliverable Description**

Report delivered to FHWA for 3 week review period.
Final report delivered in compliance with FHWA publication standards
Mathematical model and sample code
Executable software, code and user manual
Paper submitted to conference or journal
Presentation for symposium, conference or other
Time to make a decision on two parallel paths as to which is most promising to follow througjh

Work planned
Work completed
Parallel topic

| Validation Years 2 - 5 | Year 2 (4/08-3/09) | | | | Year 3 (4/09-3/10) | | | | Year 4 (04/10-03/11) | | | | Year 5 (04/11-03/12) | | | | Team |
|---|---|---|---|---|---|---|---|---|---|---|---|---|---|---|---|---|---|
| | Q1 | Q2 | Q3 | Q4 | Q1 | Q2 | Q3 | Q4 | Q1 | Q2 | Q3 | Q4 | Q1 | Q2 | Q3 | Q4 | |
| **(1) Field Validation** | | | | | | | | | | | | | | | | | |
| V1a: Use and Monitoring of Warm Mix Asphalt Sections | | | | | | | | | | | | | | | | | WRI |
| V1b: Construction and Monitoring of additional Comparative Pavement Validation sites | | | | | | | | | | | | | | | | | WRI |
| **(2) Accelerated Pavement Testing** | | | | | | | | | | | | | | | | | |
| V2a: Accelerated Pavement Testing including Scale Model Load Simulation on small test track | | | | | | | | | | | | | | | | | WRI |
| V2b: Construction of validation sections at the Pecos Research & Testing Center | | | | | | | | | | | | | | | | | WRI |
| **(3) R&D Validation** | | | | | | | | | | | | | | | | | |
| V3a: Continual Assessment of Specification | | | | | | | | | | | | | | | | | UWM |
| V3a-1: Evaluation of the PG-Plus practices and the motivations for selecting the "plus" tests. | | P | D,F | | | | | | | | | | | | | | |
| V3a-2: Detailed analysis of all PG-Plus tests being proposed or in use today, documentation of benefits and costs of these tests, and comparison with new tests | | | | P | D | | | | | | | | | | | | |
| V3a-3: Development of protocols for new binder tests and database for properties measured | | | | | | JP | | | | P | | | | | | | |
| V3a-4: Development of specification criteria for new tests based on field evaluation of construction and performance | | | | | | D | | P | P | | | JP | P | | JP | | |
| V3a-5: Interviews and surveys for soliciting feedback on binder tests and specifications | | | | | | | | | P | | | | P | | D | F | |
| V3b: Validation of the MEPDG Asphalt Materials Models and Early Verification of Technologies Developed by ARC using new MEPDG Sites and Selected LTPP sites | | | | | | | | | | | | | | | | | UNR/UWM |
| V3b-1: Design and Build Sections | | | | | | | | | | | | | | | | | |
| V3b-2: Additional Testing (if needed) | | | | | | | | | | | | | | | | | |
| V3b-3: Select LTPP Sites to Validate New Binder Testing Procedures | | | | | DP | | | P | | JP, DP | | P | | | D | F | |
| V3b-4: Testing of Extracted Binders from LTPP Sections | | | | | | | | | | | | | | | | | |
| V3b-5: Review and Revisions of Materials Models | | | | | | | | | | | | | | | | | |
| V3b-6: Evaluate the Impact of Moisture and Aging | | | | | | | | | | | | | | | | | |
| V3c: Validation of PANDA | | | | | | | | | | | | | | | | | TAMU |
| V3d: Engineered Materials Testing Plan | | | | | | | | | | P(2) | JP | P(3), JP | | | | | TAMU |

**Deliverable codes**

D: Draft Report
F: Final Report
M&A: Model and algorithm
SW: Software
JP: Journal paper
P: Presentation
DP: Decision Point

**Deliverable Description**

Report delivered to FHWA for 3 week review period.
Final report delivered in compliance with FHWA publication standards
Mathematical model and sample code
Executable software, code and user manual
Paper submitted to conference or journal
Presentation for symposium, conference or other
Time to make a decision on two parallel paths as to which is most promising to follow througjh

Work planned
Work completed
Parallel topic

# PROGRAM AREA: TECHNOLOGY DEVELOPMENT

## Work element TD1: Prioritize and Select Products for Early Development (Year 1) (AAT, WRI)

This work element has been completed. Six early development products were identified.

## Work element TD2: Develop Early Products (Year 3) (AAT, WRI)

Work Done This Quarter

Table TD2.1 summarizes the progress on the Products for Early Development. The test method for Automated Flocculation Titrimetric Analysis has been published as an ASTM standard method of test, ASTM D6703 – 07. Draft AASHTO Standards have been completed for the other 5 products; however, the Draft AASHTO Standard for simplified continuum damage fatigue analysis for the Asphalt Mixture Performance Tester, is being revised significantly based on the findings of the analyses being conducted in the continuum damage fatigue model refinement in Work Element E2e. The Draft AASHTO Standard for Determination of Polymer in Modified Asphalt was placed on the outreach portion of the ARC website at: http://www.arc.unr.edu/Outreach.html#TechDevelopmentProducts. One page product descriptions for each of these products were also prepared. These product descriptions were placed on the ARC website at: http://www.arc.unr.edu/Deliverables/ARC_Technology_Development_Product_Briefs_Mar2011.pdf, and distributed by the FHWA to the various expert task groups. The product descriptions and their purpose are discussed in greater detail in the next section.

Table TD2.1. Summary of progress on early development products.

| No. | Product | ARC Research Program | Format | Estimated Completion Data | ARC Partner | Draft AASHTO Standard? |
|---|---|---|---|---|---|---|
| 1 | Simplified Continuum Damage Fatigue Analysis for the Asphalt Mixture Performance Tester | Prior | Test Method | 9/30/2011 | AAT | Yes |
| 2 | Wilhelmy Plate Test | Prior | Test Method | Completed | TTI | Yes |
| 3 | Universal Sorption Device | Prior | Test Method | Completed | TTI | Yes |
| 4 | Dynamic Mechanical Analysis | Prior | Test Method | Completed | TTI | Yes |
| 5 | Automated Flocculation Titrimetric Analysis | Prior | Test Method | Completed | WRI | No (ASTM) |
| 6 | Determination of Polymer in Asphalt | Prior | Test Method | Completed | WRI | Yes |

Significant Problems, Issues and Potential Impact on Progress

None.

Work Planned Next Quarter

AAT will continue revising the Draft AASHTO Standard for simplified continuum damage fatigue analysis for the Asphalt Mixture Performance Tester. Based on the ratings from the ETGs, support will be provided for advancing the selected products through AASHTO for publication as Provisional AASHTO Standards.

**Work element TD3: Identify Products for Mid-Term and Long-Term Development (Years 2, 3, and 4) (AAT, TTI, UNR, UW-M, WRI)**

This work element has been completed. A total of 38 mid- and long-term products were identified. Table TD3.1 summarizes these products.

Table TD3.1. Summary of mid- and long-term technology development products.

| No. | Product | ARC Work Element | Format | Estimated Completion Date | ARC Partner |
|---|---|---|---|---|---|
| 7 | A Method for the Preparation of Specimens of Fine Aggregate Matrix of Asphalt Mixtures | M1c | Test Method | 12/31/2010 | TTI |
| 8 | Measuring intrinsic healing characteristics of asphalt binders | F1d | Test Method | 12/31/2012 | TTI / UT Austin |
| 9 | Lattice Micromechanical Model for Virtual Testing of Asphalt Concrete in Tension | F3b | Analysis Program | 2/28/2012 | NCSU |
| 10 | Cohesive Zone Modeling as an Efficient and Powerful Tool to Predict and Characterize Fracture Damage of Asphalt Mixtures Considering Mixture Microstructure, Material Inelasticity, and Moisture Damage | F3b | Performance Predicting Model | 12/31/2011 | University of Nebraska |
| 11 | Pavement Analysis Using Nonlinear Damage Approach (PANDA) | F3c | Test Method | 12/31/2012 | TTI |
| 12 | Test Methods for Determining the Parameters of Material Models in PANDA (Pavement Analysis Using Nonlinear Damage Approach) | F3c E1a | Test Method | 12/31/2011 | TTI |
| 13 | Continuum Damage Permanent Deformation Analysis for Asphalt Mixtures | E1a | Test Method | 9/30/2011 | TTI |
| 14 | Characterization of Fatigue and Healing Properties of Asphalt Mixtures Using Repeated Direct Tension Test | E1a | Test Method & Data Analysis Program | 9/30/2011 | TTI |
| 15 | Nondestructive Characterization of Tensile Viscoelastic Properties of Undamaged Asphalt Mixtures | E1a | Test Method & Data Analysis Program | Completed | TTI |
| 16 | Nondestructive Characterization of Field Cores of Asphalt Pavements | E1a | Test Method & Data Analysis Program | 9/30/2011 | TTI |

Table TD3.1 continued. Summary of mid- and long-term technology development products.

| No. | Product | ARC Work Element | Format | Estimated Completion Date | ARC Partner |
|---|---|---|---|---|---|
| 17 | Self-Consistent Micromechanics Models of Asphalt Mixtures | E1a | Analytical Model & Data Analysis Program | 6/30/2011 | TTI |
| 18 | Nondestructive Characterization of Anisotropic Viscoelastic Properties of Undamaged Asphalt Mixtures under Compressive Loading | E1a | Test Method | Completed | TTI |
| 19 | Mix Design for Cold-In-Place Recycling (CIR) | E1c | Practice | 12/31/2011 | UNR |
| 20 | Mix Design for Cold Mix Asphalt | E1c | Practice | 3/31/2012 | UNR |
| 21 | Evaluation of RAP Aggregates | E2b | Practice | 4/30/2011 | UNR |
| 22 | Identification of Critical Conditions for HMA mixtures | E2c | Practice | 12/31/2011 | UNR |
| 23 | Thermal Stress Restrained Specimen Test (TSRST) | E2d | Test Method | 9/30/2011 | UNR |
| 24 | HMA Thermal Stresses in the Intermountain Region | E2d | Model | 3/31/2012 | UNR |
| 25 | Dynamic Model for Flexible Pavements 3D-Move | VP3a | Software | 3/31/2011 | UNR |
| 26 | Bitumen Bond Strength Test ( BBS) | M1a | Test Method | Completed | UWM |
| 27 | Elastic Recovery – DSR | F2a | Test Method | 12/31/2010 | UWM |
| 28 | Linear Amplitude Sweep (DSR) | F2e | Test Method | Completed | UWM |
| 29 | Binder Yield Energy Test ( BYET) | F2e | Test Method | Completed | UWM |
| 30 | Rigden Voids for fillers | F2e | Test Method | 9/30/2011 | UWM |
| 31 | Binder Lubricity Test – DSR | E1c | Test Method | 12/31/2010 | UWM |
| 32 | RAP Binder PG True Grade Determination | E2b | Test Method / Software | 3/31/2011 | UWM |
| 33 | Single Edge Notch Bending | E2d | Test Method | 5/31/2011 | UWM |
| 34 | Binder Glass Transition Test | E2d | Test Method | 5/31/2011 | UWM |
| 35 | Asphalt Mixture Glass Transition Test | E2d | Test Method | 5/31/2011 | UWM |

Table TD3.1 continued. Summary of mid- and long-term technology development products.

| No. | Product | ARC Work Element | Format | Estimated Completion Date | ARC Partner |
|---|---|---|---|---|---|
| 36 | Planar imaging/ Aggregate Structure | E1b | Test Method/ Software | 3/31/2011 | UWM |
| 37 | Gyratory Pressure Distribution Analyzer (GPDA) | E1c | Test Method | Completed | UWM |
| 38 | Improved Oxygen and Thermal Transport Model of Binder Oxidation in Pavements | F1c | Methodology, Publication | 3/31/2012 | TAMU |
| 39 | Field Validation of an Improved Oxygen and Thermal Transport Model of Binder Oxidation in Pavements | F1c | Methodology, Publication | 3/31/2012 | TAMU |
| 40 | Validation of an improved Pavement Temperature Transport Model for use in an Oxygen and Thermal Transport Model of Binder Oxidation in Pavements | F1c | Methodology, Publication | Completed | TAMU |
| 41 | Pavement Air Voids Size Distribution Model for use in an Oxygen and Thermal Transport Model of Binder Oxidation in Pavements | F1c | Methodology, Publication | 3/31/2012 | TAMU |
| 42 | Improved Understanding of Fast-Rate, Constant-Rate Binder Oxidation Kinetics Mechanism through the Effects of Inhibitors | F1c | Publication | 3/31/2012 | TAMU |
| 43 | Improved Understanding of Fatigue Resistance Decline with Binder Oxidation | F1c | Publication | 3/31/2012 | TAMU |
| 44 | Micromechanical Properties of Various Structural Components in Asphalt using Atomic Force Microscopy (AFM) | F2d | Test and Analysis Method | 3/31/2011 | TAMU |

**Work Element TD4: Develop Mid-Term and Long-Term Products (Years 3, 4, and 5) (AAT, TTI, UNR, UW-M, WRI)**

One page descriptions of each of the mid- and long-term technology development products were prepared. These descriptions include the following:

- **Product Description.** A brief description of the product.
- **Equipment Cost and Availability.** A summary of the equipment needed, its cost and whether it is available commercially.
- **Potential Applications.** A brief description of how the research team envisions the product will be used.
- **Targeted Users.** A description of the personnel that the research team envisions will use the product. Examples are pavement design engineers, experienced asphalt mixture design technicians, etc.
- **Time and Skill Requirements.** Estimates of the time and skill required to use the product in its most likely application.
- **Recommended Next Steps.** A brief description on the next steps required to implement the product as envisioned by the research team.

A suggested product rating system was also developed based on previous work done by AAT for WRI. The FHWA refined the product rating system and forwarded it and the product descriptions to members of the various ETGs. The purpose of this survey was to help prioritize the products and to identify where additional resources should be directed. The product descriptions were also placed on the ARC website at: http://www.arc.unr.edu/Deliverables/ARC_Technology_Development_Product_Briefs_Mar2011.pdf.

The draft AASHTO Standards of the completed mid- and long- term products were placed on the outreach portion of the ARC website at: http://www.arc.unr.edu/Outreach.html#TechDevelopmentProducts. The products added to the website are:

- ARC Product 26, Standard Method of Test for "Determining Asphalt Binder Bond Strength by Means of the Bitumen Bond Strength (BBS) Test."
- ARC Product 28, Standard Method of Test for "Estimating Fatigue Resistance of Asphalt Binders Using the Linear Amplitude Sweep."
- ARC Product 29, Standard Method of Test for "Yield Energy of Asphalt Binders Using the Dynamic Shear Rheometer."

Significant Problems, Issues and Potential Impact on Progress

None.

Work Planned Next Quarter

The research team will continue with the development of the mid- and long-term technology development products. The research team will review the rankings provided to the FHWA by the ETGs.

# PROGRAM AREA: TECHNOLOGY TRANSFER

## CATEGORY TT1: OUTREACH AND DATABASES

### Work element TT1a: Development and Maintenance of Consortium Website (Duration: Year 1 through Year 5) (UNR)

Work Done This Quarter

The ARC website was maintained and updated. The ARC quarterly technical progress report, October 1- December 31, 2011, was uploaded to the ARC website. The ARC newsletter (Vol. 5, Issue 1), Summary of Deliverables, Technology Development Product Briefs, and Technology Development Products (draft AASHTO and procedures) were uploaded to the website. The following references and files were updated:

- List of Publications and Conference Proceedings under the "Publications" webpage.
- List of Presentations and Posters under the "Outreach" webpage.

The 3D-Move Discussion Group Forum was also maintained.

Significant Results

None

Significant Problems, Issues and Potential Impact on Progress

None

Work Planned Next Quarter

Continue maintaining and updating the ARC website. Update the list of Publications and Conference Proceedings. Update the list of Presentations and Posters and the list of Theses and White Papers. Post information and new releases for 3D-Move. Maintain the 3D-Move Discussion Group Forum.

### Work element TT1b: Communications (Duration: Year 1 through Year 5) (UNR)

Work Done This Quarter

Published the ARC Newsletter Vol. 5, Issue 1.

Significant Results

None

Significant Problems, Issues and Potential Impact on Progress

None

Work Planned Next Quarter

Prepare and publish the ninth ARC Newsletter.

**Work element TT1c: Prepare Presentations and Publications (All)**

Presentations

Bahia, Hussain U., Petrina T. Johannes, and Andrew Hanz, "Opportunities and Challenges in Using Emulsified Asphalt Mixtures (EAM), AEMA-ARRA-ISSA Annual Meeting, Tucson, Arizona, February 24, 2011.

Bahia, Hussain, Tim Miller, Raul Velasquez, and Amir Golalipour, "Multiple Stress Creep and Recovery: Reproducibility and Repeatability." Presented at the Binder Expert Task Group Meeting, Phoenix, AZ, March 2011.

Hanz, Andrew, Timothy Miller, Raquel Bringel, and Hussain Bahia, "Application of the Bitumen Bond Strength Test for Evaluation of Emulsion Curing and Residue Performance," AEMA-ARRA-ISSA Annual Meeting, Tucson, Arizona, February 24, 2011.

Hanz, A., E. Mahmoud, and H. Bahia, "Impacts of WMA Production Temperature on Binder Aging and Mixture Flow Number," *Journal of the Association of Asphalt Paving Technologists*, Tampa, Florida, Association of Asphalt Paving Technologists Journal 80, 2011. *Presented at Tampa annual meeting and Published in the Proceedings.*

Hanz, A., E. Mahmoud, and H. Bahia, "Asphalt Lubricity Test Evaluation and Relationship to Mixture Workability," Proceedings of the 90$^{th}$ Annual Meeting of the Transportation Research Board, Washington D.C., Transportation Board of the National Academies, 2011. *Accepted for presentation only.*

Harnsberger, P. M., M. J. Farrar, S-C. Huang, and R. E. Robertson, "Comparative Field Performance Using Asphalts from Multiple Crude Oil Sources." Presented at the 2011 Transportation Research Board Annual Meeting, Washington, DC, January 22-27, 2011.

Harnsberger, P. M., "FHWA Asphalt Research at WRI." Presented at the Rocky Mountain User-Producer Meetings, Denver, CO, February 23-25, 2011.

Hintz, C., R. Velasquez, C. Johnson, and H. Bahia, "Modification and Validation of the Linear Amplitude Sweep Test for Binder Fatigue Specification." Presented at the Transportation Research Board Annual Meeting, Washington, DC, January 2011.

Hintz, C., R. Velasquez, Z. Li, and H. Bahia, "Effect of Oxidative Aging on Binder Fatigue Performance." Presented at the Association of Asphalt Paving Technologists (AAPT) 2011 Annual Meeting, Tampa, FL, March 2011.

Luo, R., and R. L. Lytton, 2011, "Distribution of Crack Size in Asphalt Mixtures." *The Transportation Research Board (TRB) 90th Annual Meeting*, Washington, D.C., January 23-27, 2011.

Moraes, R., R. Velasquez, and H. Bahia, "Measuring Effect of Moisture on Asphalt-Aggregate Bond with the Bitumen Bond Strength Test." Poster presentation at the Transportation Research Board (TRB) Annual Meeting, Washington, DC, January 2011.

Pauli, Troy, and Will Grimes, Models ETG, "Nano-Rheology" (ARC Subtask M1b-2: Work of Adhesion at Nano-Scale using AFM; and ARC Subtask M2a-2: Work of Cohesion Measured at Nano-Scale using AFM).

Pauli, Troy, Models ETG, "Chemo-Mechanics of Bituminous Materials: Thermo-kinetic Theory of Fatigue/Healing" (ARC Subtask F1d-7: Coordinate with Atomic Force Microscopic (AFM) Analysis; and Work Element F3a: Asphalt Microstructural Model)

Planche, Jean-Pascal, "Europe's Modified Asphalt Binder Experiences." Presented at the AMAP Annual Conference, Kansas City, MO, February 15-17, 2011.

Zhang, Y., R. Luo, and R. L. Lytton, 2011, "Anisotropic Viscoelastic Characterization of Undamaged Asphalt Mixtures in Compression." *The Transportation Research Board (TRB) 90th Annual Meeting*, Washington, D.C., January 23-27, 2011.

Zhang, Y., R. Luo, and R. L. Lytton, 2011, "Microstructure-Based Inherent Anisotropy of Asphalt Mixtures." *Doctoral Student Research in Asphalt Materials and Mixtures, The Transportation Research Board (TRB) 90th Annual Meeting*, Washington, D.C., January 23-27, 2011.

Publications

Badami, J. V. and M. L. Greenfield, 2010, Maxwell Model Analysis of Bitumen Rheological Data. *J. Materials in Civil Eng.* (in press). The revised manuscript resubmitted in the prior quarter was accepted for publication. This paper parameterizes physically based rheological models using dynamic shear rheometry data.

Greenfield, M. L., 2010, Molecular Modeling and Simulation of Asphaltenes and Bituminous Materials. *Int. J. Pavement Eng.* (in press). This invited review article was accepted for publication. It tabulates and describes molecular simulations of asphaltenes and of

asphalt/bitumen systems. Some papers that apply equations of state to asphaltenes are also discussed.

Han, Rongbin, Xin Jin, Charles J. Glover. "Modeling Pavement Temperature for Use in Binder Oxidation Models and Pavement Performance Prediction," in press, *Journal of Materials in Civil Engineering*.

Hanz, A., E. Mahmoud, and H. Bahia, "Impacts of WMA Production Temperature on Binder Aging and Mixture Flow Number," *Journal of the Association of Asphalt Paving Technologists*, Tampa, Florida, Association of Asphalt Paving Technologists Journal 80, 2011. *Presented at Tampa annual meeting and Published in the Proceedings.*

Hintz, C., R. Velasquez, and H. Bahia, Healing of Asphalt Binders: State of the Art. To be submitted to the International Journal of *Road Materials and Pavement Design* (RMPD).

Li, Derek D. and M. L. Greenfield, 2011, High Internal Energies of Proposed Asphaltene Structures. *Energy Fuels*, submitted. This manuscript describes the causes of high internal energies and suggests modified structures that reduce the high energies. See text within this report.

Luo, R., and Lytton, R. L., 2011, "Distribution of Crack Size in Asphalt Mixtures." *Transportation Research Record: Journal of the Transportation Research Board*, Transportation Research Board of the National Academies, Washington, D.C., *in press*.

Pauli, A. T., R. W. Grimes, A. G. Beemer, T. F. Turner, and J. F. Branthaver. Morphology of Asphalts, Asphalt Fractions and Model Wax-doped Asphalts Studied by Atomic Force Microscopy. (In Press) *International Journal of Pavement Engineering.*

**Work element TT1d: Development of Materials Database (Duration: Year 2 through Year 5) (UNR)**

Work Done This Quarter

The following list describes the work items completed or in progress this quarter:

- Online training session completed
- User accounts enabled to production database
- Deployment plan prepared
- Bug fixes made as needed
- Continuous improvements to the Help System
- New Field Samples Form created
- General public user interface plan created and Measure Browser from prototype created

- File management system updated

Significant Results

*Online Training Session*

On February 25, 2011, an online Web-based training session was held and all ARC consortium members were invited to participate. In total, there were roughly 20 attendees. The following topics were discussed in the training session:

- As most of the users participating in the training session had not been exposed to the ARC system before, an overview of the system was provided along with a discussion of the significant features.
- Users were given a demonstration of the significant features of the ARC application, the forms that make up the application, and an overview of how to perform specific tasks.
- Finally, users were provided with a summary of new features being finalized, such as the user interface for public users.

A live training session is being planned for May 12th or May 13th at the University of Nevada, Reno campus. A hands-on training lab will be reserved for the all-day session.

*User Accounts Enabled*

Prior to the online training session, user accounts were enabled and distributed to all ARC consortium users who had requested accounts. These accounts include all organizational super users and ordinary users. Presently, there are over 30 users with access to the system. Additional users will be added, as requested.

*Deployment Plan*

Presently, the University of Nevada, Reno is hosting the ARC database and ARC application as the development and testing process is finalized. Currently, both test and production versions are being maintained. While the University of Nevada, Reno is willing to host the production version of the database, the Federal Highway Administration (FHWA) requested a set of requirements and procedures to deploy the ARC database and ARC application to other systems. This report has been prepared and forwarded to the FHWA for review. The following list summarizes the important items contained in this report:

- The ARC database and accompanying ARC application requires SQL Server 2008 to host the database, and Internet Information Server version 6 to host the ASP.NET application itself. Note that Windows Server 2003 or Windows Server 2008 can be used as the native operating systems.
- The document contains procedures to back up the ARC database from the development computers.

- The document contains procedures to restore the ARC database to the target computer. These procedures document the necessary privileges that need to be granted to the ARC database and user. Procedures to create the ARC user are also provided.
- Procedures to install the ARC application and configure IIS to run the application are also included in the document.
- Finally, procedures were also created to configure the ARC application itself. These procedures involve modifying the application's web.config file.

The development team should note that these procedures might require modification based on the configuration differences in the target environments (SQL Server, and IIS).

*Bug Fixes*

As user acceptance testing continues, small bugs are almost always detected. The development team continues to fix these bugs as they occur. These bugs include such items as refresh errors and small usability issues. As these bugs tend to be small in nature and easy to fix, they are not listed individually in this report.

*Help System*

Work continues on the Help system as modifications are made to existing forms and new forms are created. At this point, nearly all Help pages correspond to the existing application pages.

*Field Samples*

A new form was created to associate field samples with validation sections. Figure TT1d.1 shows the new Field Samples form. The Field Samples form simplifies the user interface for the Measures form, and allows each field sample to be assigned to multiple test runs via a drop down-box as shown in figure TT1d.2.

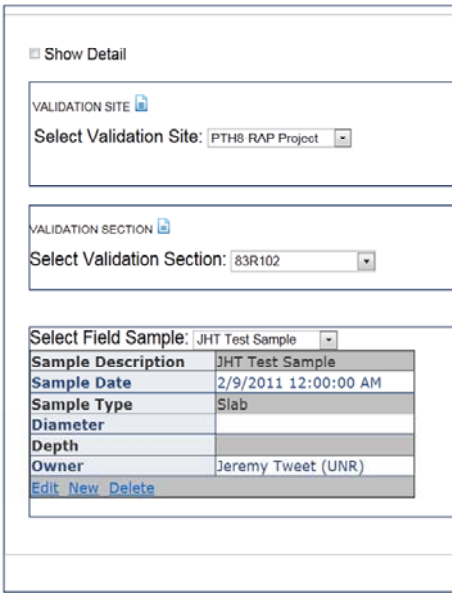


Figure TT1d.1. Field Samples form.

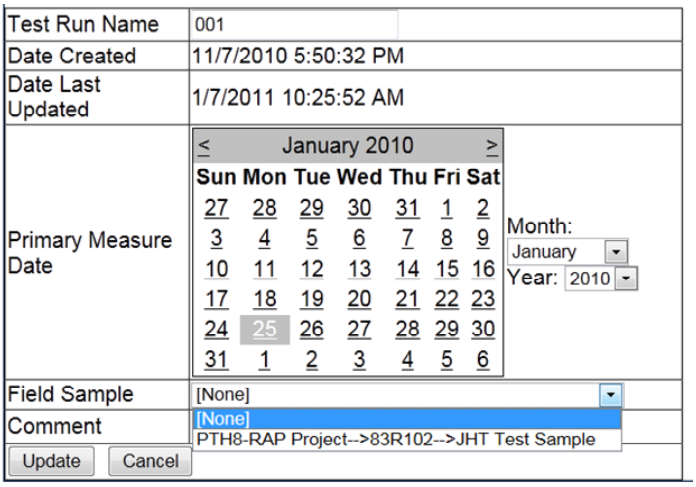


Figure TT1d.2. Revised Measures form.

*Public User Interface*

During the development process, thus far, the application and its forms have been designed and implemented so that consortium users can enter research findings into the ARC database. As stated in the last report, a major focus of development during this period was to design and implement the capabilities for data retrieval, for both consortium members and for public (non-consortium) users.

The ARC application was designed to allow access to individual forms based on the roles to which a particular user belongs. As discussed in previous reports, users are presently designated as either organizational users or organizational super users. Additionally, additional and more specific user roles are defined to give granular access to individual forms, parts of a form, or restrict the ability to edit data.

The development team sees three ways to grant read-only access to public (non-consortium) users.

1. Modify selected forms so that data in the ARC database cannot be modified. These forms could be placed in a second application. Users could access the database through this second application without authentication or identifying themselves.
2. This option would also use the second application concept described in option one. However, public users would need to self-register to use the ARC application to be granted a login and password. Public users would have read-only access to the forms created in this second application. Another possibility would be to have the ARC consortium to approve requests for user access.
3. In the third option, the same application would be used for both consortium and non-consortium users. The existing role-based infrastructure can be used to restrict access to forms or to grant limited (read-only) access to existing forms.

The user forms designed to extract research findings are either similar or identical regardless of the above options selected. Thus the "Measure Viewer" form, introduced conceptually in the last report, has been designed and partially implemented.

The page contains two sections for filtering and viewing data. The FILTERS section allows measures to be selected by the organization(s) that created the measures, and by material properties. The VIEWS section is used to describe which fields (columns) will be displayed. This page contains two different utilities for accessing data: browse mode, and export mode.

- The browse feature, though still under construction, allows flexible, online, drill-down visualization of data.
- The export mode, newly implemented, allows retrieval of any or all measure data in the database to a file, such as an Excel spreadsheet. The data returned by these utilities can be filtered by a common set of controls. Figure TT1d.3 shows part of the Measure Viewer.

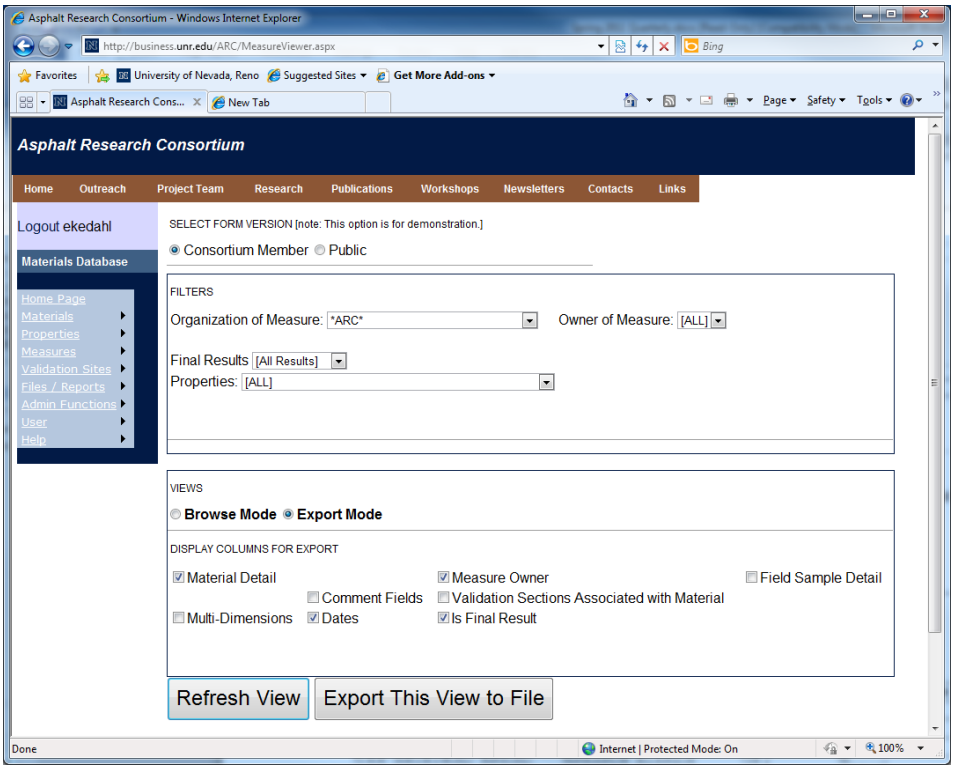


Figure TT1d.3. Measure Browser form (prototype).

The file export feature is fully functional, and should provide satisfactory data retrieval for all users. Once exported to Excel (or other spreadsheet program), the data can easily be manipulated as needed. Additional filtering capabilities will be added to this form to export only desired results, but any data can be retrieved with the current software.

A version of this form will serve as the primary access point for public users. Currently, the only difference between the public and consortium version is that the public version will only display measures which are marked as final results. While this is the only specification thus far agreed upon by the consortium, it should be a straight forward task to modify the public version to further limit the view, or provide a specialized interface. At this point, we require feedback from the consortium to determine if the public interface should differ further from the full access interface.

Still under consideration is a material comparison utility which could facilitate direct comparison of the results of 2 or more materials, e.g., mix type variants of materials with the same composition, or materials sampled at different times.

*File Management*

Improvements to the File Management system were discussed in the previous report and the hierarchical file system had been implemented, along with the infrastructure for the indexing

system. Two items remained to be finished, the user interface for this indexing system and system to create the links themselves.

The user interface for the indexing system has been implemented. Users can create any number of file groups. The infrastructure for the linking system is complete. The File Management system has also been split into two forms. The first is used to upload the files themselves. The second is used to create the file groups and link uploaded files to those groups. Figure TT1d.4 shows part of the user interface for this form.

At this point, two work items remain to be completed.

- First, while the infrastructure for the linking system is complete, final parts of the user-interface are under construction and will be completed this quarter.
- As mentioned in previous reports, a field exists in relevant tables that allow a property, measure, validation site, or other element, to be linked to a file. The user interface to store data in this field will be completed this quarter.

Additionally, based on user feedback additional filters might need to be added to simplify the process of selecting files for grouping.

Significant Problems, Issues and Potential Impact on Progress

None

Work Planned for Next Quarter

- As additional users begin to use the ARC system, small bugs will likely be found along with user interface elements that are felt to be cumbersome. Fixes will be made to repair these bugs as they arise.
- Continue work on the Help system as users find reference material unclear. Continue to modify existing Help pages and documentation to reflect current application changes.
- Finalize the file upload system and accompanying Help files.
- Develop training materials for the upcoming May 2011 hands-on workshop.

Finalize the design of the public interface and continue development based on implementation decisions made by ARC consortium members.

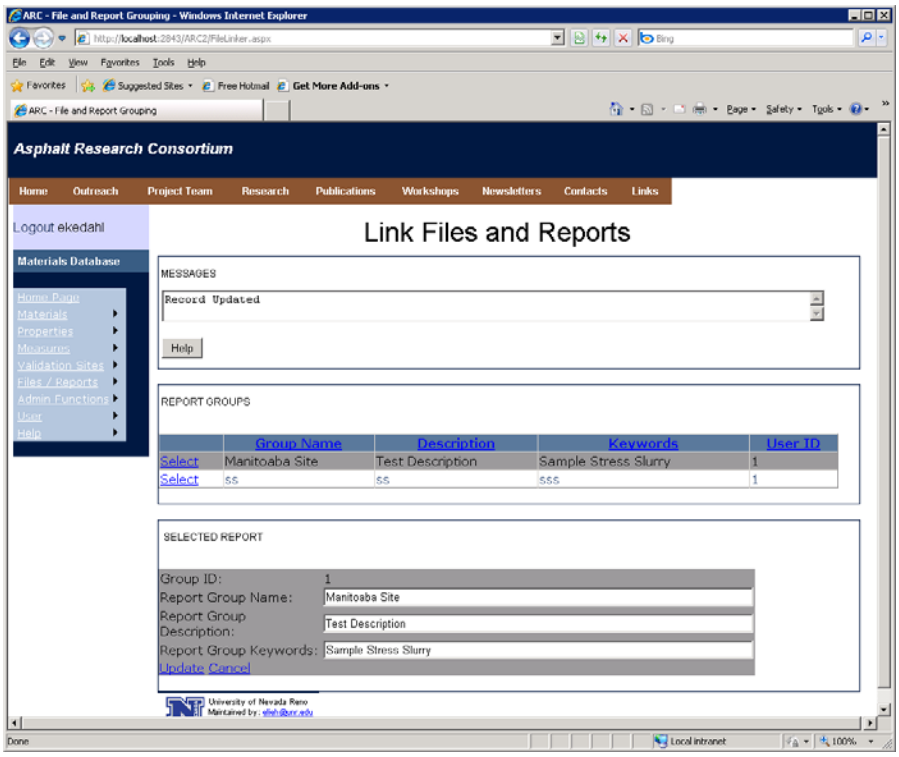


Figure TT1d.4. Link Files and Reports form.

**Work element TT1e: Development of Research Database (Duration: Year 2 through Year 5) (UNR)**

Work Done This Quarter

Uploaded the quarterly technical progress report and the ARC newsletter to the ARC website. Updated the "Publications" and "Outreach" web pages.

Significant Results

None.

Significant Problems, Issues and Potential Impact on Progress

None.

Work Planned Next Quarter

Upload the ARC quarterly technical progress report to the ARC website. Publish the ARC newsletter on the ARC website.

**Work Element TT1f: Workshops and Training (UNR lead)**

Work Done This Quarter

On February 25, 2011, an online Web-based training session was held and all ARC consortium members were invited to participate. In total, there were roughly 20 attendees. The following topics were discussed in the training session:

- As most of the users participating in the training session had not been exposed to the ARC system before, an overview of the system was provided along with a discussion of the significant features.
- Users were given a demonstration of the significant features of the ARC application, the forms that make up the application, and an overview of how to perform specific tasks.
- Finally, users were provided with a summary of new features being finalized, such as the user interface for public users.

Significant Results

None

Significant Problems, Issues and Potential Impact on Progress

None

Work Planned Next Quarter

Conduct a live training session for the ARC database on May 12$^{th}$ or May 13$^{th}$ at the University of Nevada, Reno campus. A hands-on training lab will be reserved for the all-day session.

## TABLE OF DECISION POINTS AND DELIVERABLES FOR TECHNOLOGY TRANSFER

| Name of Deliverable | Type of Deliverable | Description of Deliverable | Original Delivery Date | Revised Delivery Date | Reason for Changes in Delivery Date |
|---|---|---|---|---|---|
| TT1a: Development and Maintenance of Consortium Website | Progress report | Upload quarterly progress report and newsletter | 07/11 | N/A | N/A |
| | Newsletter | Upload newsletter | 07/11 | N/A | N/A |
| | Progress report | Upload quarterly progress report and newsletter | 10/11 | N/A | N/A |
| | Newsletter | Upload newsletter | 11/11 | N/A | N/A |
| | Progress report | Upload quarterly progress report and newsletter | 01/12 | N/A | N/A |
| | Newsletter | Upload newsletter | 03/12 | N/A | N/A |
| | Progress report | Upload quarterly progress report and newsletter | 04/12 | N/A | N/A |
| TT1b: Communications | Newsletter | Publish newsletter | 07/11 | N/A | N/A |
| | Newsletter | Publish newsletter | 11/11 | N/A | N/A |
| | Newsletter | Publish newsletter | 03/12 | N/A | N/A |
| TT1d: Development of Materials Database | Workshop | Training for "super users" and "sub users" on how to use the materials database and validation section and to evaluate the potential errors, bugs and the ease of use of the database system. | 04/11 | N/A | N/A |
| | Database | Materials database software | 03/12 | N/A | N/A |
| TT1f: Workshops and Training | Workshop | Training for "super users" and "sub users" on how to use the materials database and validation section and to evaluate the potential errors, bugs and the ease of use of the database system. | 04/11 | 5/11 | Scheduling issue |
| | Workshop | PANDA software training | 8/11 | N/A | N/A |

| Technology Transfer Year 4 | Year 4 (4/2010-3/2011) | | | | | | | | | | | | Team |
|---|---|---|---|---|---|---|---|---|---|---|---|---|---|
| | 4 | 5 | 6 | 7 | 8 | 9 | 10 | 11 | 12 | 1 | 2 | 3 | |
| **(1) Outreach and Databases** | | | | | | | | | | | | | |
| TT1a: Development and Maintenance of Consortium Website | | | | | | | | | | | | | UNR |
| TT1b: Communications | | | | | | | | | | | | | UNR |
| TT1c: Prepare presentations and publications | | | | | | | | | | | | | UNR |
| TT1d: Development of Materials Database | | | | | | | | | | | | | UNR |
| TT1d-1: Identify the overall Features of the Web Application | | | | | | | | | | | | | |
| TT1d-2: Identify Materials Properties to Include in the Materials | | | | | | | | | | | | | |
| TT1d-3: Define the Structure of the Database | | | | | | | | | | | | | |
| TT1d-4: Create and Populate the Database | | | | | | | | | | | | | |
| TT1e: Development of Research Database | | | | | | | | | | | | | UNR |
| TT1e-1: Identify the Information to Include in the Research Database | | | | | | | | | | | | | |
| TT1e-2: Define the Structure of the Database | | | | | | | | | | | | | |
| TT1e-3: Create and Populate the Database | | | | | | | | | | | | | |
| TT1f: Workshops and Training | | | | | | | | | | | | | UNR |

| **Deliverable codes** | **Deliverable Description** |
|---|---|
| D: Draft Report | Report delivered to FHWA for 3 week review period. |
| F: Final Report | Final report delivered in compliance with FHWA publication standards |
| M&A: Model and algorithm | Mathematical model and sample code |
| SW: Software | Executable software, code and user manual |
| JP: Journal paper | Paper submitted to conference or journal |
| P: Presentation | Presentation for symposium, conference or other |
| DP: Decision Point | Time to make a decision on two parallel paths as to which is most promising to follow througjh |

Work planned
Work completed
Parallel topic

| **Technology Transfer Years 2 - 5** | Year 2 (4/08-3/09) | | | | Year 3 (4/09-3/10) | | | | Year 4 (04/10-03/11) | | | | Year 5 (04/11-03/12) | | | | Team |
|---|---|---|---|---|---|---|---|---|---|---|---|---|---|---|---|---|---|
| | Q1 | Q2 | Q3 | Q4 | Q1 | Q2 | Q3 | Q4 | Q1 | Q2 | Q3 | Q4 | Q1 | Q2 | Q3 | Q4 | |
| **(1) Outreach and Databases** | | | | | | | | | | | | | | | | | |
| TT1a: Development and Maintenance of Consortium Website | | | | | | | | | | | | | | | | | UNR |
| TT1b: Communications | | | | | | | | | | | | | | | | | UNR |
| TT1c: Prepare presentations and publications | | | | | | | | | | | | | | | | | ALL |
| TT1d: Development of Materials Database | | | | | | | | | | | | | | | | | UNR |
| TT1d-1: Identify the overall Features of the Web Application | | | | | | | | | | | | | | | | | |
| TT1d-2: Identify Materials Properties to Include in the Materials Database | | | | | | | | | | | | | | | | | |
| TT1d-3: Define the Structure of the Database | | | | | | | | | | | | | | | | | |
| TT1d-4: Create and Populate the Database | | | | | | | SW, v. β | SW | | | | | | | | | |
| TT1e: Development of Research Database | | | | | | | | | | | | | | | | | UNR |
| TT1e-1: Identify the Information to Include in the Research Database | | | | | | | | | | | | | | | | | |
| TT1e-2: Define the Structure of the Database | | | | | | | | | | | | | | | | | |
| TT1e-3: Create and Populate the Database | | | | | | | | | | | | | | | | | |
| TT1f: Workshops and Training | | | | | | | | | | | | | | | | | UNR |

| **Deliverable codes** | **Deliverable Description** |
|---|---|
| D: Draft Report | Report delivered to FHWA for 3 week review period. |
| F: Final Report | Final report delivered in compliance with FHWA publication standards |
| M&A: Model and algorithm | Mathematical model and sample code |
| SW: Software | Executable software, code and user manual |
| JP: Journal paper | Paper submitted to conference or journal |
| P: Presentation | Presentation for symposium, conference or other |
| DP: Decision Point | Time to make a decision on two parallel paths as to which is most promising to follow througjh |

Work planned
Work completed
Parallel topic